23

EARTH RESOURCES TECHNOLOGY SATELLITE
FINAL REPORT

3. OBSERVATORY SYSTEM DESIGN

PREPARED FOR
GODDARD SPACE FLIGHT CENTER
NATIONAL AERONAUTICS
AND SPACE ADMINISTRATION
UNDER CONTRACT NAS5-11260

TRW SYSTEMS GROUP

IBM FEDERAL SYSTEMS DIVISION

Itek OPTICAL SYSTEMS DIVISION

RECEIVED
NASA STI FACILITY
INPUT BRANCH
AUG 1970

Reproduced by
NATIONAL TECHNICAL
INFORMATION SERVICE
Springfield, Va. 22151

FACILITY FORM 602
N70-34411 (ACCESSION NUMBER)
256 (PAGES)
CR-112495 (NASA CR OR TMX OR AD NUMBER)
(THRU) 1
(CODE) 31
(CATEGORY)

EARTH RESOURCES TECHNOLOGY SATELLITE

FINAL REPORT

Volume 3. Observatory System Design

February 11, 1970

prepared for

National Aeronautics and Space Administration
Goddard Space Flight Center

Contract NAS5-11260

item 3a

TRW Systems Group
One Space Park · Redondo Beach
Los Angeles County
California 90278

PREFACE

The final report for the ERTS Phase B/C study consists of the 12 volumes that are submitted now and additional volumes to be delivered in April covering the results of the study of the Ground Data Handling System for ERTS. The contents of the first volumes of the report are as follows:

Volume

1. (to be completed in April). Summarizes all significant conclusions of the study and indicates where the supporting analyses are presented. The system specification is included as an appendix.

2. (to be completed in April). Contains all system interface studies.

3. Describes the design of ERTS resulting from the study, to a block diagram level of detail.

4. Presents the detailed results of the study supporting the design in Volume 3, including backup tradeoffs and analyses.

5. Presents both the design of the data collection system and the supporting analyses.

6-12. Present the plans prepared for the ERTS Phase D program on the Phase B/C program.

CONTENTS

CONTENTS (Continued)

CONTENTS (Continued

CONTENTS

1. INTRODUCTION AND SUMMARY

The ERTS observatory is a reliable and versatile system capable of gathering information about the world's natural and cultural resources. It provides room and weight-carrying capability for installing a variety of sensors including specifically a multispectral point scanner, a triplet of return beam vidicon cameras and their associated electronics, a real time data collection system, and a pair of video tape recorders. It includes an attitude control system which provides accurate three-axis stabilization with the horizon and orbit plane as references and an attitude determination capability for refining knowledge of the relative and absolute location of image points. Power for continuous subsystem operation and for 20 minutes of payload operation has been included. Spacecraft monitoring and control and payload data readout can take place using either STADAN or MSFN ground stations.

While a lifetime goal of one year has been established, there is a high probability, 65 percent, that ERTS missions could continue unimpaired for three years. The ERTS design is a logical outgrowth of the OGO program and makes use not only of the technology and design developed but actually incorporates OGO spare parts in many instances. Much of the reliability and flexibility are directly traceable to the OGO program.

OGO assemblies have been retained intact where possible. All of the manual override features of OGO attitude control have been retained, as have the alternate modes of control. In adapting OGO to ERTS, four principles have been consistently applied:

- The highest possible reliability for a first launch must be achieved.
- A useful life of three years is desired.
- Growth capability should be provided.
- Implementation of the design must be possible within a relatively short schedule and low cost.

The simplest acceptable approach to a design problem has been sought. For attitude determination it has been found possible to employ the same

data that guides the spacecraft. For orbit adjustment a highly reliable though somewhat inefficient (in weight) system has been adapted.

Some measures which might have improved performance have been rejected because of cost implications. A more efficient array configuration is possible, for example, but costs for qualification tests are an over-riding deterrent. A smooth array drive during picture taking is technically possible but it is simpler and much less expensive to simply turn off the array drive with the sensor ON signal.

Like OGO, ERTS is a rectangular parallelepiped (Figure 1-1) with one side always facing earth in flight. Like OGO it employs two large solar arrays which are oriented toward the sun on a rotating support shaft. Unlike OGO the ERTS solar array shaft is always aligned with the velocity vector, accomplished by using an OGO gyro package to function as a gyrocompass controlling ERTS in yaw.

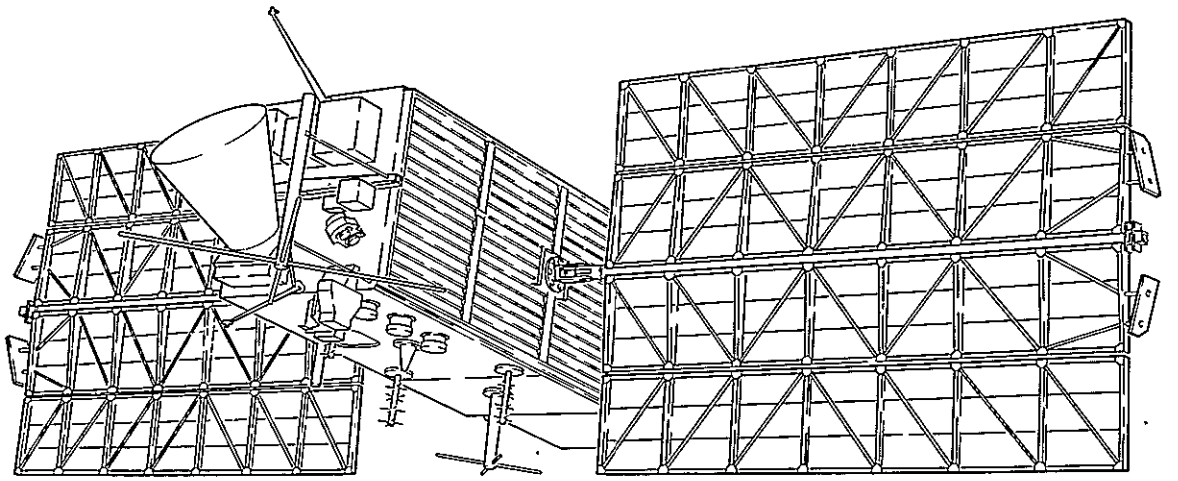

Figure 1-1
ERTS SPACECRAFT CONFIGURATION

The spacecraft folded for launch is dimensionally the same as OGO (Figure 1-2). Array tips are at the OGO positions with respect to the shroud. The tips of the attitude control booms are fixed in position as close to the shroud as possible.

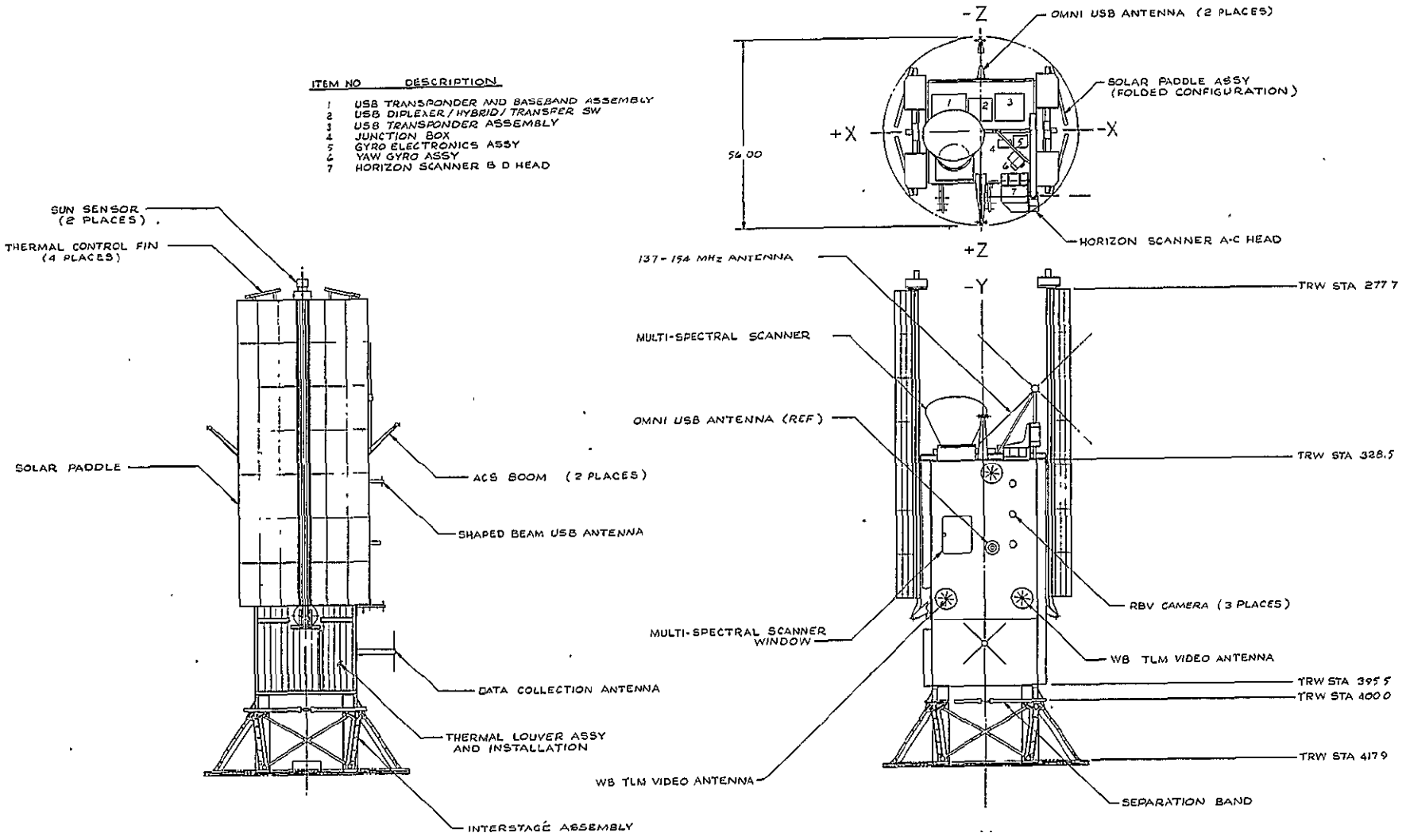

Figure 1-2
ERTS FOLDED FOR LAUNCH

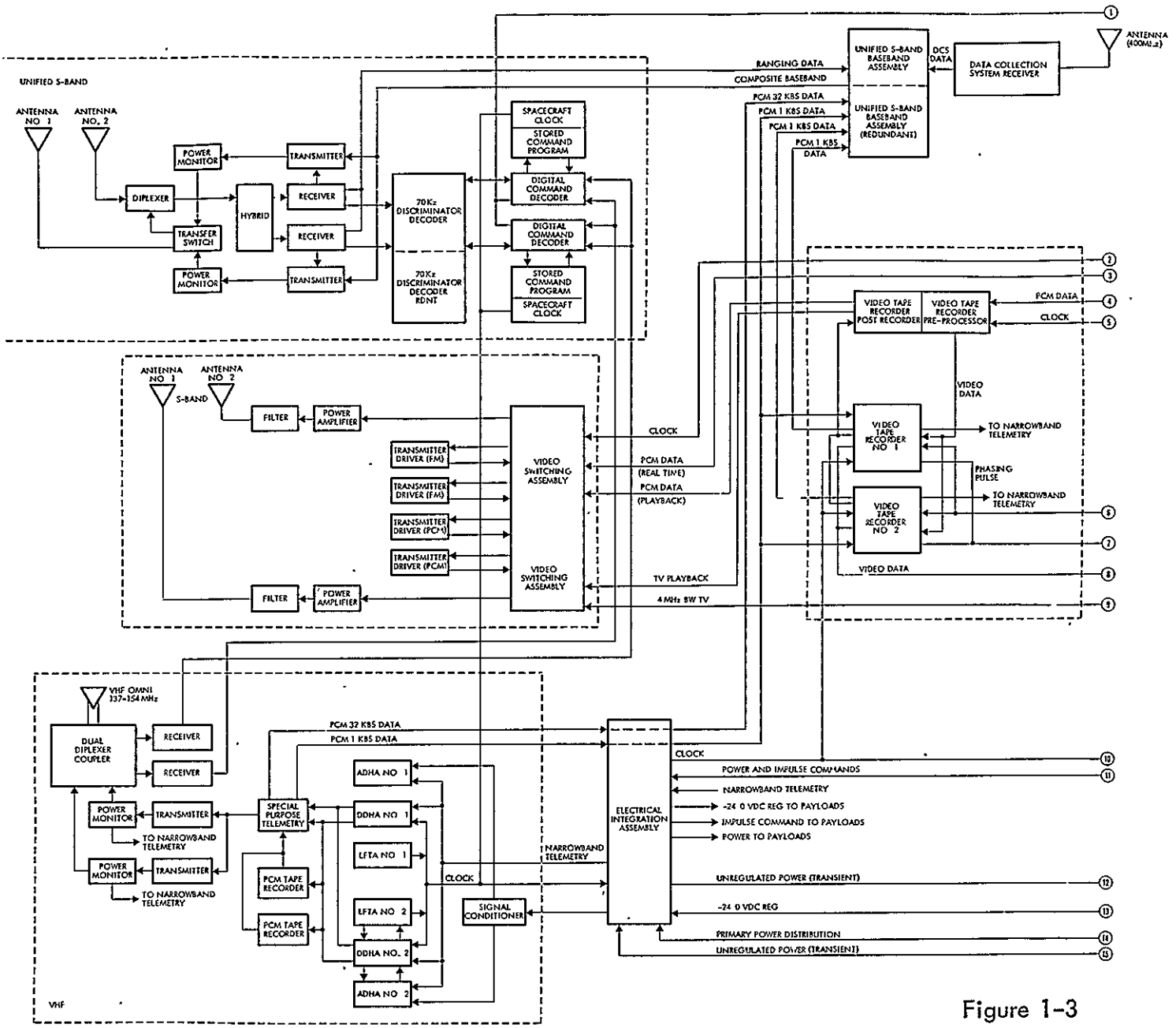

Figure 1-3

Earth pointing information is measured by horizon trackers which continuously track the earth's edge in four directions. Like OGO control of the body and array is by bang-bang servo systems utilizing reaction wheels (three axis) along with gas jets to occasionally unload wheel momentum. In concept the entire attitude control system is little changed from OGO, and most of the equipment employed is identical. The principal performance features of ERTS are given in Table 1-1, and subsystem relationships are shown in Figure 1-3.

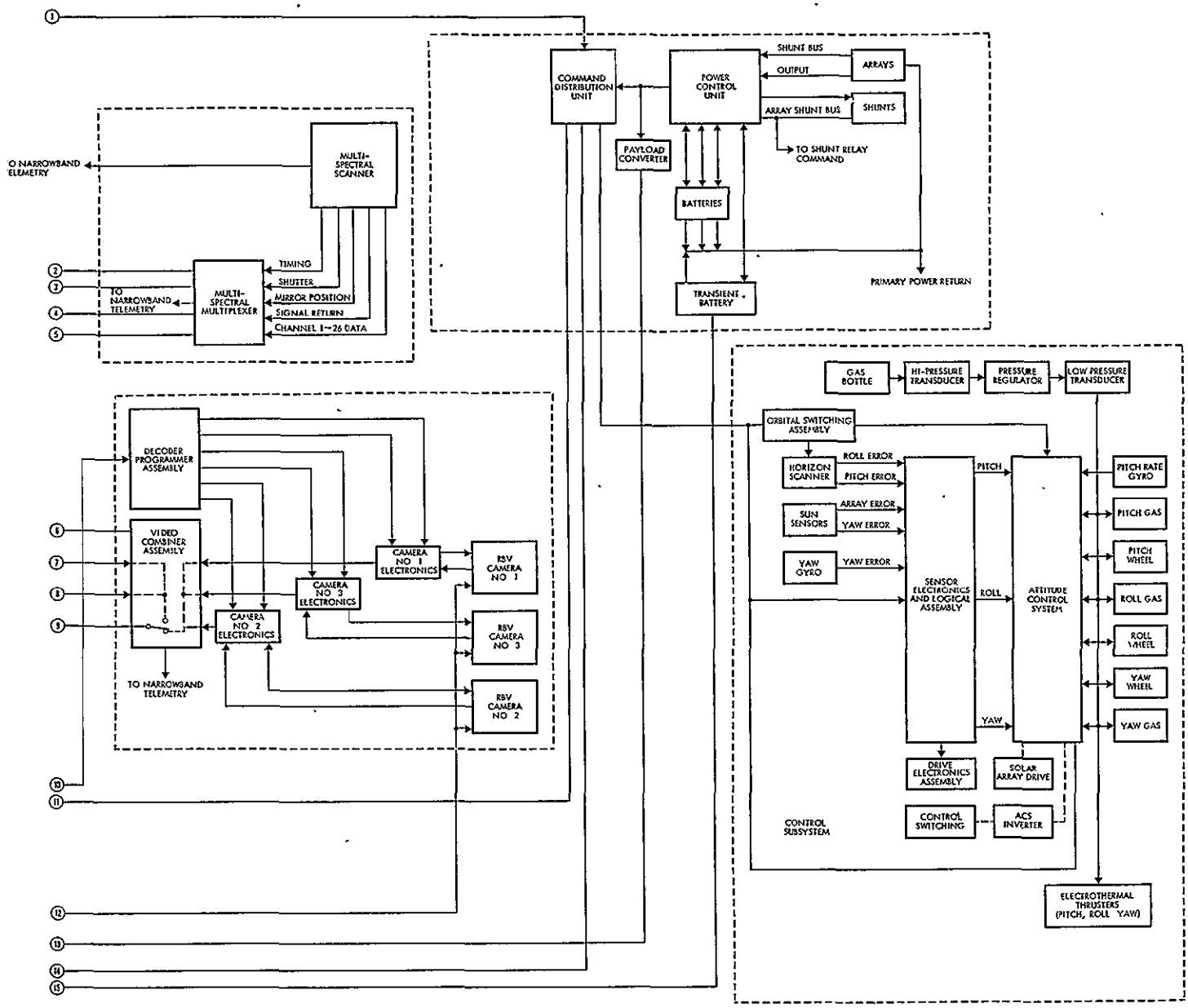

ERTS SYSTEM functional block diagram

The precision orbit for ERTS is achieved with a velocity trim of the spacecraft after release from the Thor-Delta. For this purpose simple thermal thrusters are added to the existing OGO pneumatic system, providing more correction capability than is anticipated to eliminate injection errors.

Thermal control of ERTS is unchanged from OGO except for added aluminized teflon surfaces under the standard thermal louvers. In the

Table 1-1. Key Spacecraft Performance Features

	Desired	Planned
Orbit adjustment, ft/sec	48	70
Payload		
Weight, lb	450	500
Volume, ft^3	12	18
Power load, minutes/orbit	20	>20*
Temperature ^oC	20 ± 10	±10
Life, years	1	>1
Boost vehicle	Thor-Delta	Thor-Delta
Attitude Control		
Earth pointing, pitch, roll, deg	0.7	0.5
Orbit plane pointing, deg	0.7	0.7
Body rates, deg/sec	<0.04	<0.011
Picture element accuracy, naut mile	<2	<2
Commands	256	358
Execute from store	>30	64
Store capacity	>100	127/254
Power margin RF links		
Command, db	>26	23
Telemetry, db	>6	7
Data system, narrowband		
Accuracy, bits	8	8
Sample rate, kilobits/sec	1	1/32
Storage capacity, hours	2	12
One-year reliability	0.7	0.85

*30 minutes for 9:30 am orbit crossing of equator

ERTS orbit, sun shines on each louvered panel briefly during each revolution and a reduced panel absorptivity is needed. Multiple layers of aluminized Mylar generally insulate all body surfaces except the two louvered panels of the array facing sides.

The ERTS solar array is 16 percent larger in area than on OGO (Figure 1-4) achieved by filling in the unused sections of the OGO array; the external dimensions of the array are unchanged. Charge control makes

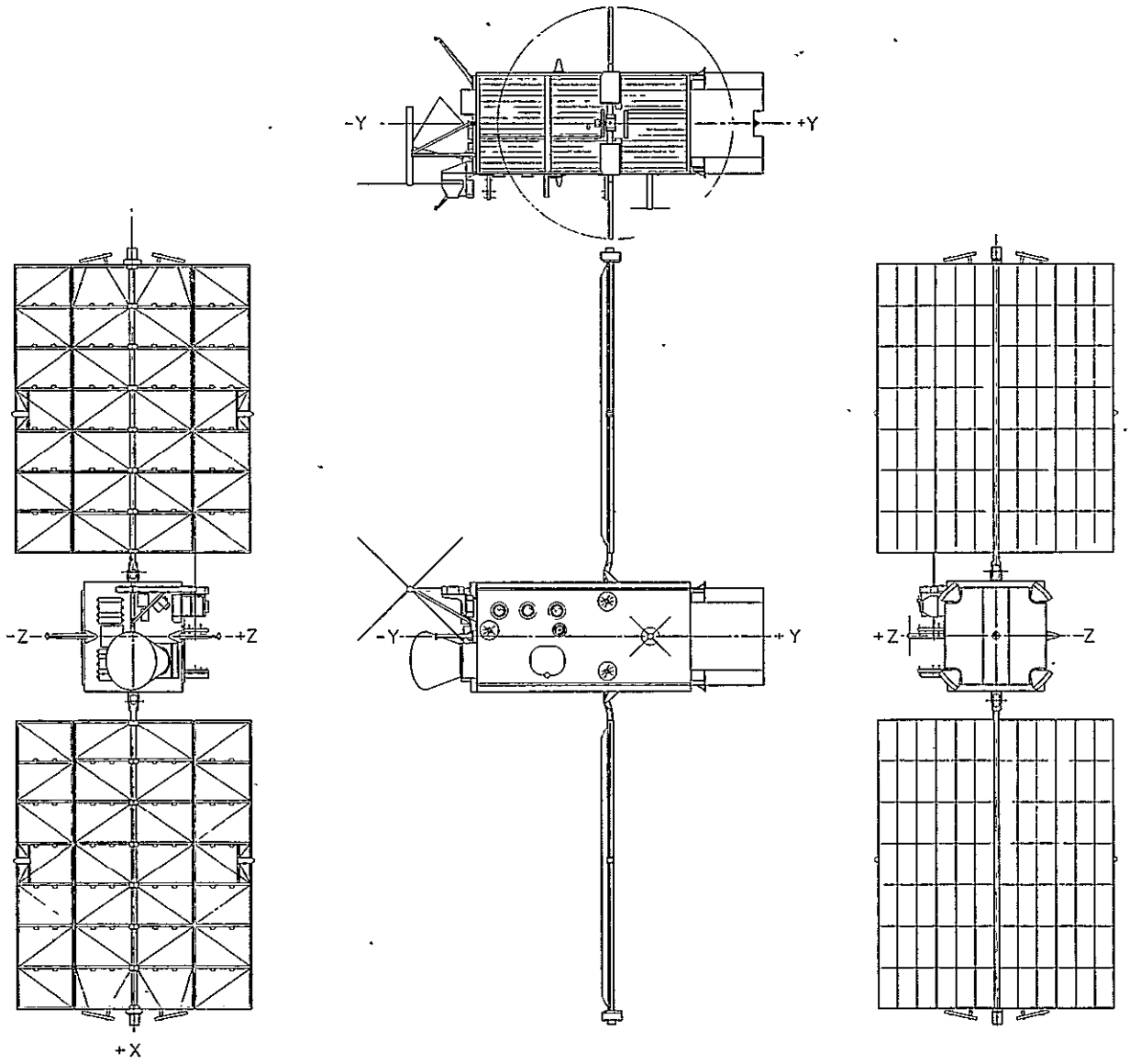

Figure 1-4
ERTS DEPLOYMENT ARRANGEMENT

use of the OGO power control unit, shunting part of the array strings with OGO power transistor thermal fins when power is excessive. Spacecraft voltages are all developed with OGO distributed converters. Regulated -24 volts for the ERTS payload is supplied from a new high-power converter. Power available for payload operation varies with time of year and launch and is shown on Figure 1-5.

Communication functions of ERTS are more diverse than on OGO in that sensor data transmitted is extremely high rate and telemetry and command communication is quad-redundant. Six transmitters and four

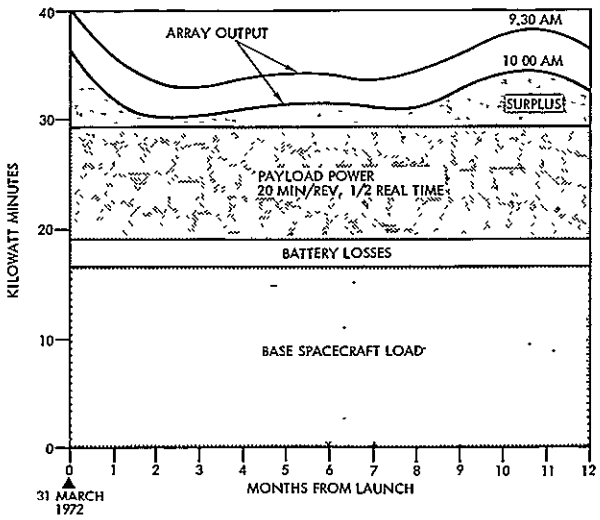

Figure 1-5
ELECTRICAL POWER during first year of operation

receivers are employed. Four links are S band and four are VHF. Two 10/20 watt S band video transmitters relay sensor video data while a redundant pair of 0.5-watt unified S-band transponders accomplish tracking, command, and telemetry functions. STADAN-compatible equipment performs these same three functions at VHF.

The volume and variety of command and telemetry required for the ERTS mission is not far short of the final OGO requirements. Almost the entire command decoding and distribution system of OGO is retained in ERTS. OGO telemetry formatting and handling equipment is retained intact in ERTS as are the command receiver and decoders. A new ERTS need for stored, delayed-execution commands is provided by a stored command programmer. The OGO digital tape recorders are used at half speed to store narrowband telemetry data for delayed transmission.

Table 1-2 summarizes the specific performance requirements of Study Specification S-701-P-3 and the performance of the observatory described here.

Table 1-2. Summary of Specified and Actual Spacecraft Performance

S-701-P-3 Paragraph	Requirement	Performance Achieved
6.1a	Sun synchronous orbit 9:30 +30 min -0 node crossing	Power system provides 20 minute operation at year end with 30-minute launch slip
6.1b	Correct injection errors	Orbit adjust system will correct all 3σ injection errors.
	Adjust sensor swath sidelap	Full adjustment provided
6.1c	Control attitude to local vertical and velocity vector	This is done
6.1d	Orbit sidelap 10 percent	ΔV system can adjust as accurately as orbit can be measured
6.1e	Swath coincident to ±10 n mi at 18-day intervals	ΔV system can adjust as accurately as orbit can be measured
7.1a	Payload weight at least 450 pounds	Structure can accommodate 495 pounds above current spacecraft weight
7.1b	Volume minimum 12 cubic ft for payload	Payload volume is now about 18 cubic feet
7.1c	Earth viewing area to be 125 percent of initial sensor requirements	Feasible by redistributing assemblies
7.1d	Area for MSS space-looking cooler	Is accommodated in current design
7.2	Minimum life, 1 year	Expendables sized for 3 years; wear out designs 1 year or more
7.3	Predict misalignments	Initial alignment by shim to 0.1 deg, measured to 0.01 deg
		Thermal shift less than 0.007 deg
7.4	Recommend a launch vehicle	Thor-Delta is acceptable. Adaptation costs are truly minor. No known performance incompatibility
7.4.1	State principal moments of inertia	I_{xx} 210 slug ft^2 I_{yy} 250 slug ft^2 I_{zz} 390 slug ft^2
	State cross products of inertia	Less than 7.5 slug ft^2
	Plot allowable uncompensated momentum and moment from 0 to 100 Hz	See Section 1, Vol. 4
7.5	Pointing error less than	Spacecraft design provides
	Pitch 0.7 deg	0.5 deg
	Roll 0.7 deg	0.5 deg
	Yaw 0.7 deg	0.7 deg
	Body rates less than	Spacecraft design provides
	Pitch 0.04 deg/sec	<0.011 deg/sec
	Roll 0.04 deg/sec	<0.008 deg/sec
	Yaw 0.04 deg/sec	<0.011 deg/sec

Table 1-2. Summary of Specified and Actual Spacecraft Performance (Continued)

S-701-P-3 Paragraph	Requirement	Performance Achieved
7.5.1	Demonstrate can null initial rates	Demonstrated in orbit with OGO. Design remains the same
	Reacquire four times	Done many times with OGO spacecraft
	Show ΔV compatible with attitude control	No spacecraft maneuvers required, yaw gas must be turned on by ΔV command, fully compatible
	Locate picture elements to ±2 n mi	±2 n mi is feasible
	Goal for location accuracy one-resolution element	About 1000 ft is feasible with ground truth, etc.
7.6.1	Dual uplink 154 and 2106.4 MHz 256 commands	This is provided Provides 358 commands
7.6.1.1	Execute 30 different commands from store	64 provided
	100 executions Override stored command Verify store Reliable address	127 provided (254 in the two stores) Real-time override Does that 7-bit address
7.6.1.2	Command reliability	All critical commands require arming. Shut off timers on loads over 1 ampere
	Command System Redundancy	Fully redundant throughout
7.6.1.3	Command RF power margin*	
	STADAN >26 db USB >26 db	17.6 db 34.3 db
7.6.2	Narrowband telemetry	
	136-138 MHz transmitter 2287.5 MHz transmitter 8-bit accuracy	Provided Provided Provided
	Transmission rate 1 kbit/sec Storage at 1 kbit/sec or less	1 kbit/sec or 32 kbit/sec 1 kbit/sec
	Playback 32 kbit/sec or less Simultaneous RT and PB over USB Link margin for bit error; $1/10^6$	32 kbit/sec Provided
	VHF Link* USB Link*	17.7 db 4.5 db [2.6 db 32 kbit/sec; 4.3 db 32 kbit/sec]
7.6.3	Wideband telemetry	
	2 carriers about 2265 MHz Real time and video playback simultaneously Commandable 20 watt mode Link power budget at 10 watts	Carriers at 2230 and 2265 MHz Provided Provides 10 and 20 watt modes
	30-ft dish S/N ratio** 85-ft dish S/N ratio**	Provides 38.7 db RBV, 4.4*** db MSS Provides 43.7 db RBV, 8.9*** db MSS
	Cross strapping	4 drivers. See Section 9.4

Table 1-2. Summary of Specified and Actual Spacecraft Performance (Continued)

S-701-P-3 Paragraph	Requirement	Performance Achieved
7.6.4	Tracking	
	Beacon carrier: 136-138 MHz	137.86 MHz
	USB transponder compatible MSFN	Provided
	Beacon on continuously	Provided
	Redundant transmitters	
	VHF	2 provided
	USB	2 provided
7.6.5	Data Storage	
	Video units GFE	All provisions made
	Narrowband	
	Existing space qualified unit	OGO unit is used
	Capacity >2 orbits data	7 orbits/2 recorders
	Playback/record ratio >20/1	32/1
7.6.6	Timing	
	Common clock for PCM, (command and wideband systems)	Provided
	Timing signals	
	Pulse trains as Attach. I, II, II	All provided
	Coded clock	Binary, 1.152 sec
	Update known to 1-bit time of PCM	Provided
	Clock reset	Not provided
7.7	Power	
	20 minutes payload power/revolution	Provided
	50% RT, 50% PB	Provided
	Seasonal sun line variations	Provided
7.8	Thermal	
	Payload Environment 20 ± 10°C	Provided
7.9.1	Orbit adjust	
	Eccentricity less than 0.006	<0.001 provided
	Swath overlap ~10%	Provided
	Westward progression	Booster provides
	18-day swath coincidence <±10 miles	≪10 miles
	Estimate injection residuals	~39 ft/sec 3σ
	Specify operation use	See Section 10
	Verify orbit	
	Altitude 496 n mi	492.6 n mi
	Inclination 99.04 deg	99.085 deg
	Predict	
	Orbit parameter variation/year	100 ft altitude/year
	Need for orbit trim after ΔV	0.007 ft/sec/year****
	Tradeoff size ΔV system versus drift	Zero drift is easy

*Above 6 db system margin.

**p-p signal/rms noise; above 6 db margin

***Margin above BER 1×10^{-6} and above 6 db system margin

****TRW recommends this trim be accomplished but it is left to user discretion

CONTENTS

2. STRUCTURE

The ERTS structure supports the various subsystems and payload members. It includes the following major assemblies:

- Basic frame. Supports the payload members and spacecraft subsystems
- Solar array assembly. Supports the solar cell modules, charge controls, sun sensors, drive mechanism and related electrical equipment
- Miscellaneous appendages. Supports antennas and attitude control thrusters
- Interstage. Supports the entire observatory during launch and permits separation from the Thor Delta N after injection

2.1 BASIC FRAME

The basic frame taken from OGO is a parallelepiped of approximately 31 x 32 x 67 inches (see Figure 2-1). All primary structural elements are constructed of aluminum alloy. Four 7075-T6 aluminum alloy extrusions form the longitudinal edge members (longerons) of this box to which 5/8-inch thick aluminum core honeycomb panels with aluminum face sheets are attached. These panels form the sides of the box and are referred to as the X (horizon facing) and Z (nadir and zenith facing) panels. The Z panels are hinged to provide equipment access. In contrast to OGO the X panels extend 23 inches beyond the longerons at the +Y end. Additional Z doors are also provided at this end to form a compartment for holding the video tape recorders and their associated electronics assemblies. Figure 2-2 illustrates equipment placement in the ERTS structure.

All requirements concerning volume, weight, and earth-viewing area for payload members are met with the proposed structure. Accommodation of the MSS with its radiative cooler for ERTS-B is illustrated in Figure 2-3. The same figure indicates the earth viewing area provided for the MSS and the RBV's.

All of the sensors are mounted directly to the basic structure of the spacecraft. These members are extremely rigid and experience less

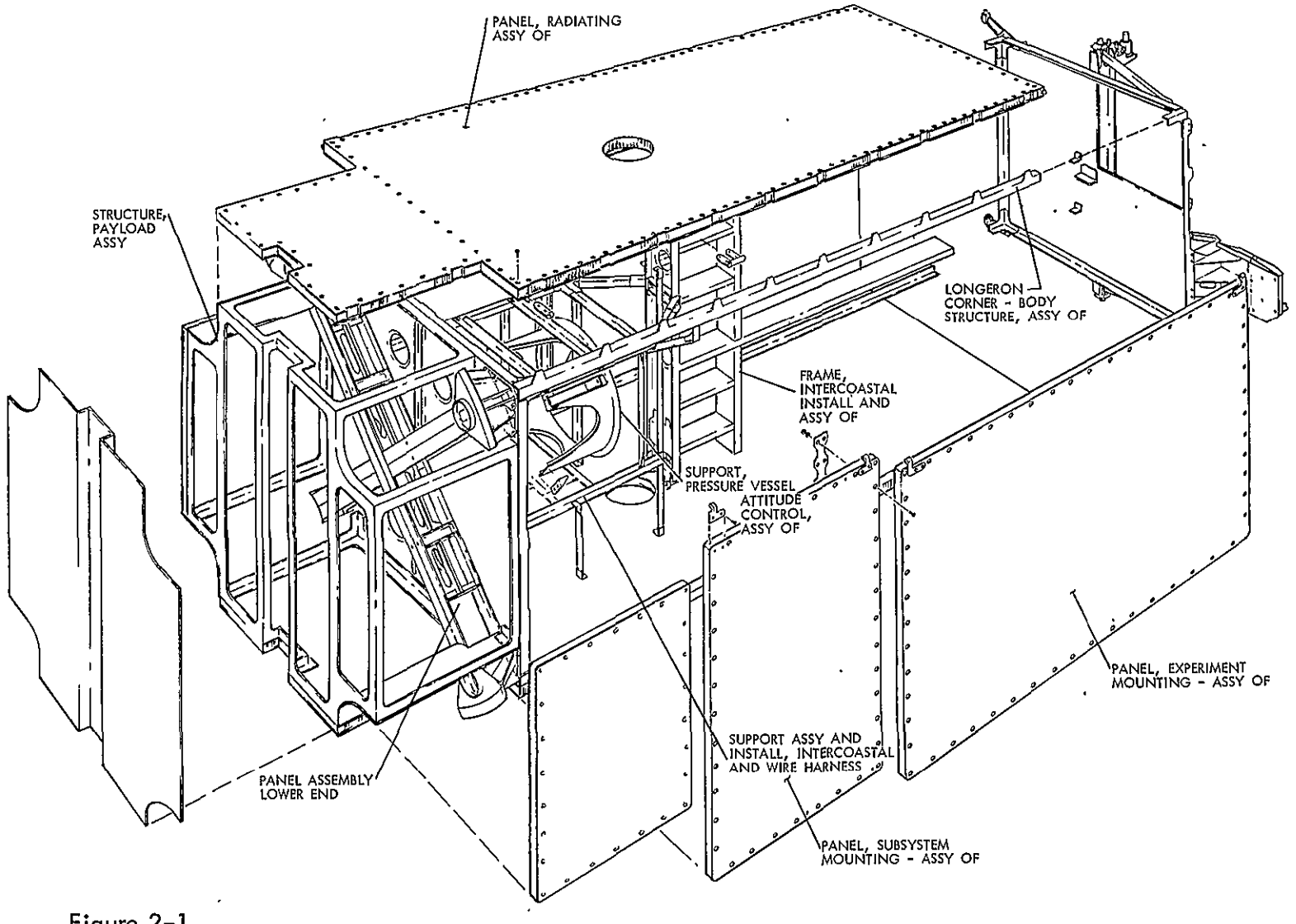

Figure 2-1

THE ERTS MAIN BODY is identical to that of OGO except that honeycomb panels (such as those used on OGO 5 and 6) are substituted for the corrugated core sandwich panels to improve panel stiffness.

PRECEDING PAGE BLANK NOT FILMED.

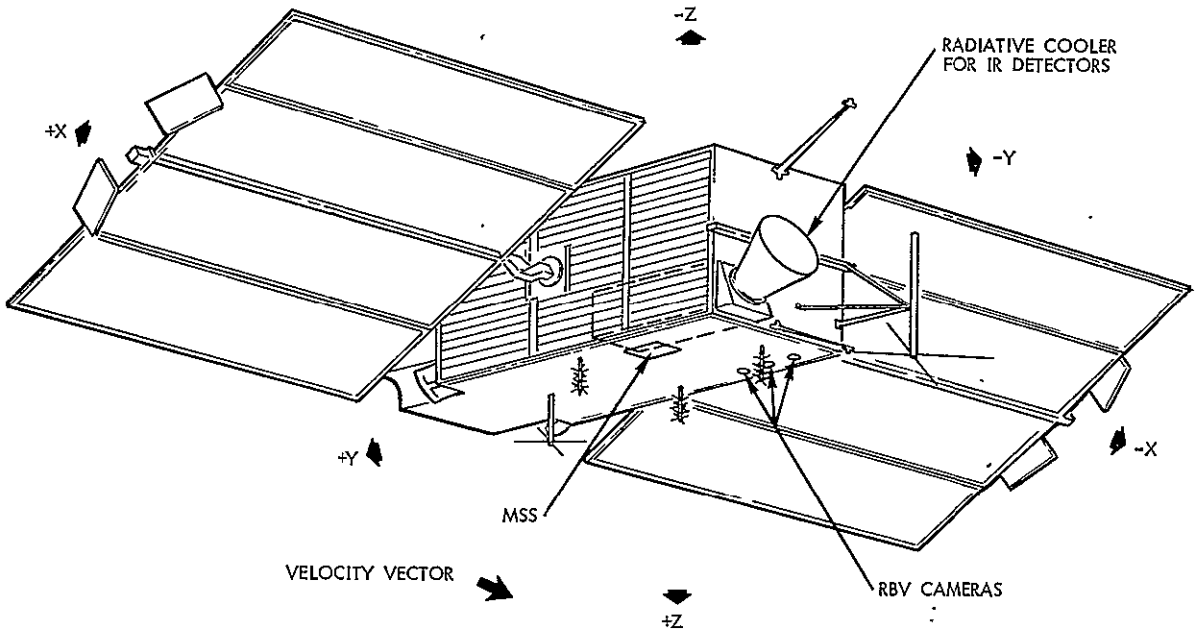

Figure 2-3

RADIATIVELY COOLED MSS is readily accommodated in OGO, which contains more than 18 ft^3 of unassigned volume for payload with easy access to the radiating panels and earth-viewing face.

thermal deformation than the panels. The horizon scanner heads are mounted on a special bracket which is designed to reduce thermal gradients and maintain alignment between the heads and the spacecraft structure (Figure 2-4). The RBV cameras are mounted on a thermally stable platform which is, in turn, mounted to the basic ERTS structure. The MSS is attached directly to the basic structure close to the attitude sensors. The yaw gyro is mounted behind the horizon scanner bracket close to the basic structural elements and the payload sensors. Alignment uncertainty between these units can be held to less than 0.1 degree. The uncertainty results from thermal deformation of the mounting brackets and basic structure, launch vibration, and structural relaxation in changing from a 1-g to a 0-g field. Compensation for the latter is possible.

Four 356-T6 aluminum alloy castings are attached to the aft end of the spacecraft body, one at each corner in line with the longerons, and are utilized to transmit all primary loads to the interstage structure.

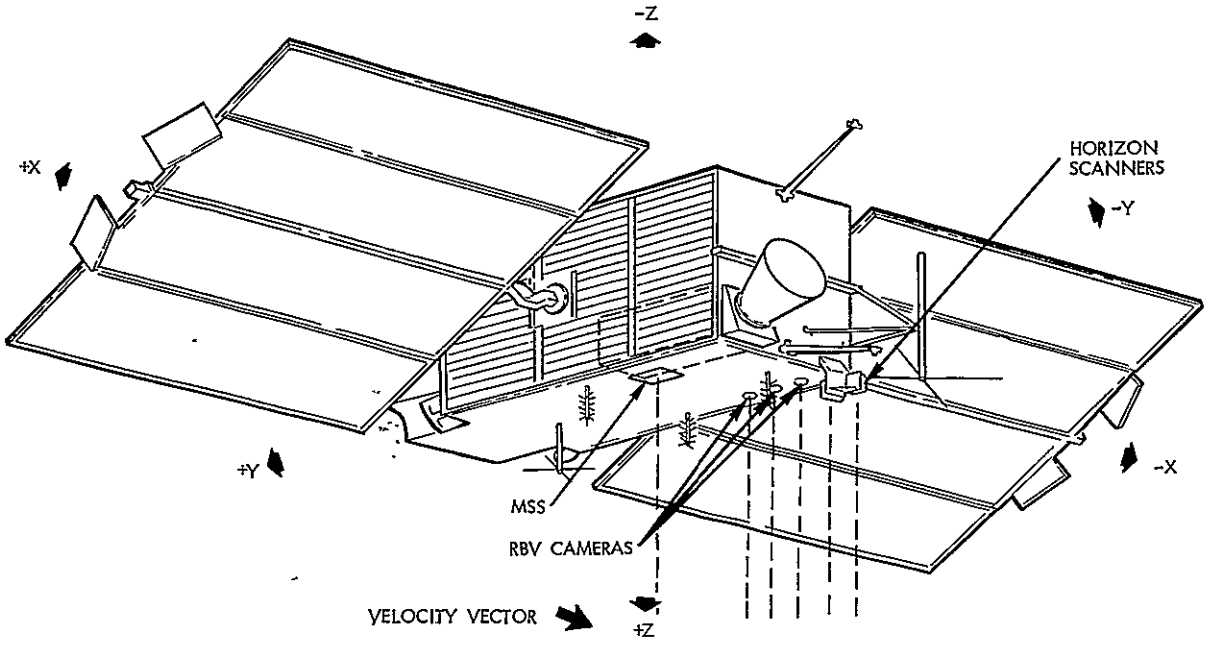

Figure 2-4

SENSOR AND HORIZON SCANNER ALIGNMENT is based on precision orthogonality between the two dual-tracker assemblies by ground alignment of each tracker to the precisely machined mounting bracket. Attachment is straightforward since payload alignment does not rely on spacecraft references.

These corner fittings are attached in plane to 7075-T6 diagonal beams which are designed to react the separation band preload and "kick" load induced by the interstage truss structure. Subsystem assemblies are supported also by an internal 2024-T42 aluminum alloy sheet metal assembly, referred to as the intercostal, which is attached at either edge to the radiating panels. Located at the forward end of the body assembly are four machined aluminum "bathtub" fittings which serve to react hoisting loads and for attaching the roll rings.

2.2 INTERSTAGE

The machined 7075-T6 aluminum alloy interstage truss structure provides an efficient load path between OGO and the Delta. It consists of four bipod legs designed to carry the major loading axially in each leg element (Figure 2-5). To provide margin over OGO, the interstage is cross braced to reduce interstage warping under lateral loads, and

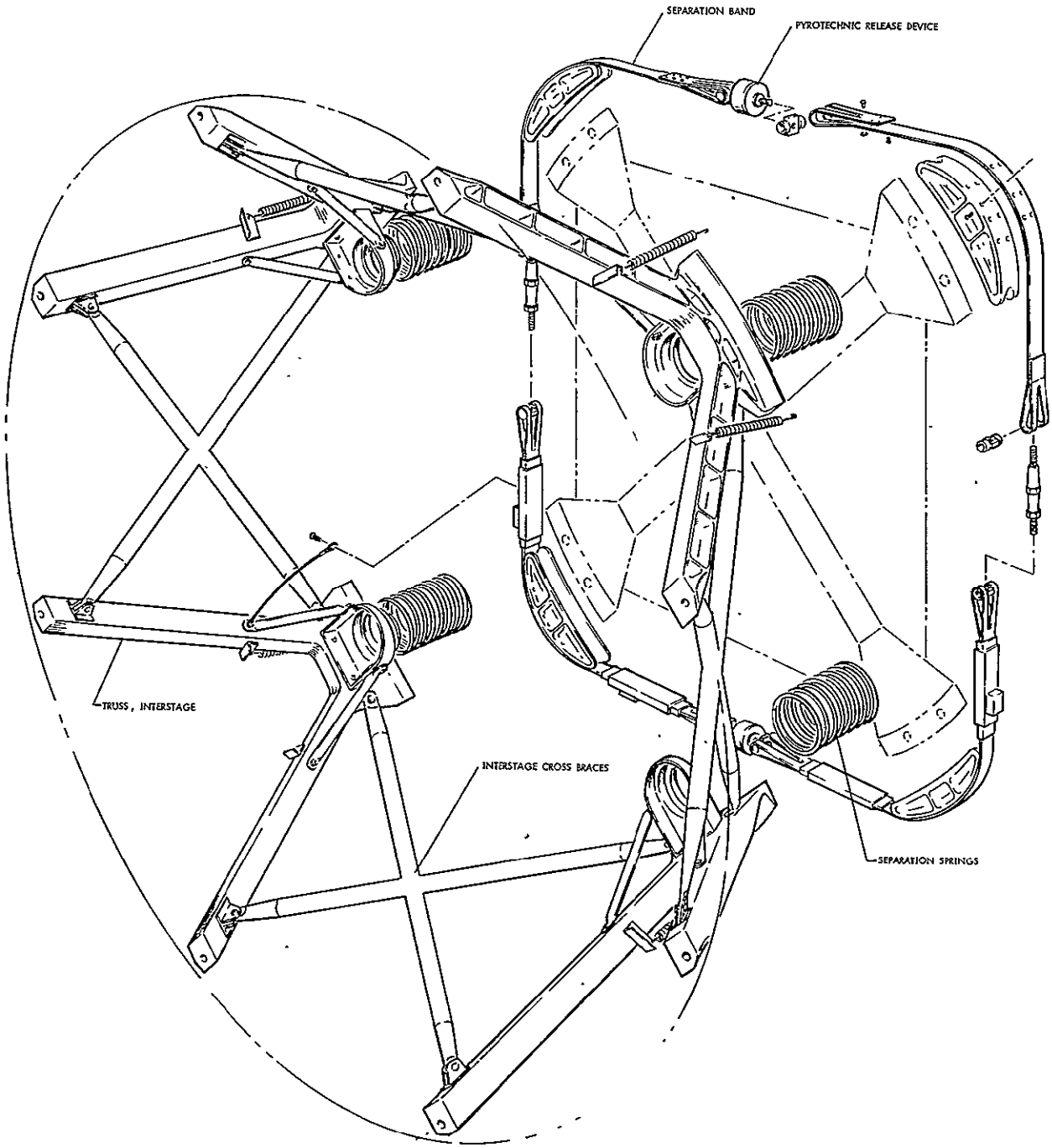

Figure 2-5

INTERSTAGE AND SEPARATION SYSTEM is modified slightly from OGO's to support the increased forward and side loads.

the bipod wall thickness is increased to support longitudinal loading in the ERTS environment. The bipod elements accommodate a beam-column loading which results from the combination of the primary axial load and the bending moment induced by the compressed separation springs. The vertical load is reacted equally in each of the four bipods Horizontal "kick" loads are produced by the in-plane bipod reactions; however, these loads are reacted by the diagonal beams attached to the aft end of the spacecraft body structure. At separation, the vertical load produced by the separation springs is reacted in similar fashion, i.e., the "kick" loads are reacted by the truss members which connect adjacent bipods on the sides of the spacecraft. The bipod legs attach to the Delta through an adaptor ring which is only slightly different thant the one used with Agena in attaching OGO.

The lateral load, which is applied near the spacecraft center of gravity, is beamed to the spacecraft/interstage separation plane. The beamed loads can then be carried as axial loads in the bipod elements.

The observatory is secured to the interstage assembly by a 7075-T6 aluminum alloy segmented V-type clamp assembly which is thicker than its OGO counterpart (Figure 2-5). This assembly is jointed by two redundant explosive actuated release assemblies.

2.3 SOLAR ARRAY

Figure 2-6 portrays details of the array structure. Largely the same as OGO, the array has the same outside dimensions but will mount solar modules at the in-board corners (cut out in OGO and at the holes provided in OGO for the solar-oriented experiment packages.

The solar paddles, each of which supports solar cell modules, a sun sensor, and charge controls, are constructed basically of 2024 aluminum alloy. The substrate of the solar cell module is a 13 x 5.9 x 0.041-inch plate of beryllium with a beryllium stud brazed at each of the four corners. The main spar of the solar paddle is an extruded square tube of 2024-T42 aluminum alloy which is bolted to a typical hinge assembly at its in-board end. The hinge assembly of each paddle

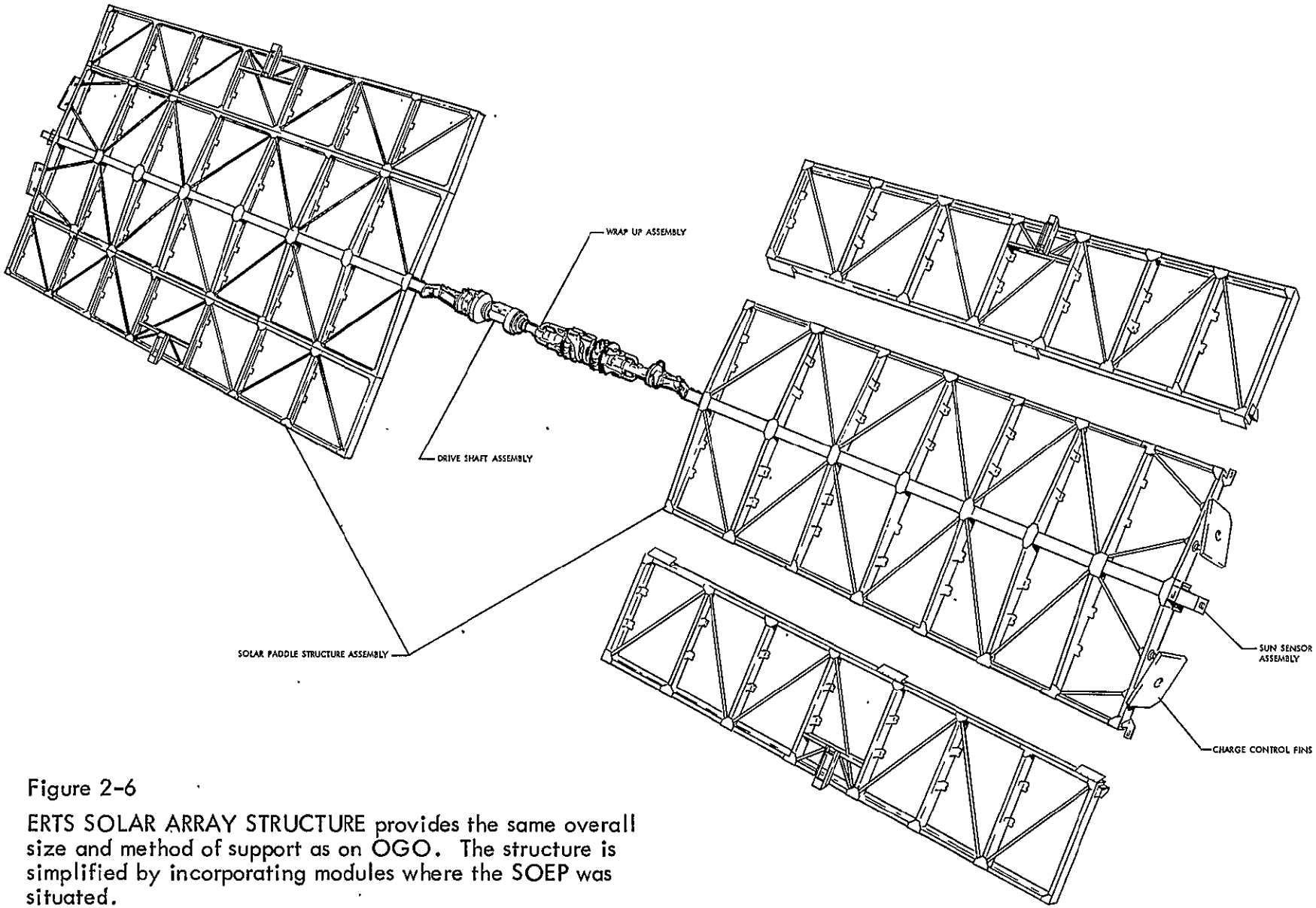

Figure 2-6

ERTS SOLAR ARRAY STRUCTURE provides the same overall size and method of support as on OGO. The structure is simplified by incorporating modules where the SOEP was situated.

is bolted to the solar array shaft (Figure 2-7) which in turn is supported by Elgiloy compression springs contained within a fitting which is bolted to the +X and -X spacecraft honeycomb panels. The two outer panels of each paddle are folded over the main panel and secured to the spacecraft body assembly with a single release yoke assembly. The release system is shown in Figure 2-8. An explosive valve initiates deployment of the solar array. Additional impulse is also provided by a spring-loaded kick-off mechanism. The stroke of the kick-off mechanism is of sufficient length to insure that the release yoke clears the release mechanism. Telemetry is provided by a microswitch at the beginning and completion of the array deployment.

2.4 APPENDAGES

ERTS, in contrast to OGO which had 13 deployable appendages, has only the solar array described in the previous section. There are, however, two fixed booms which provide lever arms for the attitude control thrusters and a fixed structure extended from the body for the VHF antenna. The thruster booms though shorter than those on OGO and not hinged at the base are essentially the same. The VHF antenna support structure is new, replacing a deployable boom on OGO.

2.5 MASS PROPERTIES

Total observatory weight now rests at 1433 pounds for ERTS-A and 1448 pounds for ERTS-B, an increase of 144 pounds over that in June 1969. Payload weight increase was 51.8 pounds. A compartment was added to the main structure to house the video tape recorder which added 23.2 pounds to the structure weight, a 24-volt battery was added to the power subsystem to provide power for the RBV shutters (4.3 pounds), an additional 12 modules were added to each solar paddle to offset the increased power loss caused by the additional shadow effects resulting from the video tape recorder enclosure (13.0 pounds), and the unified S-band communication system was added (33.2 pounds) to make the communication system compatible with the MSFN.

The current weight and other mass properties data (Table 2-1) do not reflect a contingency. Satellite mass properties are presented by mission event for both configurations in Table 2-2. The moments of

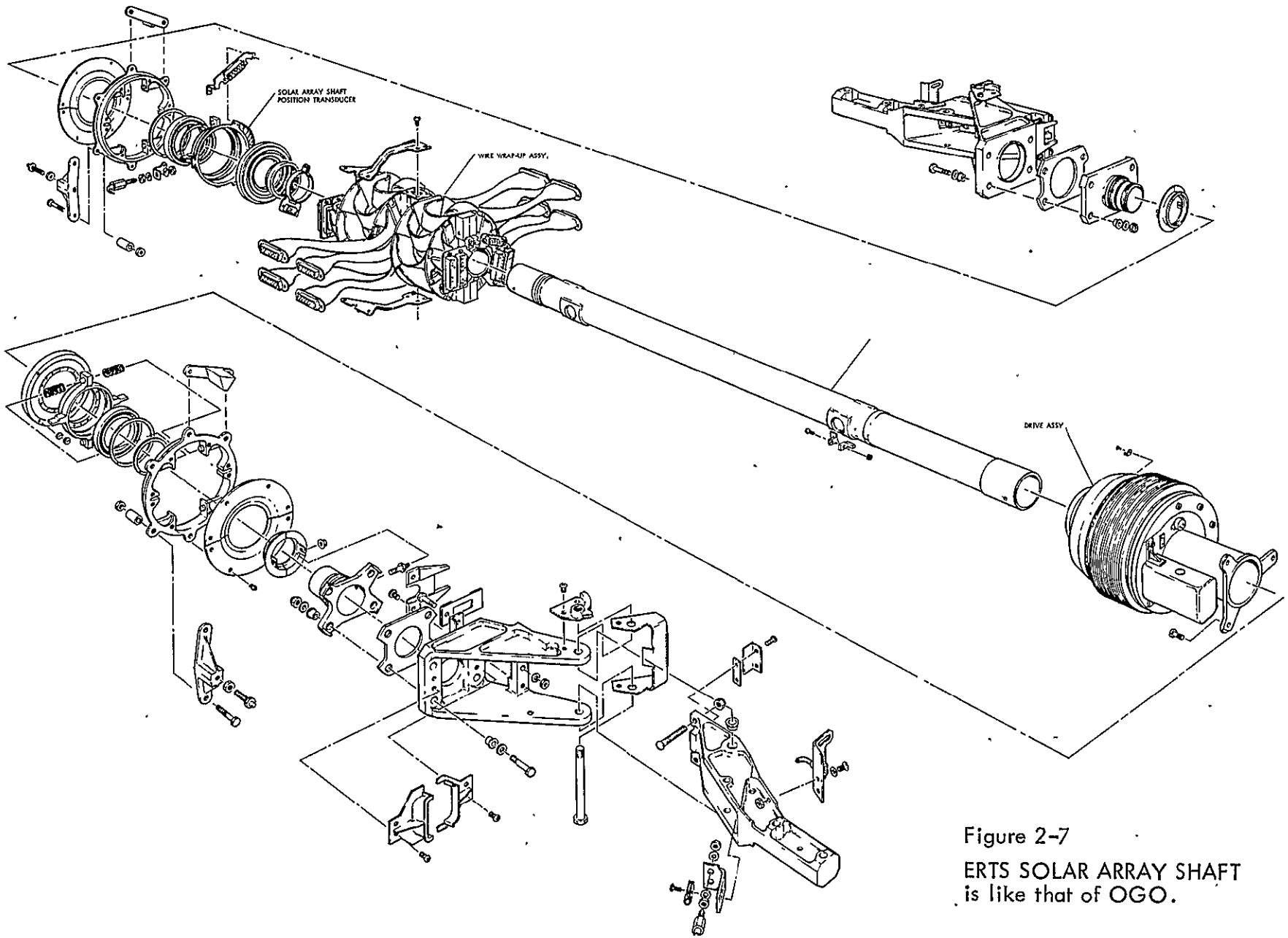

Figure 2-7
ERTS SOLAR ARRAY SHAFT is like that of OGO.

Figure 2-8

ERTS ARRAY RELEASE SYSTEM is unchanged from OGO. Only one deployment sequence is needed, and additional elements can be added if desirable.

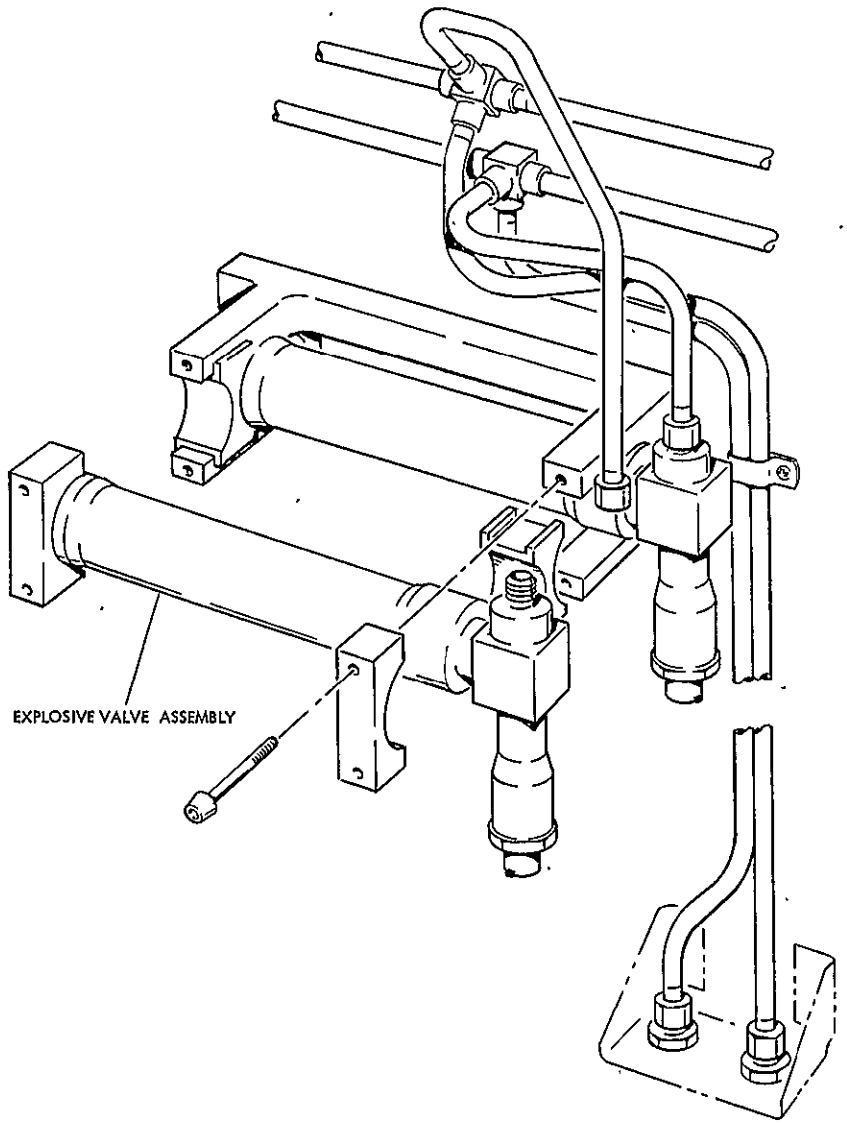

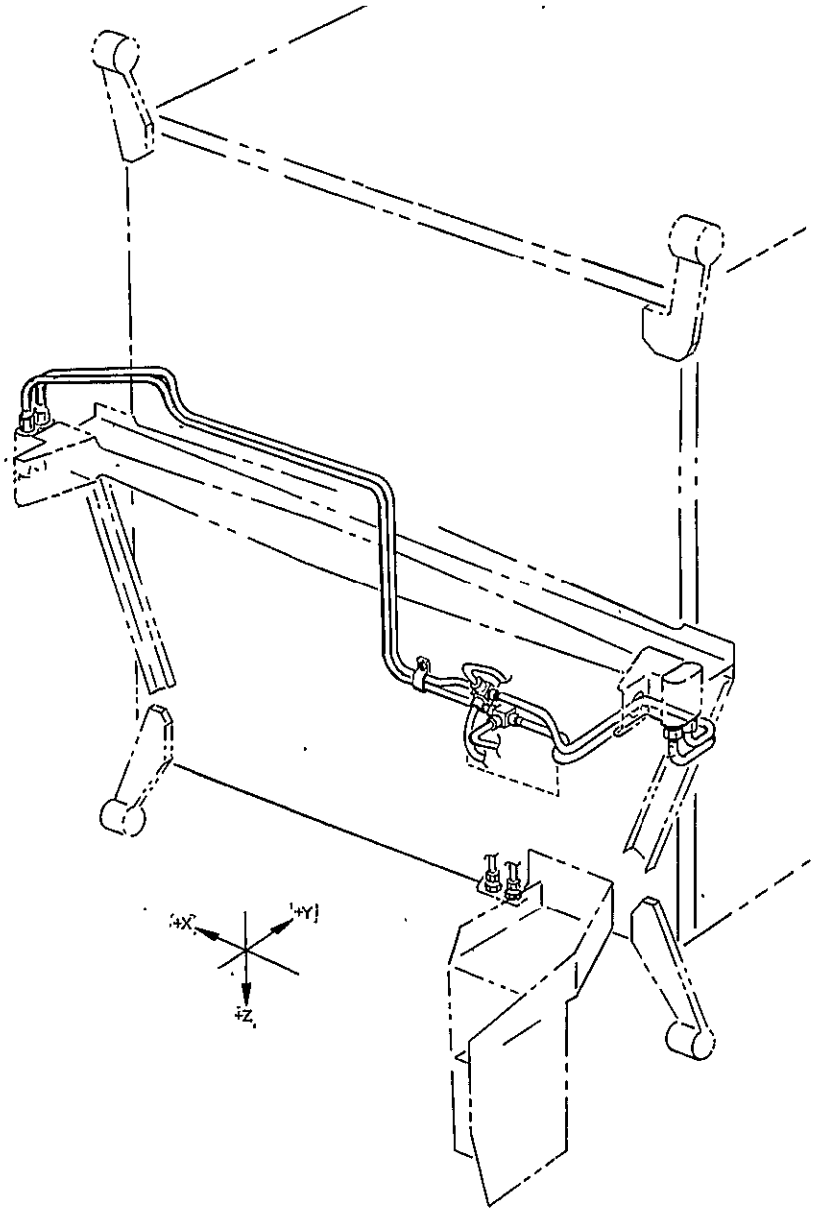

Table 2-1. Detailed Weight Breakdown for ERTS

	Current Status Weight (lb)		
Structure and Temperature Control			175.4
Main box structure		105.0	
Forward end panel	5.5		
Aft end panel	13.5		
Experiment panels (upper) (2)	20.0		
Experiment panels (lower) (2)	12.0		
Radiating panels (2)	25.0		
Intercostal	7.4		
Longerons (4)	4.4		
Miscellaneous structure	8.0		
Interstage attach fittings (4)	8.2		
Interstage release mechanism	1.0		
Temperature control		26.5	
Forward panel insulation	1.5		
Aft panel insulation	1.0		
Experiment panel insulation	6.0		
Louver system	16.0		
Thermal paint	0.5		
Reflector surface	1.5		
Booms and support structure		20.7	
Nozzle booms (2)	2 7		
Antenna supports (4)	3.0		
Horizon scanner support	5.5		
Appendage release system	9.5		
Video tape recorder enclosure		23.2	
Attitude Control System			209 1
Electronics and drive mechanisms		97.7	
Yaw gyro unit (1)	3.0		
Gyro electronics unit (1)	1.6		
Horizon scanner electronics	6.8		
Horizon scanner heads (2)	8.8		
Sun sensors (2)	-2.0		
Sensor electronics and logic	11.7		
Z-reaction wheel (1)	9.9		
X-reaction wheel (1)	4.9		
Y-reaction wheel (1)	4.9		
Attitude control unit	12.0		
Attitude control inverter	8.8		
Array drive mechanism	5.3		
Solar array drive electronics	7.5		
Rate gyro unit	1.4		
Control switching assembly	4.2		
Orbital switching	4.4		
Solar array shaft transducer	0.5		
Pneumatic system		98 9	
Pressure vessel (OGO 6 type)	27.4		
Pressure vessel support	3.8		
Nozzles, valves, plumbing	6.2		
Krypton gas (4000 psi)	57.0		
Thermal thruster system nozzles, heaters lines, and hardware	4.5		
Solar array shaft and mounting provisions		12.5	
Solar array shaft installation	10.5		
Subassembly mounting hardware	1.0		
Reaction wheel mounting	1.0		
Power Supply			234.5
Solar arrays (beryllium substrates)		118.0	
Solar array (+X paddle)	59.0		
Solar array (-X paddle)	59.0		
Battery packs (2)		62.0	
Battery, 24 volt		4.3	
Charge control units (4)		8.0	

Table 2-1. Detailed Weight Breakdown for ERTS (Continued)

	Current Status Weight (lb)		
Converters		41.2	
Converter No. 2 (2)	3.4		
Converter No. 5	2.0		
Converter No. 6	2.0		
Converter No. 7	0.7		
Converter No. 8	0.7		
Converter No. 9	2.4		
Converter (experiment bus) 24.5 volt	16.0		
Power control unit	14.0		
Subsystem mounting provisions		1.0	
Electrical Integration			146.5
Command distribution unit		23.0	
Junction boxes		9.8	
Central J-box 3A5	4.6		
Junction box 3A7	5.0		
Junction box 3A13	0.2		
Momentum control unit		1.1	
Payload integration assembly		27.5	
Subsystem harnesses		84.1	
Attitude control harness No. 1	7.5		
Power and communication (harness Nos. 2, 12, 13, 14, 15, 18, 19, 24, 29, 30, 37)	25.0		
Harness No. 3	11.0		
RF harness No. 4 (S-band cabling)	3.0		
Harness No. 5	1.0		
Horizon scanner harnesses No. 9	3.1		
Solar array rotating harness Nos. 10, 11, 26	2.4		
Harness Nos. 7, 8, 20 (yaw gyros)	3.0		
Analog commutator harness No. 23	7.0		
Deploy antenna harness No. 31	0.2		
Solar array power harnesses	8.0		
Interstage harnesses Nos. 1, 3, 36	2.7		
Harness No. 41	3.0		
Solar array wrap-up	2.6		
Ordnance jumper No. 25	0.2		
Solar array deployment harnesses	0.1		
Range and range rate antenna cables	0.3		
Cable clamps, mounting hardware, etc.	2.0		
Subsystem mounting provisions		1.0	
Communications and Data Handling			209.1
Communications		100.7	
Unified S-band transponder assembly (2)	20.6		
Unified S-band baseband assembly	2.5		
Command receiver (2)	3.2		
Diplexer coupler	2.5		
Digital decoder (2)	10.4		
Transmitter (137 MHz, 0.5 watt) (2)	3.0		
Antenna (Unified S-band omni) (2)	1.2		
Antenna (Unified S-band shaped beam)	0.6		
Unified S-band diplexer, hybrid/transfer switch	3.5		
Special purpose telemetry	0.6		
Power monitors (2 watt) (2)	0.6		
Transmitter driver (4)	10.0		
Antenna, video (wideband telemetry) (2)	1.2		
TWT power amplifier	19.5		
Stored command programmer/clock (2)	15.0		
Data collection system receiver	2.5		
Antenna (137 to 154 MHz)	1.8		
Reject filter (wideband) (2)	2.0		
Data handling		107.4	
Analog data handling units (2)	16.0		
Digital data handling units (2)	35.0		
Signal conditioner	1.1		

Table 2-1. Detailed Weight Breakdown for ERTS (Continued)

	Current Status Weight (lb)		
Low frequency timing unit (2)	14.6		
Tape recorder transports (2)	22.8		
Channel switching assembly	3.0		
Digital integration unit	2.5		
Subsystem mounting provisions		1.0	
Interstage and Separation System			23.0
Interstage structure		23.0	
Total ERTS Spacecraft			997 6
Payload			435.2
Payload equipment		402.2	
RBV TV cameras (3)	93.6		
Video tape recorder/transport and electronics	68.0		
Multispectral scanner ERTS-A	105.0*		
Video tape recorder/transport and electronics	68.0		
Data collection system	5 8		
RBV electronics (3)	36 0		
RBV camera controller	7.0		
Scanner signal processor	9.8		
Video combiner	9.0		
Payload interface		33.0	
Payload harness and structure	33.0		
Total ERTS-A satellite weight			1432.8

*Note ERTS-B multispectral scanner includes an IR cooler assembly and weighs 120.0 pounds.

ERTS-B weight summary	Weight (lb)
ERTS-B spacecraft	997.6
ERTS-B payload	450.2
Total ERTS-B satellite weight	1447.8

inertia about the yaw and pitch axes as depicted in Table 2-2 have increased significantly (approximately 82 slug-ft^2 each) over June 1969. This increase is due principally to the addition of the video tape recorders and their enclosure to the aft end of the satellite, and due also to the solar array paddle revision.

A mass distribution for ERTS-A is presented in Figure 2-9 with comparative data for OGO 6 for reference.

Table 2-2. Sequenced Mass Properties Data

Mission Event	Weight (lb)	Center of Gravity (Satellite Station)			Moment of Inertia ($slug\text{-}ft^2$)			Product of Inertia ($slug\text{-}ft^2$)		
		X	Y	Z	I_{xx} (roll)	I_{yy} (pitch)	I_{zz} (yaw)	I_{xy}	I_{xz}	I_{yz}
ERTS-A										
Satellite at launch (includes adaptor)	1432 8	400.3	363.1	400.5	308	65	316	1.3	-0.8	-1.6
Satellite at separation (solar array paddles and antennas stowed)	1409.8	400.3	362.3	400.5	296	62	304	1.4	-0.8	-1.6
Satellite at separation (solar array paddles and antenna deployed, solar array at 180 degrees)	1409.8	400.3	367.8	400.5	210	251	393	1.2	-0.8	-2.4
ERTS-B										
Satellite at launch (includes adaptor)	1447.8	400.4	362.7	400.5	316	67	324	1.3	-0.1	-1.6
Satellite at separation (solar array paddles and antennas stowed)	1424.8	400.4	361.9	400.5	304	64	314	1.6	-0.2	-1.4
Satellite at separation (solar array paddles and antennas deployed, solar array at 180 degrees)	1424.8	400.4	367.3	400.5	217	251	400	0.2	-0-	-2.2

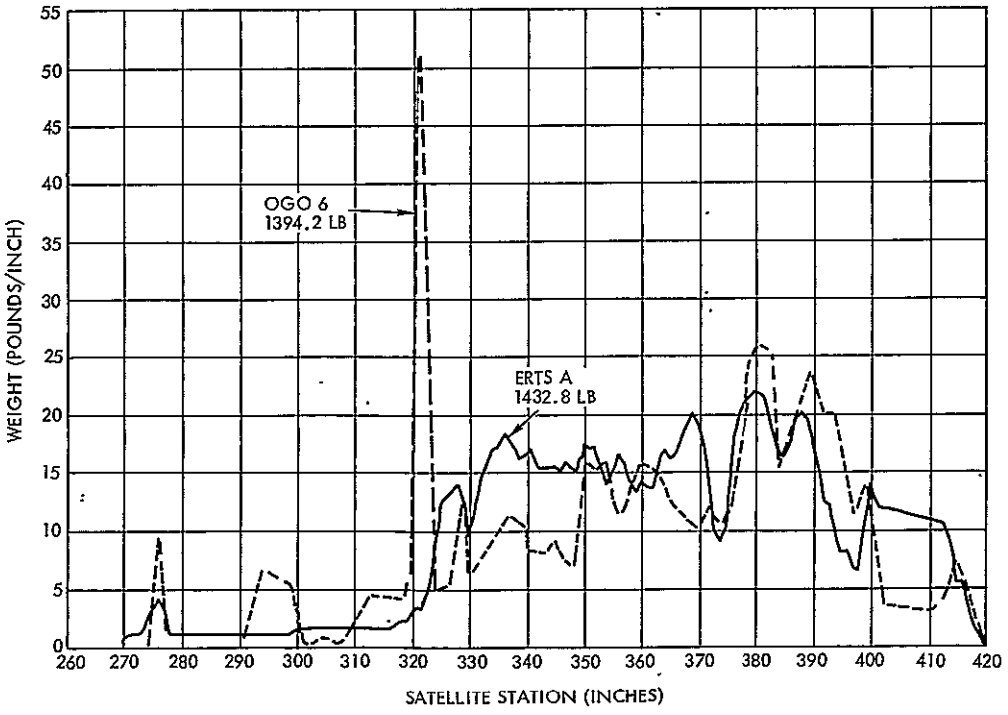

Figure 2-9

MASS DISTRIBUTION FOR ERTS-A, satellite at launch, including interstage.

3. ATTITUDE CONTROL SYSTEM

The ERTS attitude control system establishes and maintains the body orientation aligned to the local vertical and the orbit plane; it orients the solar array so as to achieve maximum solar power; it develops signals which after ground processing provide a precision measure of the spacecraft's attitude and, through a sequence of modes, permits control reacquisition should any circumstances cause loss of stabilization. The accuracy with which it performs these functions is shown on Table 3-1.

Table 3-1. Control System Normal Mode Performance Maximum Errors

	Pitch	Roll	Yaw
Body pointing, deg	0.39	0.44	0.65
Body rates, max. deg/sec during picture taking	0.008	0.011	0.011
All other normal mode, deg/sec	0.028	0.075	0.03
Attitude determination, deg (1σ)	0.05	0.05	0.07
Solar array			
Pointing error, deg		8	
Slew rate, deg/sec		1.5	

3.1 SUMMARY DESCRIPTION

The earth horizon as located by any three of four CO_2-band horizon scanners and their associated electronic circuits provides a reference for determining the local vertical (Figure 3-1). Roll and pitch error signals are developed whenever the body Z axis drifts from the local vertical about either of these axes. Similarly a gyrocompass assembly provides a yaw reference by detecting whenever the X axis does not lie in the orbit plane. Sun sensors mounted on the solar array provide a 4π steradian field of view and indicate deviations about two axes between the array perpendicular and the sun line. The error signal about the array axis controls the angle about the roll axis of the array with respect to the body. The other error signal is used only during acquisition.

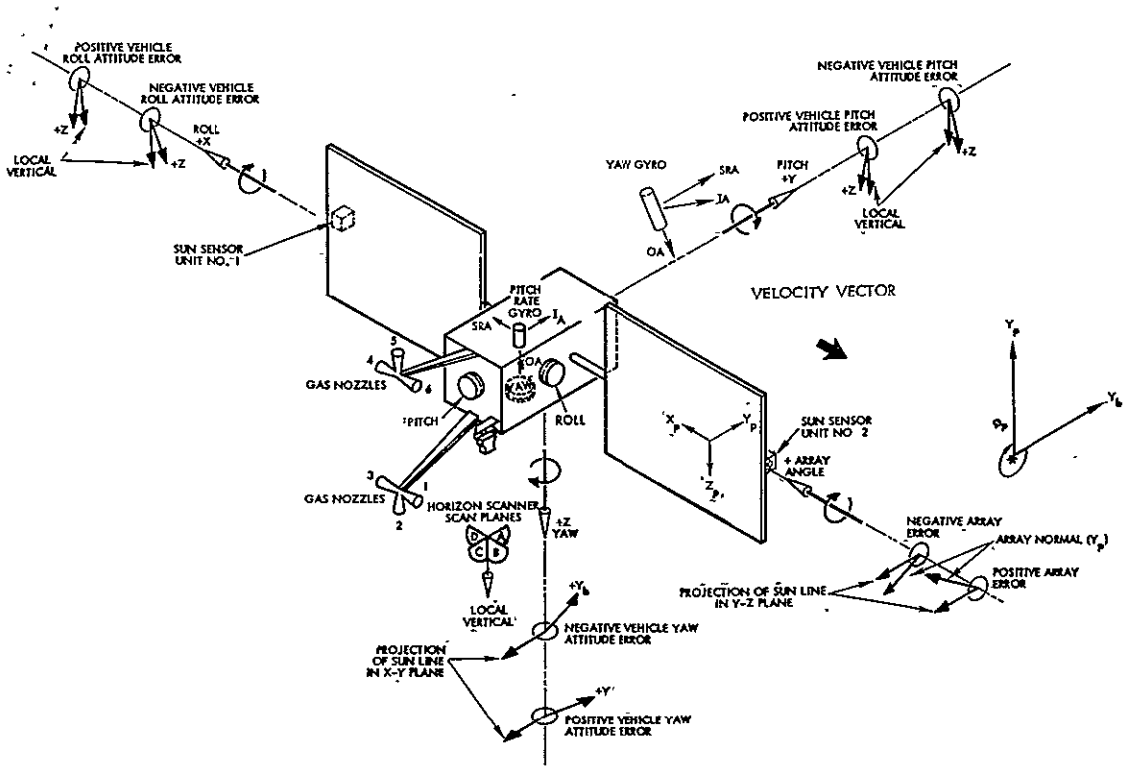

Figure 3-1
ATTITUDE CONTROL COORDINATE SYSTEM

Body control is effected (Figure 3-2) by a pneumatic system (for angular momentum removal) and a reaction wheel system (for momentum storage). The pneumatic assembly provides torques about the X, Y, and Z axes in either a positive or negative sense during the acquisition mode. The same is true of the reaction wheel assembly. In normal control the yaw pneumatic system is disabled, and the pitch and roll pneumatic systems remove components of secular momentum stored in the reaction wheels. Torque to rotate the solar array is provided by a small servo motor through a 24,000:1 gear train.

The spacecraft portion of attitude determination for ERTS is accomplished entirely with the attitude control equipment. One alteration is made to the OGO reaction control wheels in the use of position rather than velocity indicators. Cumulative wheel position for each axis, horizon sensor error signals, yaw gyrocompass error signal, and solar array angle constitutes the attitude determination data telemetered to the ground. On the ground a computer-implemented Kalman filter is used to calibrate,

CONTENTS

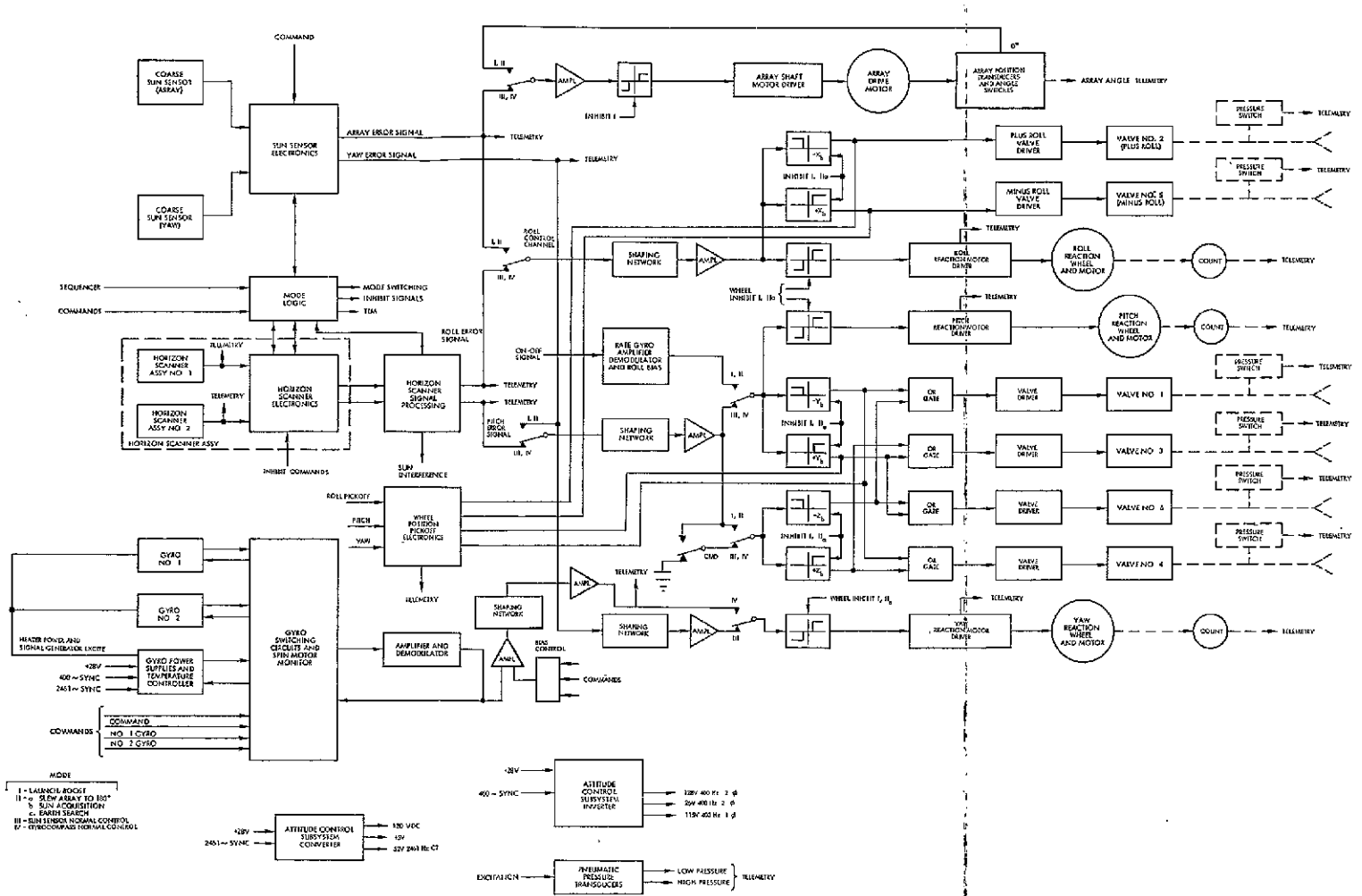

Figure 3-2
ATTITUDE CONTROL SUBSYSTEM
block diagram

FOLDOUT FRAME

FOLDOUT FRAME

PRECEDING PAGE BLANK NOT FILMED.

smooth, interpolate, and combine the spacecraft telemetered data together with additional inputs such as ephemeris data, mass property models, torque models and ground truth when available to yield an accurate record of spacecraft yaw, pitch, and roll. Additional details on the theory of attitude determination are contained in Volume 4 Section 6. Details of the ground processing software will be treated in the ground data processing report.

The control system operates in a "bang-bang" mode, i.e., control signals apply full positive, full negative, or no torque. The pneumatic jets and the wheel for each axis are operated in parallel with the pneumatic deadband set at 2.5 times the wheel deadband so that normally all control is effected by the wheels. Should a wheel saturate (achieve limiting speed in either direction), a short pneumatic pulse would remove enough momentum from the system to re-establish control by the wheel. In normal operation without picture taking, however, a wheel tachometer signal calls for pneumatic removal of 25 percent of the wheel momentum whenever half saturation speed is achieved. This automatic momentum removal technique is disabled during picture taking leaving enough additional momentum storage capability in the wheel to assure that no gas discharges occur before the cameras are turned off again.

The ERTS attitude control concept is taken from OGO with the addition of a fourth or "normal" mode of control using a gyrocompass to align body to orbit plane.

During boost, the outputs from the sensors and the inputs to the torque sources and drive mechanisms are inhibited. After separation the subsystem operation is in two phases: acquisition and normal control. The acquisition phase consists of three modes: array slew, sun acquisition, and earth search. The normal control phase is entered when the gyrocompass mode is commanded from earth and the resulting transient has settled out.

The acquisition phase of control system operation has been designed to orient the vehicle to the required references given arbitrary initial angular errors and body angular rates up to 1 deg/sec about all three axes as could occur following separation from the booster and deployment

of the solar array. During the array slew mode the sensitive axis of the solar array is driven to a position parallel to the $+y_b$ axis. The sun acquisition mode is provided in order to align the pitch ($+y_b$) axis with the sun and establish a constant rate about this axis. Error signals for control in this mode are provided by the sun sensors and the pitch rate gyro. By pointing the body at the sun initially in this fashion, the solar array is rapidly oriented for maximum charging of the batteries. The fields of view of the four horizon scanners intersect on the $+Z_b$ axis. During the earth search mode the control system configuration is the same as that for sun acquisition and hence as the spacecraft rotates this axis sweeps out a plane. As the vehicle progresses in orbit this plane must intersect the earth, at which time such rotation ceases and earth acquisition is complete with the Z_b axis properly oriented to the local vertical. The yaw gyrocompass mode is then entered by connecting the yaw gyro rate output signal to the yaw axis control channel, resulting in a spacecraft slew which positions the roll axis in the orbital plane, the normal cruise orientation. Earth acquisition can be inhibited by ground command. Yaw gyrocompass control can only be effected while under ground control.

Acquisition of the observatory reference axes is initiated at a predetermined time after separation from the launch vehicle, and at any time when one or more references are lost. The sequence of acquisition ensures that the time is minimized during which the solar array is not oriented toward the sun. Acquisition of the remaining reference axis minimizes the time of acquisition consistent with other system constraints. A period not to exceed 90 minutes is required for alignment of the observatory X axis in the orbital plane.

The observatory stabilization and control subsystem is designed to control the orientation of the observatory and its solar array throughout the life of the observatory in orbit. It maintains this stabilization within the following tolerances.

- Earth Pointing Accuracy: the earth reference axis stabilized within 0.7 degree of the line from the earth's instantaneous geometric center to the spacecraft.

- Orbit Plane Orientation Accuracy: the observatory roll axis stabilized within 0.7 degree of the orbit plane.

- Angular Velocity: less than 0.011 deg/sec, exclusive of the orbital rate of the observatory. This requirement is relaxed by a factor of 10 when the imaging sensors are not operative.

- Sun Pointing Accuracy: the face of the solar array oriented about the observatory roll axis within 8 degrees of the sun when it is visible. The array is inherently oriented correctly on emerging from an eclipse.

- Angular Velocity: the angular velocity of the solar array relative to the main spacecraft body less than 1.5 deg/sec.

The attitude control system for ERTS is obtained by making minor modifications to the OGO attitude control system. Most of the changes involve deletion of functions not required for ERTS. One new package (the orbital switching assembly) is required, a relatively simple electronics package which provides mode switching into the gyrocompass mode and some telemetry functions. The comprehensive system block diagram is shown on Figure 3-3.

The horizon scanner electronics are redesigned to improve the scanner performance for attitude determination and to improve manufacturability. The magnetic bistable amplifiers in the attitude control assembly are being replaced with mechanically and electrically interchangeable units of solid state design. This change is necessitated by the smaller control hysteresis required for ERTS compared to OGO. These changes are within the state of the art and hence present no developmental risks.

3.2 HORIZON SCANNER

The horizon scanner subsystem measures pitch and roll attitude errors with respect to the horizon. Four independent horizon tracker signals are combined to generate these error signals for control and for attitude determination. See Figures 3-4 and 3-5. The system is conceptually the same as the advanced OGO horizon scanner developed by ATD for GSFC but with improvements and modifications to achieve better performance. Redundancy is inherent since any three of the four tracker signals suffice for deriving both error signals. The equipment has the following characteristics:

- Size and Weight: dual tracking head, each (2 per system) 115 in.^{3}, 6.0 lb; electronics assembly 187 in.^{3}, 6.5 lb

- Power: 10 watts nominal; 13 watts maximum

- Optics: detector; immersed thermistor bolometer; FOV of 1.2 degrees; and spectral range of 14 to 16 microns

- Outputs: Pitch and Roll: DC voltage linear to 10 deg; logic: sun alarm and track check signal from each of four track heads; telemetry: Full scale position, expanded scale position, and radiance level from each of four track heads, plus temperature, all telemetered.

- Accuracy, attitude determination, 1 deg range. Allows for removal of predictable errors by suitable ground processing.

Horizon Tracker Instrument Errors	
Long term biases	0.084 deg (3σ)
Short term noise	0.048 deg (3σ)
Horizon model accuracy	0.048 deg (3σ)
Atmospheric Variability	0.048 deg (3σ)
	0.12 rss (3σ)
Bandwidth	0.17 Hz

- Accuracy, Attitude Control: 10 degree range, includes pitch roll computation errors, three head operation, in-flight use of uncorrected data.

Horizon Tracker position error near null	0.102 deg (3σ)
Sensor head-Control axis alignment	0.070 deg (3σ)
Earth Oblateness and Seasonal Horizon altitude variation caused biases	0.13 deg (3σ)
Horizon Atmospheric Variability and uncertainty	0.084 deg (3σ)
Noise	0.096 deg (3σ)
Bandwidth	1.0 Hz

3.2.1 Operation

The horizon scanner system uses four infrared search-track units to track points separated in azimuth by 90 degrees on the earth's horizon. Each unit employs a servo circuit to search for and track the horizon. The servo of each tracker includes a mirror, a telescope, a thermistor

PRECEDING PAGE BLANK NOT FILMED.

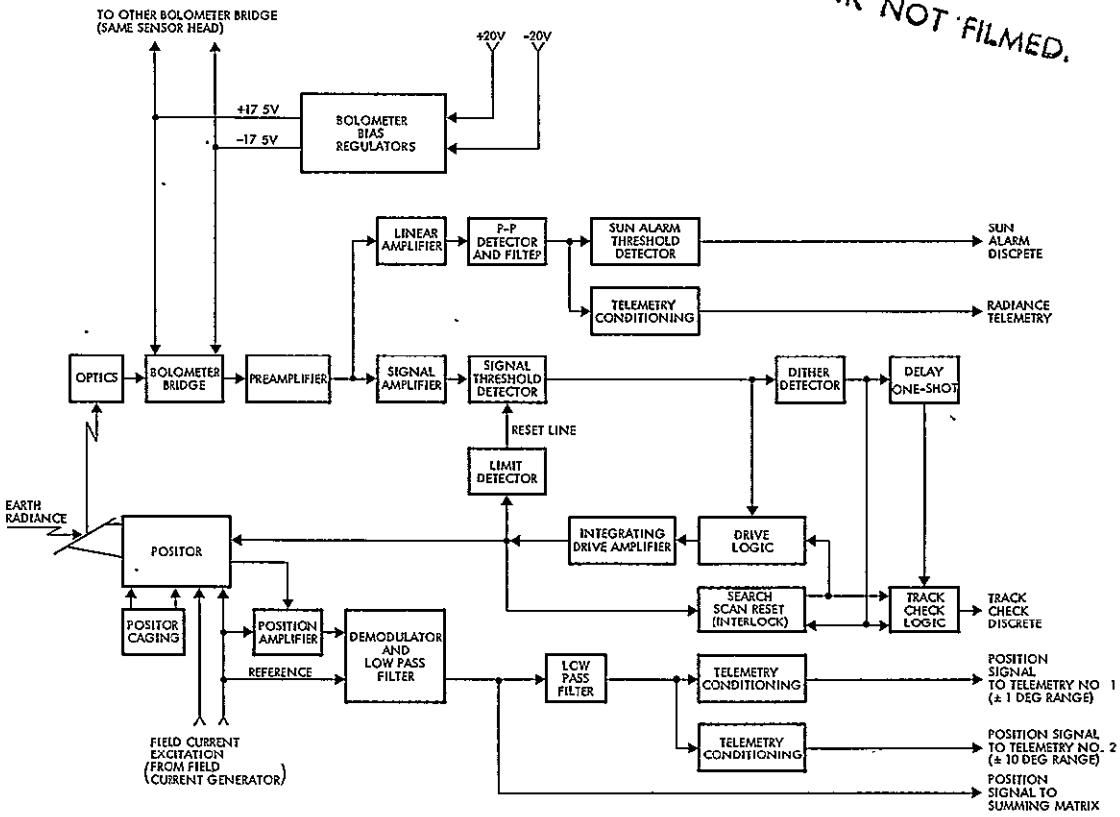

Figure 3-4

ERTS HORIZON SCANNER block diagram, single tracking loop (one of four)

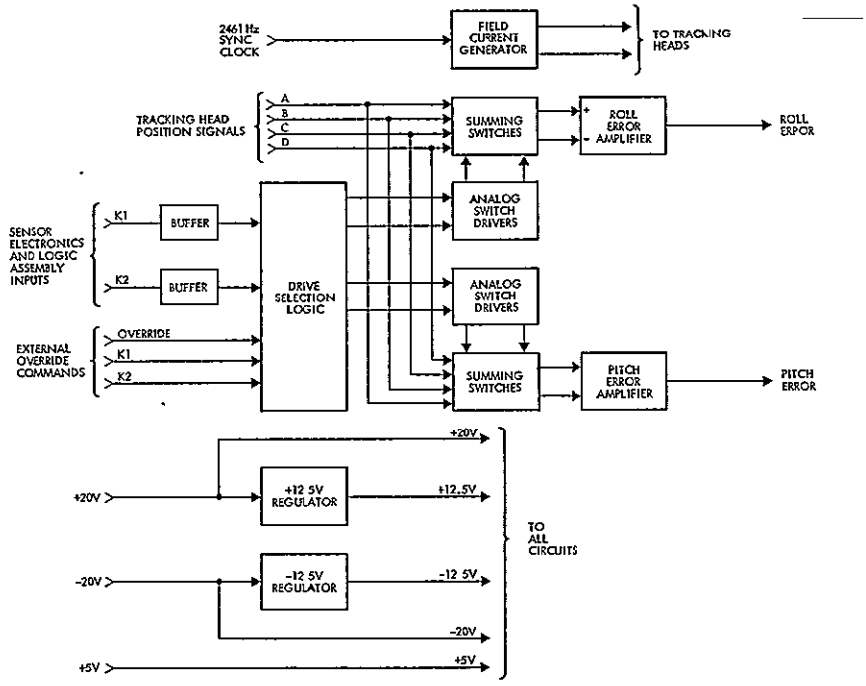

Figure 3-5

HORIZON SCANNER block diagram of common electronics

bolometer, a signal preamplifier, a signal amplifier, a threshold detector and a scan mirror drive amplifier. The servo circuit is intentionally made to oscillate at a controlled amplitude and at a controlled frequency. Movements of the mirror in response to the servo oscillations cause the telescope field of view to scan the horizon. If this oscillation is centered on the horizon the resulting bolometer output after amplification and thresholding will appear as a 50 percent duty-cycle square wave. De-centering of the horizon causes the duty cycle to change proportionately introducing a DC component into the waveform whose sense indicates whether the center of scan is above or below the horizon. The DC component is amplified and applied to the mirror along with the oscillating drive signal in the polarity necessary to reduce the horizon de-centering. Thus the DC signal necessary to re-center the horizon is a direct measure of the angular displacement of the horizon from a nominal position (approximately 30 degrees below the horizontal plane).

Logic is provided to verify whether the scanning loop is oscillating about a suitable earth edge. This operates by examining the amplitude of the radiance and frequency of the oscillation. If this logic output is not true, the mirror drive loop is modified by switching to a search mode, in which the mirror is scanned slowly by a triangular sweep between its angular extremes. Acquisition of an edge is permitted only during the downward portion of the scan (from space toward earth).

The angular displacement signals are amplified, demodulated, and fed to a switching matrix to develop the pitch and roll signals. Logic supplied to the horizon scanner actuates switching circuits in the scanner to select the appropriate three of the four angular-position signals supplied for computing the local vertical. The switching logic is derived in one of two ways, depending on ground command. In the automatic mode the control system bases the tracker head selection on sun presence and tracking-check information from each tracker. In the command mode, a ground command overrides the automatic logic to permit ground command selection of the three desired tracker heads. The three angular output signals are fed via the matrix to two summing amplifiers which read out vehicle attitude in terms of pitch and roll. If one tracker fails, the fourth tracker is automatically chosen (or selected by command) and

the system continues to operate. Manual head selection will be used for avoidance of moon tracking (See Volume IV Section 5). All four of the independent tracker head positions are telemetered to the ground for use in the attitude determination function. Two telemetry signals are provided for each head: one reproduces the full linear range of tracker head position, and another provides an expanded scale about the nominal angle for more precise attitude determination.

3.2.2 Scan Mechanism

The horizon scanner concept is based on the use of a positor drive for the scan motion. This drive utilizes a flexure-pivot suspension to provide motion without sliding surfaces or friction. The mechanism used is identical to the advanced OGO version of the positor, shown as Figure 3-6, and is similar to the original OGO unit but with improvements for linearity and producibility.

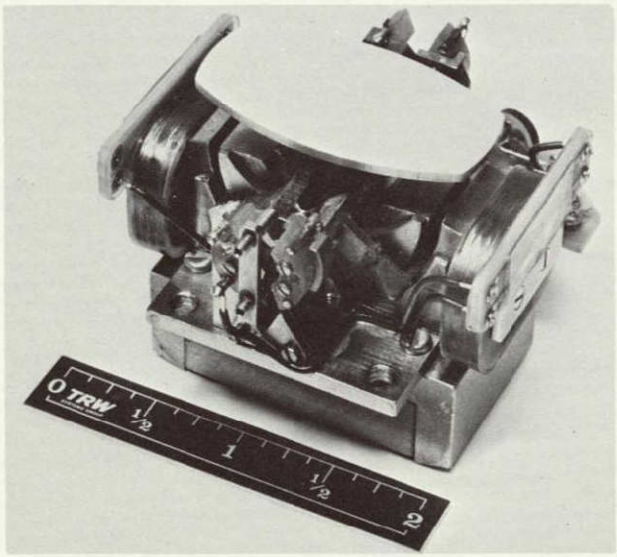

Figure 3-6
ADVANCED OGO SCAN MECHANISM
showing D'Arsonval type movement and mirror table

Scanning is by means of a mirror mounted on the rotor of a permanent-magnet-type torquer. Two coils that can move in a cylindrical air gap are also connected to the rotor. A pair of flexure pivots connects the rotor to the base structure. Each pivot consists of two flat springs attached to the rotor and to the base in such a way as to form an X. The flat sides of the springs are perpendicular to the plane of the X and the rotor turns about an axis perpendicular to the X, passing through its center point. The electrical connections to the rotor coils are through the flexure pivots. The base structure contains a permanent magnet, a laminated iron magnetic structure to form the air gap, and two AC reference coils.

If a DC current is applied to the rotor coils, the rotor assumes an angular position proportional to the current. The mirror can be made to scan about some desired angle through the application of a direct current plus a varying current to the rotor coils. The total angular motion for ERTS is ±10.75 degrees, resulting in a total optical range of ±21.5 degrees.

The AC reference coils are used to set up a small-amplitude high frequency (2461 Hz) flux change in the air gap. A high frequency signal with an amplitude proportional to the angular position of the rotor from the mechanical null position is therefore present in these rotor coils. An accurate linear indication of position is then obtained which is independent of the flexure-pivot spring rate.

3.2.3 Optics

Each tracker-head assembly (Figure 3-7) contains two trackers which scan in the same plane but with fields of view separated 180 degrees in azimuth. The two heads are mounted at right angles to each other so that the trackers scan in vertical planes with respect to vehicle coordinates but separated in azimuth by 90 degrees. Incident infrared radiation is reflected from the scanning mirror into the telescope. Rotation of the scan mirror gives each tracker a search-and-track capability over an approximately 43-degree range in the scan plane. The telescope assembly consists of three optical elements: an oval aperture mask in the plane of the aperture, a lens filter coated to obtain system optical response from 14 to 16 microns, and a germanium-immersed thermistor bolometer at the focal plane of the lens.

3.2.4 Electronics Assembly

The electronics assembly (Figure 3-8) contains servo, readout, and logic circuits and a voltage regulator for internal power.

The readout circuits include the field current generator, individual position amplifiers and demodulators for each tracker, the switching matrix, and two summing amplifiers. The field current generator supplies the 2461 Hz excitation signal to the field coils for the mirror mechanisms. The induced voltages are amplified, demodulated, and then combined in the switching matrix and summing amplifiers provide the pitch and roll

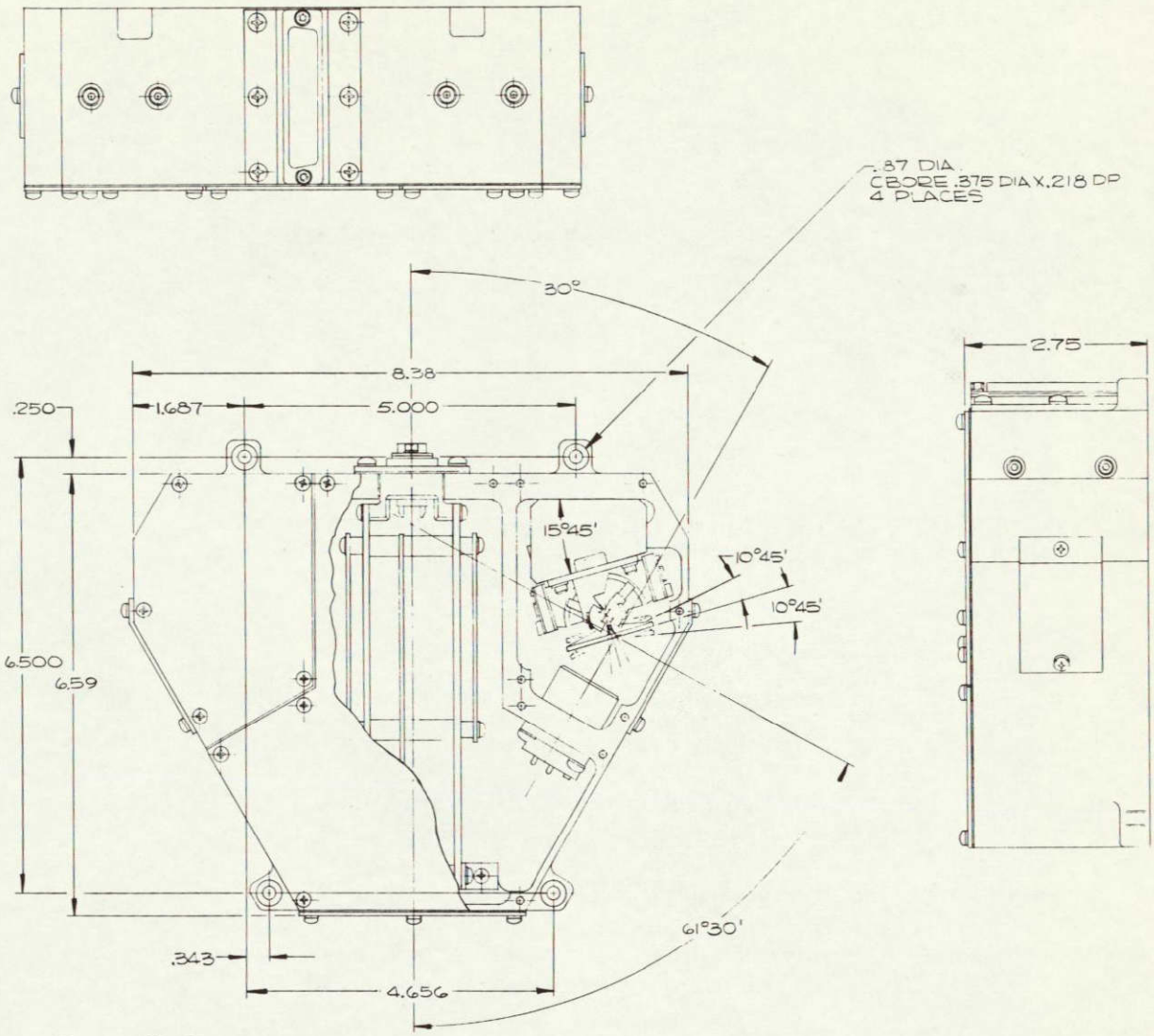

Figure 3-7
ERTS TRACKER HEAD ASSEMBLY

outputs. Additional filtering and buffering is provided for the telemetry signals.

Tracking-check circuits furnish the output signals that confirm that the trackers are tracking the earth's horizon. During the search, the interlock circuits prevent possible lock onto a gradient within the earth by allowing lock only while the line of sight is searching in a downward direction. The sun-alarm circuit furnishes a logical output signal to indicate when the sun is being tracked.

The voltage regulator circuit supplies ±17.5 VDC for the critical low-noise circuits and ±12.5 VDC for other circuits.

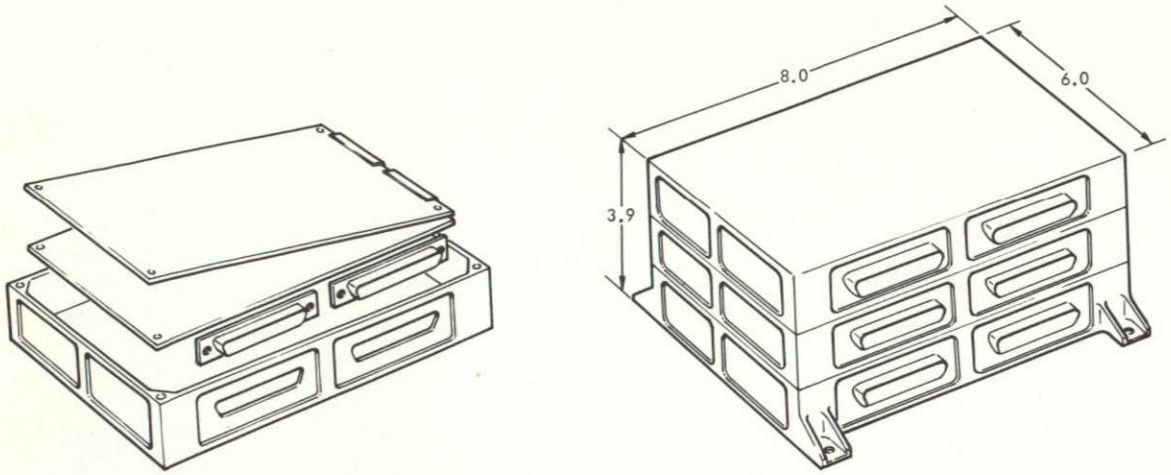

Figure 3-8
CONCEPTUAL DESIGN of the exterior and mounting technique for the HORIZON SCANNER ELECTRONICS

3.2.5 Implementation

The ERTS horizon scanner is similar to that developed under the advanced OGO program, with some modifications and improvements.

- The mirror scanning mechanism is identical, permitting use of the remaining units now at GSFC.
- The optical channel is the same except that one filter is replaced to provide a spectral bandpass of 14 to 16 microns to provide more usable signal energy while still making use of the CO_2 absorption band earth profile.
- The head assembly is modified such that the null pointing angle of each mirror is at 61.5 degrees from the Z axis, corresponding to the 492 nmi altitude, rather than 43 degrees as previously noted. This permits greater accuracy for attitude determination and reduces power.
- The electronics use more contemporary and currently available components.

The tracking head assemblies are packaged in the same manner as in the advanced OGO horizon scanner. The one change of significance is in rotating each scanning axis null. The electronics is housed using a standard TRW electronics package. Printed circuit boards are assembled into slices, which in turn are bolted together to form an assembly. Advantages of this technique include the convenience of handling discrete subassemblies for manufacture and test and the fact that a large number

of similar units have successfully undergone a variety of space environment tests.

3.3 YAW GYROCOMPASS

The yaw gyrocompass (Figure 3-9) consists of the yaw gyro assembly and the gyro electronics assembly. The yaw gyro assembly contains two MIG gyros, gyro transfer relays, an amplifier demodulator module, a temperature controller module, and a miscellaneous circuit module. The gyro electronics assembly contains three modules which provide B+, 400 Hz motor power, 2461 Hz AC and a spin motor monitoring function. See Zone 2 of Figure 3-2.

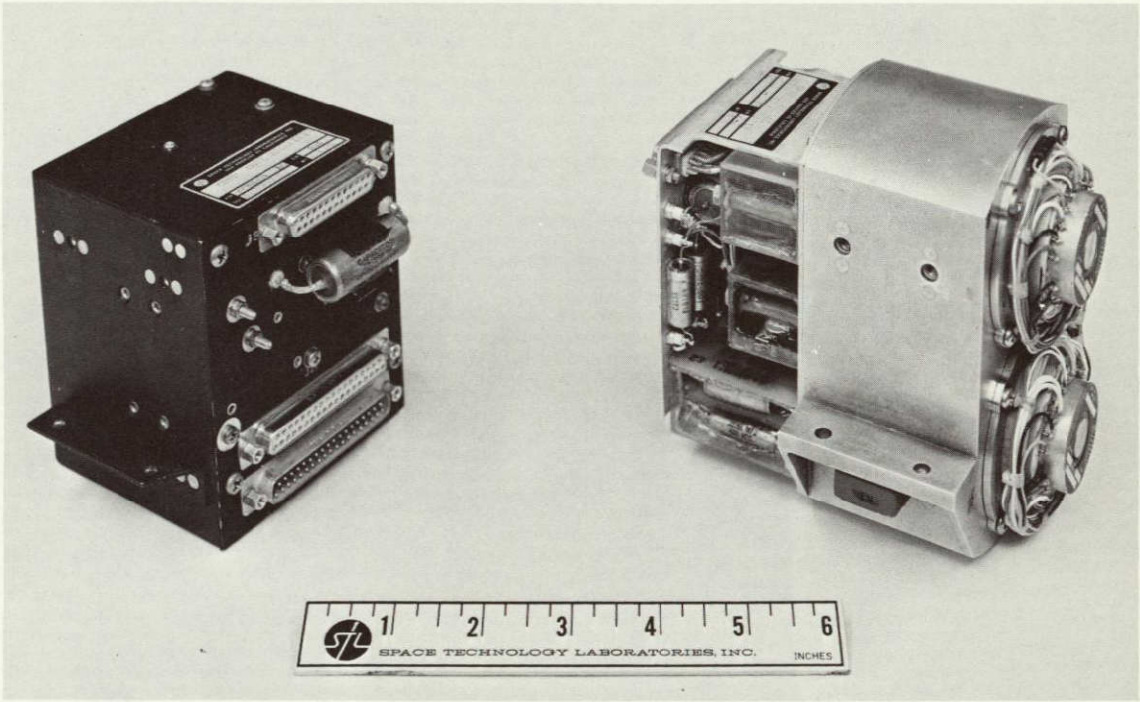

Figure 3-9
YAW GYROCOMPASS SUBSYSTEM consists of the yaw gyro and gyro electronics assemblies

The yaw gyro assembly detects errors in the alignment of the spacecraft roll axis relative to the orbit plane. When the roll axis moves out of the orbit plane, a component of the orbital angular rate appears along the gyro input axis. This rotational rate is accompanied by a precessional

torque about the gyro gimbal through normal gyroscopic action. A servo action initiated with a gyro pick off signal which is amplified and demodulated and applied to the torquer generator creates an electronic torque balancing the precessional torque. The electronic torque is proportional to the torquer current and therefore this current is a direct measure of the component of orbital rate lying along the gyro input axis. This current also passes through a monitoring resistance in series with the torquer to produce an output voltage whose scale factor is approximately 48 volts/deg/sec. In Mode 4 this voltage is the yaw error signal which initiates yaw wheel motion so as to reorient the observatory about its yaw axis and return the gyro input axis to the orbit plane. After suitable conditioning this error voltage is telemetered to earth as one component of the attitude determination input.

To provide damping in the yaw control loop, rate feedback is created by tipping the input axis of the gyrocompass upward by 45 degrees.

3.4 RATE GYRO ASSEMBLY

During acquisition after solar orientation has been established, the spacecraft is made to rotate about its pitch axis in search of the horizon. The rate gyro assembly taken directly from OGO establishes the reference to control this pitch rate. The gyro itself includes both a motor speed sensor and a gimbal torquer through which the required rate bias is applied. Direct current and two-phase, square wave power for this assembly are furnished by external supplies.

The gyroscope in the pitch rate gyro assembly (Figure 3-10) is a ±20 deg/sec instrument with the gimbal stops moved to limit full scale range to ±3 deg/sec. The range reduction results in a lowering of the effective hysteresis to less than 0.005 deg/sec. Since the gyroscope selected for the assembly includes a gimbal torque generator, rate error signal null offset is easily obtained to establish the earth search rate. A DC current (13 milliamperes) in the gyroscope torque generator provides a bias which is calibrated to obtain a rate error signal null with a nominal input rate of -0.49 deg/sec. This produces the specified earth search rate for acquisition.

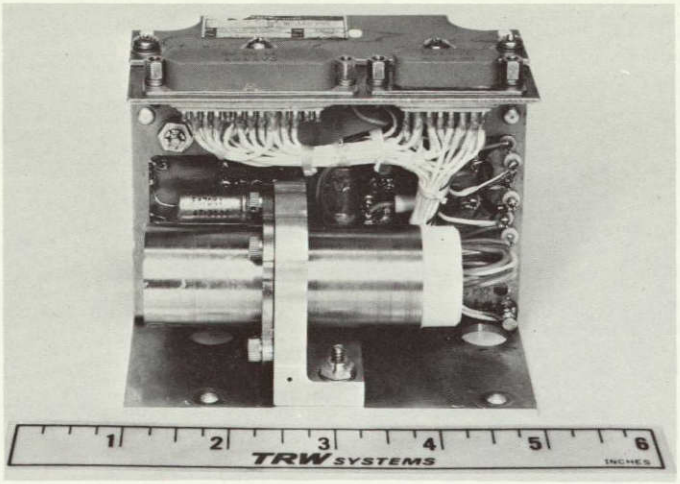

Figure 3-10

PITCH RATE GYRO ASSEMBLY incorporates a subminiature rate gyroscope, signal amplifying and demodulating electronics, and telemetry processing circuits.

The gyro spin motor is a two-phase hysteresis synchronous motor operating on 26-volt square wave, 400-Hz power. The motor draws approximately 3 watts of power while running and 4 watts while starting. Motor run-up time is typically 20 seconds. The wheel turns at 24,000 rpm, developing an angular momentum of 30,000 gm cm^2/sec. It runs only from launch to initial earth acquisition and during any reacquisition sequences.

The spin motor rotation detector consists of four small magnets mounted in the rim of the gyro wheel. The flux from these magnets interacts with the windings of the torquer coil to produce an AC signal at its terminals. The frequency of the signal is proportional to wheel speed, being 1600 Hz when the wheel is running in synchronism with the 400-Hz supply.

The gyro gimbal is supported on both ends by means of ball bearings. In addition, a torsional spring is attached between the gimbal and case on one end. Metallic paddles attached to the gimbal displace silicone fluid through flow gaps which compensate for variation in fluid viscosity by changing gap areas in relation to gyro temperature. The temperature compensator produces gimbal damping which is 0.6 ± 0.3 of critical over the temperature range of 0 to 180°F. The sizing of this damping, the torsional spring and the gimbal moment of inertia produce a gyro natural frequency between 15 and 18 Hz.

The gimbal torquer consists of case-mounted permanent magnets coupled with a laminar stack which provides the flux path. A single gimbal-mounted coil is placed in the flux path air gap. Direct current through this winding produces the torque on the gimbal.

The signal pickup is a variable reluctance microsyn excited by square wave power. A precision metal film resistor in series is used to

swamp out pickoff resistance variations due to temperature, and series capacitor is used for tuning. The voltage waveform in the secondary of the signal generator is sinusoidal.

Excitation supplied to the gyroscope spin motor from the spacecraft static inverter is unfiltered two-phase square wave voltage. Signal generator excitation is single-phase square wave filtered to produce sine wave rate error signals to the gyro signal amplifier.

The spring restrained rate gyro has the following characteristics:

- Size: 1 inch diameter, length 2.0 inches
- Weight: 4.5 ounces
- Angular momentum: 3×10^4 gm cm^2/sec
- Range: ±3 deg/sec
- Sensitivity, scale factor: 200 millivolts/(deg/sec)
- Torquer scale factor: 0.08 deg/sec-ma (trimmed to 0.04 deg/sec-ma by means of an external shunting resistor)

The gyro signal amplifier and demodulator convert the suppressed carrier, low level AC signal from the gyroscope to a DC rate-related signal of sufficient power to drive the bistable amplifier of the drive electronics assembly pitch channel. A power gain of 42 db in the signal amplifier-demodulator provides 125 microamperes to the bistable amplifier, sufficient for wheel turn-on. The gyro signal amplifier is a three-stage, solid state, AC amplifier. Printed circuit board construction is used for the signal amplifier and demodulator. Phase sensitive gyro signal demodulation is provided by a full wave ring demodulator.

3.5 SUN SENSOR

The sun sensor is used to detect position of the sun with respect to body yaw (Y) axis and with respect to the sensitive array pointing direction. The yaw output is used to point the spacecraft during sun tracking; the array error output is used to position the array. The sun sensor, a modernized version of the OGO coarse sun sensor, consists of a +X and a -X unit (see Figure 3-11) which are mechanically and electrically interchangeable. The +X unit is attached to a sun sensor bracket assembly at the extremity of one solar array and the -X unit is attached to an identical assembly on the opposite solar array to prevent any possibility of control

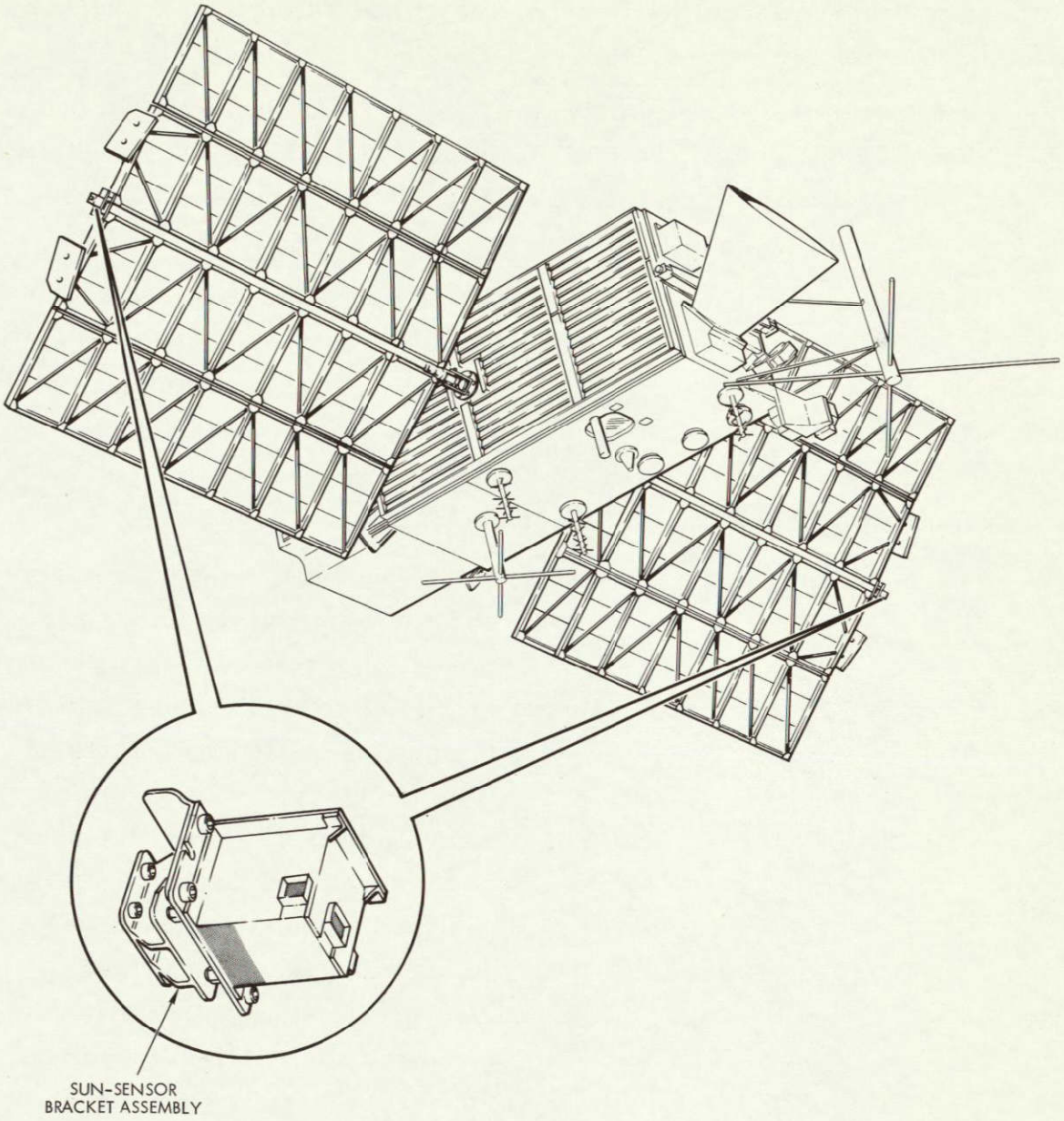

Figure 3-11

A SUN SENSOR ASSEMBLY is mounted on each end of the spacecraft X axis

loss due to shading of the detectors by the spacecraft. Each unit consists of three silicon solar cells, associated circuitry, a temperature monitoring thermistor, thermal provisions, and structural members.

Each sun sensor unit weighs approximately 1 pound and occupies 4 x 4.5 x 3 inches. No power is consumed by the sensors except that required to excite

the temperature monitoring thermistor. The unit operating temperature is maintained between 40 and 140°F by passive techniques (Section 9).

All detectors are 1 x 0.5 cm n-on-p silicon solar cells with a bulk resistivity of 10 ohm-cm. The inherent radiation resistant characteristic of these cells limits the expected degradation output signal due to radiation to less than 8 percent after two years in orbit.

The yaw sensor consists of two solar cell detectors and two scale-factor adjustment resistors; one detector and one resistor in each unit. See Figure 3-12. The output of these detectors are parallel-summed at the input of the sensor electronics and logic assembly. Each detector provides angular-position information about an axis normal to the solar array axis over a field of view of 2π steradians.

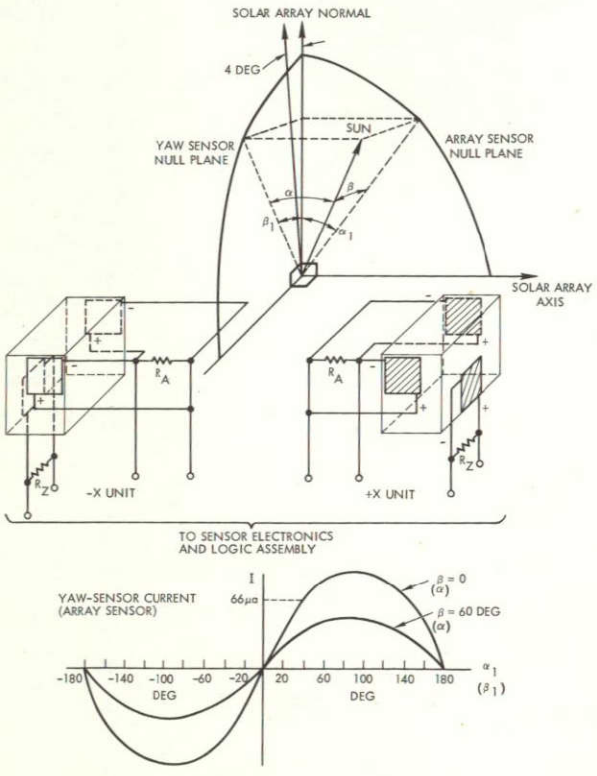

Figure 3-12
SUN SENSOR SCHEMATIC showing representative error signal

The array sensor consists of four solar cell detectors and two scale-factor adjustment resistors; two detectors and one resistor in each unit. The outputs of the two detectors are parallel-summed in their respective units. Each detector provides angular-position information about the solar array axis over a field of view greater than π but less than 2π steradians. A 4-degree bias for earth albedo is built into the unit. The fields of view of a sensor may be limited by shadows of the spacecraft but when one detector in one unit is shaded the corresponding detector in the other unit will be fully illuminated.

3.6 SENSOR ELECTRONICS AND LOGIC ASSEMBLY

The sensor electronics and logic assembly (SELA) amplifies and frequency shapes the error signals for array control, roll, pitch, and

Mode 3 yaw channels. In addition, it defines the switching between the various modes of the control system, controls the redundant states of the horizon scanner, and processes a number of telemetry signals. It is the nerve center of the attitude control system. In terms of hardware, the assembly contains magnetic amplifiers and welded electronic modules with both analog and digital transistor circuits. The unit is illustrated in Figure 3-13. The block diagram of this unit is little changed from OGO and is shown on Figure 3-3. The unit itself offers from OGO only in deletion of circuits not needed in the ERTS mission: small earth, fine sun sensor, yaw wheel logic and pitch and roll error demodulators (the last are placed in the horizon scanner electronics on ERTS).

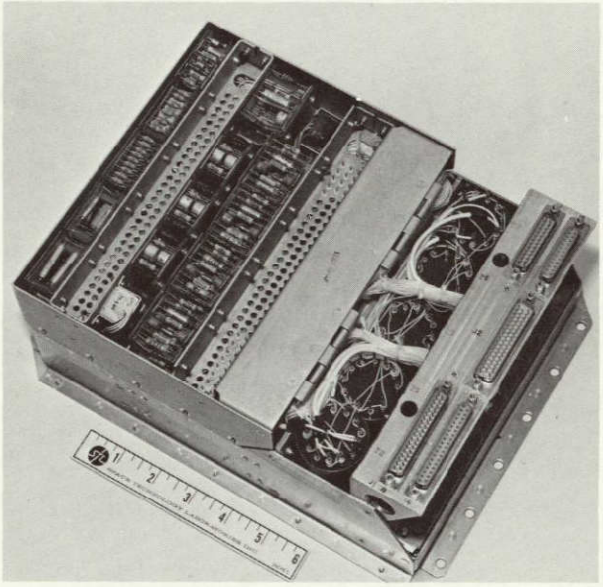

Figure 3-13
EXTERIOR VIEW OF THE SENSOR ELECTRONICS AND LOGIC ASSEMBLY. Engineering model, modules not encapsulated, cables not clamped.

The various control modes are used during acquisition and for re-acquisition should stabilization be lost. Provision is made for the system to step automatically through its modes arriving at the proper stabilized orientation or to advance only under ground control. In a typical acquisition after launch both aspects would be employed. The available modes, nominally in the order of their activation during launch are:

- Mode 1. Boost. Mode 1 is the status from countdown until a start command is received. Power is supplied to most functions but all drive, wheel, and pneumatic bistables are inhibited.

- Mode 2a. Array Slew. Mode 2a is provided to drive the array to 0 degrees for sun acquisition and cage it there. The only uninhibited actuator is the solar array drive motor. After array caging Mode 2b is automatically entered.

- Mode 2b. Sun Acquisition. All actuators are active in Mode 2b with the array caged, the roll axis driven by the array sun sensor, the yaw sun sensor connected to the yaw channel, and the pitch rate gyro used for pitch control. As in OGO the gyro is biased to establish an earth search rate of 0.49 deg/sec in pitch.

- Mode 2c. Earth Search. Mode 2c is identical to Mode 2b except that the automatic logic for transition to Mode 3 is enabled. The transition takes place when horizon-sensor track checks indicate that at least three sensors have acquired the earth.

- Mode 3. Sun Sensor Normal Control. Mode 3 is a completely stabilized mode but with the sun rather than the gyrocompass as yaw reference. It is identical to the normal control state for OGO, with all functions operative other than yaw pneumatics. For ERTS this mode is transitory, leading, on command into the gyrocompass mode. It also offers backup control capability.

- Mode 3a. Sun Sensor Reacquisition Delay. Mode 3a is entered if two or more horizon tracker heads indicate loss of lock in Mode 3. In Mode 3a only the array drive controller is uninhibited. If during a timed 7-minute interval three or more track checks occur simultaneously, Mode 3 is re-entered; otherwise the system recycles to Mode 2a.

- Mode 4. Gyrocompass Normal Control. Mode 4, the ERTS operational control configuration, is identical to Mode 3 in the pitch and roll channels but uses the gyrocompass as the yaw attitude reference.

- Mode 4a. Gyrocompass Reacquisition Delay. Mode 4a parallels 3a except for the retention of the gyrocompass error signal in yaw. All controllers, other than the array drive, are inhibited.

Modes 4 and 4a have been appended to the OGO mode structure, with Mode 4a using logic and switching identical to that of Mode 3a, and 4 involving a change from Mode 3 only in the yaw error signal connection. Entry into Mode 4 is not controlled by the SELA, but is controlled in the orbital switching assembly by ground command.

Although mode sequencing is automatic, key maneuvers such as earth acquisition (entrance into Mode 2c) can be inhibited by ground command. ERTS retains this override capability, used with great success during OGO operations. The sequence in which the attitude control switches between modes is best described by reference to

Figure 3-14. Switching between modes by means of the automatic sequence can occur only in the directions given by the solid arrows on the figure. Modes 1, 2a, 2c, 3, and 4 may be entered from any other mode (dashed arrows) and held by means of ground command. Three commands sent

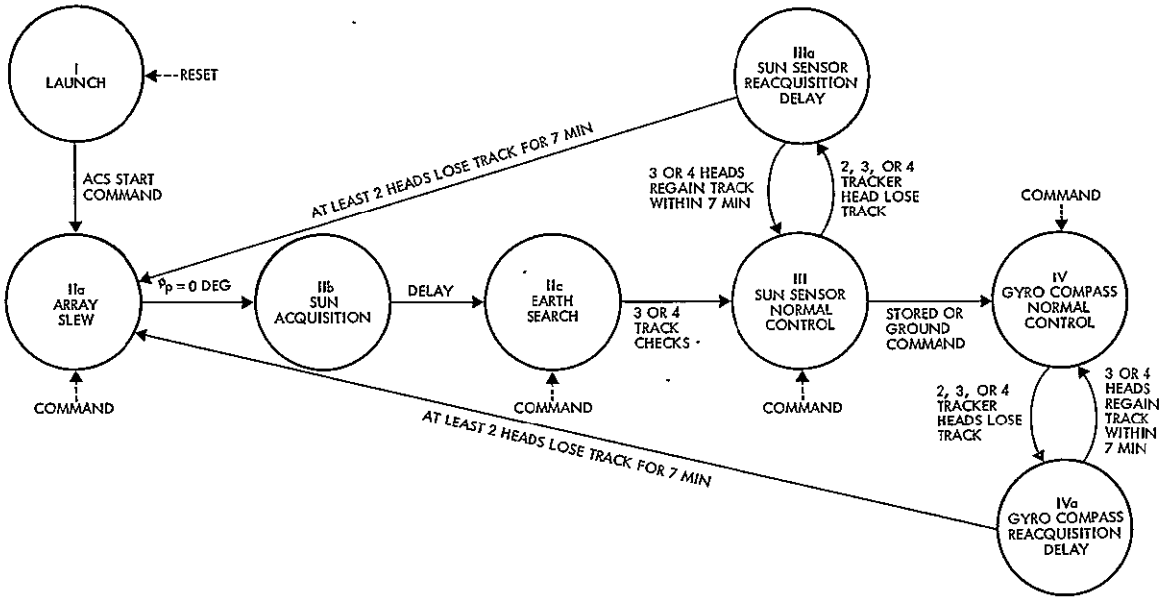

Figure 3-14
ERTS MODE STRUCTURE

sequentially (enable, select mode, execute) are required to effect the nonautomatic entrance to Mode 2a, 2c, 3 or 4. The command enable, if left on, inhibits all of the automatic sequence logic. In addition, the system may be reset into Mode 1 from any other mode before launch by grounding a reset hard line (dotted arrow). A description of the switching conditions into various modes is as follows:

- Into Mode 1: from any mode by reset; from any mode by command Mode 1.
- Into Mode 2a: from any mode by command Mode 2a; from Mode 3a after system has been in Mode 3a for 7 minutes (because two or more horizon scanner heads have lost a horizon); same for Mode IVa.
- Into Mode 2b: from Mode 2a upon receipt of a signal, which indicates that the solar array shaft is caged at 0 degrees.

- Into Mode 2c: from any mode by command Mode 2c; from Mode 2b after the system has been in that mode for a chosen time period.

- Into Mode 3: from any mode by command Mode 3; from Mode 2c when three or more of the horizon scanner heads indicate track check on earth; from Mode 3a if three or more of the horizon scanner heads reacquire the horizon before the 7-minute Mode 3a time delay period has expired.

- Into Mode 3a: from Mode 3 if two or more of the horizon scanner heads lose the horizon (immediately returns to Mode 3 if any three of the heads reacquire the horizon). Command Mode 3 will result in Mode 3A if fewer than three of the horizon scanner heads are tracking.

- Into Mode 4: from any mode by command Mode 4; from Mode 4A if three or more of the horizon scanner heads reacquire the horizon before the 7-minute Mode 4a time delay period has expired.

- Into Mode 4A: from Mode 4 if two or more of the horizon scanner heads lose the horizon (immediately returns to Mode 4 if any three of the heads reacquire the horizon). Command Mode 4 will result in Mode 4a if fewer than three of the horizon scanner heads are tracking.

When the attitude control system is in Mode 1, 2 or 3 the yaw error signal processing circuits amplify the low level yaw error voltage, frequency shape it to provide rate stabilization, and reamplify it for transmission to the attitude control assembly. A yaw error telemetry signal is also provided. The yaw circuits within the SELA consist of two linear magnetic amplifiers with a resistive-capacitive lead-lag network between them to provide the frequency shaping. Input error signal to this control channel comes from the yaw sun sensor. Rate feedback to provide damping is derived in the lead-lag network. The transfer function of this network is:

$$F(S) = \frac{\theta_o}{\theta_i}(S) = K\frac{(\tau_1 S + 1)}{(\tau_2 S + 1)}$$

where

$$\tau_1 = 15^{+5}_{-10} \text{ sec}$$

$$T_2 = 1.5^{+0.8}_{-1.0} \text{ sec}$$

K = constant

In addition to the lead and lag corner frequencies specified above, there are several lags which occur in the actual circuits. These are all well above the desired 3 Hz nominal bandwidth of the sensor input signals and do not affect the operation of the system.

Following the shaping network the signal is amplified in a second magnetic amplifier. The output of this goes to the attitude control assembly where it drives level detectors to operate the yaw reaction wheel and gas jets.

The telemetry conditioning circuit filters, scales and biases the control signal for delivery to the telemetry system.

In Modes 1 and 2 when the solar array is caged the array error signal processing circuits are similar to those for yaw. The output after passing through a shaping network, however, drives the roll channel. During Modes 3 and 4, the array error controls the array channel in the drive electronics assembly directly from the first preamplifier without shaping.

No shaping network is required for control of the solar array shaft, because damping is provided by friction of the drive and by dynamic braking. A shaping network is required in the SELA array/roll channel during Mode 2 since no damping exists for the vehicle itself (this network is also connected during Mode 1 but has no effect since all control is disabled in that mode). The shaping-network transfer function is

$$F(S) = \frac{\theta_o}{\theta_i} = K \frac{(T_3 S + 1)}{(T_4 S + 1)(T_7 S + 1)}$$

where

$$T_3 = 12.5^{+3.8}_{-1.6} \text{ sec}$$

T_4 = 1.25 ±0.16 sec

T_7 = 0.199 ±0.025 sec

K = constant

The array telemetry conditioning circuit is identical to that in the yaw channel except that a different set of dividing resistors are used to equalize the two telemetry scale factors.

The roll error channel, during Modes 3 and 4, consists of a frequency shaping network and an amplifier to process the error signals from the horizon scanner. During Modes 1 and 2 the horizon scanner portions of the circuit are used only for telemetry.

The source of roll error information is the earth edge tracking horizon scanner. The relation between roll angle and the resulting roll error signal as supplied to the SELA is shown in Figure 3-15.

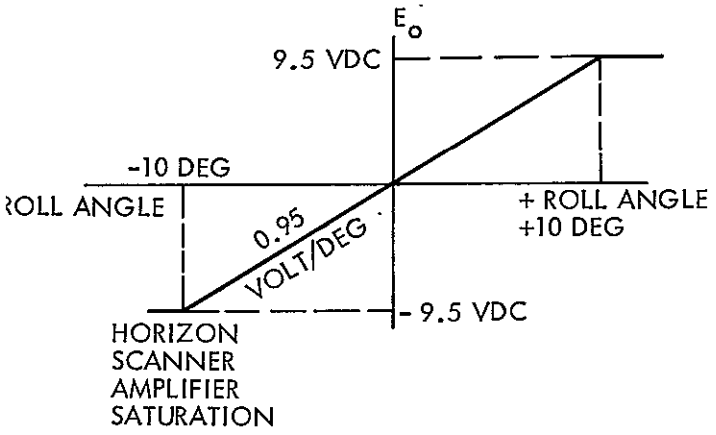

Figure 3-15
ROLL ERROR SIGNAL

The time-varying DC voltages are filtered by a lead-lag shaping network to provide derived rate information. This network is the same as that used for the roll channel in Modes 1 and 2 except that it is slightly more complex, as given below.

$$F(S) = \frac{\theta_o}{\theta_i}(S) = \frac{(T_3S + 1)K}{(T_4S + 1)(T_7S + 1)^2}$$

where

$T_3 = 12.5^{+3.8}_{-1.6}$ sec

T_4 = 1.25 ±0.6 sec

T_7 = 0.199 ±0.025 sec

K = constant

The additional pole associated with T_7 is used to filter out the 16.5 Hz hunting noise which exists on the output of the horizon scanner. In modes 1 and 2 a mode relay removes the unneeded components associated with this pole.

An output amplifier follows the shaping network to amplify the signal before it goes to the attitude control assembly to control the roll reaction wheel motors and valves.

A telemetry signal is provided on the input to determine the amplitude of the roll error. Except for scale factor, this is the same circuit as in the yaw and array channels, and consists of a resistive voltage divider with RC filter to scale the signal and a circuit which adds +2.50 volts to the scaled signal to accommodate the 0- to 5-volt telemetry system.

The pitch error channel duplicates that for roll in Modes 3 and 4, except that no mode switching is involved in the SELA, the input being permanently connected to the horizon scanner. This includes inputs, outputs, scale factors, polarities, and filter time constants.

During earth search and acquisition the pitch channel is controlled by a biased pitch rate gyro rather than by the horizon scanner. Switching is done in the attitude control assembly by a relay. The relay, in turn, is energized during Modes 1 and 2 by a signal from the SELA.

The horizon scanner redundancy logic consists of gates and bistable amplifiers. The amplifiers control logic within the horizon scanner assembly selecting which three of the four tracker heads to use in deriving pitch and roll error signals. By means of the proper switching, any three of the four may be used in the event of failure of the fourth, provided it is possible to detect the failure.

Associated with each of the analog tracking head outputs is a "tracking check" discrete signal. The tracking check signal is "true" only when that particular scanner is tracking a thermal discontinuity (such as a horizon). The sun interference signal is "true" only when the sun location is such that it saturates the bolometer associated with that scanner. Thus, the indication of a properly-operating scanner head

is that its tracking check signal (A, B, C, or D) is true, and its sun interference signal (a, b, c, or d) is false. The "true" signals are between +5 and +10 volts, while the "false" signals are between 0 and +0.7 volts.

The combinations of scanners which are to be used under different conditions, and the computations required for each case, are listed in Table 3-2. The a', b', c', and d' in this table refer to the analog outputs of each independent scanning head. Four combinations definable by the state of two relays exist.

The sensor electronics and logic assembly outputs defining the two states come from bistable magnetic amplifiers located in the assembly. Inputs to the magnetic amplifiers consist of gates which define the states in order to implement Table 3-2.

The required gate equations are:

$$\text{(State No. 1 On)} = \overline{A} + \overline{D} + a + d$$

$$\text{(State No. 2 On)} = \overline{B} + \overline{D} + b + d$$

Table 3-2. Scanner Combinations with Required Computations

Pitch	Roll	Scanner Status	State 1	State 2
$\frac{b' - d'}{2}$	$a' - \frac{b' + d'}{2}$	All operating or A, B, D operating, C out	Off	Off
$\frac{b' - d'}{2}$	$\frac{b' + d'}{2} - c'$	B, C, D operating, A out	On	Off
$\frac{a' + c'}{2} - d'$	$\frac{a' - c'}{2}$	A, C, D operating, B out	Off	On
$b' - \frac{a' + c'}{2}$	$\frac{a' - c'}{2}$	A, B, C operating, D out	On	On

where the signals a, b, and d are the sun interference signals and $\overline{A}$, $\overline{B}$, and $\overline{D}$ are the complements of the corresponding tracking check signals.

Note that the gates described by the above equations will hold the output in some specific state for all possible combinations of scanner head

operation while only those combinations in which three or four scanner heads are properly tracking provide useful two-axis error information. Logic to sense the remaining combinations (two or fewer heads tracking) is provided for as part of Modes 3A and 4A and is used to inhibit operation of the entire system for short periods of time and then recycle the acquisition sequence if normal tracking has not commenced.

Ground command override of these computed states is provided in the horizon scanner electronics so that a preferred set of three scanners can be selected during periods of moon interference.

The power for the assembly is derived from an external converter and inverter. The power supply circuits within the assembly consist of capacitive noise filters plus a negative 3-volt regulator

Certain sensor electronics and logic assembly functions which were embodied on OGO are not necessary on ERTS.

- There is no need to acquire the earth from large distances therefore the small earth detectors have been deleted.
- The fine sun sensor is not needed for ERTS because of the absence of sun-oriented experiments requiring precision solar array alignment. On ERTS, solar array alignment is necessary for power only, and hence, pointing errors up to 8 degrees can be allowed, resulting in a maximum of 1 percent decrease in power output. Furthermore, during portions of the orbit the angle between the solar array shaft and sun line reach 65 degrees, making a fine sun sensor with its ±17-degree field of view unusable. As a consequence the fine sun sensor intensity circuit has been deleted.
- The pitch and roll horizon scanner electronics error signals on ERTS are DC voltages as opposed to suppressed carrier AC voltages utilized on OGO, and hence demodulation is not required.
- The yaw wheel logic is also unnecessary on ERTS since the condition requiring it will not be encountered.

The existing flight SELA will be utilized in its present configuration with these unnecessary functions intact but not connected to the spacecraft wiring harness. They will be connected in such a way that a failure in them would not jeopardize normal ERTS attitude control operation. Subsequent SELA's will be built with these functions deleted, but all of

the SELA's will be wired such that they are electrically interchangeable. Using the existing SELA, without rework, results in a significant cost savings with no significant degradation in reliability. With the newly fabricated SELA's, it will reduce cost to leave out the unneeded functions and delete their functional tests from the test procedure.

Because the SELA on ERTS is identical with the one on OGO except for deleted functions, it is not necessary to requalify the unit. Its packaging configuration is also identical with that of OGO, thus allowing use of all OGO test procedures and test sets.

3.7 ATTITUDE CONTROL ASSEMBLY

The attitude control assembly (Figure 3-16) supplies controlled two-phase AC power to the roll, pitch, and yaw reaction wheel motors, and DC power to the reaction jet solenoid valves. Both wheels and jets create torques for controlling the angular positions of the spacecraft about the pitch, roll, and yaw axes. The control signal inputs to the attitude control assembly are supplied by the sensor electronics and logic assembly, by the rate gyro assembly and by the orbital switching assembly. The attitude control assembly block diagram is shown on Figure 3-3. The assembly is conceptually the same as OGO but requires lower hysteresis switching to reduce body rates on ERTS.

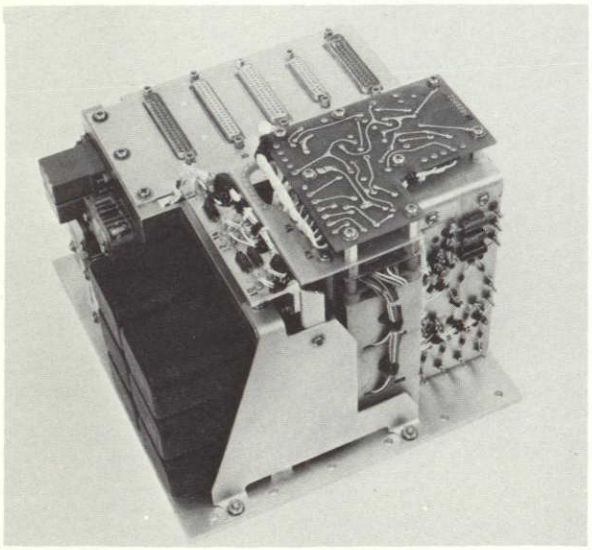

Figure 3-16
ATTITUDE CONTROL ASSEMBLY as shown was used on OGO. ERTS unit will substitute solid-state switching for magamp bistables.

The hardware for implementation consists of bistable amplifiers driving AC motor driver magnetic amplifiers, and bistable amplifiers driving transistor valve drivers. Relays provide switching for the various modes.

Drive functions in the attitude control assembly are accomplished in the following sequence. Each channel contains two double-ended

bistable amplifiers whose inputs are in series. The outputs of one of the double-ended bistables for each channel supply inputs to a motor driver magnetic amplifier; and the outputs of the other bistable (for each channel) supply inputs to the network for driving the gas jet solenoids. The motor bistables are biased to turn on at 50 microamperes corresponding to ±0.4 degree error and the valve bistables are biased to turn on at 125 microamperes corresponding to 1.0 degree error. Hysteresis for all channels is 10 percent in order to achieve tighter limit cycle performance than on OGO.

The bistable outputs supply 0 VDC when "off" and 9.5 VDC when "on." The outputs cannot exist in the region between 0 and 9.5 VDC except in transient. The bistables are double-ended, which means that one output is triggered by positive inputs, and the other output is triggered by negative inputs. Only one output can be "on" at a time.

Each motor driver magnetic amplifier has two outputs -- one with fixed phase and one with reversible phase. The two are separated in phase by ±90 degrees. When turned "on," each output supplies 105 VAC rms square wave to one of the motor windings. A delay circuit in the roll and yaw wheel circuits prevents the associated motor driver magnetic amplifier from reversing direction for 5 seconds.

The valve drivers are transistors which ground the solenoids (supplied with 28 volts) when their inputs are energized. Figure 3-3 shows the logic network for energizing the valve drivers. The gating required to operate the correct individual or pair of thrusters is implemented with diodes in redundant quads.

Relays are located inside the assembly for control signals for the various modes. All drive outputs are inhibited during Modes 1 and 2a by opening relay contacts which thereby remove 2461-Hz power from the bistable amplifiers. During Modes 3 and 4, the yaw gas bistable input is removed by a relay actuated from the SELA. In Mode 4, yaw gas may be enabled by separate ground command for use during ΔV maneuvers. Mode 4 is enabled by a relay in the orbital switching assembly.

The ERTS attitude control assembly is basically identical with the OGO assembly except for reaction wheel count telemetry and motor direction telemetry. These functions are now incorporated in the orbital switching assembly in ERTS.

The bistable magnetic amplifiers used on OGO will be replaced with solid state versions, achieving the same function with much tighter tolerance control on trip point and hysteresis parameters. The new units will be electrically and mechanically interchangeable with the old units. As a result of the bistable change, the new attitude control assembly will require a qualification test.

The existing OGO flight spare assembly will be modified to the extent that it will be mechanically and electrically identical to the "new build" attitude control assemblies for ERTS.

3.8 DRIVE ELECTRONICS ASSEMBLY

The function of the drive electronics assembly (Figure 3-17), is to control two-phase AC power to the solar array shaft motor. Its block diagram is incorporated in Figure 3-3. As with the attitude control assembly, the output is "bang-bang," i.e., either full power or no power is applied. The input for the solar array drive circuit is the sun sensor array signal, supplied by the sensor electronics and logic assembly during Modes 3 and 4, and is the solar array shaft position signal as supplied by the sine output of the solar array shaft position resolver during Mode 2. The solar array drive circuit is inhibited during Mode 1 and whenever the payload is functioning. The solar array drive circuit voltage applied to the reference phase winding of the motor remains energized for approximately 1 to 3 seconds after the voltage to the control phase of the motor has been de-energized; this provides dynamic braking for the motor. The drive electronics assembly also provides a signal to the SELA to signify that the solar array is at 0 degrees. The SELA uses this signal during acquisition to initiate the next acquisition mode after the solar array has been aligned to 0 degrees.

The drive electronics assembly also processes two signals from the solar array shaft resolver to provide voltages which vary from 0 to 5 volts

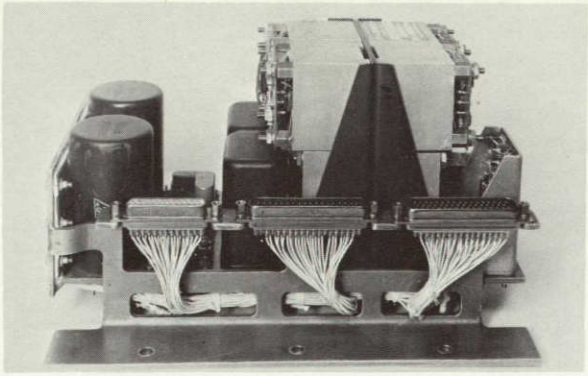

Figure 3-17
DRIVE ELECTRONICS ASSEMBLY
provides control power for the solar array motor.

to telemetry for determining shaft position. Also a three-level analog signal conveys the forward-off-reverse state of the motor drive signals.

The solar array drive circuit is a three-stage amplifier consisting of a low level DC magnetic amplifier, a double ended bistable magnetic amplifier, and an AC motor driver magnetic amplifier, all in tandem. The motor driver has two outputs—one with fixed phase and one with reversible phase. The two are separated in phase by ±90 degrees. The reversible phase output is rectified and delayed, then fed back into the fixed phase control input which turns on the fixed phase output. This allows the fixed phase output to remain energized after the reversible phase output has been de-energized, providing dynamic braking on the motor.

Array angle information is obtained from a resolver rotating with the solar array shaft. The solar array shaft position resolver has two 2461 Hz amplitude-modulated square wave outputs, one of which is proportional to the sine of the shaft angle and the other to the cosine. The output of each is an AC signal whose phase is reversed to convey negative values. Identical circuits in each channel demodulate these signals converting them to DC voltages which vary between 0 and 5 volts over the range of resolver angles.

There are mode control relays in the drive electronics assembly which are activated by the SELA for inhibiting the solar array drive during Mode 1. One of the relays also switches the input of the solar array drive circuit to either the sun sensor array signal or to the sine component of the shaft position signal. The null position for the solar array shaft when driven by the shaft position signal is at 0 degrees.

The ERTS drive electronic assembly derives from the OGO assembly with the deletion of the orbital plane experiment package drive

channel. The existing OGO spare drive electronics will be used on ERTS without change but with the unused channel not connected to the spacecraft wiring harness. Subsequent units will have these functions deleted. Since these changes are minor, the ERTS drive electronics assembly will not be requalified.

3.9 ORBITAL SWITCHING ASSEMBLY

The orbital switching assembly is a new unit which houses the hardware to convert the OGO concept to ERTS. It is a low-risk design utilizing proven electronic devices and packaging techniques. It contains the following discrete functions:

- Yaw gyro frequency shaping
- Yaw gyro drift offset
- Mode 4 control
- Reaction wheel revolution counters
- Pitch and roll reaction wheel momentum controllers
- Yaw gas enable
- Inhibit circuits for solar array drive and pitch and roll gas

A block diagram of the assembly is shown in Figure 3-18.

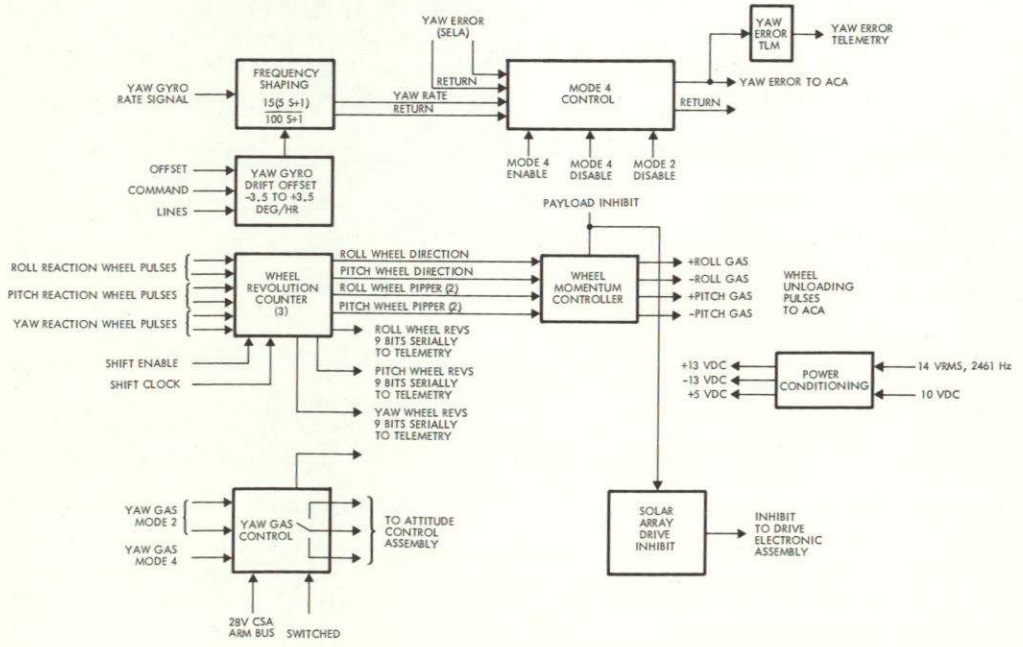

Figure 3-18
ORBITAL SWITCHING ASSEMBLY block diagram

The yaw gyro frequency shaping and drift offset circuits consist of a summing amplifier which adds a ground commandable offset signal to the gyro signal, a frequency shaping network, and an output amplifier to provide gain. The transfer function of the shaping circuit is:

$$F(s) = K \frac{(\tau_7 S + 1)}{(\tau_8 S + 1)}$$

where

$\tau_7 = 5 \pm 1$ second

$\tau_8 = 100 \pm 20$ seconds

$K \cong 15$

The amplifier output goes to the attitude control assembly (in Mode 4) where it drives level detectors to operate the yaw reaction wheel and, when enabled, the yaw gas jets.

Yaw gyro drift offset is provided by a set of logic switches driving a resistor ladder network. The logic switches decode three input ground command lines into one of eight possible states. The output of the ladder network is one of eight possible voltages added to the yaw gyro signal at the input of the yaw gyro frequency shaping network.

The commandable offset can handle a combination of gyro and electronic circuit drifts up to ±4.0 deg/hr in its eight possible steps as follows: ±0.5, ±1.5, ±2.5, ±3.5 deg/hr. The maximum uncompensated drift error under these conditions is ±0.5 deg/hr which corresponds to a contributed yaw bias error term of ±0.2 degree.

Switching of the input to the yaw drive circuits between the sun sensor signal (Modes 1, 2, and 3) and the yaw gyro is accomplished in the Mode 4 control relay.

Reaction wheel revolution counters provide telemetry for the three reaction wheels in the ERTS attitude control system. There are three identical circuits, one for each wheel. Each consists of analog circuitry to condition the outputs of two Hall effect sensors associated with each wheel, a digital counter

and a storage-shift register. The information provided by these circuits is the net number of one-eighth revolutions each wheel has moved from some arbitrary zero position. Eight magnets located on each wheel induce pulses in the two Hall effect sensors independent of wheel speed. Each pulse is approximately 5 ± 1 degree wide and the two sensors on each reaction wheel overlap by 2.5 ± 1 degree. The 20-millivolt output of each sensor is amplified and thresholded against a reference voltage to provide a standard logic level output. There is a small amount of hystereses in the thresholding process to significantly increase noise immunity, although the Hall effect sensors already have signal-to-noise ratios of about 10 to 1. The order of occurrence of the pulses from the two sensors determine whether each pair should add or subtract from the count accumulating in the 16-bit up-down counter. At the appropriate telemetry word of each frame the contents of each counter are parallel transferred to an 16-bit shift register and on two successive words shifted out serially to the telemetry system. Maximum wheel speed is 1300 rpm giving rise to a maximum pipper rate of 174 pulses/second.

The reaction wheel momentum controller circuits detect when either the roll or pitch reaction wheel reaches 50 percent of its maximum speed and issue a gas valve command to reduce that speed to 37 percent of maximum. This function is intended to insure that at least 50 percent of each wheel's momentum storage capability remains when the payload begins taking pictures thus guaranteeing that neither wheel will saturate during the 20-minute period of payload operation.

This function is normally enabled. It may be disabled by either an inhibit signal from the payload, or by ground command. This is accomplished by disabling the output stage so that it may still be turned off despite a failure anywhere in the circuits previous.

The circuit operates by feeding one of the logic level pipper signals from the reaction wheel revolution counter circuit into a one-shot multivibrator and filtering the output to obtain a DC level which is proportional to wheel speed. This voltage is compared to a reference voltage representing 50 percent wheel speed. The comparator, which has a hysterisis characteristic, then fires a one-shot multivibrator whose output is gated with a wheel direction signal to momentarily actuate a gas firing in the proper direction to unload the wheel. There are two complete circuits, one for the roll axis and one for the

pitch axis. No controller is necessary on the yaw axis since its reaction wheel has more than enough momentum storage capability for that axis, and its gas control is normally inhibited. The gas pulse which is issued by these circuits is scaled to reduce the reaction wheel rpm (and hence momentum) to 37 percent of maximum speed for each channel.

Yaw gas may be allowed to fire during Mode 4 by actuation of the yaw-gas control relay. Yaw gas may be necessary during the velocity correction maneuver to manage the potentially increased yaw torques produced by the thruster misalignment relative to the spacecraft center of gravity.

This function is implemented by interrupting the yaw channel mode control relay in the attitude control assembly with a relay in the orbital switching assembly. A ground command enables the function, and either a ground command or Mode 2 command disables it.

Because solar array motion would affect picture quality, array drive is inhibited during image sensor operation. The solar array drive inhibit is implemented with a pair of switching transistors which short out the error signal in the drive electronics assembly.

The orbital switching assembly uses the "new ERTS boxes" packaging technique which is described in (Section 3.2). The unit consists of two slices, one three-board slice and one two-board slice. The boards in the three-board slice are all identical and constitute the three reaction wheel revolution counters. There are 66 parts on each board, or 198 parts in the slice. The two-board slice contains 160 parts or about 80 parts per board. These two boards hold the remaining six functions.

Most circuit elements in the orbital switching assembly are company-stocked TRW preferred parts. The integrated circuit logic elements are the low power type, to conserve spacecraft power. All other components are readily available TRW PT specified parts.

3.10 CONTROL SWITCHING AND MOMENTUM CONTROL ASSEMBLIES

The functions added by the control switching assembly (Figure 3-19) are:

- Gas logic control
- Gas jet disable control

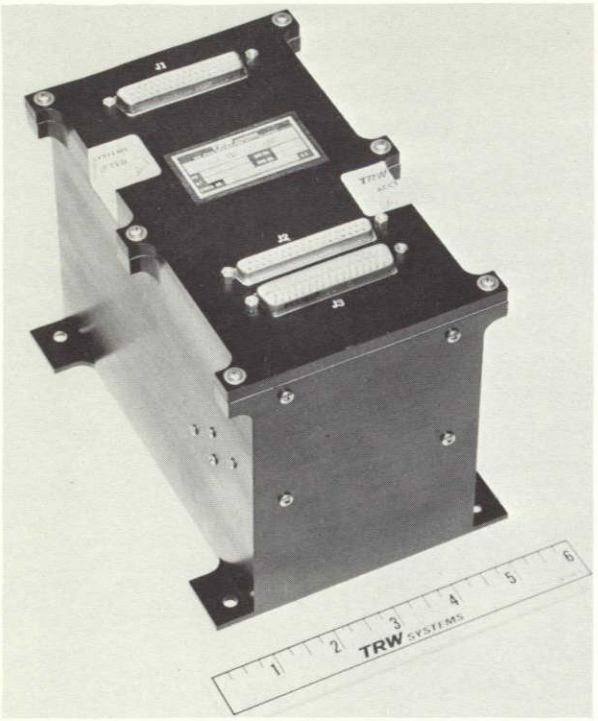

Figure 3-19
CONTROL SWITCHING ASSEMBLY

- Momentum control
- Pitch rate gyro control

This assembly has been used in OGO 3 and later observatories. it allowed increased flexibility in operating OGO 3 and 4 and saved these spacecraft from early gas depletion. It is unchanged for ERTS. It permits control of gas firings which may be caused by noise or body oscillations. This function, which is implemented in +roll, -roll, +pitch, and -pitch, may be enabled by ground command when the attitude control system is not in Modes 1 or 2. Gas firings are minimized by inhibiting the gas solenoid drivers for a nominal 15 seconds after the turn-on of the reaction motor magnetic amplifiers. To enable the gas logic control, two commands are required, spin arm command and a gas logic enable command.

Inhibition of any or all gas jets (+ roll, - roll, + pitch, + yaw, and - yaw) may be inhibited by ground commands. To inhibit gas firing, two commands are required, a spin arm command and a gas jet disable command. To return the spacecraft to normal, an enable command is required after first arming the bus.

The momentum control assembly, shown in Figure 3-20, allows gas to be emitted in any of the six directions by ground command. An arm command and the appropriate spin axis selection commands are required. Upon transmission of these commands, the appropriate gas valves are driven on for 1.2 seconds and then automatically cut off by a timer.

3.11 INVERTER ASSEMBLY

The inverter assembly (Figure 3-21) supplies AC power to the magnetic amplifiers, reaction wheels, and solar array shaft motor and is

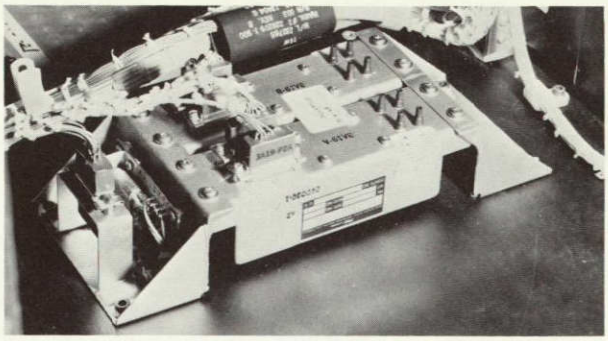

Figure 3-20
MOMENTUM CONTROL ASSEMBLY provides manual control of control gas jets.

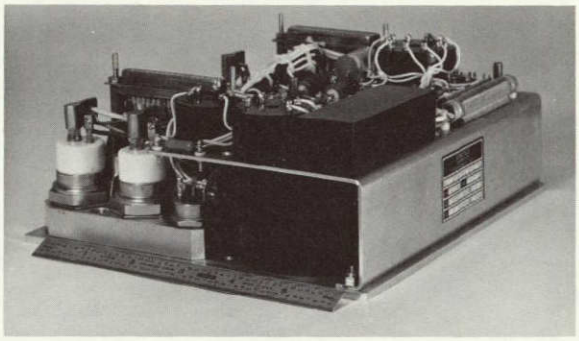

Figure 3-21
ACS INVERTER ASSEMBLY supplies 400 Hz square wave power.

used for pitch rate gyro excitation. The inverter provides unregulated 400-Hz power to operate reaction wheels and motors, and regulated 400-Hz power for precision requirements. Total power output is 70 va continuous power plus 400 va on a low (wheel on) duty cycle. The inverter employs a precision 400-Hz oscillator and high power switching output transistors.

3.12 REACTION WHEEL ASSEMBLIES

Three reaction wheel assemblies are used on ERTS, one each in roll, pitch, and yaw. These units are the same type as used on OGO and are manufactured by Bendix Corporation.

Each wheel assembly consists of an inertia wheel, a two-phase motor, wheel position indicator, and a thermistor, mounted in a hermetically sealed housing. Figure 3-22 shows the outline dimensions of the wheels. Figure 3-23 is a cutaway view of the yaw wheel illustrated by an OGO pitch or roll wheel, which has its connections on the top of the housing. One of the modifications proposed by the vendor, to locate the connector on the base of the housing, is incorporated in Figure 3-22. This arrangement, a minor modification, greatly facilitates assembly.

The inertial wheels are balanced precisely, with the weight concentrated in the rim to attain a high inertia-to-weight ratio. The motor is an inside-out two phase induction motor. The squirrel cage rotor of the motor is assembled as part of the inertial wheel, which is mounted in

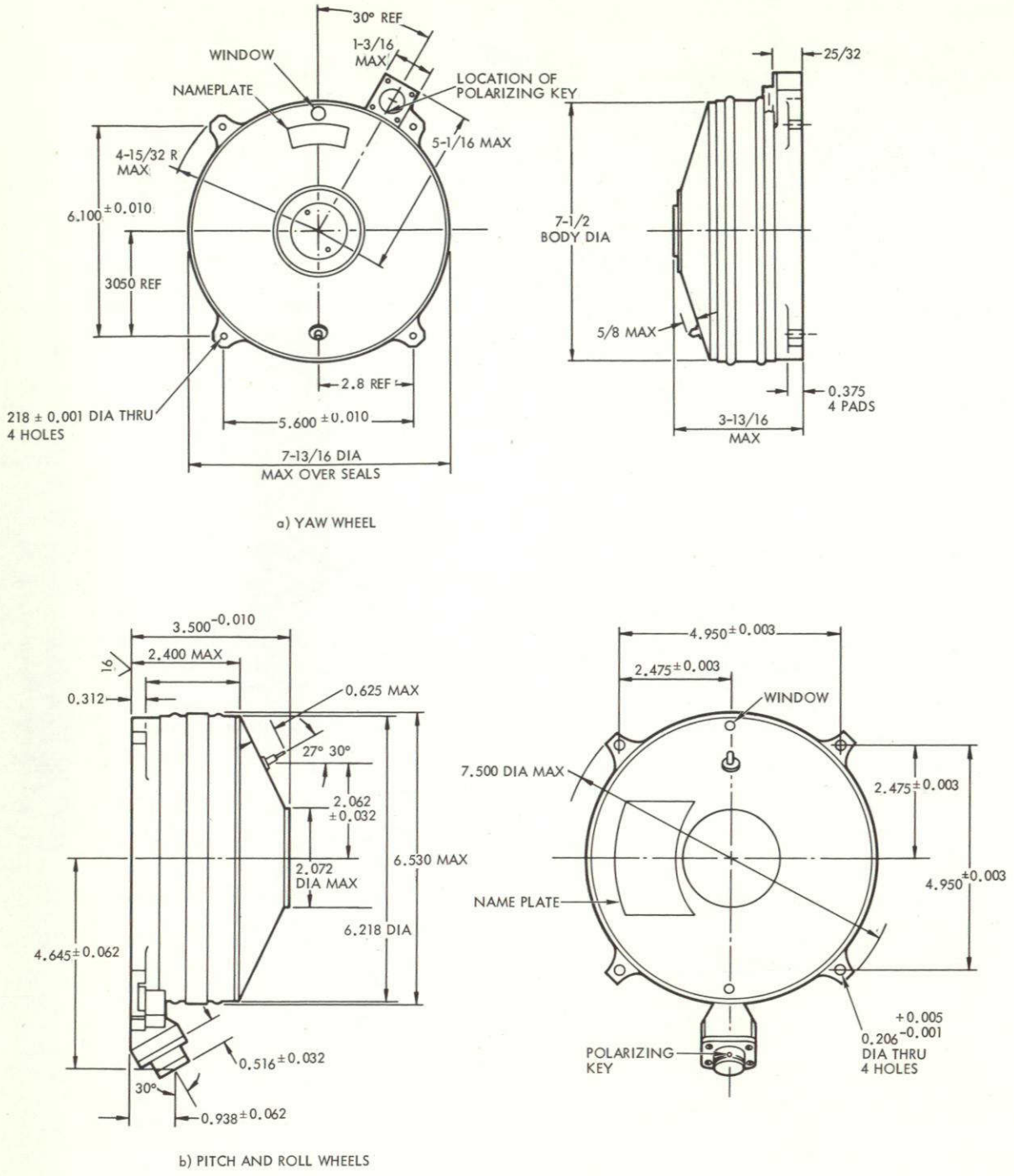

Figure 3-22

REACTION WHEEL ASSEMBLY outline drawings

two size R-8 deep-groove precision bearings. The reaction wheel contains a Hall effect device used as a position indicator, a second minor change in these wheels relative to those on OGO. This device produces a pulse output once per 1/8th revolution, the amplitude of which is independent of wheel speed. The pulses are be counted to determine the

Figure 3-23
CUTAWAY OF THE YAW REACTION WHEEL

number of turns the wheel has made, and the time between pulses conveys wheel speed information.

3.12.1 Operation

The reaction wheels apply torque to the spacecraft for controlling the angular positions about the pitch, roll, and yaw axes. The power to drive the reaction wheels is supplied by the attitude control assembly. As power is applied to one of the reaction wheels, the motor torque accelerates or decelerates the rotor, changing its angular momentum. The reaction torque associated with this change is transmitted through the unit mounting pads to the spacecraft structure, thus torquing the spacecraft in response to control commands.

The momentum storage capability of the roll and pitch, reaction wheels are identical (Table 3-3). The required momentum capacity of each reaction wheel system is established by three considerations: (1) required vehicle maneuvers, (2) cyclical disturbance torques, and (3) temporary storage for momentum resulting from noncyclic disturbance torques.

3.12.2 Design

The wheel and rotor assembly are the only moving parts. These consist of the wheel, the squirrel cage rotor of the motor, two precision ball bearings, two lubricant storage rings, two labyrinth lubricant seals, and the wheel position magnets.

The motor is a 32-pole, two-phase induction unit. The field windings are enclosed within the rotor and mounted to the stationary portion of the housing, while the rotor completely surrounds the stator.

Table 3-3. Reaction Wheel Characteristics

	Pitch/Roll	Yaw
Stall torque, in.-oz	4	10
Moment of inertia, slug ft^2	0.0025	0.01
Maximum speed, rpm	1250	1250
Momentum storage, ft-lb-sec	0.4	1.66

The motor operates on two-phase, 400 Hz, 115 volts rms, square wave voltages which are 90 degrees out of phase.

The bearings that support the wheel are Barden Type R8, Class III. The lubricant reservoirs are porous nylasint plastic washers impregnated with Plexol 201 type lubricant. In case of failure of the hermetic seal of the case, labyrinth seals are provided to decrease the lubricant evaporation rate.

To provide the capability for sensing very slow wheel speed, the position indicator has been changed from the velocity sensitive magnetic pickup used in the last of the OGO's to a Hall effect device. This device consists of powdered indium arsenide crystals mounted on a suitable substrate. It measure 0.125 x 0.100 inch and is 0.020 inch thick.

The device has a DC resistance of 42 to 50 ohms and requires 30 milliamperes of excitation current, thus a DC electrical source of about 1.5 volts is used for excitation. As shown in Figure 3-24, when plates A-A are attached to each end of the device, the current normally would flow in a laminar manner from one electrode to the other. Two additional electrodes, B-B, are attached to perpendicular surfaces of the device. The magnetic field represented by the arrows labelled ϕ travels through the device in a direction mutually perpendicular to the two sets of electrodes. With this arrangement, the output voltage is given by $V_{out} = KI_{in}\phi$.

With the reaction wheel configuration, the spacing between the Hall device and excitation magnet, nominally 0.005 inch, and an output of at least 0.02 volt is obtained. Bench tests have verified that this output level can be readily attained. Since the output impedance of the device is

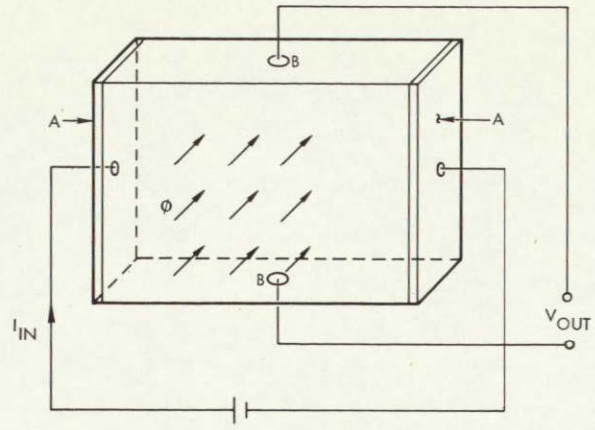

Figure 3-24
HALL EFFECT DEVICE

low, noise interference is not likely to be a problem. An amplifier in the orbital switching assembly amplifies the output to the level required by the remaining control logic. To achieve bidirectional counting, two Hall devices are installed.

A thermistor is mounted near the lower bearing of the wheel housing to monitor the temperature of the motor stator and lower bearing during tests as well as in flight.

The leads from the reaction wheel assembly are brought out through a hermetically sealed connector that is soldered to the base housing. The leads are soldered into the pins and the pins potted in a plastic material.

The assembly is packaged in a flat, dome-shaped, two-piece cylindrical can, as shown in Figure 3-22. Mounting pads, the electrical connector, the evacuation tube, and the window are also shown in that figure. The window is provided for observing the rotation of the wheel during ground tests. The window is first plated and then soldered to a metal insert set in the case which has the same temperature coefficient of expansion. This technique has been successfully qualified and flown on the Vela spacecraft.

The two-piece cylindrical can is a hermetically sealed magnesium housing filled with a mixture of helium and oxygen at 2 psia. A special ring seal and tear strip are provided to permit easy opening and closing of the hermetic seal during inspection and assembly.

As manufactured, the angular momentum vector is within 0.05 degree of perpendicular to the plane of the mounting pads. The allowable alignment error budget for the wheel assembly is ±0.02 degree. This accuracy is achieved by inserting shims under the mounting pads during acceptance testing.

3.13 PNEUMATICS

A conventional cold gas expulsion system applies control torques about the three spacecraft axes upon command from the attitude control assembly. The ERTS pneumatic system differs little from that of OGO. The lower body rates together with reduced body inertias compared to OGO permit lower control torques. The pneumatic booms can thus be shortened from the OGO configuration, and the shorter length allows the booms to be fixed to the body, eliminating the need for post launch deployment. All other pneumatic components are unchanged, thus allowing the use of many OGO spare components for ERTS. A schematic of the pneumatic system is shown in Figure 3-25. Figure 3-26 shows the installation of the system in ERTS.

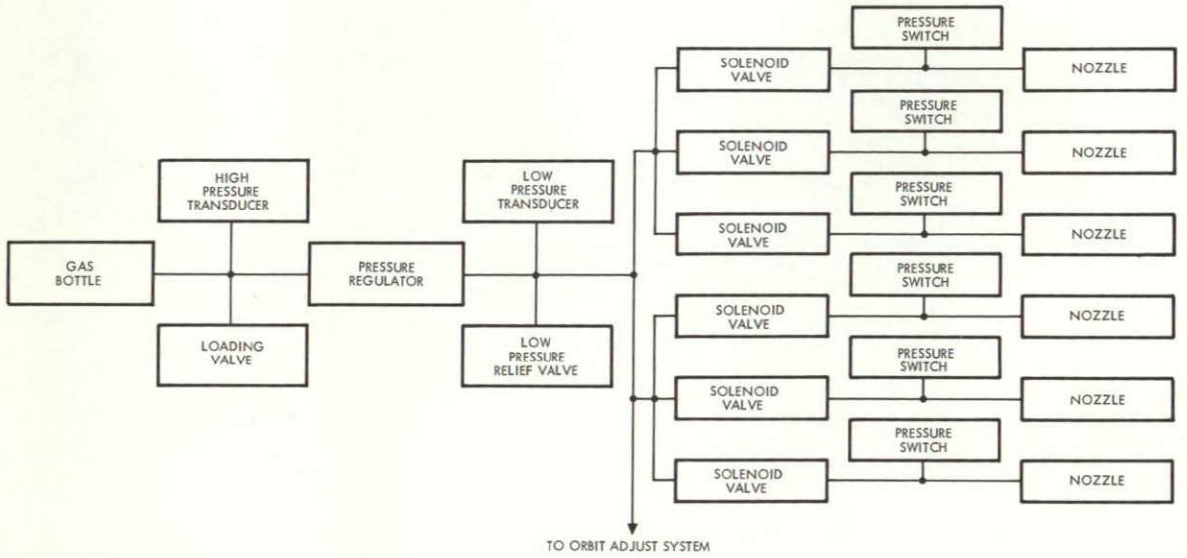

Figure 3-25

ERTS ATTITUDE CONTROL PNEUMATICS SYSTEM uses all OGO flight-qualified components

The system includes a storage vessel (or propellant tank) filled with krypton under high pressure, a pressure regulator and relief valve, six solenoid valves, six pressure switches, six boom-mounted nozzles, high and low pressure transducers, a fill valve, and the tubing and manifolding necessary to connect the system components. The working fluid is krypton, an odorless, tasteless, colorless, non-toxic, inert gas.

As heavy as water at 4000 psi, krypton delivers a low specific impulse, but allows a large total impulse to be stored in a given volume.

Table 3-4 summarizes the capabilities of the pneumatics system for attitude control. The system also provides propellant at a regulated pressure for the orbit adjust system, described in Section 10.

Table 3-4

Capabilities and Characteristics of the Attitude Control Pneumatics System

Thrust level, lb	0.05
Specific impulse, sec	37
Propulsive efficiency (minimum, percent)	95.6
Propellant storage pressure, $lb/in.^2$	4000
Propellant supply pressure, $lb/in.^2$	50
Propellant weight ($1299\ in.^3$), lb	57*
Attitude control, lb	5.4
Leakage, lb	1.5
Residual (50 psia), lb	0.8
Attitude control total impulse, lb-sec	200

*Includes 49.3 pounds for orbit adjustment.

3.13.1 Pressure Vessel

The pressure vessel is a welded titanium sphere with an internal volume of 1299 cubic inches. At 4000 psia, the vessel stores 57 pounds of krypton, 7.7 pounds for attitude control, leakage and residuals, the remainder for orbit adjustment. The vessel is designed for a maximum storage pressure of 5175 psia. The system capability can therefore be increased if necessary.

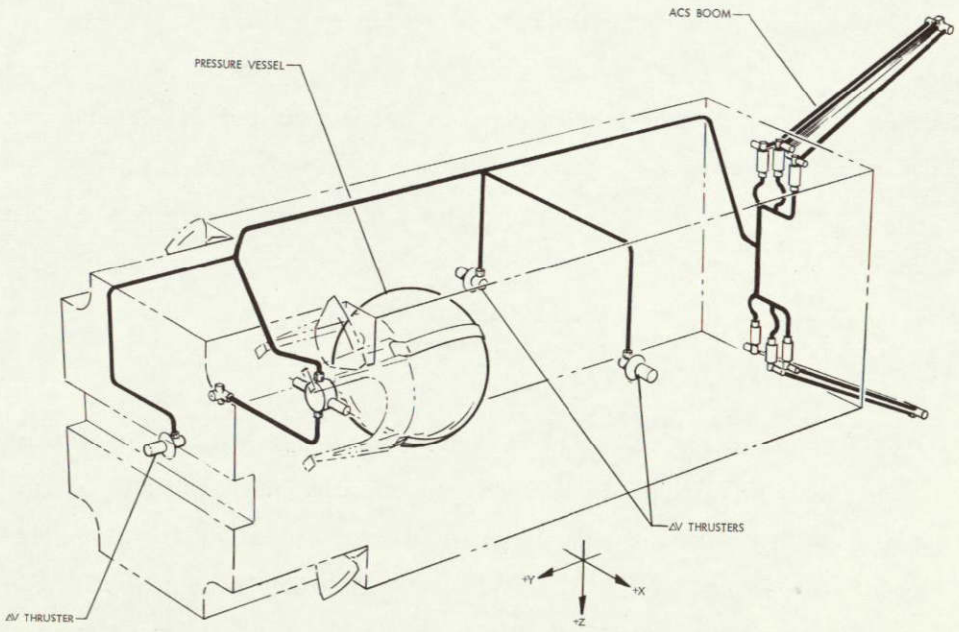

Figure 3-26

PNEUMATIC SYSTEM installation includes thermal thrusters described in Section 10.

3.13.2 Pressure Regulator and Relief Valve

The regulator reduces the pressure of the krypton to a constant level of 50 psi for delivery to the valve-nozzle combinations. The regulator assembly also includes a relief valve and manifolding for the high and low pressure transducers. The relief valve protects the regulated pressure side of the pneumatics system in the event of thermally induced gas expansion in the line between the regulator and solenoid valves or internal leakage of the regulator. The pressure transducers provide telemetry signals for monitoring the system status.

3.13.3 Solenoid Valve

The solenoid valves control the flow of propellant to the nozzles and thus control the thrust. The valve is a coaxial unit incorporating a single actuating coil and a poppet with a hard seat. No measurable leakage has occurred on the 36 valves flown on six OGO's. The propellant leakage allowance for ERTS should therefore be available for additional attitude control capability.

3.13.4 Nozzles and Booms

The booms provide a 4-foot lever arm for yaw and roll and 2.25-foot for pitch. The booms are gold-plated to increase their temperature in sunlight, and the propellant lines mounted on the booms act as heat exchangers to increase the propellant temperature and delivered specific impulse. The nozzles have a throat diameter of 1/32 inch and an expansion ratio of 80. The nozzle propulsive efficiency is greater than 95 percent. Pressure switches upstream of the nozzles are used for telemetry verification of thruster operation.

3.14 ARRAY DRIVE MECHANISM

The array drive mechanism (Figure 3-27) is an electromechanical device which uses the unique wabble gear principle. Input excitation is 115 volt, 400 Hz, two-phase, square wave power supplied by a static inverter. The prime mover is a size 11 servo motor with gearhead. The output rotation is approximately 1.5 deg/sec at an output load torque of 50 in-lb. The system application on ERTS as on OGO uses the drive in an on-off mode of operation.

Figure 3-27
EXTERIOR VIEW of the array drive mechanism

As shown in Figure 3-28, motion is transmitted from the servo motor through a 40:1 gear head. The gear head output pinion meshes with a 139-tooth ring gear, providing another reduction of 6.04:1.

The outer surface of the ring gear carrier is not concentric with the drive mechanism centerline, but is accurately machined to an axis which is skewed at an angle of 2 degrees 14 minutes with the drive centerline. Mounted on the skewed surface are two larger diameter bearings, also of small cross section and angular contact. The outer races of the two skew-mounted bearings hold a flange to which the input wabble gear is attached. All of the mechanism

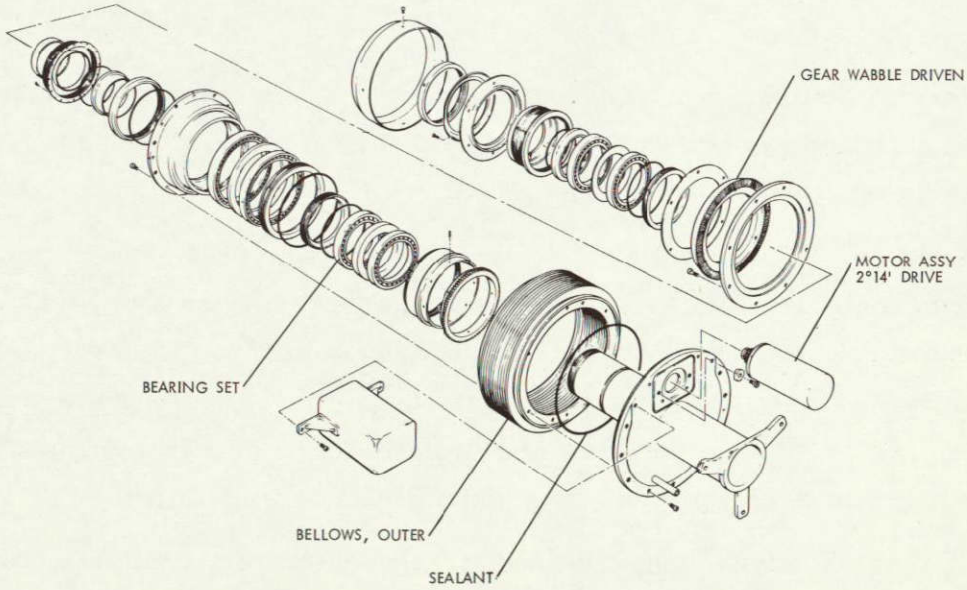

Figure 3-28
EXPLODED VIEW of the array drive assembly

described above, including the motor gearhead, is contained in a welded bellows hermetic seal. The two bellows, an inner and an outer assembly, also serve as load-carrying members to convey the load torque to the structure by constraining the input wabble gear from rotation.

The final drive members of the mechanism are the wabble gears. The input wabble gear is constrained to its irrotational wobbling motion by the bellows assemblies. This gear has 100 teeth. The output wabble gear is completely in mesh with the input gear at one point only. The output gear has 99 teeth, and is mounted so that it rotates about the main centerline of the drive mechanism. The wabble gear mesh provides 99:1 reduction. The output wabble gear carrier is held by split outer race bearings of small cross section. Attachment to the load shaft is by means of a key. A Belleville washer slip clutch between the output gear and its carrier limits the torque to 500 in-lb. Total speed reduction, motor to output shaft, is about 24, 000:1.

3.15 ATTITUDE AND RATE DETERMINATION

Body attitude and rate data is needed for accurate determination of picture element positions. Attitude data is primarily required to meet the requirement for 2 nautical mile accuracy in absolute element location of RBV and MSS pictures. Body rate data is used to remove geometric error in MSS pictures. Further discussion of this method is included in Volume 4, Section 7.

The ERTS design obtains earth pointing from horizon trackers to determine attitude error in pitch and roll. Error from the yaw gyrocompass is used for yaw pointing data.

Body rates are not directly measured by any on-board instrument. Instead the primary forces producing spacecraft motion are measured indirectly through counting reaction wheel revolutions. This wheel position data is used together with pointing history from trackers and gyrocompass to develop precise short term relative pointing history. This process is accomplished in ground digital computation.

Characteristics of the instrumentation used for measuring and telemetering this data for later use are

	Sample Rate (sec)	Least Count	Full Scale
Pitch error	1.152	0.01 deg	±2.5 deg
Roll error	1.152	0.01 deg	±2.5 deg
Yaw error	1.152	0.01 deg	±2.5 deg
Pitch wheel position	1.152	1/8 Rev.	8192 Rev.
Roll wheel position	1.152	1/8 Rev.	8192 Rev.
Yaw wheel position	1.152	1/8 Rev.	8192 Rev.

CONTENTS

4. COMMUNICATION SYSTEM

4.1 FUNCTIONAL DESCRIPTION

The ERTS communication subsystem transmits spacecraft data to and receives commands from the earth. In addition it cooperates with ground-based tracking networks to permit measurement of range and range rate for precision orbit determination.

The data communicated includes digital telemetry at 1 and 32 kbits/sec and video data at rates corresponding to 4 MHz bandwidth and 15 Mbits/sec. Telemetry data is processed and supplied to the communication system by data processing equipment described in Section 5. Video data is generated by payload sensors which operate intermittently in generating pictures of the earth.

Six carrier frequencies are used for communication and the system as a result of redundancy, includes four receivers and six transmitters plus incidental power monitoring and switching equipment. Antennas and radio frequency coupling or diplexing equipment makes up the antenna subsystem described in Section 6. Figure 4-1 shows the entire communication subsystem in block diagram and Table 4-1 summarizes its operating characteristics.

For convenience the communication subsystem is partitioned into three assemblies grouped by carrier frequency and function:

- STADAN-VHF equipment
- Unified S-band equipment
- Wideband video equipment (S-band)

In most respects the VHF and the USB systems provide redundant functions as far as the spacecraft is concerned. Their presence, however, permits status checking and commanding from two of NASA's principal tracking and data acquisition networks. Tracking differs between these networks, STADAN providing angle tracking data only while the MSFN can provide range and range rate as well as angle information.

The VHF communication equipment, Figure 4-2, incorporates two redundant 0.5 watt, 137.86 MHz transmitters for 1 kbit/sec real-time

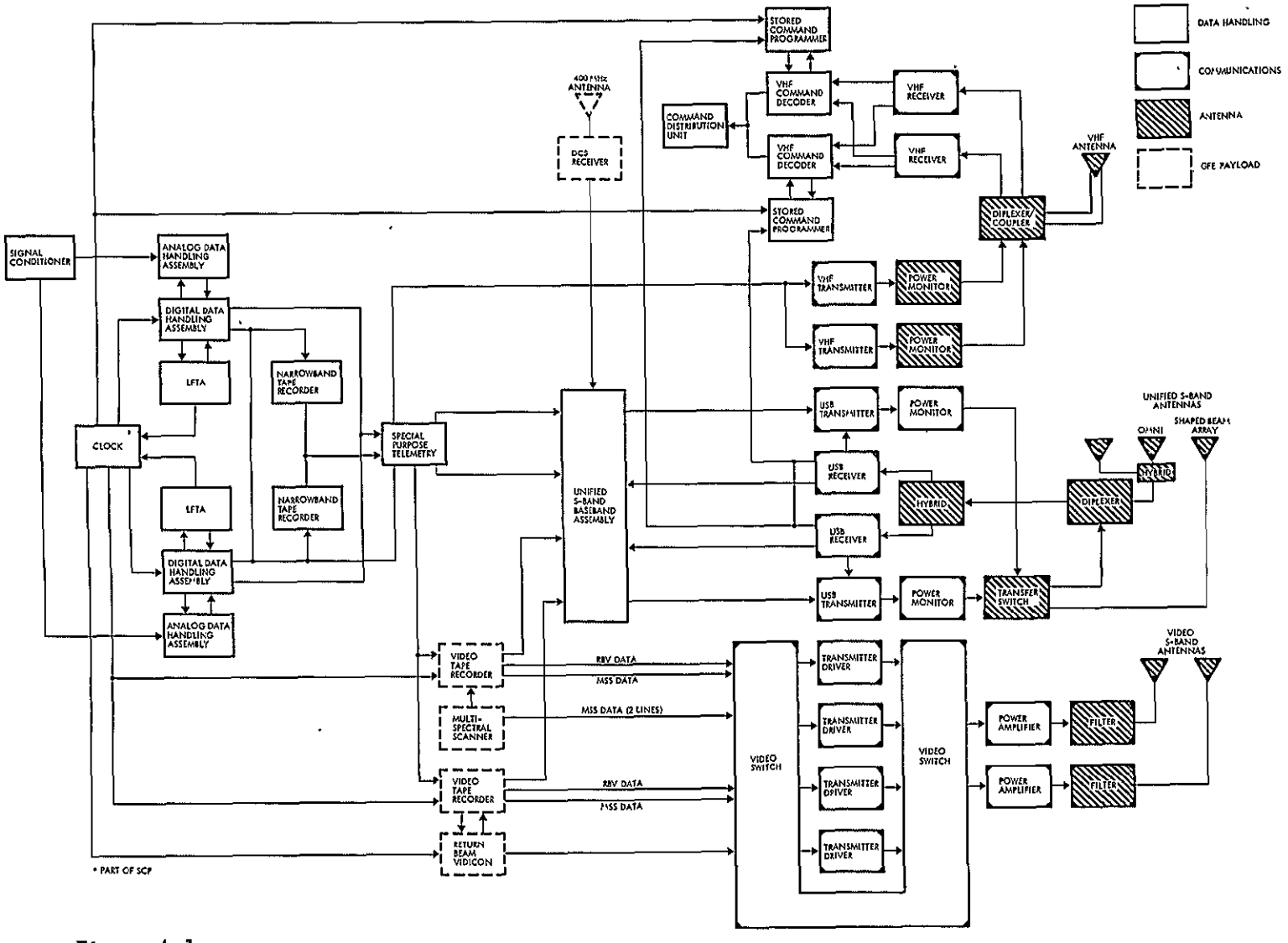

Figure 4-1
COMMUNICATION SUBSYSTEM block diagram

Table 4-1. Communication Subsystem Characteristics

	Carrier Frequency (MHz)	Modulation Type	Sub Carriers (kHz)	Noise Figure (db)	Power Output (watts)	Link Margin (db)
Receivers						
VHF command	154.2	AM-FSK	8 to 8.6	4		23.6
S-band command	2106.4	PM		9		40.3
Transmitters						
VHF data	137.86	PM			0.5	23.7*
Video 1	2229.5	FM			10/20	37.7**
Video 2	2265.5	FM			10/20	9.4**
Ranging data	2287.5	PM	165		0.8	20.8
SCO data			225			7.2
			300			
			1.024			
			1.25			

*1 kbit/sec

**Ref. 30 ft Antenna

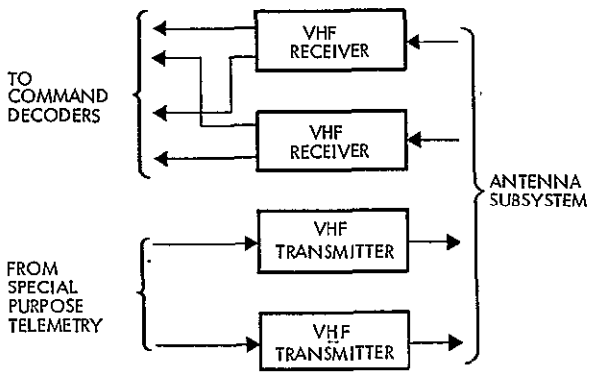

Figure 4-2
VHF COMMUNICATION ASSEMBLY provides tracking, telemetry, and command compatible with STADAN

telemetry and for tracking. These transmitters can also be used to send 32 kbits/sec stored telemetry from the narrowband tape recorders. Two 154.2-MHz AM command receivers operate continuously in linear polarization diversity, providing both equipment and functional redundancy. These are retuned OGO receivers; the receivers for the first spacecraft are already fabricated and tested.

The unified S-band communication assembly, Figure 4-3, provides uplink commands and downlink communications for real-time and stored telemetry, DCS 100-kHz bandwidth analog data, and 1 kbit/sec timing and attitude data for each of the two payload video tape recorders.

The unified S-band communication assembly includes two unified S-band transponders. Each transponder consists of a phase-lock receiver,

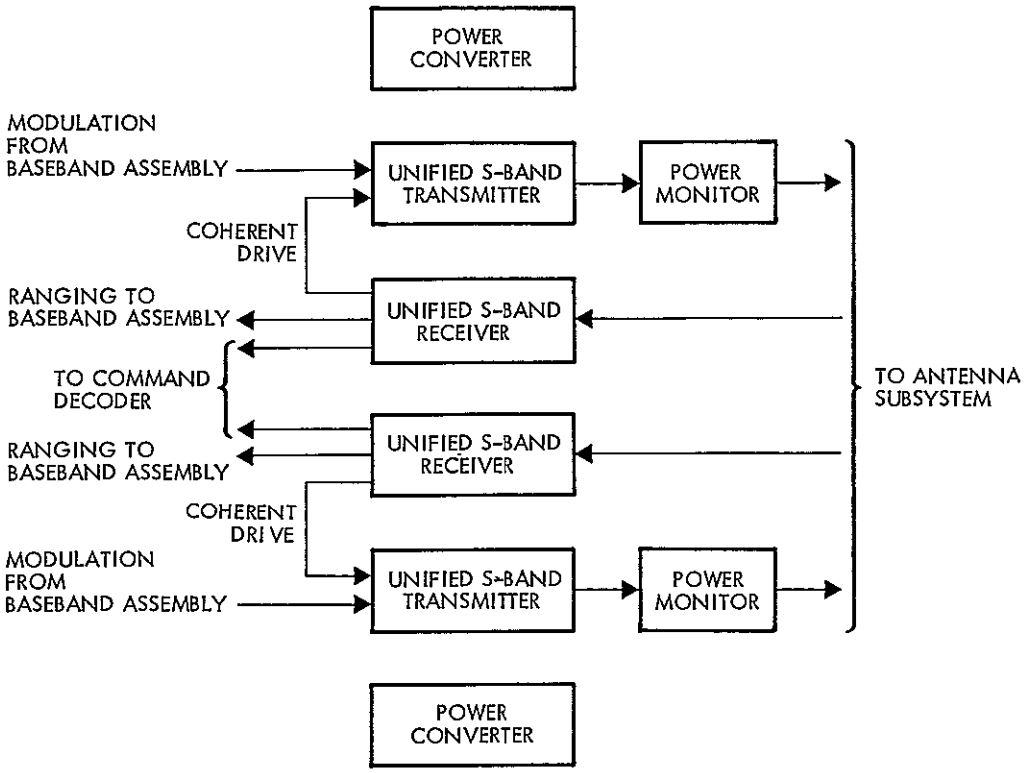

Figure 4-3

UNIFIED S-BAND COMMUNICATION ASSEMBLY provides tracking, telemetry, and command compatible with the MSFN

an 800-milliwatt transmitter, a power monitor, and a power converter. The 2287.5-MHz transmitter can be operated coherently with the uplink carrier or from its own stable crystal oscillator. Its output is phase modulated by the composite baseband from the baseband assembly unit to generate the composite baseband structure shown in Figure 4-4 and described in Table 4-2.

In normal operation, two transmission modes are used. For acquisition and ranging, only the ranging function, the 1.024 MHz DCS data subcarried and the 1.25 MHz 1 kbps data subcarrier are transmitted. After acquisition and ranging have been accomplished, the ranging function is replaced by the ranging clock at the ground station, and the 165, 225 and 300 kHz SCO's are turned on, by command, on the spacecraft and then the composit signal consisting of ranging clock and five subcarriers is transmitted. The 165, 225 and 300 kHz subcarriers are turned off during acquisition and ranging to avoid possible interference.

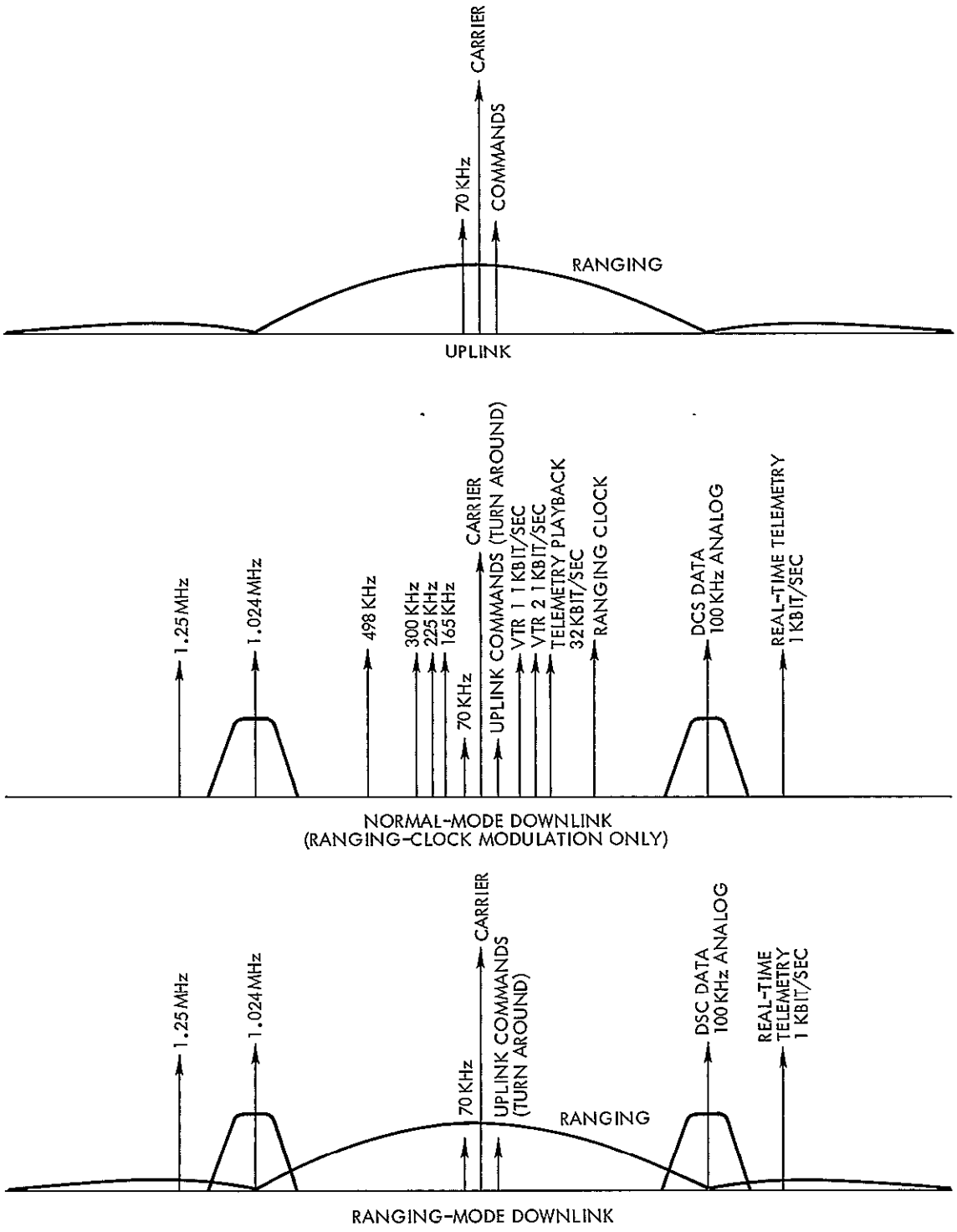

Figure 4-4
UNIFIED S-BAND SIGNAL SPECTRUM

Table 4-2. Unified S-Band Downlink Subcarrier

Data	Type	SCO Frequency	Carrier Peak Deviation (radian)
Video tape recorder 1	1 kbit/sec Manchester coded data	165 kHz	0.32
Video tape recorder 2	1 kbit/sec Manchester coded data	225 kHz	0.38
Telemetry Playback data	32 kbit/sec Manchester coded data	300 kHz	0.63
DCS data	100 kHz analog centered at 65 kHz hard limited	1.024 MHz	1.04
Real-time telemetry	1 kbit/sec Manchester coded data	1.25 MHz	0.29
Ranging	Hard limited ranging code plus uplink command signal	Baseband	0.1

During launch or whenever the spacecraft is not earth oriented, all subcarriers other than the 1.25-MHz real-time telemetry carrier will be turned off to permit utilization of all the downlink RF power in the communication of telemetry data. When 32 kbits/sec real-time telemetry is being generated, it is transmitted on the 300-kHz subcarrier normally used for telemetry playback, and the 1.25-MHz subcarrier modulation is removed.

The transponders are turned on and off as units so that the proven TETR transponder design may be utilized without modification. Only one receiver at a time will be operated to eliminate any possibility of one receiver locking to spurious signals from the other. Switching can always be accomplished via the VHF command system in case the operating unified S-band receiver fails.

The wideband video data assembly, Figure 4-5, transmits the data from the multispectral scanner and the return beam vidicon at 2229.5 and 2265.5 MHz. The data can be real-time or play-back from one of the two video tape recorders. The wideband video data assembly accepts six inputs: 14.8 Mbits/sec NRZ data from the MSS, 4 MHz-bandwidth analog data from the RBV's, and data of each type from each of the two video tape recorders. All the data is conditioned for downlink transmission, and any two inputs can be transmitted on the two downlinks.

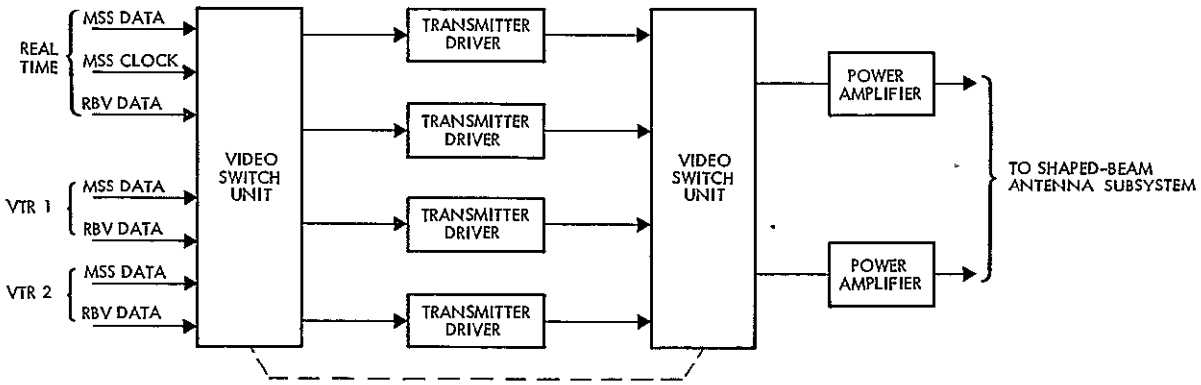

Figure 4-5

WIDEBAND VIDEO ASSEMBLY transmits payload data to S-band ground stations.

The assembly consists of a video switch unit, four transmitter drivers and two 10/20 watt traveling wave tube amplifiers. The video switch unit conditions the inputs and connects one to the 2229.5-MHz modulation input and one to the 2265.5-MHz modulation input. The four transmitter-drivers consist of two redundant units at each downlink frequency. Two transmitter-drivers are energized, one at each frequency, and these generate the two modulated S-band downlink signals. The video switch unit normally connects one downlink signal to each traveling wave tube amplifier. It also can connect a combined signal consisting of both S-band carriers either TWT amplifier input.

The TWT amplifiers are dual-mode 10- and 20-watt output units, similar to those flown on Mariner 1969. They normally operate in the 10-watt mode with a single carrier. If a TWT amplifier failure should occur, the remaining TWTA amplifies both carriers in the 20-watt mode. This mode is less efficient since power is lost due to intermodulation and some allowance must be made for signal level imbalance in the output. As shown in Section 6.2, however, the power is sufficient to provide acceptable system operation, with reduced margin. This system provides TWT amplifier redundancy without either the penalty of an extra TWT amplifier or the loss of efficiency resulting from dual-frequency operation in normal operation.

4.2 COMMUNICATION POWER BUDGETS

Power budgets for the ERTS communication links are detailed in Volume 4 and summarized in Table 4-3. The margins are seen to exceed the 6-db system margin and 20-db additional command margin requirements in all cases except the VHF command link. This link is unchanged from OGO and is considered acceptable in view of the actual command powers available at STADAN stations and the acceptable OGO experience.

Table 4-3. Summary of Power Budgets for ERTS Communication Links. All values are in db.

Link All Margins are Above a 6-db System Margin	Margin (DB)
VHF command (uplink)	17.6
VHF 1 kbit/sec downlink	17.7
VHF 32 kbit/sec downlink (Note 1)	2.6
VHF carrier beacon	24.3
Unified S-band command (uplink)	34.3
Unified S-band ranging (Note 4)	17.8
Unified S-band normal mode downlink (Note 4)	4.2
Unified S-band unstabilized mode downlink (Note 4)	9.7
Wideband RBV downlink, 30 ft station, normal mode (Note 2 & 4)	38.7
Wideband RBV downlink, 40 ft station, normal mode (Note 2)	37.7
Wideband RBV downlink, 85 ft station, normal mode (Note 2)	43.7
Wideband RBV downlink, 30 ft station, single TWTA mode (Note 1, 2 & 4)	37.2
Wideband RBV downlink, 40 ft station, single TWTA mode (Note 1 & 2)	36.2
Wideband RBV downlink, 85 ft station, single TWTA mode (Note 1 & 2)	42.2
Wideband MSS downlink, 30 ft station, normal mode (Note 3 & 4)	4.4
Wideband MSS downlink, 40 ft station, normal mode (Note 3)	3.4
Wideband MSS downlink, 85 ft station, normal mode (Note 3)	9.4
Wideband MSS downlink, 30 ft station, single TWTA mode (Note 1, 3 & 4)	2.9
Wideband MSS downlink, 40 ft station, single TWTA mode (Note 1 & 3)	1.9
Wideband MSS downlink, 85 ft station, single TWTA mode (Note 1 & 3)	7.0

Notes:
1. Not a normal operating mode.
2. Communication Link SNR with 6 db margin.
3. Referenced to 10^{-6} bit error probability.
4. In compliance with verbal information at the ERTS Interim Report on 15 January 1970, the system noise temperature used for the USB link and the Wideband link (30 ft antenna) is 125°K instead of the 250°K and 160°K shown in GSFC Design Specifications S-701-P-3. [This provides an added margin of 3 db on the USB signals and 1 db on the Wideband (30 ft antenna) signals].

4.3 VHF COMMUNICATION ASSEMBLY

4.3.1 VHF Transmitter

The ERTS VHF transmitter is a new design. Recent advancements in semiconductor technology and electronic components make it possible to design, develop, and build a 138-MHz transmitter which will outperform earlier VHF transmitters. These advancements, with the design considerations listed below, have been applied to the ERTS design:

- Simplicity
- Reliability
- High DC to RF efficiency
- Elimination of a converter by operation off the +28 volt buss
- Minimum filtering
- Minimum tuning
- A phase modulator which is insensitive to environmental changes

The local oscillator in the transmitter (see Figure 4-6) is a two-stage crystal-controlled oscillator utilizing a seventh overtone crystal at 138.86 MHz and two 2N918 transistors. The output of the oscillator is -10 dbm and the frequency stability over temperature and aging is ±0.002 percent. No multiplication or filtering is required. The oscillator is followed by a conventional 2N918 amplifier, which has a gain of +12 db, to provide +2 dbm signal to the phase modulator.

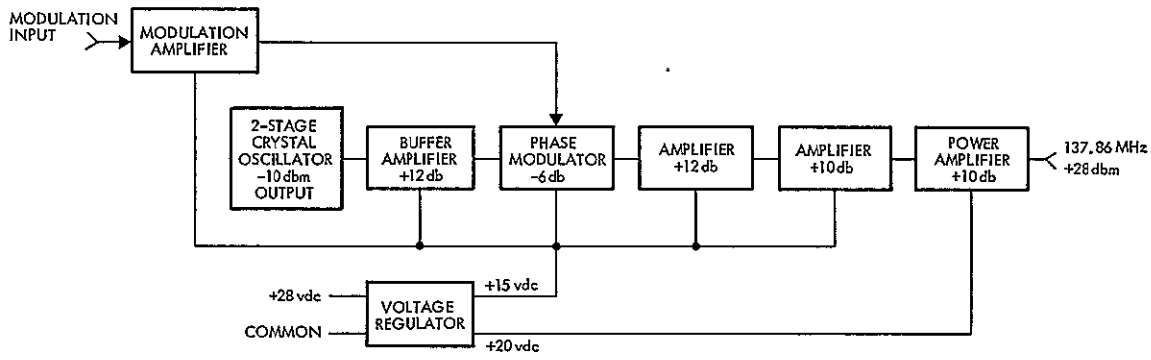

Figure 4-6
ERTS VHF 137.86 MHz TRANSMITTER block diagram

The modulator (Figure 4-7) biphase modulates the 138-MHz carrier by ±71 degrees which keeps a small fraction of the total power in the carrier. The center-tapped secondary of a transformer generates two carrier-frequency signals that are 180 degrees out of phase. The center tap of a series tuned circuit connected between the transformer ends creates a signal 90 degrees out of phase with either end. The weighted addition of this with the other two signals creates a pair ±71 degrees or 1.25 radians from it. An exclusive "or" diode switching circuit under control of the telemetry data selects one of the pair for further amplification.

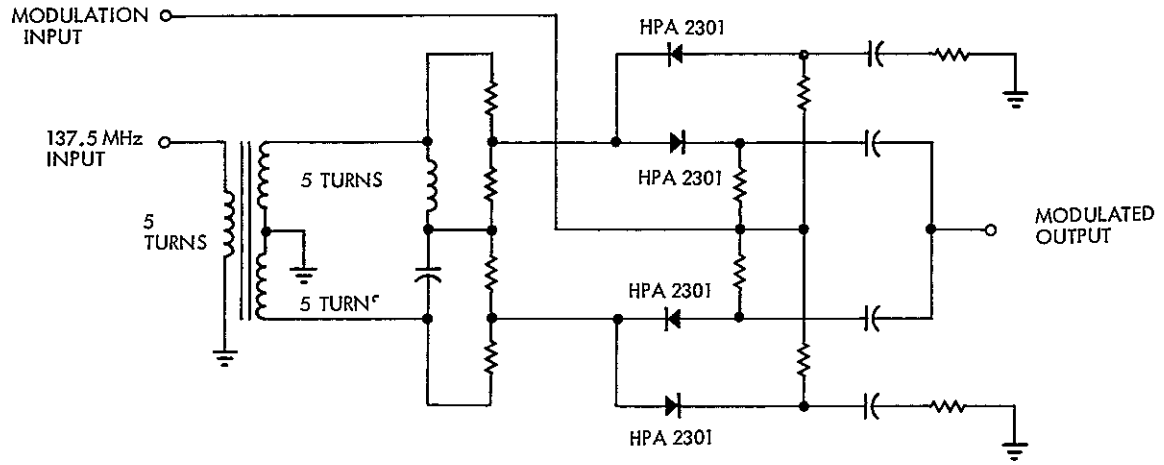

Figure 4-7
ERTS PHASE MODULATOR

The voltage regulator is a series type with +15 and +20 volt outputs. The drain on the +15 volt line is 17 milliamperes, and on the +20 volt line 47 milliamperes, resulting in a transmitter dissipation of 1.5 watts for a 23-volt input and 2.2 watts for a 33-volt input. At 28 volts the nominal efficiency is over 35 percent.

The salient features of the transmitter are as follows:

- RF Output Level: a minimum of 0.5 watt into a 50 ohm load over the required environmental conditions.
- RF Output Frequency: determined by the internal oscillator at 137.86 MHz.
- Frequency Stability: ±0.002 percent over the required environment.

- Load Impedance: 50 ohms with a maximum VSWR of 2.0:1 over the bandwidth of interest and all phase angles.
- Minimum 10-db Bandwidth: ±45 kHz referred to the output center frequency when modulated with a 1 kilobit signal.
- Modulation Input Impedance: 600 ohms ±10%.
- Modulation Input Levels:

  (1) +1.3 vdc, +0.03 -0.02 vdc

  (0) +0.2 vdc, +0.10 -0.15 vdc
- Unmodulated Spectral Bandwidth: With no modulating signal applied, all spurious responses and harmonics are more than 60 db below the carrier.
- Input Power:

  +23v input ≤ 1.5 watts

  +28v input ≤ 1.80 watts

  +33v input ≤ 2.20 watts
- Volume and Weight: 3 x 8 x 1.5 inches, 1.5 pounds

Mechanically, the VHF transmitter consists of one RF component board assembly mounted in an egg-crate, machined housing, with two covers having Metex type RF gasket material. The unit is RF tight.

The component board assembly is a two-sided aluminum gold-plated board utilizing press-in teflon terminals. Chomeric type flat gaskets are provided for internal shielding on the board. The RF input and output connectors are PT2-89/1 connectors.

4.3.2 VHF Command Receiver

The OGO command receiver is a space qualified unit whose reliability has been proven by its zero-failure record on all OGO missions. It can be adapted to the ERTS mission without affecting its reliability by three minor changes:

- Change crystals: to meet ERTS frequency assignments
- Replace 2N1197 transistors: no longer available; high reliability equivalents are available
- Remove relay K-1; signal present: not used for ERTS

The change in frequency assignments requires slight retuning of the first local oscillator chain. Replacing the 2N1197 transistor with a high-reliability equivalent part and removing the relay do not degrade performance. Relay removal reduces power consumption of the unit when a signal is present by 0.4 watt. In addition, soldered rather than welded circuits are used for economy.

The dual conversion receiver (see Figure 4-8) receives and demodulates an amplitude modulated RF signal and feeds the demodulated information to the output through three separate audio channels. The receiver, all solid state, contains an RF amplifier, two mixers, two IF amplifiers, two local oscillators, two AGC loops, a linear AM detector, audio amplifiers, a signal present (squelch) circuit, and a voltage regulator.

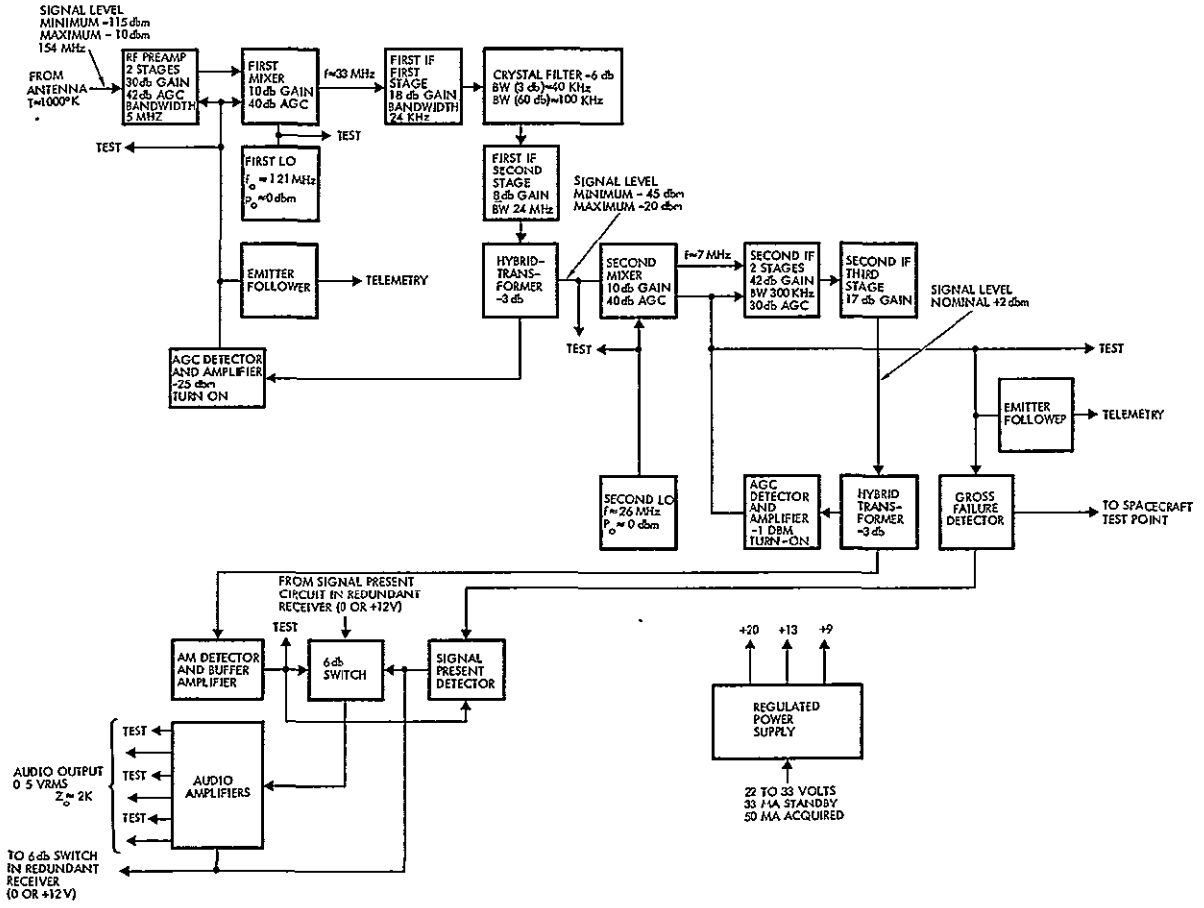

Figure 4-8
ERTS COMMAND RECEIVER block diagram

The gains of the RF amplifier and first mixer are controlled by the first AGC loop, and the gains of the second IF amplifier and mixer are controlled by the second AGC loop to give a dynamic range of over 100 db. The 40-kHz bandwidth of the receiver is set by a crystal filter in the first IF amplifier. Both local oscillators are crystal controlled to within ±0.002 percent over the temperature range. The output of the second IF amplifier drives the diode AM detector at a constant level of approximately 0 dbm. The detector drives three audio amplifiers, whose gains are independent of their transistor parameters, to provide three isolated out channels. The detector also drives the signal-present circuit which detects an RF signal above -115 dbm and turns the audio amplifiers on or off accordingly. The audio amplifiers are also automatically turned off in case of a failure in the receiver so that no noise is present at the output.

The consistent performance of the receiver over the wide temperature range results from temperature compensation in the AGC loops, signal present circuit, and voltage regulator. The voltage regulator supplies constant voltages to the transistors for input voltage varying from +23 to +52 volts.

Unit Specifications

Frequency	154.2 MHz
Sensitivity	-115 dbm for squelch operation
Noise figure	Less than 4 db
IF bandwidth	40 kHz
Modulation	Amplitude
Output (each of three channels)	0.5v rms ±0.05v at 85 percent modulation from -15 to -115 dbm
	0.5v rms ±0.095v at 85 percent modulation from 1 to 11 kHz
Power requirements	1 watt at +28 volts (standby) 1.2 watts at +28 volts (with signal)
Input voltage tolerance	+23 to +33 volts (50 volt transient)

Temperature range	-5 to +45°C
Interference	60 db spurious response rejection 60 db IF rejection
Intermodulation and harmonic distortion	Less than 10 percent

The receiver (see Figure 4-9) occupies a rectangular box with a volume of 63 cubic inches, excluding connectors. The power, test, and antenna connectors are mounted on one face. All circuits are constructed on two flat metal plates. The RF circuitry is on one side of each plate and DC circuitry and interconnecting cables are on the other. The covers have integral shields which fit around groups of circuits to reduce coupling. A wrap-around bracket joins the two circuit boards and their covers.

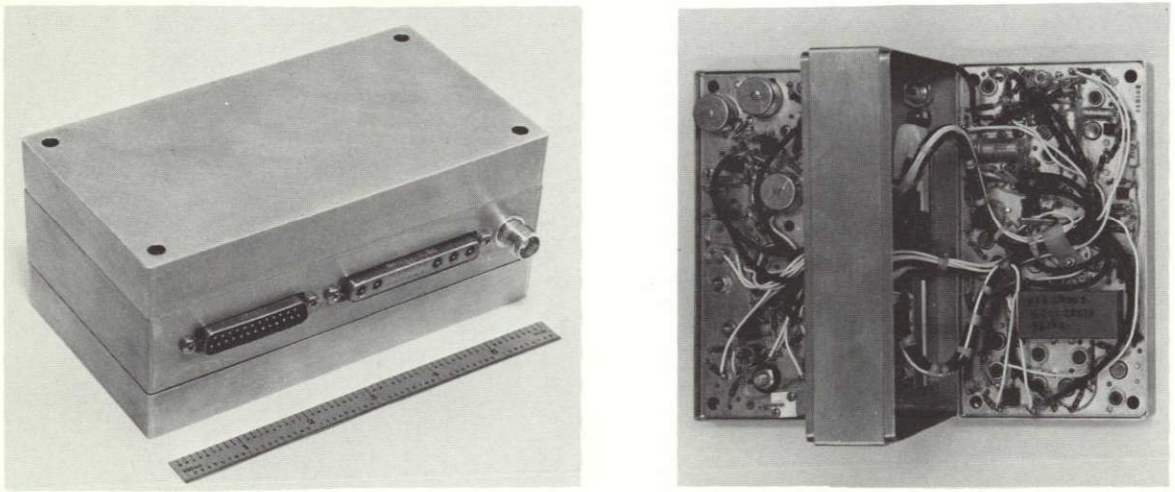

Figure 4-9
VHF COMMAND RECEIVER weighs 1.8 pounds and measures 6.2 x 3.9 x 2.6 inches

Interboard wiring is dressed in this area between the two boards, and the connectors and the power lead RF filter are mounted to this bracket.

4.3.3 Power Monitor

The 0.5-watt, 137.86-MHz RF power monitors for ERTS are a modified version of the 10-watt, 136-MHz power monitor used on OGO. They employ stripline assemblies to measure the power delivered to the antennas by the 0.5-watt VHF transmitters and the power reflected from the antennas

due to impedance mismatch. Directional couplers sample RF power from the transmission lines between the transmitters and antennas and rectify this power to give DC voltages that are proportioned to the forward and reverse power.

The increase in frequency from the 136.2 MHz of OGO to 137.86 MHz requires no redesign. The increase in sensitivity from 10 to 0.5 watt requires a minor change in the detector circuits and a decrease in the DC output level.

Specifications for the RF power monitor are:

- Center frequency — 137.86 ± 0.2 MHz
- RF line impedance — 50 ohms nominal
- RF line VSWR — ≤1.2:1 when terminated into 50 ohms
- Directivity — ≤18 db between the monitoring circuits
- Insertion loss — ≤0.2 db in the forward direction
- Detector output — positive polarity with the following levels:

Forward Readings	
Power out	output voltage
0.5 w	0.35 ± 0.1 vdc

Reverse Readings	
Power out	output voltage
0.5 w	0.035 ± 0.1 vdc

- Detector resistance — ≤2000 ohms

4.4 UNIFIED S-BAND TRANSPONDER

Communication with the MSFN tracking stations takes place with a TETR-developed on-board unified S-band transponder. This unit enables the telemetering of real-time and stored housekeeping data and of DCS data, the commanding of all spacecraft functions and the derivation of range and range-rate data from MSFN stations.

This transponder has been flown on TETR satellites as an aid in evaluating the NASA Manned Space Flight Network and the training of

network personnel. This unified S-band compatible transponder offers the following features:

- Flight proven performance and reliability
- Minimum size, weight, and power consumption
- Demonstrated compatibility with the MSFN ground stations
- Qualified to stringent environments
- Receiver high-loop gain results in low static phase error and high tracking rates
- Receiver offset frequency prevents false lock.

Because of these advantages of the TETR transponder (Figure 4-10), it has been adapted for ERTS. The adaption calls for the following modifications:

Unit	Modification
• Receiver	The amplifier following the wideband phase detector is changed to an emitter follower.
• Transmitter	No modification
• Power converter	The primary power requirements are changed from 11 to 14 vdc to 22 to 33 vdc. This configuration is the same as for the Air Force Programs 777 and 949.
• Power monitor	No modification.

When an uplink carrier is received by the unified S-band transponder, the carrier transmitted back to earth is coherent in the frequency ratio of 221/240 to that received. This coherence coupled with turn-around pseudo-noise ranging modulation permits accurate determination and tracking of the spacecraft ephemeris. Commands superimposed on a 70-kHz subcarrier are stripped from the carrier in the receiver's phase detector. Telemetry information comprising a series of IRIG and other subcarriers in phase modulated on the downlink carrier. A block diagram of the unified S-band transponder is illustrated in Figure 4-11.

The 800-mw transmitter operates at an output frequency of 2287.5 MHz. It has two operational modes, coherent and noncoherent.

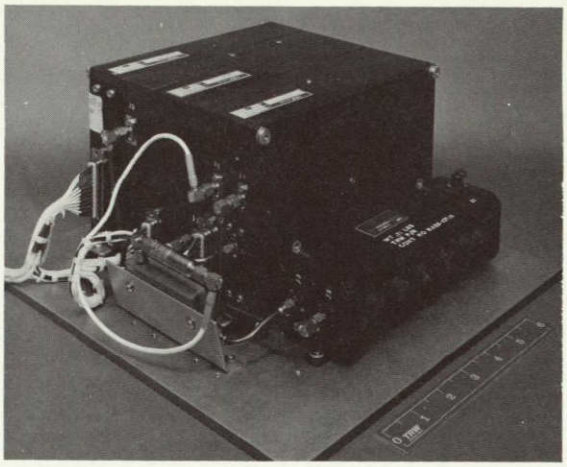

Figure 4-10

THE TETR TRANSPONDER is adapted to the ERTS S-band communication link with two minor modifications. The diplexer is shown on the right.

In the coherent mode the transmitter receives drive signals from the receiver; in the noncoherent mode it is driven from a self-contained crystal oscillator. The transmitter output is phase modulated by a composite signal from the baseband assembly unit, which contains the ranging code and subcarriers. The transmitter provides two telemetered functions, temperature and transmitter power level, derived through a directional coupler, detector, and amplifier.

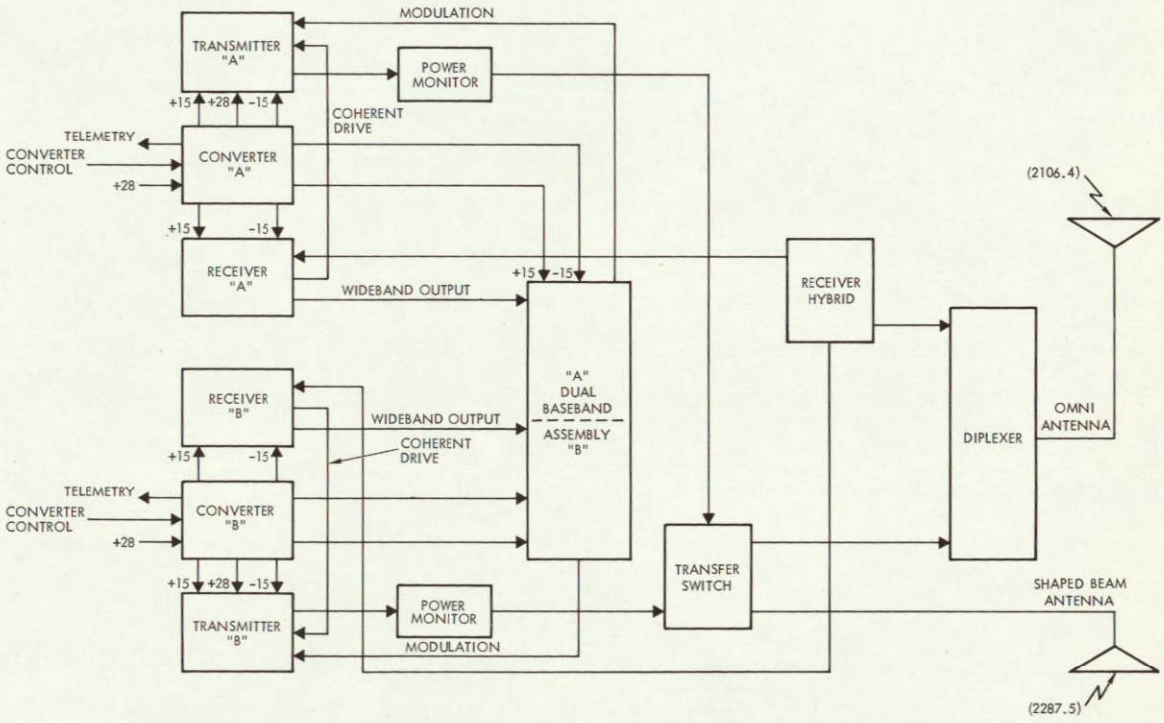

Figure 4-11

THE UNIFIED S-BAND SYSTEM for ERTS consists of redundant receivers, transmitters, converters, and power monitors

The power converter is a DC-DC converter operating from the spacecraft bus voltage and providing power to the transponder. The converter can be commanded on-off from the ground. The converter also supplies telemetry signals which are proportional to its output voltages.

4.4.1 Receiver

In the receiver (Figure 4-12), the received signal at 221f* (2106.4 MHz) is heterodyned in the first mixer with the local oscillator signal at 216f to give an output of 5f, approximately 47.7 MHz. The output of the first IF amplifier at 5f is heterodyned in the second mixer with a signal at 5f $-f_r$ to give an output at f_r, which is 13.3 MHz. The signal at f_r is amplified and bandlimited in the second IF amplifier and applied to three phase detectors. A wideband phase detector demodulates the wideband (subcarriers) information on the received signal. A second and narrowband loop phase detector drives an operational amplifier (loop filter), which in turn controls the VCO operating at a frequency of 2f. The VCO signal is multiplied by 108 to 216f and injected into the first mixer to close the loop.

In addition, the VCO signal is multiplied by five and mixed with a signal at $2f_r$ from the reference oscillator to give an output of 10f $-2f_r$. This signal is divided by two to generate the 5f $-f_r$ signal inputted at the second mixer. The reference oscillator signal at f_r is also used as the reference signal for the phase detectors. The feedback to the VCO controls its frequency and phase such that each mixer injection signal is maintained in precisely the relations indicated above and so that the IF and reference injections at the loop phase detector are very nearly in phase quadrature. The output of the VCO at 2f is subsequently multiplied by five, providing the 10f coherent drive for the transmitter.

A third phase detector operating with its reference shifted 90 degrees senses the presence of a signal at threshold level or above and disables squelch amplifier at the output of the wideband and narrowband loop phase detectors. No AGC is used. Instead, the receiver is designed to limit on noise when no signal is present.

*f is the frequency of a pseudo signal to which all other signals can be related. It is approximately 9.5 MHz.

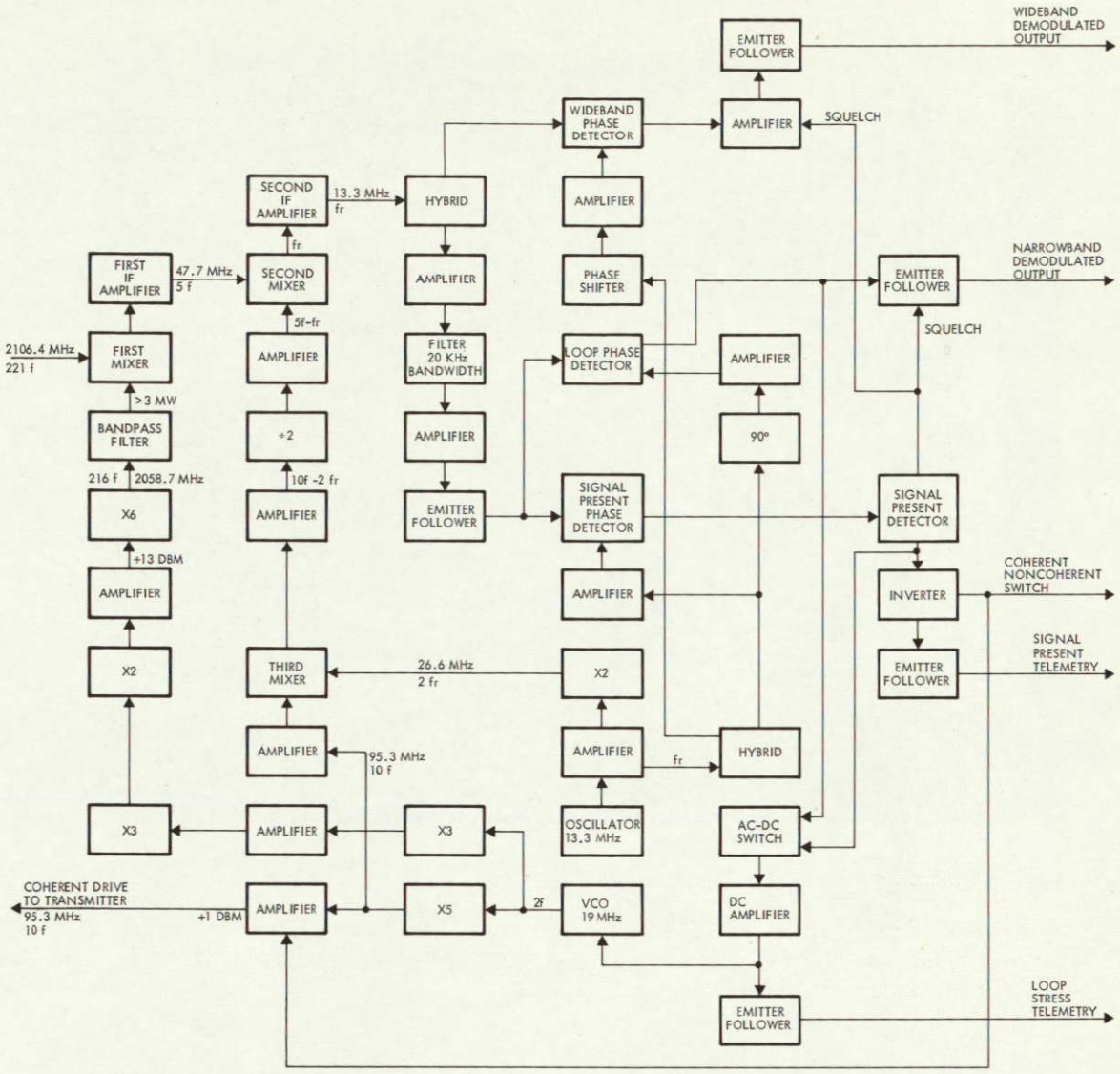

Figure 4-12
UNIFIED S-BAND RECEIVER block diagram

The phase-lock loop parameters are based upon those used for the TETR receiver (shown in Figure 4-13):

Noise figure	10 db max
Predetection bandwidth	20 kHz
Loop noise bandwidth	$2B_{LO}$ = 800 Hz
Threshold (0 db S/N in loop)	-135 dbm

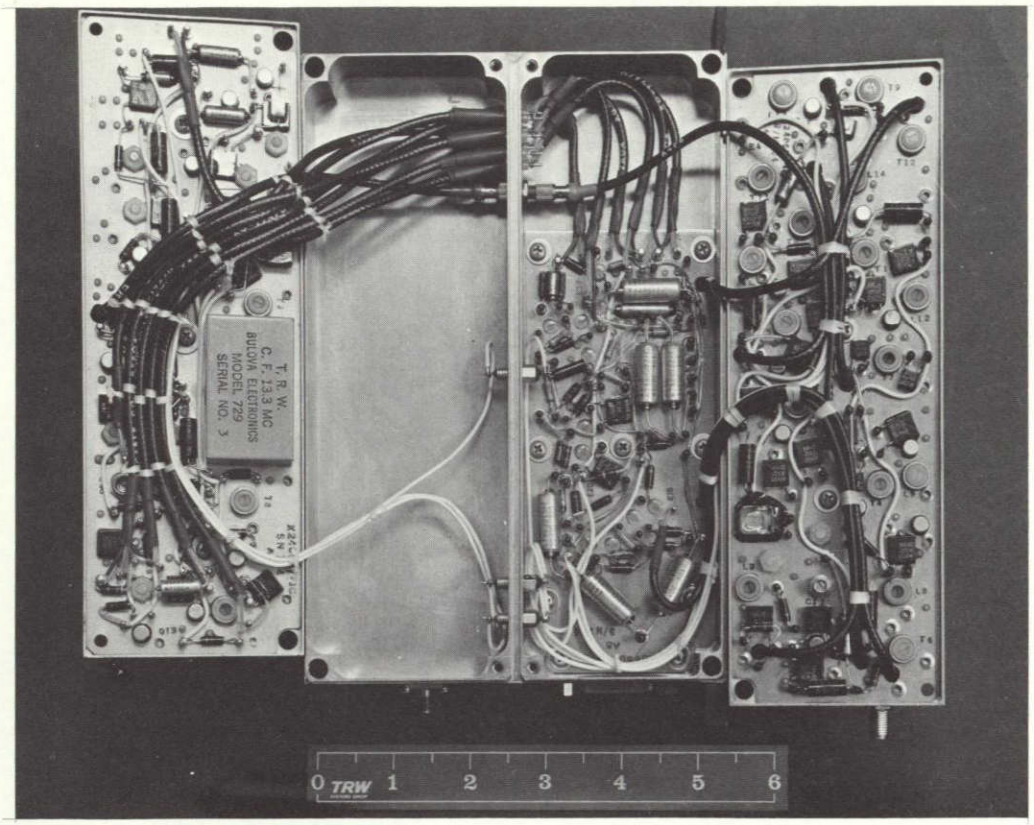

Figure 4-13

THE UNIFIED S-BAND RECEIVER measures 7.25 x 5 x 3.25 inches, weighs 4 pounds, and consumes 80 ma at -15 volts and 25 ma at 15 volts for a total dissipation of 1.6 watts.

Suppression factor at -135 dbm (based on a -14 db S/N in the 20 kHz predetection bandwidth)	0.18
Damping factor at threshold	$\delta = 0.707$
Natural resonant frequency at threshold (ω_n)	755 radians/sec
Natural resonant frequency at -125 dbm	1310 radians/sec
Loop noise bandwidth at -125 dbm	$2 B_{LO} = 1870$ Hz
Damping factor at -125 dbm	1.22
S/N in 1870 Hz loop noise bandwidth at -125 dbm	6.3 db

Suppression factor at -125 dbm (based on a -4 db S/N in the 20 kHz predetection bandwidth)	0.54
Maximum sweep rate for a 20 degree peak acquisition error at -125 dbm	95 kHz/sec
Natural resonant frequency at strong signals	1780 radians/sec
Damping factor at strong signals	1.67
Loop noise bandwidth at strong signals	3240 Hz
Acquisition error for a 360 kHz/sec sweep rate at strong signals	$\phi = \frac{\dot{\omega}}{\omega_n^2} = \frac{2\pi(360) \cdot 10^3}{(1.78)^2 \cdot 10^6}$ = 0.71 radian or 41 degrees
Maximum sweep rate for a 20-degree peak acquisition error at strong signals	177 kHz/sec
Sweep range at -125 dbm once receiver is acquired	±185 kHz minimum
Phase detector scale factor	1 volt/rad
VCO scale factor	500 Hz/volt
Multiplication ratio	110.5
DC amplifier gain	105
Total gain at -125 dbm	1.97×10^7
Total gain at strong signal levels	3.65×10^7
Static phase error at -125 dbm for a 185-kHz offset	$\phi = \frac{\Delta\omega}{G} = \frac{2\pi(185) \cdot 10^3}{1.97 \cdot 10^7}$ = 0.059 radian or 3.4 degrees

From these values, it can be seen that the static phase error is low because of the DC amplifier gain, allowing the receiver to track signals with a high sweep rate. The receiver threshold (set by the signal present detector circuit) is set at -125 dbm to give a 6-db S/N in the loop. If the

threshold were set at a stronger signal level, which can easily be done, the loop bandwidth would be larger and the dynamic phase error for a given sweep rate at threshold would decrease.

4.4.2 Transmitter

The transmitter (Figure 4-14) produces nominally 1 watt and a minimum of 800 mw of power at 2287.5 MHz. Drive power at 95.3 MHz is obtained from an internal crystal oscillator stage stable to ±0.002 percent in the noncoherent mode or from the receiver in the coherent mode. A solid-state switch, controlled by the signal-present voltage from the receiver, selects either the coherent or noncoherent drive and feeds it to a buffer amplifier.

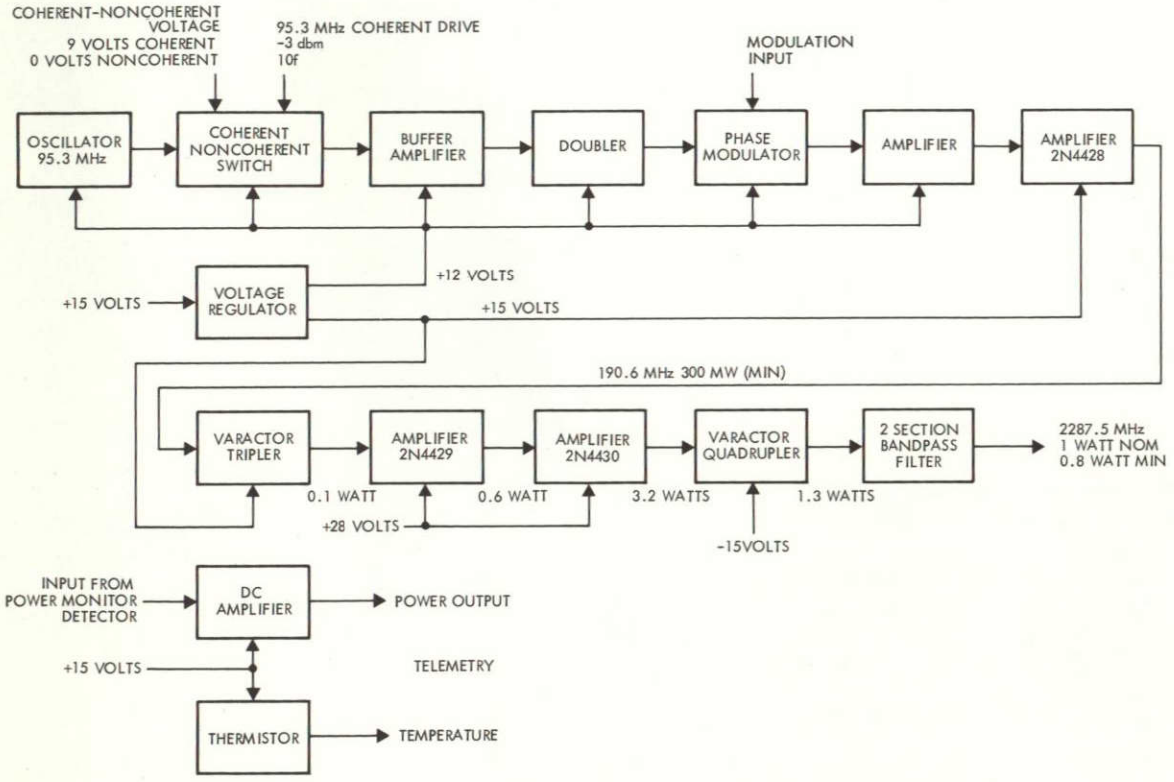

Figure 4-14
UNIFIED S-BAND TRANSMITTER is all solid state

The signal is amplified by the buffer to 1 mw. Following this a frequency doubler stage drives a conventional phase modulator-amplifier stage to produce approximately 8 mw at 190.6 MHz. A buffer amplifier then delivers 50 mw of drive to the last amplifier stage on the low-level

board. The last stage delivering 300 mw at 190.6 MHz is coaxial-connected to the low level tripler stage on the high level board.

The conversion efficiency of the low-level tripler is 33 percent giving 100 mw at 571.8 MHz. A power gain of 7.5 db in the next amplifier stage brings the power level to 0.6 watts and a last stage of amplification brings the power to 3.2 watts at 571.8 MHz. Finally, a high level 40 percent efficient quadrupler stage gives 1.3 watts at 2.287 gHz. A 5-db loss in a two-section bandpass filter reduces the output power to 1.0-watt nominal and 0.8-watt minimum over the specified environmental temperature range.

The transmitter current consumption is shown below.

Voltage (v)	Nominal Current (ma)	Maximum
+28	310	340
+15	105	120
-15	2	3

The nominal power dissipation is 8.7 watts giving an overall efficiency of 11.5 percent for a 1-watt output. The TETR unit, to be applied without modification to ERTS, is shown in Figure 4-15.

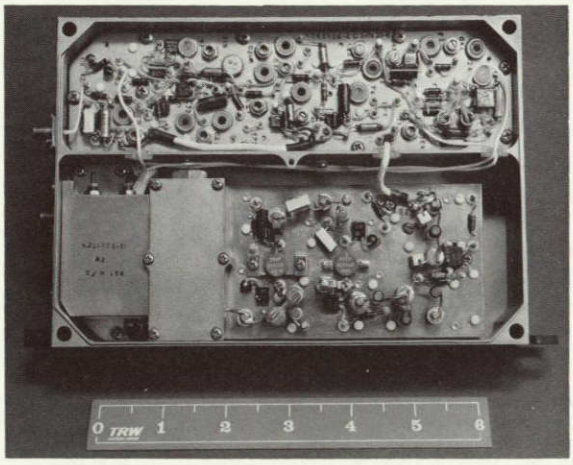

Figure 4-15
THE UNIFIED S-BAND TRANSMITTER measures 7.25 x 5 x 1.6 inches and weighs 2 pounds.

4.4.3 Power Monitor

The power monitor samples the RF output of the transmitter and provides a telemetry voltage proportional to that output power. The unit consists of a directional coupler, diode detector, and DC amplifier. The 20-db directional coupler is an OSM 20054-20 unit which operates at S band and feeds an RF signal to the detector. The OSM 20080 detector drives the DC amplifier located in the transmitter whose output is then used as the telemetry voltage.

The directional coupler measures 1/2 x 2-7/16 x 2-5/32 inches and weighs 1.75 ounces. The detector is 3/8 inch in diameter, 2 inches long, and weighs 0.6 ounce.

4.4.4 Converter

As shown in Figure 4-16, power is applied at connector J1 through EMI and L-C filters to the power switching transistors. An on/off control enables the 6 kHz driver oscillator circuit, which then powers the timing circuit. This circuit in turn controls the switching of the power switching transistors. The volt-second reference inductor controls the duration of drive to the power switching transistors. This time is determined directly by the value of line voltage applied to the converter and so the response is independent of feedback loops of the circuit.

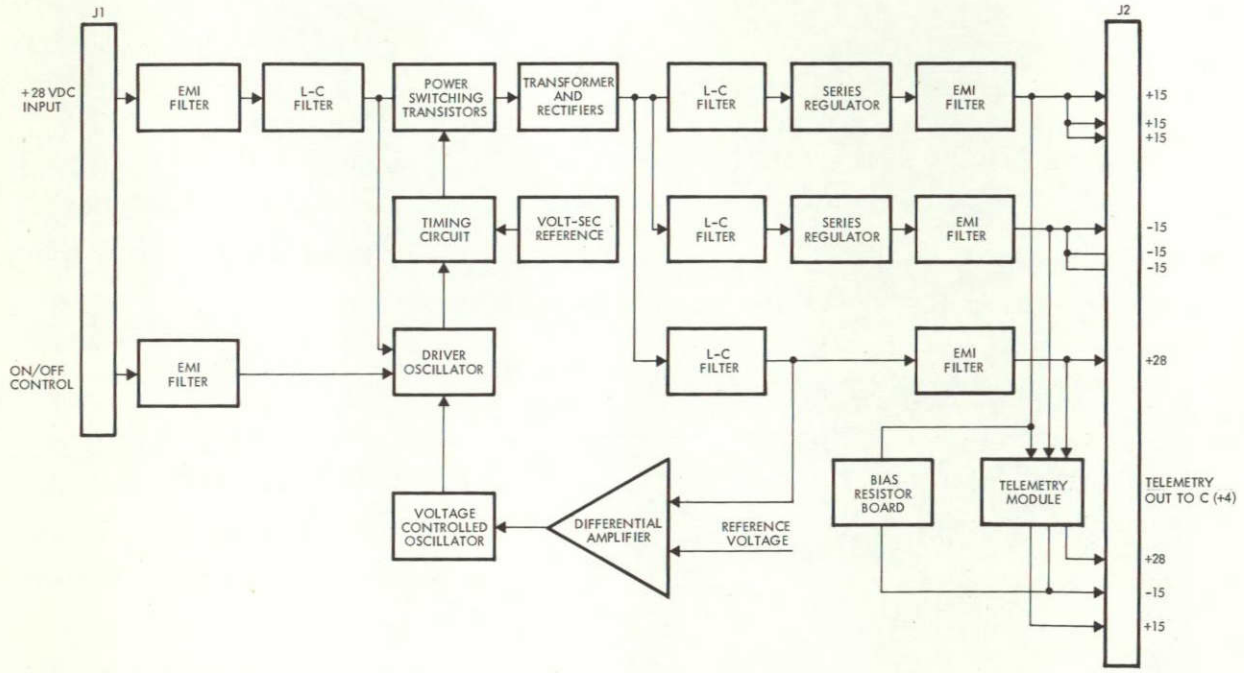

Figure 4-16
UNIFIED S-BAND TRANSPONDER CONVERTER block diagram

The power switching transistors provide the chopped DC power to the transformer and rectifier circuits. Filtered outputs are routed through two series regulators to supply the +15 and -15 vdc outputs. The +28 vdc output is monitored for voltage level by differential amplifier circuit referenced to a zener diode voltage. The output of this circuit

determines the voltage applied to a voltage-controlled oscillator circuit. The frequency of this oscillator determines the frequency of the driver oscillator circuit since the frequency of the free-running driver oscillator is several kiloHertz below the normal 10 kHz of the voltage-controlled oscillator.

At all of the voltage outputs EMI filters are provided. Each output is monitored by a resistor network in the telemetry module, providing an output of approximately +5 vdc at the nominal voltage for each output. The output impedance of the telemetry networks is approximately 8 kohms. The bias resistor board shown makes provision for a positive output for the -15 vdc telemetry voltage.

The converter operates from a +22 to +33 vdc signal and regulates the +15, -15, and +28 vdc lines to ±2 percent. The ripple on the +15 and -15 volt lines is 10 mv peak-to-peak maximum and 100 mv peak-to-peak maximum on the +28 volt line. The converter efficiency is nominally 80 percent and never drops below 75 percent for all load and input conditions. The TETR converter is shown in Figure 4-17.

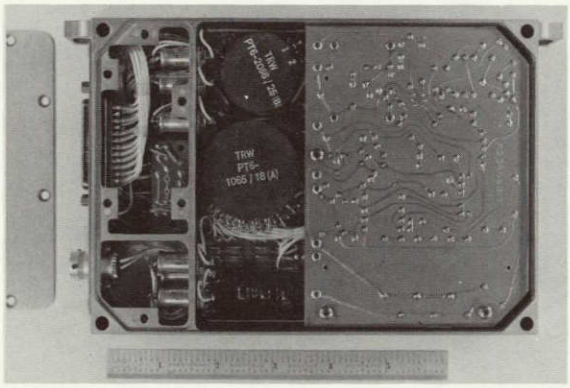

Figure 4-17
THE S-BAND CONVERTER measures 7.25 x 5 x 1.25 inches and weighs 2 pounds.

4.5 WIDEBAND VIDEO ASSEMBLY

4.5.1 Video Switch Unit

The video switch unit provides switching between six baseband inputs and four FM exciters. It also handles RF switching between the exciter outputs and two TWT amplifiers.

For baseband switching (Figure 4-18), latching relays are used to select an input directly from the MSS scanner in the real-time mode, or from one of two tape recorders in the playback mode. The inputs are processed by a high speed comparator and filter. The comparator senses a digital 1 or 0 from a widely varying RBV signal, and, accordingly, the output level shifts between two preset values.

The comparator maintains the frequency shift of the FM exciters constant regardless of the MSS input levels. The filter shapes the baseband signal so that the RF output spectrum of the channel carrying the MSS signal is contained within a 20-MHz band. Latching relays are also used to select an analog input directly from the RBV or from one of two tape recorders. Each of the analog inputs has an input pad, using select-in-test resistors, to individually adjust the modulation sensitivity. The baseband switching section also provides termination for unused data and clock outputs from the MSS.

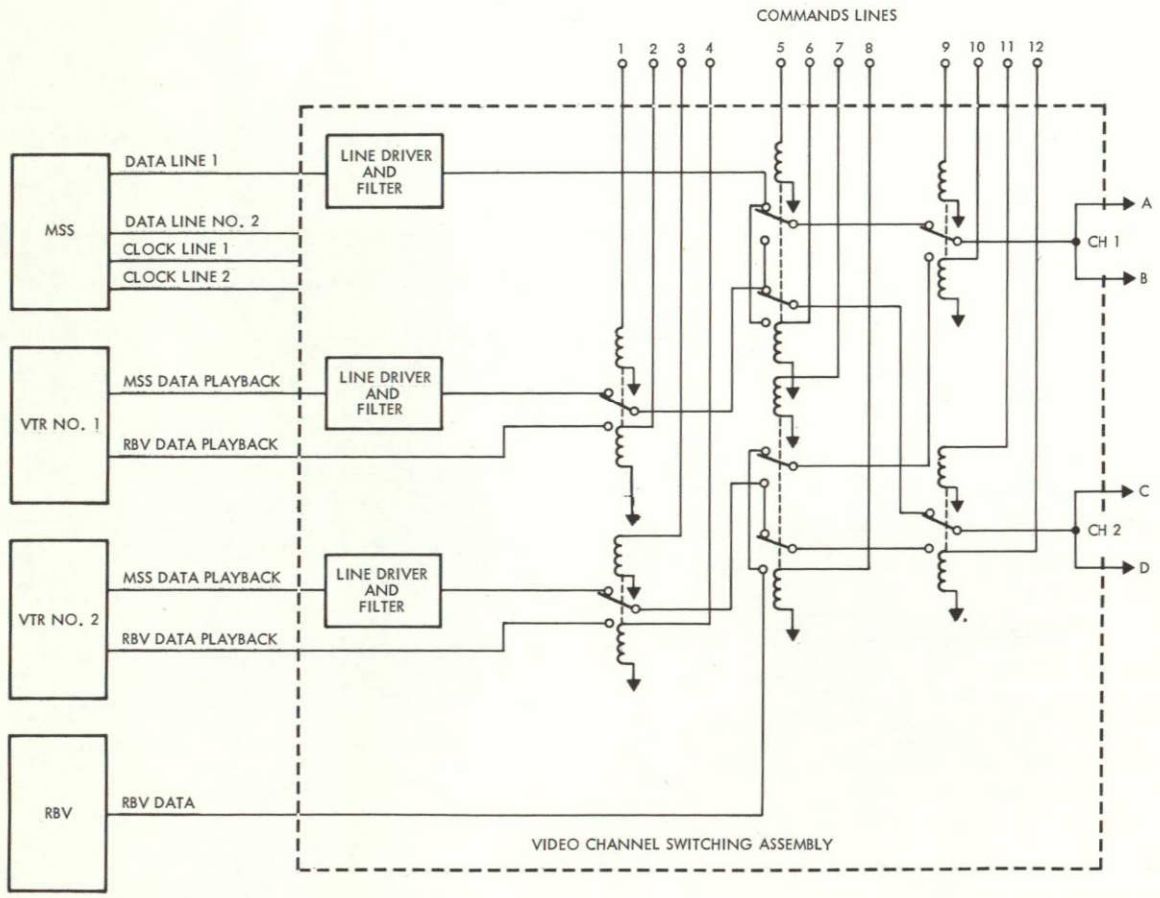

Figure 4-18
BASEBAND SWITCH

Switching between the driver outputs and the TWT's (Figure 4-19) is by four 3-db couplers and a mechanical transfer switch. In the normal mode, the input signal is split by the first coupler and recombined by the second coupler. The combining scheme requires that one of the lines

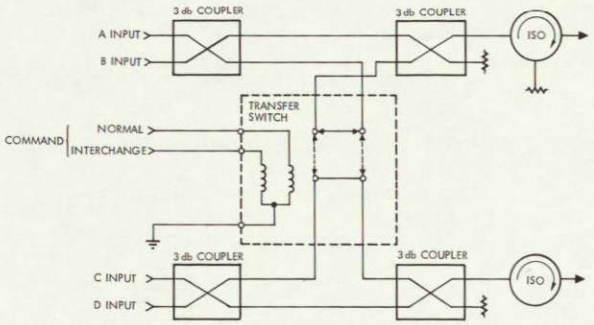

Figure 4-19
RF CHANNEL SWITCH

connecting the two couplers be a quarter wave longer than the other. With this arrangement half of the input at either of the input ports appears at the output port. In the cross strap mode each carrier is split by the input couplers and half of each carrier is recombined in the output couplers. The average powers at the output ports for the normal and cross strap modes are equal. The peak power in the cross strap mode goes to twice the average power. Loss in the switching assembly are estimated as follows:

Isolator loss	0.20
Combining loss	3.00
Input coupler loss	0.25
Output coupler loss	0.25
Switch loss	0.30
Cable loss	0.40
Phasing loss	0.10
Total	4.5 db

Maintaining phase loss below 0.1 db requires a dimensional tolerance on the length of the interconnecting cables of ±0.04 inch.

The RF channel switching circuitry uses outside purchased parts with 3 mm coaxial fittings. The components will be assembled on a metal plate and use semi-rigid coaxial cable for the interconnections.

The baseband switching circuitry is housed in a metal box and mounted on the same plate as the RF channel switch. Baseband inputs

and output enter and leave the box through 3 mm coaxial connectors, the command and power input lines enter the box through a 15-pin cannon connector. Inside the box, relays, active circuits, and filters are installed on a printed circuit board.

4.5.2 Transmitter Driver

Modulation of the S-band carrier with the video data takes place in the transmitter driver. In this unit (whose block diagram is shown in Figure 4-20) the wideband video input is amplified and applied to an FM deviator operating at the output frequency. To obtain the required frequency accuracy, the deviator is stabilized by a crystal-reference-sampling AFC loop. The sampling AFC loop eliminates frequency errors found in conventional AFC loops which are caused by discriminator instability and DC offset in direct coupled amplifiers. The accuracy of the sampling AFC loop is limited only by the stability of the reference source and the resolution of the discriminator.

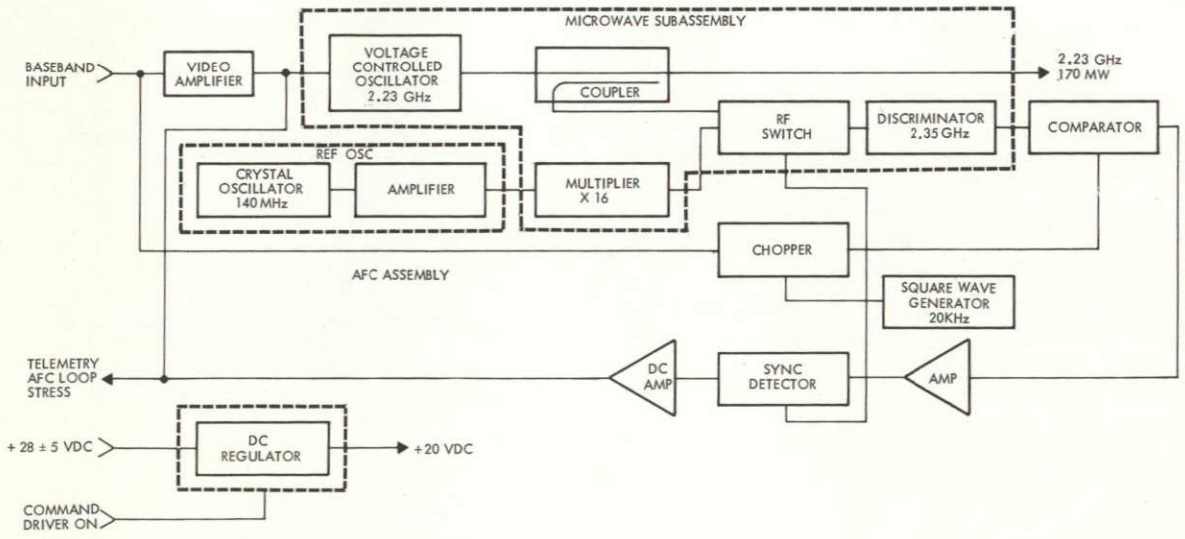

Figure 4-20
ERTS TRANSMITTER DRIVER

A portion of the deviator's output and a reference frequency are alternately switched through a discriminator. The output of the discriminator is a square wave at the switching frequency, whose amplitude is proportional to the frequency difference between the two sources. The

discriminator's output is capacitively coupled to comparator circuit where a sample of the data input is subtracted from it. The data sample is chopped so that it is applied to the comparator only when the deviator is connected to the discriminator. This comparison is made to remove the portion of the frequency difference between the two RF sources which is due to low frequency data input modulating the deviator. The comparator prevents the AFC loop from tracking out modulating signals within the loop bandwidth.

The square wave output from the comparator is amplified in a relatively simple operational amplifier. Since the amplifier is AC coupled, large gains can be obtained without compensating for DC offsets. The synchronous detector following the amplifier extracts the frequency error information from the square wave by grounding the output when the reference is being sampled and passing the level shift when the deviator is being sampled.

A low pass filter integrates the detector's output and applies it to the deviator to close the AFC loop. Performance characteristics of the transmitter driver are given in Table 4-4.

Construction of the transmitter driver includes four subassemblies:

- Microwave subassembly contains the VCO (2.23 or 2.26 GHz), X16 multiplier, coupler RF switch and discriminator. All of the components with the exception of the discriminator cavity are constructed on a single alumina substrate using micro stripline techniques. The discriminator cavity is machined from Invar stock.

- Reference oscillator subassembly contains a crystal oscillator operating at 140 MHz and a power amplifier with an output of about 100 mw. The circuitry is constructed on a removable metal terminal board.

- AFC subassembly contains the comparator, chopper, square wave generator, 20 kHz amplifier, sync detector and video amplifier. Construction is on a removable, double-sided printed circuit board with integrated circuits and discrete components.

- Power conditioner contains a series switching regulator and all of the input filtering required to meet the conducted interference requirements of the EMC specification. The circuitry is constructed as an integral part of the transmitter driver housing.

Table 4-4. Characteristics of the Transmitter Driver in the Wideband Video Assembly

Frequency	2229.5 or 2265.5 GHz
Absolute stability	±0.005%
Power output	170 mw ±20%
Modulation	
Type	FM
Frequency response	DC to 15 MHz ±1 db
Deviation	±10 MHz peak
Linearity	±2% BSL from 0 to 10 MHz
DC input	
Voltage	28 ± 5 vdc
Power	5 watts maximum
Size	2 x 3 x 6 in.
Weight	2.5 lb

4.5.3 Power Amplifier

The traveling-wave tube amplifier in the ERTS wideband video assembly (Figure 4-21) is a single integrated package having a similar design to that which was flown on Mariner Mars 1969 and which is to be flown on Mariner Mars 1971. A WJ-274-9 TWT has been substituted for the Hughes 242H TWT, however. The overall length of the TWT amplifier package must be increased from 9.5 to 10.5 inches (Figure 4-22) to accommodate the longer WJ-274-9 TWT. Depending on the results of mechanical design analysis this change may require a partial requalification (shock and vibration only).

The use of the WJ-274-9 TWT raises the package efficiency from 17.5 to 26 percent. Less time is anticipated for procurement as well, since a single subcontractor provides the tube as well as other components

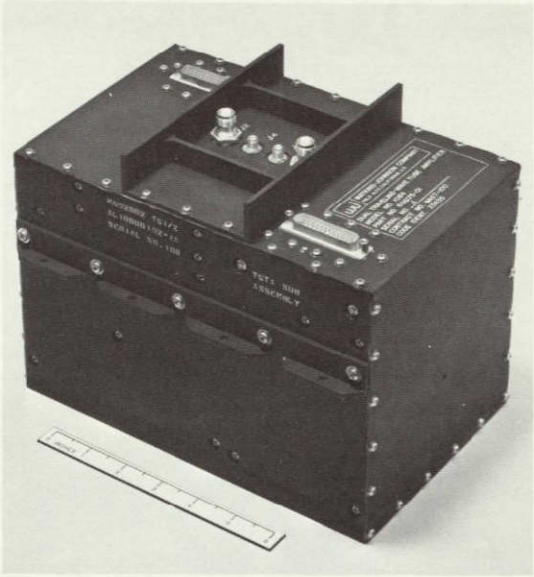

Figure 4-21
TWO TWT AMPLIFIERS are combined into a single RF-tight enclosure

in the amplifier. Both the Mariner Mars 1969 TWT amplifier and the WJ-274-9 TWT have been qualified to Jet Propulsion Specification TS 500437B, 13 December 1967.

The original WJ-274 was developed under contract to the NASA Langley Research Center to develop an extremely lightweight high efficiency 20-watt TWT. As a result of this early contract, Watkins-Johnson Company completed the development of a tube which weighed 1.2 pounds including the capsule, occuplied a volume of approximately 8 cubic inches and had an overall efficiency of 35 percent at the 20-watt level at 2.3 gHz.

In a later contract with the NASA Marshall Space Flight Center, the WJ-274 was produced as the WJ-274-1 and space qualified for the WJ-1014-1 amplifier, which is flown in the Saturn V. Approximately 25 of these tubes have been delivered in completed amplifiers to either Marshall Space Flight Center or to the Federal Systems Division of the International Business Machine Corporation for use on the Saturn V.

Subsequently, the NASA Langley Research Center supported additional work on the WJ-274 to upgrade its efficiency. The resulting improved design was assigned the type number, WJ-274-9 (Figure 4-23). Briefly, the results were as follows: overall efficiency, including heater power, of 42.2 percent at 2.30 gHz and greater than 41 percent from 2.11 to 2.39 gHz with a saturated output power of 25 watts and a saturation gain of 34 db.

Two of the WJ-274-1 TWT's and one WJ-274-6 are on extended life test at the Jet Propulsion Laboratory. As of October 1969, the WJ-274-1 TWT's S/N 29 and S/N 30 had respectively accumulated 16,700 and 15,000

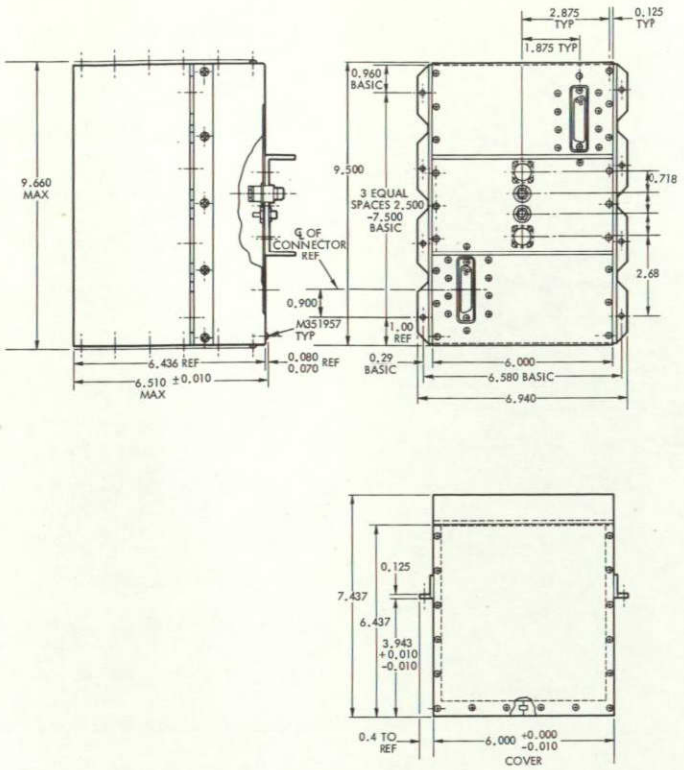

Figure 4-22

DIMENSIONS OF THE TWTA are unchanged from the Mariner Mars configuration except for an extension of the length from 9.5 to 10 inches.

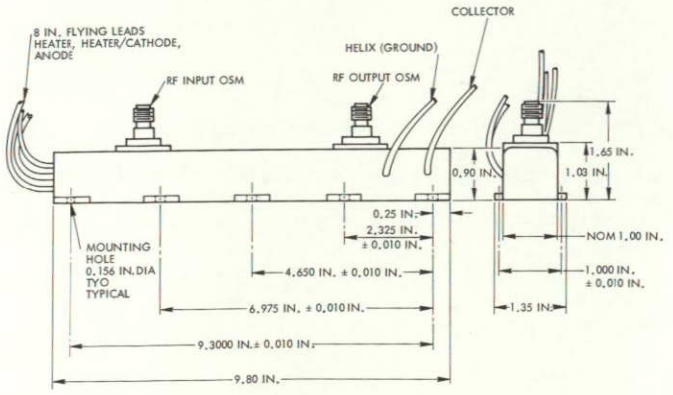

Figure 4-23

OUTLINE DRAWING of the WJ-274-9 traveling wave tube

hours. WJ-274-6 S/N 3 had accumulated 13,000 hours. No significant changes in performance have been noted.

A summary of the principal characteristics of the WJ-274-9 follow.

Performance	10-Watt Mode Typical	10-Watt Mode Guaranteed	20-Watt Mode Typical	20-Watt Mode Guaranteed
Frequency, gHz	2.2-2.4	2.2-2.4	2.2-2.4	2.2-2.4
Power output, saturated, watts	13	12	26	24
Gain, saturation, db	30	28	32	31
Efficiency, %	33	30	40	38
Electrical Requirements	**Typical**	**Range**	**Typical**	**Range**
TWT voltages				
Anode, vdc	1580	1580 ± 100	2020	2020 ± 100
Helix, vdc	1470	1470 ± 100	1550	1550 ± 100
Collector, vdc	980	980 ± 100	1075	1075 ± 100
Heater, vrms	3.5	3.5 ± 0.5	3.5	3.5 ± 0.5
TWT currents				
Anode, ma	0.2	0.5 max.	0.4	0.5 max.
Helix, ma	4.0	10.0 max.	8.0	10.0 max.
Collector, ma	32.0	40.0 max.	44.0	60.0 max.
Heater, amp	0.8	0.9 max.	0.8	0.9 max.

Environmental Characteristics	
Heat sink temperature	$-20^{\circ}C$ to $+85^{\circ}C$
Vibration	
Sinusoidal (2 min/octave)	0.5 inch double amplitude, 5 to 18 Hz ± 20g, peak, 18 to 2000 Hz
Random (5 min/axis)	20-59 Hz at 0.4 g^2/Hz 59-126 Hz at 9 db/octave 126-700 Hz at 0.4 g^2/Hz 700-900 Hz at -18 db/octave 900-2000 Hz at 0.09 g^2/Hz
Acceleration (1 min/axis)	100 g
Shock	75 g, 11 ms

The WJ-1084 power supply assembly (Figure 4-24) consists of the following subassemblies.

- Current limiter (Figure 4-25)
- Regulator (Figure 4-26)
- Low voltage converter (Figure 4-27)
- High voltage converter (Figure 4-28), mounted on a common magnesium baseplate and encased in a single RF-tight module.

The WJ-1084 power supply was qualified at Jet Propulsion Laboratory for its use on Mariner-Mars 1969. Since no design changes are required to meet the ERTS mission, the power supply assembly retains its qualification status.

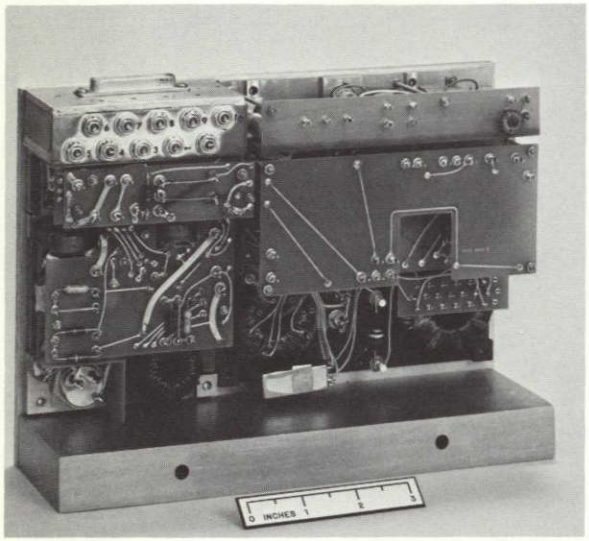

Figure 4-24

POWER SUPPLY for the TWTA is unchanged from its use on Mariner Mars

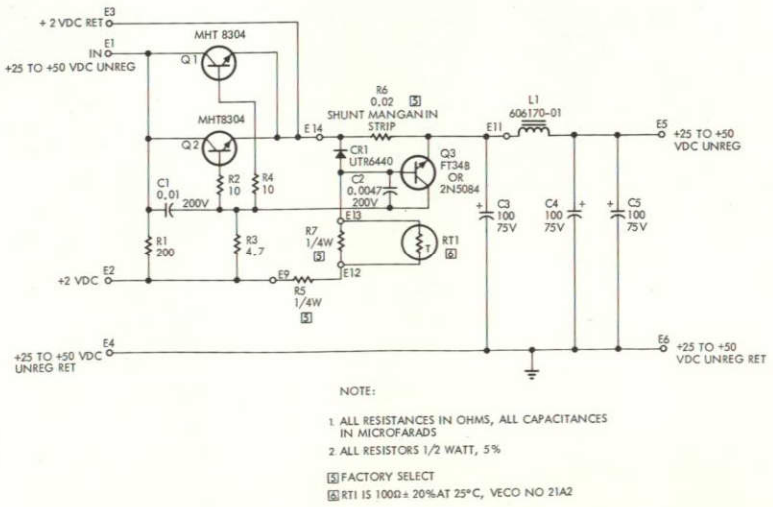

NOTE:

1. ALL RESISTANCES IN OHMS, ALL CAPACITANCES IN MICROFARADS
2. ALL RESISTORS 1/2 WATT, 5%

[5] FACTORY SELECT

[6] RT1 IS 100Ω ± 20% AT 25°C, VECO NO 21A2

Figure 4-25

CURRENT LIMITER for TWTA power supply

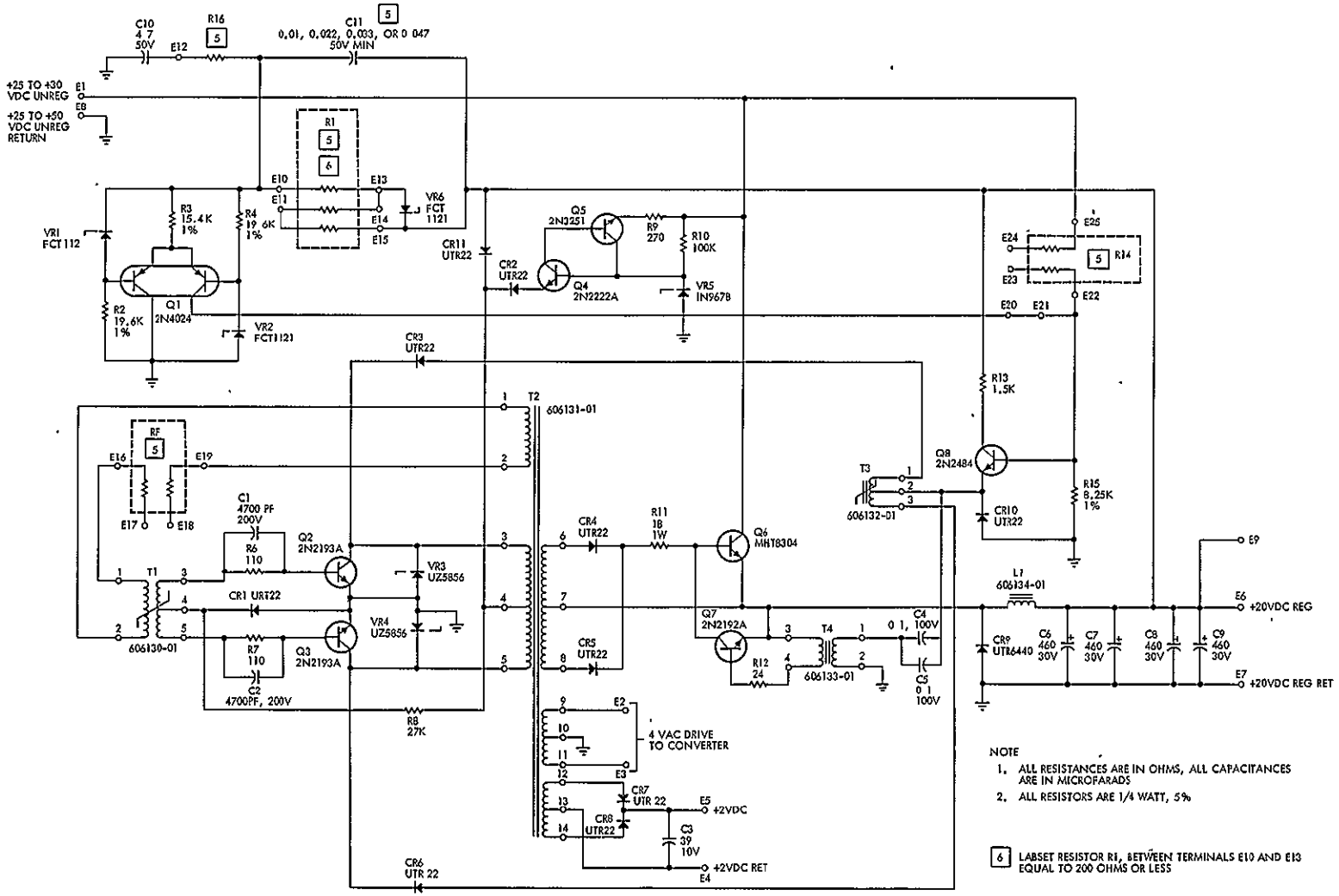

Figure 4-26
REGULATOR for TWTA power supply

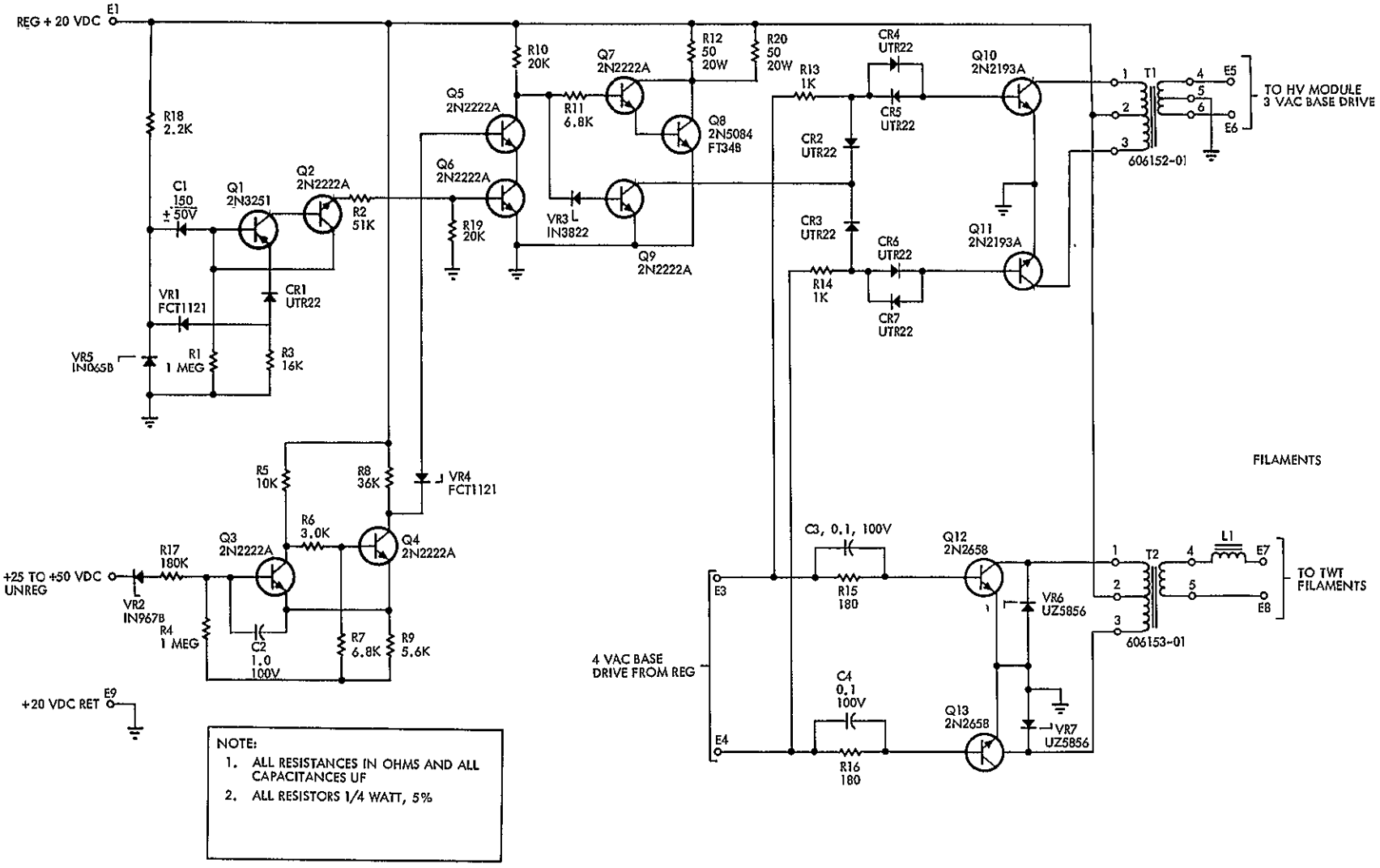

Figure 4-27
LOW VOLTAGE CONVERTER for TWTA power supply

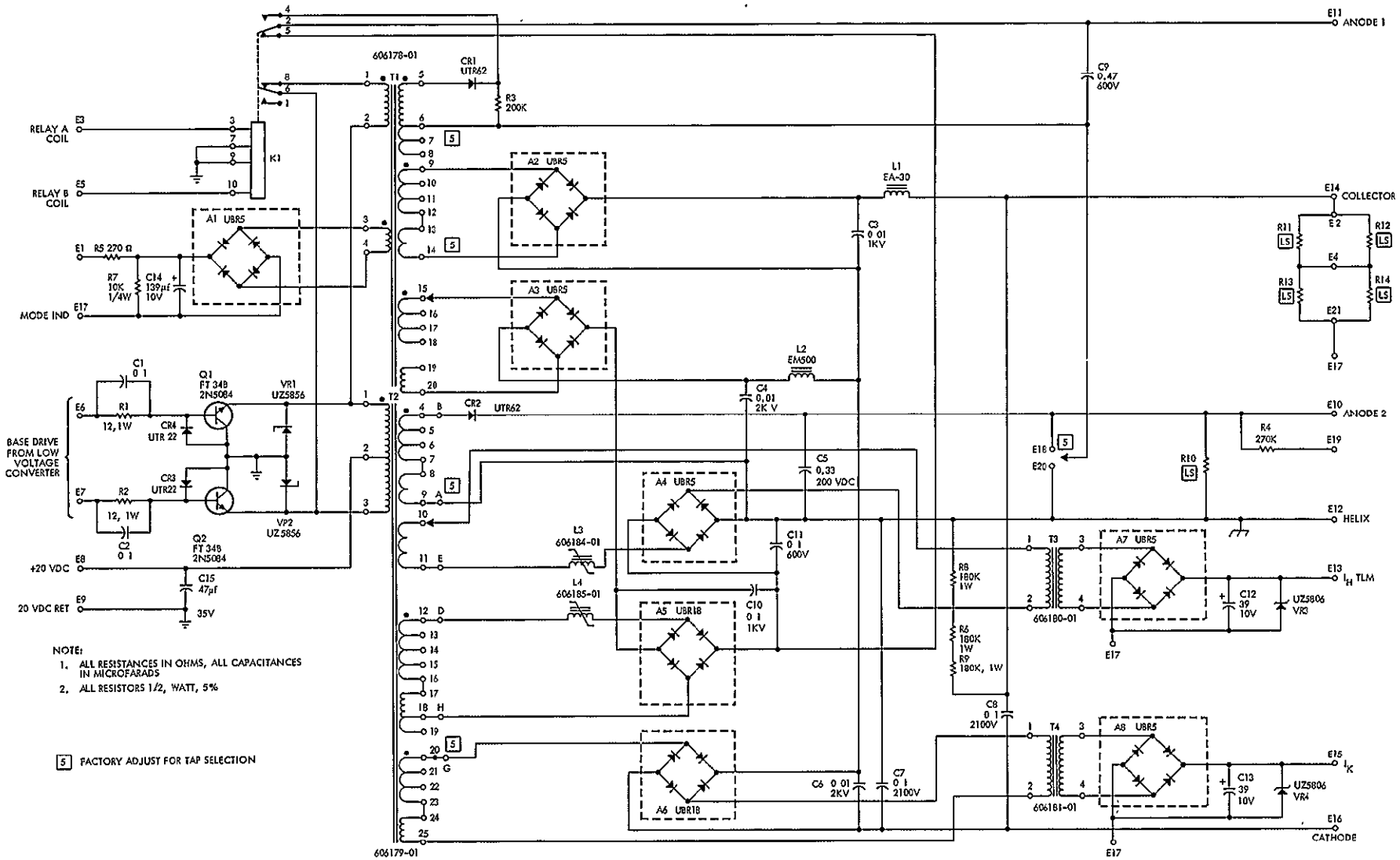

Figure 4-28
HIGH VOLTAGE CONVERTER for TWTA power supply

CONTENTS

5. DATA HANDLING SUBSYSTEM

The ERTS data handling subsystem, Figure 5-1, formats the spacecraft housekeeping and experiment telemetry for downlink transmission and decodes the uplink command data. Storage is provided for housekeeping telemetry and commands so that the spacecraft can be exercised and monitored when it is not in view of an ERTS ground station. The data handling subsystem also contains the spacecraft clock which provides timing signals to several observatory subsystems and generates a binary time word which is inserted in the telemetry data frame and which also controls the execution of stored commands.

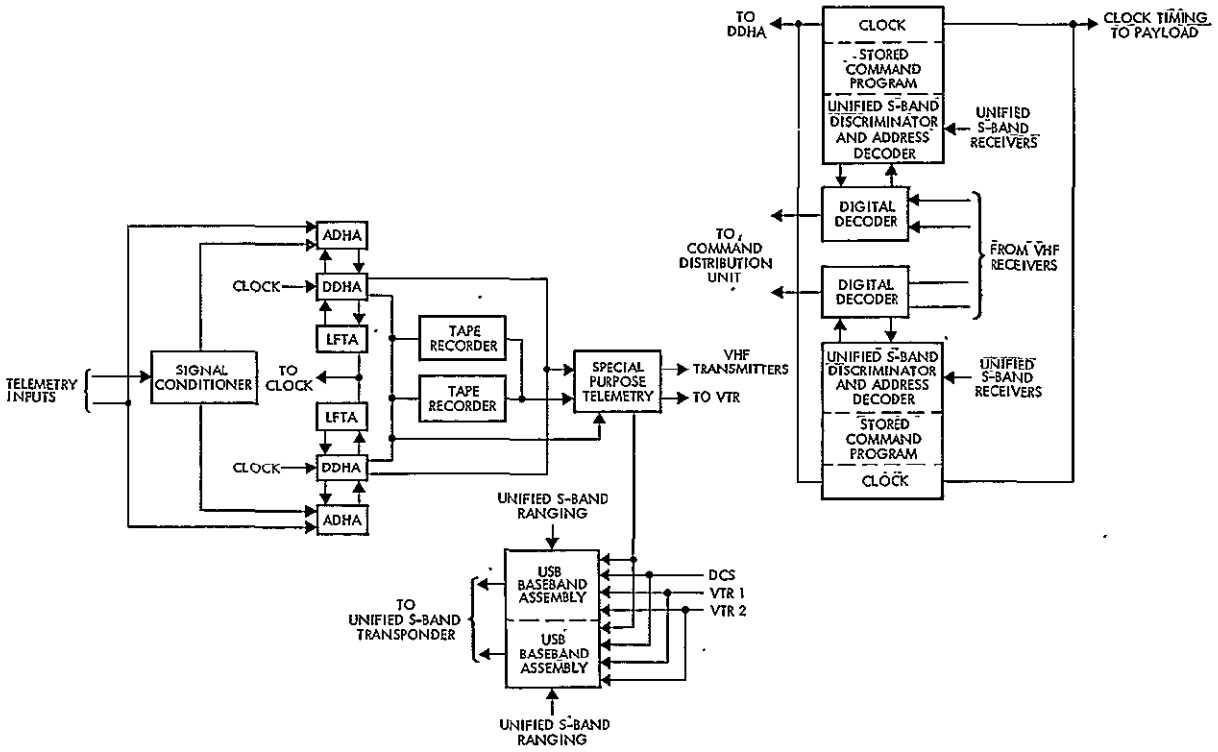

Figure 5-1

DATA HANDLING SUBSYSTEM for ERTS incorporates only one entirely new unit, the stored command programmer.

The ERTS data handling subsystem is derived from the flight-proven OGO data handling subsystem. The ERTS subsystem has additional redundancy; both equipment and functional. Additional capabilities

have been incorporated to provide the greater downlink data capacity required for ERTS and to provide for highly flexible operation with tracking, telemetry, and command capabilities through either MSFN or STADAN.

The flight-proven OGO hardware has been retained as much as possible. The most complex single items in the data handling subsystem, the digital data handling assemblies, are unmodified from the successful OGO design. The units to be used for the first spacecraft are already fabricated and tested and require only a post-storage verification test.

The analog data handling assemblies require the installation of unity-gain inverters to provide negative signal capability. The modification requires module installation in available space within the unit along with a wiring change. The units for the first spacecraft are already fabricated and tested but will require re-acceptance testing after the installation of the inverters.

The low frequency timing assemblies and the command decoders require only minor wiring changes, consisting of bringing out wires that previously had only internal connections. The units for the first spacecraft are fabricated and tested but will require a partial re-acceptance test after the wiring changes.

The tape recorders will be manufactured using OGO drawings and procedures with slight changes which reflect the improvements in the state of the art since the OGO recorders were designed and provide the 32:1 playback ratio required for the ERTS mission.

The special purpose telemetry unit will be modified significantly to provide redundant data signal level-setting and switching.

The unified S-band baseband assembly adapted from the AF Program 949 spacecraft is significantly modified by adding additional subcarrier oscillators and commandable modes.

A newly designed and breadboard-tested stored command programmer assembly is the only unproven unit in the data handling subsystem.

5.1 FUNCTIONAL DESCRIPTION

5.1.1 Housekeeping Telemetry

ERTS utilizes two completely redundant sets of telemetry data handling equipment. The narrowband digital data can be transmitted over a 137.86-MHz VHF link and/ or a 2287.5-MHz unified S-band link. The system has two main functions, data handling and data storage. The data handling equipment groups each consist of one digital data handling assembly and one analog data handling assembly. One equipment group normally processes data for real time transmission and the other processes data into storage. These operations can be independent or simultaneous. The normal assignments of the equipment groups can be reversed by command.

Telemetry data are accepted in four formats: positive analog voltage, negative analog voltage, bilevel digital, and 9-bit serial digital. Bilevel digital inputs are conditioned and combined to form analog voltages. All of the analog voltage inputs, including those generated by bilevel inputs, are multiplexed and converted into digital format by the analog data handling assembly. The output of this assembly is a parallel digital data signal which is combined with the 9-bit serial digital data telemetry inputs in the digital data handling assembly, thus forming a single serial signal of digital housekeeping telemetry.

The serial data outputs from the redundant equipment groups are supplied either to the tape recorders or to the special purpose telemetry for immediate transmission by the VHF or unified S-band links. Switches within the special purpose telemetry unit allow real time data and stored data playback to be directed, by command, to the appropriate transmission path. Additionally, the special purpose telemetry unit provides 1 kilobit data for the two video tape recorders within the payload.

The equipment groups are supplemented by redundant low frequency timing assemblies and clock assemblies to generate the master oscillator frequencies, payload clock signals, coded spacecraft time and other low frequency timing required. Either assembly can be selected by command. Two real time telemetry bit rates, 1 kbit/sec and 32 kbits/sec, are provided. Data storage is at 1 kbit/sec and playback at 32 kbits/sec.

The data handling system normally provides 1 kbit/sec data for both the VHF and the unified S-band link and 32 kbits/sec playback data to the unified S-band link only. Alternate modes can be selected by command to provide 32 kbits/sec real time data to both the VHF and unified S-band links or to provide 32 kbits/sec playback data on the VHF link. Whichever mode is selected, the digital housekeeping telemetry stream is the only modulating signal on the VHF link.

5.1.2 Other Downlink Data

The data handling subsystem generates a composite baseband signal for the unified S-band link which includes both real time and playback housekeeping telemetry data, DCS analog data, 1 kbit/sec data signals from each of the two video tape recorders, and the unified S-band ranging signal. All of these data signals are modulated on subcarrier oscillators except the ranging signal, which is left at baseband. The composite signal is phase modulated onto the unified S-band downlink (Section 4.4).

5.1.3 Command

The command decoder system, four-way redundant, provides both VHF and unified S-band communication access through each of two fully redundant paths.

Each VHF command link accepts OGO-type FSK baseband from either VHF receiver. The baseband is demodulated in the input stage of the digital decoder and the resulting serial data stream is transferred to the stored command programmer unit. Here the data stream is checked for proper 7-bit address, whether or not it is a real-time or stored command and if it has priority over other activities. Real time commands have top priority over all except in-process real time commands and are executed immediately through the command distribution unit. Stored commands require a prior real-time, enable command before they will be accepted by the stored command programmer. Once commands are stored in the programmer, comparison of their time tag with the spacecraft clock time recurs every 64 msec. Stored commands are executed through the digital decoder and the command distribution

unit when the spacecraft time matches the time tag stored with the command.

Demodulation of the unified S-band command signal takes place in the stored command programmer unit. The command format, similar to the Apollo command format, consists of 1 kbit/sec subbit data biphase modulated on a 2-kHz tone, plus a 1-kHz synchronization tone, all frequency modulated on a 70-kHz subcarrier. Portions of the stored command programmer unit extract the 1 kbit/sec subbit data, decode the five subbit code into a 200 bits/sec data stream, detect the proper address, and deliver real time commands to the digital decoder and stored commands to memory. The operation of the system then is identical to that for VHF commands whether for real time execution or for storage.

5.2 DIGITAL DATA HANDLING ASSEMBLY

Basic formating and timing for telemetry are executed in the digital data handling assembly shown in Figure 5-2. In addition, the unit contains all the necessary gates for digital inputs and provides shift pulses to external shifting accumulators. The unit also provides timing and sequence signals for the analog data handling assembly.

Figure 5-2
THE DIGITAL DATA HANDLING ASSEMBLY for ERTS is unmodified from OGO

The nominal characteristics of the digital data handling assembly are as follows:

Output

Real time:	Serial bit train in Manchester code (one: true-false; zero; false-true) to special purpose telemetry.
Data storage:	Serial bit train in NRZ code (one: true; zero; false) to narrowband tape recorder and special purpose telemetry (then to wideband video tape recorders).
To analog data handling assembly:	High frequency timing and sync down to approximately 5000 Hz
	61 matrix signals for analog gate control
	4 multiplexer select signals
	1 aperture gate signal
	9 A-D converter timing signals
To low frequency timing assembly:	128 kilobit clock
	64 kilobit clock, various control signals
	(time accumulation counter readout, time status)
To digital word shifting accumulators:	Shift pulses, inhibit pulses, signal bus

Input

From low frequency timing assembly:	Bit rate clock time accumulator readout status and synchronization
From analog data handling assembly:	8 A-D converter output signals
Commands:	9 lines from the digital decoder provide message commands
	20 lines from the command distribution unit provide relay commands such as bit rate operation mode
Power requirements:	-6 volts, 1.8 watts maximum +9 volts, 5.7 watts, maximum +16 volts, 4.2 watts maximum

Weight:	18 pounds maximum
Size:	650 cubic inches maximum

Three lines from the DDHA and a shifting accumulator are associated with each serial digital measurement. The shifting accumulator is used as a buffer between the source and the data handling assembly. Shift pulses occur on one line at the bit rate in use and are present whenever an equipment group is on. These pulses clock the data out of the shifting accumulator, are nominally 0.75 microsecond wide, and have a true level of +10 volts.

An inhibit pulse on a second line indicates that a particular input is being sampled and is unique to each serial digital measurement. It is at the true level (+5 to +11 volts) for the sampling period of the particular measurement. It gates the shift pulses to the shifting accumulator. It also inhibits accumulation of data during accumulator readout.

Serial spacecraft digital inputs from the shifting accumulator occupy the third line. A true level of this signal is a voltage between +5.2 to +9.0 volts, a false level being between ±0.65 volt.

Words are arranged in a predetermined format within a main multiplexer and two submultiplexers. The main frame, 128 words long, is generated by a sequence of gate openings which select data for insertion into the frame sequence. The basic format of data is conveniently represented by a chart with 128 spaces (Figure 5-3). Certain time slots are reserved for digital words (indicated by "D" in Figure 5-3). Others are reserved for analog words (indicated by "A"), and some may take either (indicated by A/D). Twelve time slots (1, 2, 3, 33, 34, 35, 65, 66, 67, 97, 98, 99) are allocated to fixed words having specific assignments.

Each word in the 128-word frame consists of 9 bits. A serial digital measurement may use all of these 9 bits, but only 8 are used for analog words. The unused bit in each analog word is processed as a binary zero. Since each word contains 9 binary bits, the frame is 1152 bits long. Words 1, 2, and 3 always possess the same sequence of binary digits and are used for frame sync, to indicate the start of

FRAME SYNCHRONIZATION 1	2	3	A 4	A 5	A 6	A 7	A 8
D 9	D/A 10	D/A 11	D/A 12	A 13	A 14	A 15	A 16
D 17	D 18	D 17	D/A 20	A 21	A 22	A 23	A 24
D 25	D/A 26	D/A 27	D/A 28	A 29	A 30	A 31	A 32
ACCUMULATED TIME 33	34	35	A 36	A 37	A 38	A 39	A 40
D 41	D/A 42	D/A 43	D/A 44	A 45	A 46	A 47	A 48
D 49	D 50	D 51	D/A 52	A 53	A 54	A 55	A 56
D 57	D/A 58	D/A 59	D/A 60	A 61	A 62	A 63	A 64
IDENTIFICATION WORDS 65	66	67	A 68	A 69	A 70	A 71	A 72
D 73	D/A 74	D/A 75	D/A 76	A 77	A 78	A 79	A 80
D 81	D 82	D 83	D/A 84	A 85	A 86	A 87	A 88
D 89	D/A 90	D/A 91	D/A 92	A 93	A 94	A 95	A 96
SUBMULT #1 97	SUBMULT #2 98	SUBMULT #3 99	A 100	A 101	A 102	A 103	A 104
D 105	D/A 106	D/A 107	D/A 108	A 109	A 110	A 111	A 112
D 113	D 114	D 115	D/A 116	A 117	A 118	A 119	A 120
D 121	D/A 122	D/A 123	D/A 124	A 125	A 126	A 127	A 128

D = DIGITAL INPUT

A = ANALOG INPUT

D/A = DIGITAL OR ANALOG INPUT

Figure 5-3

BASIC TELEMETRY FORMAT

each 128-word group. Words 33, 34, and 35 are allocated to spacecraft time (accumulated 1.152-second intervals), which requires 25 bits. Words 65, 66, and 67 provide information on the state of the telemetry system (described in detail later). Words 97, 99, and 99 are devoted to conveying submultiplexer data.

Three submultiplexers are used to expand the data handling capacity of the system. Each submultiplexer consists of 128 time slots. Certain time slots are devoted to analog and others to serial digital gates as in the main multiplexer. The assignment of analog and digital words for submultiplexer No. 1 is shown in Figure 5-4. Since one word of the submultiplexer is sampled each time the entire main multiplexer is sampled, the sampling rate is 1/128th of the main multiplexer multiplexer sampling rate. Each word from submultiplexer No. 1 is inserted into the main frame in word 97. This submultiplexer is devoted to payload information.

1 D	2 D	3 D	4 D	5 D	6 D	7 D	8 D
9 A	10 A	11 A	12 A	13 A	14 A	15 A	16 A
17 D/A	18 D/A	19 D/A	20 D/A	21 D/A	22 D/A	23 D/A	24 D/A
25 A	26 A	27 A	28 A	29 A	30 A	31 A	32 A
33 D/A	34 D/A	35 D/A	36 D/A	37 D/A	38 D/A	39 D/A	40 D/A
41 A	42 A	43 A	44 A	45 A	46 A	47 A	48 A
49 D/A	50 D/A	51 D/A	52 D/A	53 D/A	54 D/A	55 D/A	56 D/A
57 A	58 A	59 A	60 A	61 A	62 A	63 A	64 A
65 D	66 D	67 D	68 D	69 D	70 D	71 D	72 D
73 A	74 A	75 A	76 A	77 A	78 A	79 A	80 A
81 A	82 A	83 A	84 A	85 A	86 A	87 A	88 A
89 A	90 A	91 A	92 A	93 A	94 A	95 A	96 A
97 A	98 A	99 A	100 A	101 A	102 A	103 A	104 A
105 A	106 A	107 A	108 A	109 A	110 A	111 A	112 A
113 A	114 A	115 A	116 A	117 A	118 A	119 A	120 A
121 A	122 A	123 A	124 A	125 A	126 A	127 A	128 A

D = DIGITAL EXPERIMENT
A = ANALOG EXPERIMENT
D/A = DIGITAL OR ANALOG

Figure 5-4
SUBMULTIPLEXER NO. 1 FORMAT

Submultiplexers Nos. 2 and 3 are reserved for monitoring spacecraft performance. Typical measurements are bus voltage, transmitter temperatures, tape recorder status, and solar paddle position. Operation is similar to that of the submultiplexer No. 1 except that data is inserted into words 98 and 99 of the frame.

During certain critical periods of spacecraft operation, submultiplexer No. 2 can be accelerated to the main multiplexer rate, providing a higher frequency response for critical functions. In this mode all main frame data is displaced except the fixed words, which displace those submultiplexer No. 2 words normally assigned to time slots 1, 2, 3, 33, 34, 35, 65, 66, and 67. In the accelerated submultiplexer mode, no submultiplexer No. 1 nor No. 3 data is telemetered except word 97 in submultiplexer No. 1 and word 99 of submultiplexer No. 3.

Certain telemetry bookeeping functions are conveyed in main-frame fixed-words 65, 66, and 67. The first seven bits in word 65 indicate the position of a submultiplexer, i.e., which submultiplexer word is being read in a particular frame. This word applies to all three submultiplexers. The eighth bit of a binary 1 indicates that some relay command has been executed. The ninth bit indicates whether the equipment group is being used for real time or stored data processing.

Provision is made for indicating the telemetry mode for both equipment groups in the format of each. Word 66 conveys mode information about the equipment group generating it, and word 67 conveys mode information about the opposite equipment group.

The first bit of word 66 or 67 is true if the appropriate equipment group is generating real time data and is false if it is generating data for storage. A true condition in bits two and three indicates, respectively, that the telemetry is in the main multiplexer or accelerated submultiplexer mode. Only one of these signals can be true at a time. The last six bits are left blank. Figure 5-5 illustrates a typical sample of words 65, 66, and 67.

A relatively large number of inputs are provided to permit flexibility in the selection of data. The number of analog and serial digital

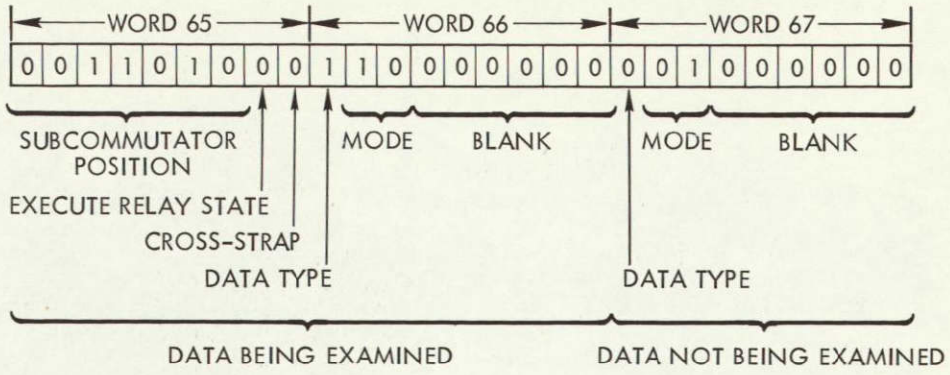

WORD 65 - SUBCOMMUTATOR POSITION 26
- EXECUTE RELAY UNENERGIZED
- NORMAL CROSS-STRAPPING

WORD 66 - REAL TIME DATA BEING TRANSMITTED
- MAIN COMMUTATOR MODE

WORD 67 - STORED DATA NOT BEING TRANSMITTED
- ACCELERATED SUBCOMMUTATOR MODE

Figure 5-5
EXAMPLE OF WORDS 65, 66, and 67

gates per multiplexer are shown below, along with the number of time slots that can be devoted to either analog or serial digital words.

	Data Quantities		Selectable
	Analog	Digital	Time Slots
Main multiplexer	96	48	28
Submultiplexer No. 1	112	40	24
Submultiplexer No. 2	88	12 (fixed)	0
Submultiplexer No. 3	88	4 (fixed)	0

5.3 LOW FREQUENCY TIMING ASSEMBLY

The low frequency timing assembly (Figure 5-6) provides various timing and synchronizing signals for spacecraft subsystems as well as bit rate selection. It also contains the spacecraft clock which accumulated approximately 1-second pulses for a total capacity of 2^{25} counts. This accumulated time is read out once in each main frame. The assembly

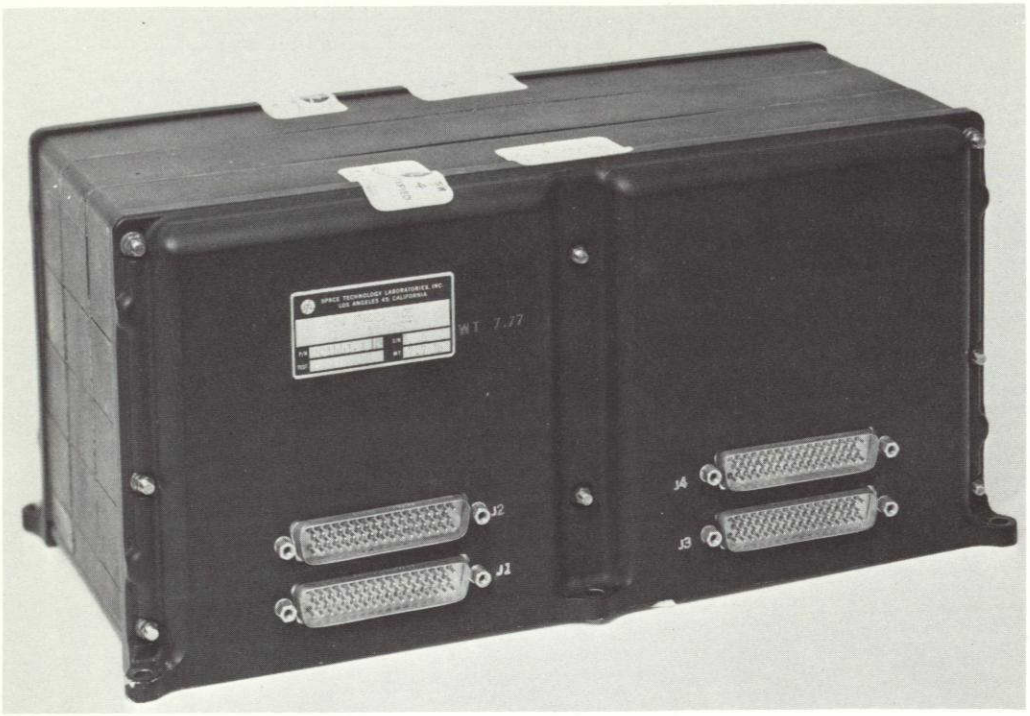

Figure 5-6

LOW FREQUENCY TIMING ASSEMBLY for ERTS is the OGO assembly with minor wiring changes.

controls the bit rate being used by the command. The following are its nominal characteristics:

Inputs:	64 kbit clock 128 kbit clock Various control signals
Outputs, timing available:	3555.0 pulses/sec 222.0 pulses/sec 13.8 pulses/sec 0.868 pulses/sec 0.0543 pulses/sec 0.00340 pulses/sec
System synchronization:	4923 pulses/sec, 0 degree 4923 pulses/sec, 180 degree 800 pulses/sec
Bit rate selection real time:	2 kHz (clock) (1 kbit/sec) 64 kHz (clock) (32 kbit/sec)

Time accumulation:	One pulse per 1.152 seconds 2^{25} pulse count storage
Tape recorder sync:	400 Hz square wave
Bit and word signals:	Bit: 1 kHz Word: 1/9 kHz
Telemetry signals time accumulation:	3 words, 9 bits each on 9 lines to digital data handling assembly
Status:	1 word, 9 bits maximum on same 9 lines
Data frame sync:	0.868 pulses/sec to synchronize both equipment groups to the time accumulator
Power requirements:	-6 volts, 0.29 watt maximum +9 volts, 4.10 watts maximum +16 volts, 0.15 watt maximum
Weight:	8.1 pounds maximum
Size:	360 cubic inches maximum

5.4 ANALOG DATA HANDLING ASSEMBLY

The analog measurements on ERTS are time multiplied and converted (shown in Figure 5-7) into digital words prior to transmission or storage by the analog data handling assembly. Each input consists of a single lead and a return. The nominal characteristics of the assembly are:

Input level:	0 to +5.120 volts or 0 to -6.375 volts
Fault protection:	$\pm$ 33.5 volts
Quantization:	8 bits (20 millivolts per bit nominal)
Sampling time:	74 microsec
Capacity:	384 analog inputs
Output:	8 lines indicating the binary values of converted inputs

Power requirement:	+16 volts ± 1% 25 ma maximum
	-16 volts ± 1% 10 ma maximum
	+9 volts ± 1% 75 ma maximum
Weight:	15 pounds maximum
Size:	350 cubic inches maximum

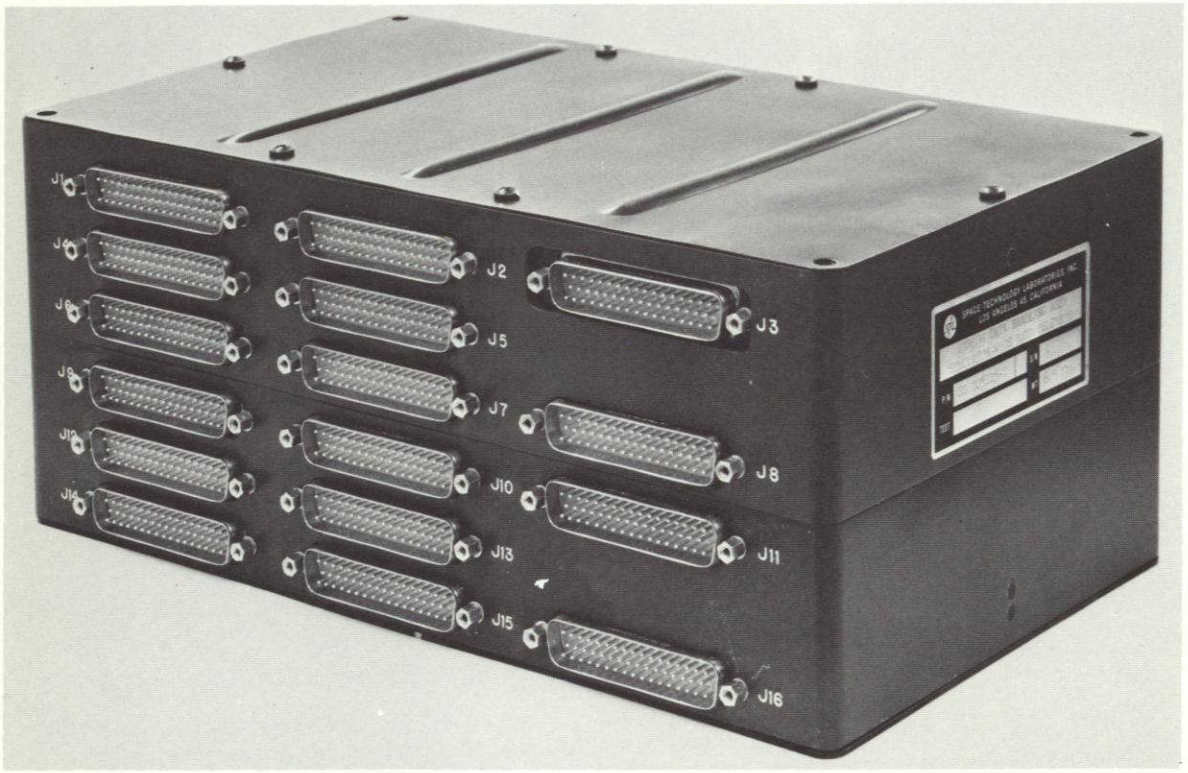

Figure 5-7
THE ERTS ANALOG DATA HANDLING ASSEMBLY is identical to that of OGO

Negative analog inputs from the payload are multiplexed and converted to positive (0 to +5.120 volts) signals prior to conversion to digital. Positive inputs are multiplexed and directly connected to the analog-to-digital converter. Inputs are quantized to eight bits (255 increments) ± 10 millivolts. Analog measurements are sampled for 74 microseconds for A-D conversion at either bit rate. The conversion process takes 58.6 microseconds; the additional 15.4 microseconds being used for charging stray capacitances to the input signal level before the

comparison process is started. Nominal input loading is 1 microampere from the source over the full input voltage range. Negative payload signals with less than 8000 ohms resistive and 50 picofarad capacitive source impedance are quantized to 1 percent accuracy. Positive analog outputs are quantized to 1 percent accuracy from sources of 1000 ohms resistive and 100 picofarad capacitive impedances.

Supercommutation of analog payload inputs, both within and between equipment groups, can occur in the payload integration assembly by merely connecting the analog gates. Thus one lead can be brought from a signal source, providing its output impedance meets the requirements, and can feed a number of gates in the two multiplexers in each equipment group. Since two equipment groups are contained in the spacecraft, it may be desirable to parallel analog inputs to both the real time and the data storage equipment groups, although since the two loads operate at different word rates direct paralleling can result in transients which may reduce conversion accuracy.

The analog data handling assembly basically consists of a large number of analog gates and an A-to-D converter. The gates are grouped into sets according to the multiplexer to which they are assigned. They funnel to one line and feed the A-D converter, which is sampled by the digital data handling assembly for insertion of the converter analog information into the telemetry frame.

Each multiplexer consists of a group of first level gates, eight second level gates, and a third level gate. The three levels are a means of grouping and subgrouping the transmission gates to reduce cross talk, minimize capacitive loading on any input, and reduce failure modes. These first level gates are arranged in groups of eight to form modules with all of the gates (in a single module) driven simultaneously from one driver. Each multiplexer is arranged into a gating matrix to simplify drive requirements and to conserve power.

This matrix drive technique is accomplished by making use of two simultaneous signals. As shown in Figure 5-8, a word select signal in the y-axis closes a group (module) of first level analog gates. A second word select signal in the x-axis selects one of the second level gates of

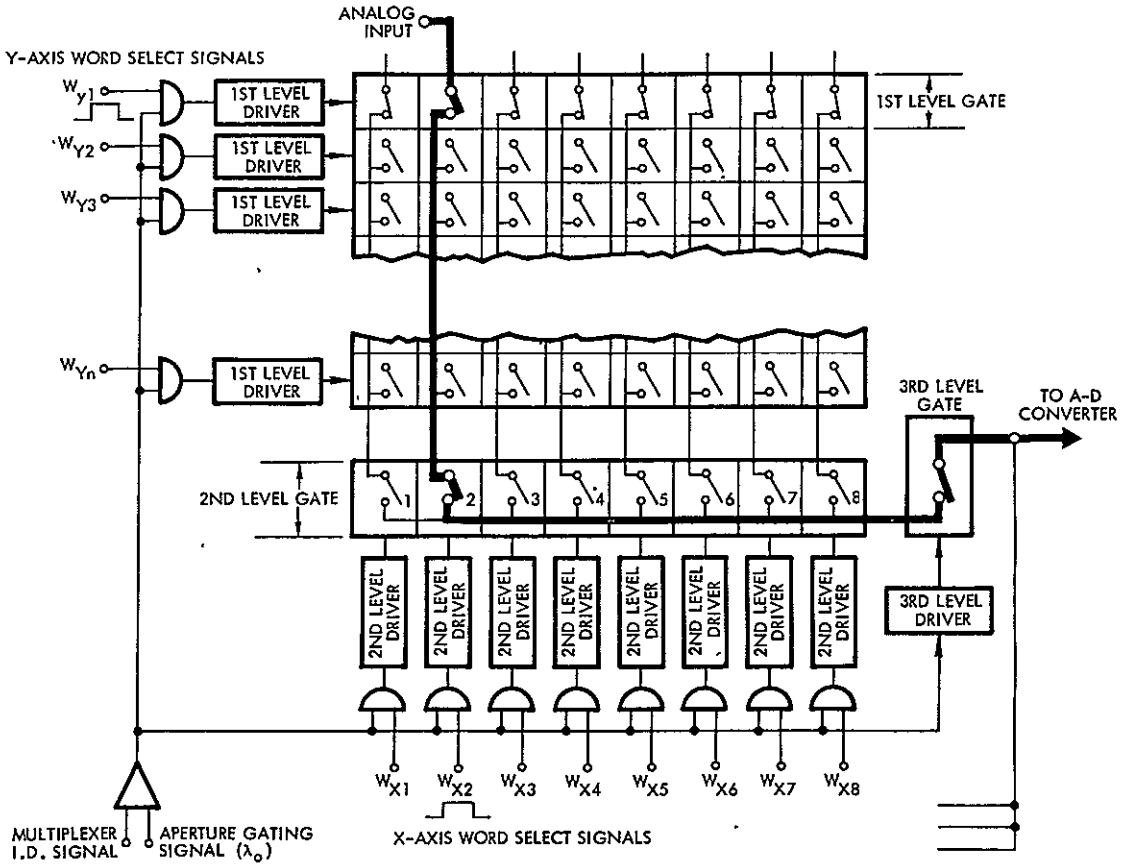

Figure 5-8
ANALOG GATING in the analog data handling assembly

the multiplexer. With the output of each first level gate within a single module connected to the input of a different second level gate, it is possible to sample any of the inputs by proper selection of the two word select signals. All positive-input second-level gate outputs of a multiplexer are connected in parallel to the third level gate through an isolation amplifier. Negative signal inputs are routed through second level gates that feed an inversion amplifier before the third level gate. This third level gate provides the required isolation between the five multiplexer groups.

The exact period that the three levels of gating are closed (sampling or aperture time) is controlled by an aperture gating signal (λ_o). This signal, present during each word, is supplied to each multiplexer group. A fourth signal, the multiplexer identification, is conditioned true for

only one multiplexer at a time, and in this way several multiplexer groups can share common x-y matrix word select signals. The aperture gating and multiplexer identification signals are AND gated to control multiplexer operation in such a way as to reduce power requirements (keep all drivers off during multiplexer dead time). The heavy line in Figure 5-8 illustrates an analog input signal path. In this example y-axis word select signal, W_{y1}, closed the eight first level gates in the top module and x-axis word select signal, w_{x2}, closed the second level gate number 2.

All analog transmission gates are two-transistor inverted configurations to produce (when closed) minimum offset potential and minimum impedance to the signal path. In the open position and when power is removed, they present a high impedance to reduce cross talk.

The A-to-D converter quantizes the input analog signals to eight-bit resolution at either of the system readout bit rates. The A-to-D conversion technique is the compressed half-split sampler type.

The A-to-D converter (Figure 5-9) contains a comparator, digital timing gates, a register (flip flops a_1 through a_8) for storage, and a digital-to-analog converter (switches and ladder adder). The register flip flops drive the D-to-A switches, which in turn define accurate voltage levels with the use of the ladder adder. The ladder adder applies binary weights to the register positions starting with a_1 as the most significant weight (2.56 volts) through a_8 with the least significant weight (20 millivolts).

Eight successive comparisons are made in ever decreasing portions of full scale until the voltage of the input signal is known to within one quantization level. The quantization level is nominally 20 millivolts out of the full scale of 0 to 5.120 volts. (Negative input signals are inverted and multiplied by a scale factor to produce positive 0 to 5.120 volts.) As shown in Figure 5-10, at the end of the sampling period (following time B_8) the register flip flops are left in states representing the binary equivalent of the analog signal voltage. If these eight states are interogated at the readout bit rate, a serial string of bits representing the

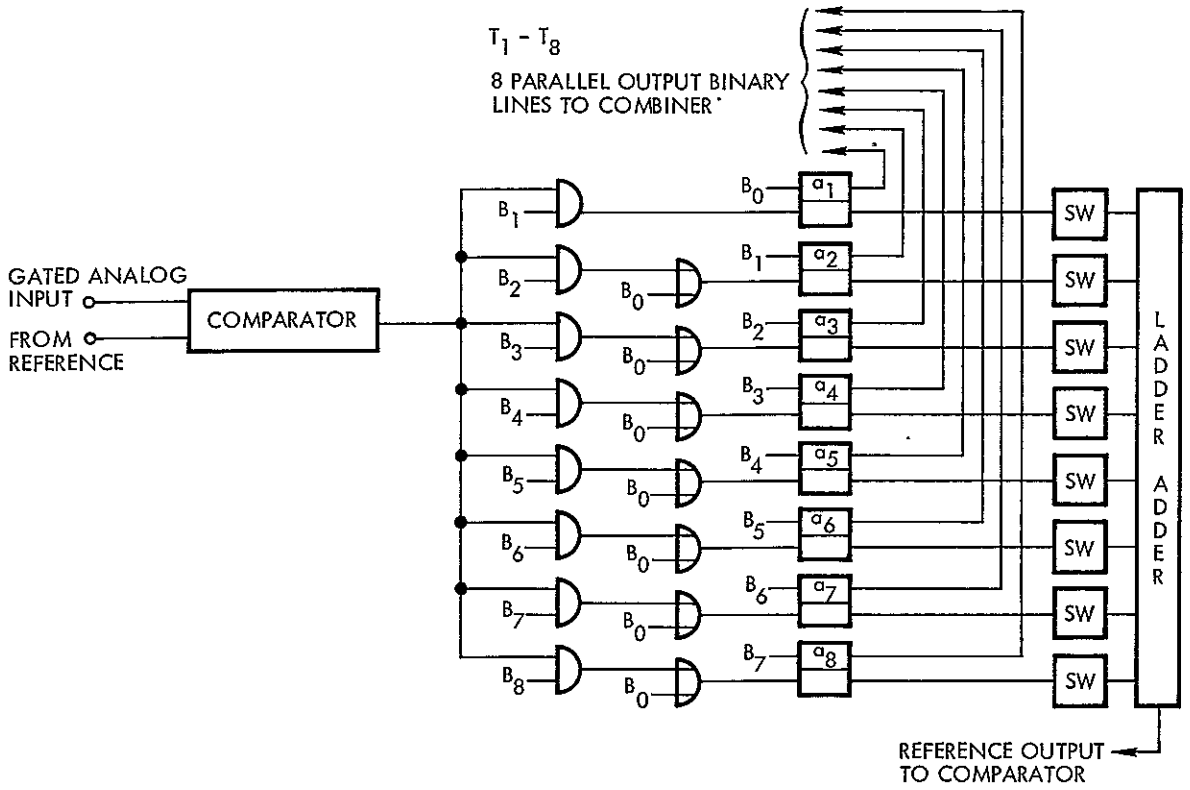

Figure 5-9

ANALOG-TO-DIGITAL CONVERTER in the analog data handling assembly

		LOGIC TIMING								
FLIP FLOP	STATE	B_0	B_1	B_2	B_3	B_4	B_5	B_6	B_7	B_8
a_1	1	B_0								
	0		$B_1 \cdot C$							
a_2	1		B_1							
	0	B_0		$B_2 \cdot C$						
a_3	1			B_2						
	0	B_0			$B_3 \cdot C$					
a_4	1				B_3					
	0	B_0				$B_4 \cdot C$				
a_5	1					B_4				
	0	B_0					$B_5 \cdot C$			
a_6	1						B_5			
	0	B_0						$B_6 \cdot C$		
a_7	1							B_6		
	0	B_0							$B_7 \cdot C$	
a_8	1								B_7	
	0	B_0								$B_8 \cdot C$

Figure 5-10

TRUTH TABLE for A-D encoding in the analog data handling assembly

analog signal voltages is obtained. Figure 5-11 shows the time relationships between the input signal aperture gating period, the logical timing pulses (and therefore actual conversion time), and the readout bit rate. The fact that the A-to-D conversion period is compressed or less than a full word time differentiates the technique from a conventional half-split sampler, where the conversion follows the readout bit rate. Figure 5-11 shows that the A-to-D conversion rate is independent of readout bit speed and that readout is initiated during conversion time in the case of the faster bit speed of 32 kbits/sec. As shown, however, no ambiguity exists since conversion always starts before and proceeds at a faster rate than readout.

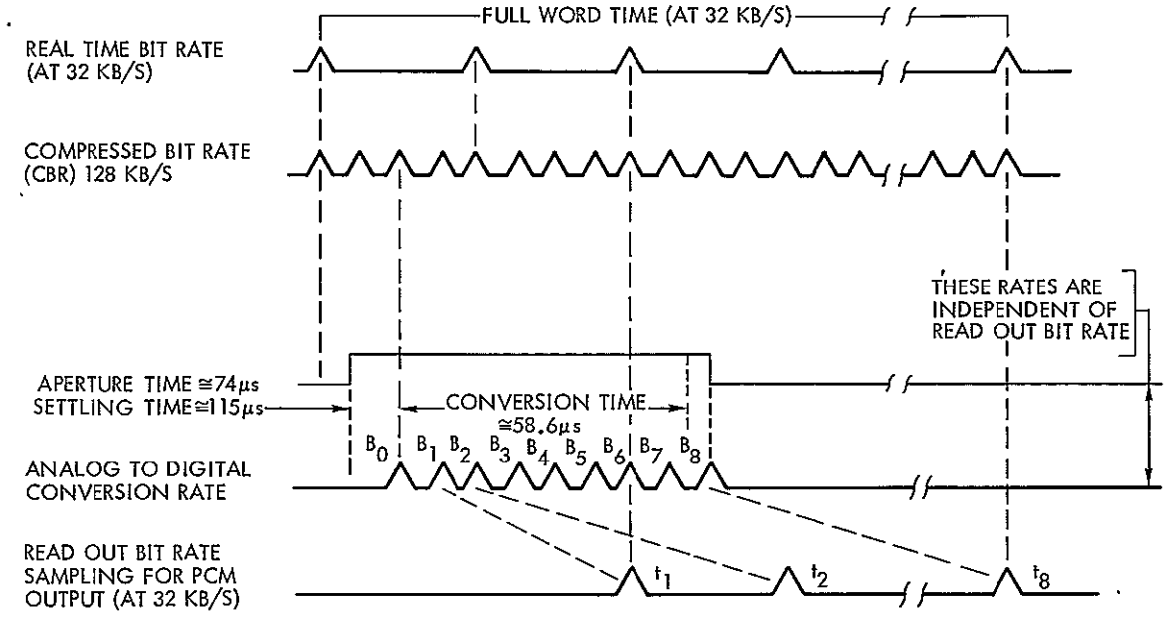

Figure 5-11

COMPARATOR TIMING. This example illustrates logic timing for the maximum real-time bit rate of 32 kbits/sec.

To provide calibration of the D-to-A converter in flight, specific voltages are generated within it and are telemered in the spacecraft submultiplexers. Thus, the telemetered value of the voltage can be compared with its design value to check on the calibration.

5.5 NARROWBAND TAPE RECORDER

The narrowband tape recorder (Figure 5-12) consists of two units, an unpressurized electronics package and a pressurized transport containing the tape and drive mechanisms. The recorder uses a reel-to-reel tape storage system. During recording, tape passes by the heads to another reel; playback occurs by reading the data out as the tape travels back to the first reel. Thus the playback data is transmitted backward with respect to that recorded. The nominal characteristics are as follows:

Signal input:	1 kbit NRZ data
Signal output:	Manchester PCM code, data playback in reverse chronological order (one: false-true; zero: true-false), 32 kbits
Control inputs from low frequency timing assembly:	Word rate
	Bit clock
	400 cycle square wave
Pressurization:	Internal argon atmosphere, pressurized as required (presently 16 pounds nominal)
Power requirements:	28 volts DC +5.5v, -4.5 volts 7.5 watts, average, recording (maximum) 17.0 watts, average, reproduce (maximum) 0.11 watts, average, standby (maximum)
Weight:	17.75 pounds maximum
Size:	Electronics: 260 cubic inches maximum Tape transport: 780 cubic inches maximum

The only changes in the ERTS recorders from OGO are:

- Type G-6 grease in the record motor-gear train and the playback motor instead of the type O-11 and O-16 oils previously used.
- A disc brake rather than the drum brake on OGO. This results in elimination of solenoid capacitors and simplifies brake adjustment.

- Optical end-of-tape detection
- 32:1 playback-to-record ratio by increasing record speed by a factor of 2

The first three changes represent state-of-the-art improvements since the OGO recorders were fabricated. These changes should increase the reliability of the ERTS recorders. The fourth change is a gear change to meet ERTS requirements and slightly improves tape recorder signal-to-noise ratio.

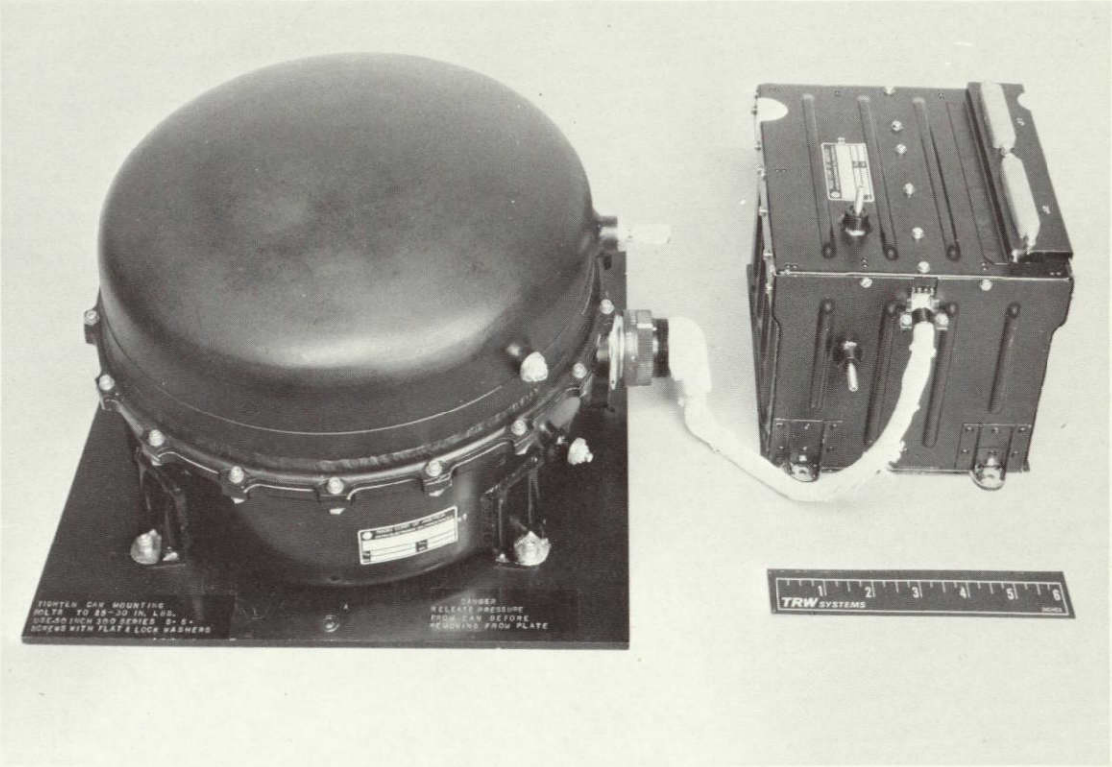

Figure 5-12

FOR ERTS THE OGO NARROWBAND TAPE RECORDERS are modified slightly for improved reliability and S/N

5.6 STORED COMMAND PROGRAMMER

The stored command programmer permits commands to be executed independently of ground station viewing (see Figure 5-13). The stored command programmer memory receives commands, addresses, and time tags via the command link, stores the commands and provides

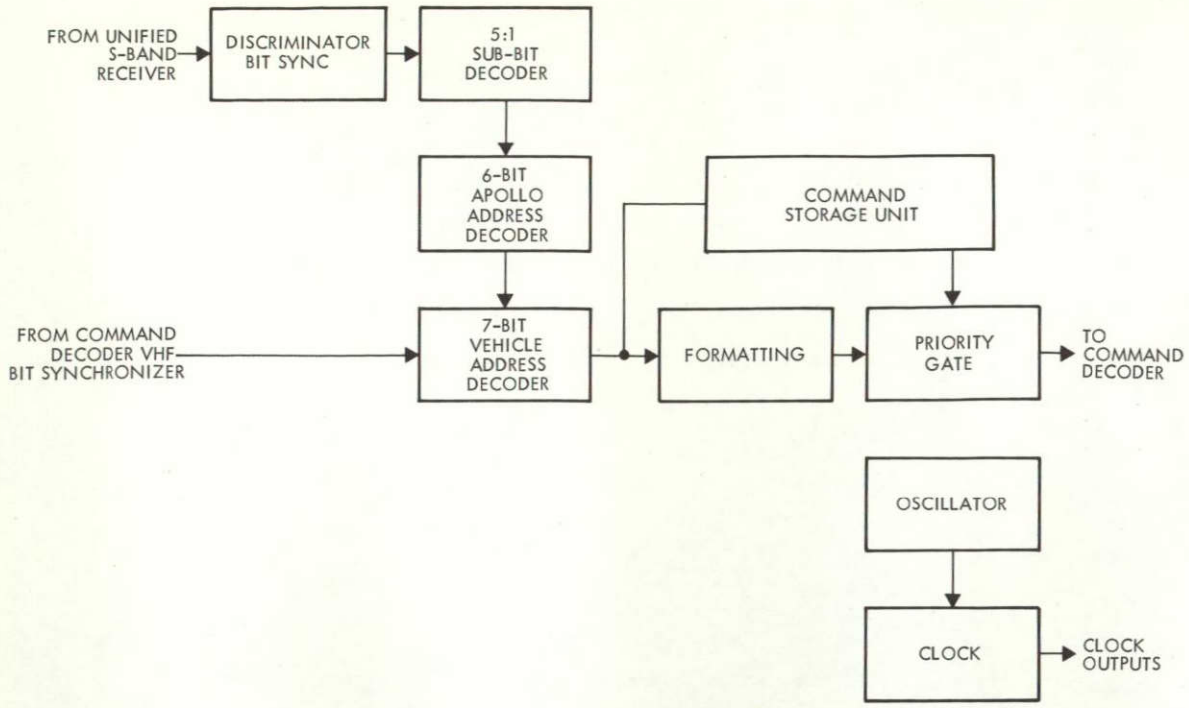

Figure 5-13

ERTS STORED COMMAND PROGRAMMER contains spacecraft clock circuitry and circuits for detecting commands to be stored.

for their execution at the time defined by their time tags. The functional characteristics of the memory are:

- 127 usable words of storage plus one synchronization word. The synchronization word must be sent via the command link each time the memory is filled.
- 40-bit digital command message format
- 25 bits per stored word (18 time tags, 6 command, 1 parity)
- 64 different commands selectable
- 0.5 sec command centers approximately
- 37-hour time cycle
- Total telemetry verification of memory contents in 74 seconds at 1 kbit/sec.
- Four modes of operation (standby/verification, clear, fill, process) entered by matrix command

- Telemetry of mode ID, message parity, and command parity data is provided
- Real time commands have priority over stored commands

The memory interfaces with the rest of the spacecraft as shown in Figure 5-14.

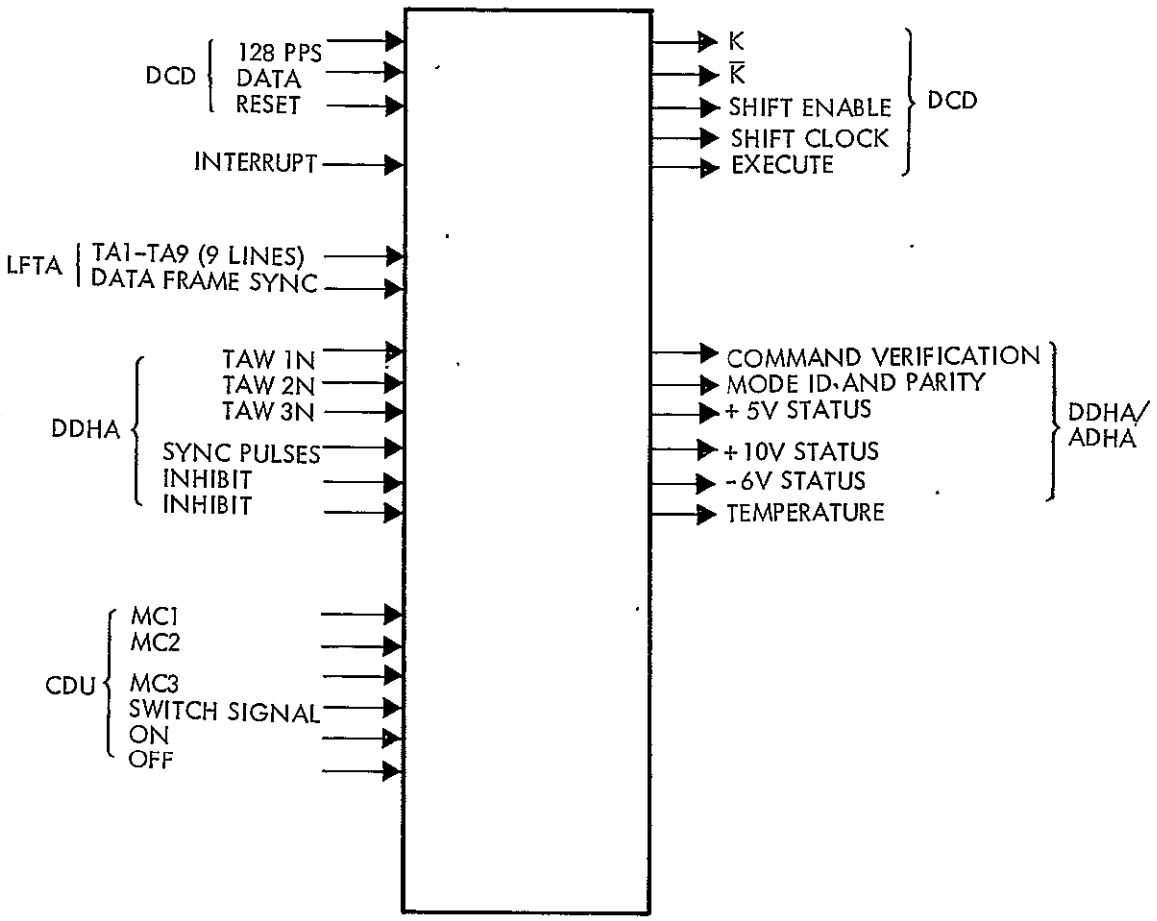

Figure 5-14

THE STORED COMMAND PROGRAMMER interfaces functionally with six other spacecraft assemblies

As shown in Figure 5-15, the power converter provides +15, +5, and -5 volts to the programmer. The clock driver receives a 100 kHz signal from the clock and generates two 50-kHz signals, phase 1 and phase 2, for use throughout the programmer. The mode decoder receives coded mode commands from the command distribution unit and

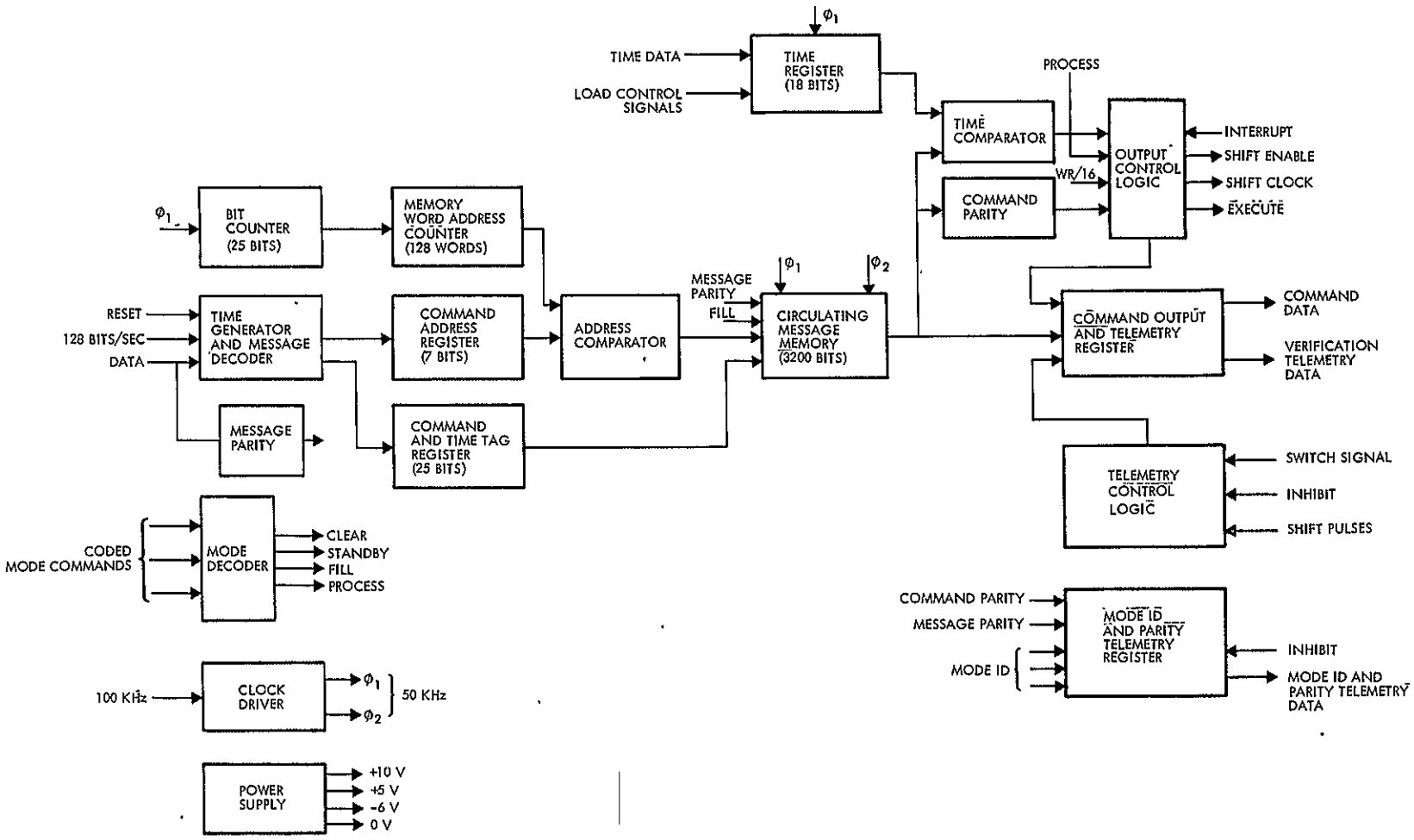

Figure 5-15

STORED COMMAND PROGRAMMER block diagram showing logic, store, clock, and telemetry

produces one of four mode signals (standby, clear, fill, process) to control operations.

Serial data enters the message decoder. If the command is a real time matrix command it is ignored. If it is to be stored, the timing generator is started and the various parts of the message are separated. The 7-bit word address enters the command address register and the remaining 25 bits (6 command, 18 time, and 1 parity) are shifted into the command and time ID register. The contents of the command address register and of the memory word address counter are compared in the address comparator. If they are alike, the contents of the command and time ID register are shifted into the circulating memory if message parity is correct and the programmer is in the fill mode. As the contents of the memory are circulated once, each 64 msec parity is checked on each word and each word is temporarily stored in the command output and telemetry register.

Time data is transferred to the circulating time register and the data is circulated. In the process mode the 18 time bits of each word are compared to the contents of the circulating time register. When they are alike, the 6-bit command is shifted out of the command output and telemetry register to the command decoder. The interrupt signal from the pre-decode logic prevents the transfer of data when a real time command is being received. An execute signal is sent to the command decoder after the data transfer is completed.

5.7 UNIFIED S-BAND SUBBIT DETECTOR, ADDRESS DETECTOR, AND PRIORITY LOGIC

The unified S-band uplink data transmission is compatible with the Apollo digital command system. Each information bit in the command is encoded into five subbits. The subbit rate is 1 kbit/sec. The ERTS subbit detector decodes the five groups into information bits which, when further decoded provide vehicle address and command information.

The input to the subbit detector, generated by the 70 kHz discriminator and bit synchronizer, provides serial NRZ data bit stream in 5-bit encoded form and a clock or sync signal coherent with the data bits. The input bit rate is 1 kbit/sec.

Two outputs of the bit detector are a serial bit stream resulting from the 5-bit decoding and bit synchronizing pulse at 200 bits/sec. The VHF link bit detection utilizes the OGO command decoder bit detection circuits and at the OGO bit rate of 128 bits/sec.

Both VHF and unified S-band command channels have their respective address decoder register and detection gates. Sensing of correct address information initiates restructuring of message and routing to the command decoder, command distribution unit, and stored command programmer. The restructuring consists of generating a 3-bit address compatible with OGO equipment (vehicle address) and substituting this address in the message format for the vehicle address. To execute this restructuring, the information of the transmitted message is delayed to follow the newly generated address. The selection of output is controlled by priority logic gates for routing to the command decoder and stored command programmer.

The real time command will always take over the stored command except during the critical period during which a stored command has been decoded and is in the process of being transferred to the command distribution unit. At other times the detection of acceptable address through either real-time command link will negate the stored command.

These functions require 30 integrated circuits and consume approximately 1 watt of converter power. The enclosure provided for the stored command programmer accommodates the new requirements for unified S-band and increased addressing capability.

5.8 UNIFIED S-BAND DISCRIMINATOR AND BIT SYNCHRONIZER

The discriminator and bit synchronizer (Figure 5-16) incorporates a 70-kHz frequency discriminator and a 1 kbit/sec bit synchronizer. It receives its input from the wideband data output of the receiver and provides two outputs, command data bit stream and command clock.

The wideband data input is in the form of a composite signal. The portion of interest to the synchronizer is a 70-kHz subcarrier, which is frequency modulated with 1 and 2 kHz signals. The 2-kHz signal is biphase modulated with 1 kbit/sec command data.

The discriminator block diagram is shown in Figure 5-16. The 70-kHz component of the wideband data is filtered and limited at the input. This signal is then amplified and split to two emitter followers. The emitter followers drive a Roung-Travis configured discriminator. The demodulated signal is then amplified and filtered to drive an emitter follower output circuit.

The bit synchronizer (Figure 5-16) separates the 1-kHz synchronization tone and the 2-kHz PSK signal by filtering. The 2-kHz PSK signal is then amplified and becomes the reference signal to the phase detector. The phase detector is followed by an emitter follower to output the command data bit stream. The 1-kHz synchronization tone is brought out through an emitter follower as the command clock data.

A highly stable redundant clock system (Figure 5-17) provides those frequencies required by the experiments and those required by

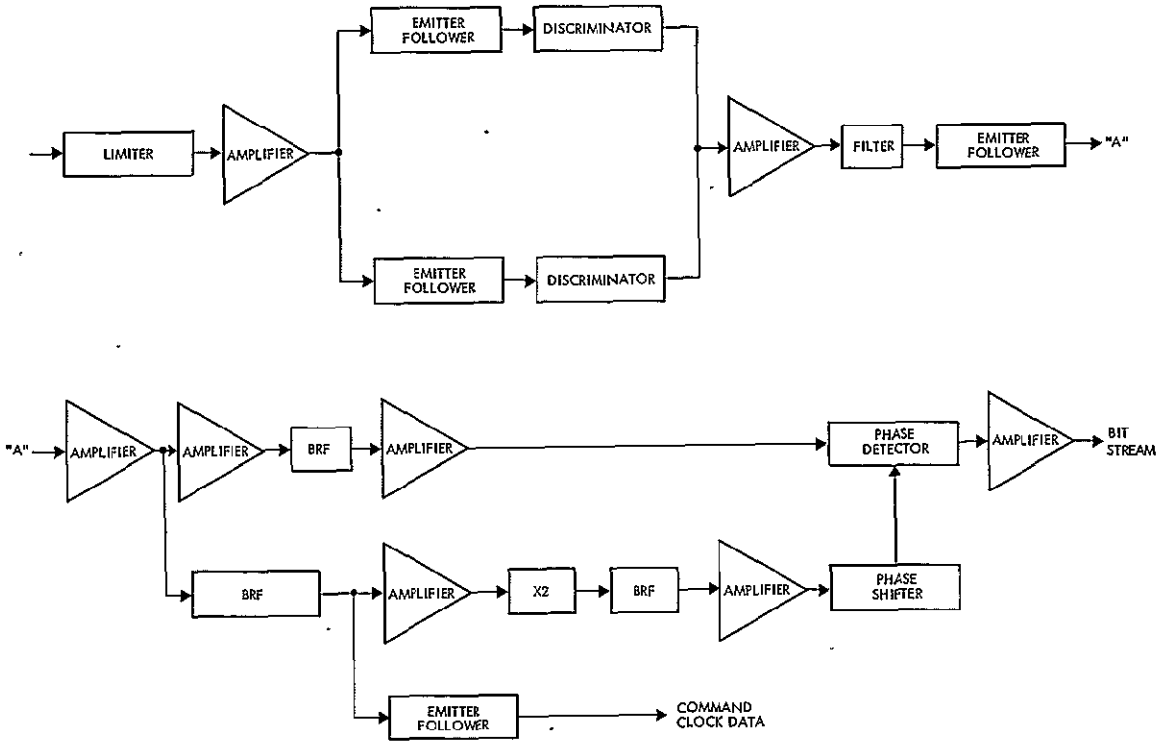

Figure 5-16

THE UNIFIED S-BAND DISCRIMINATOR AND BIT SYNCHRONIZER operates from +15 volts DC and requires 40 milliamperes

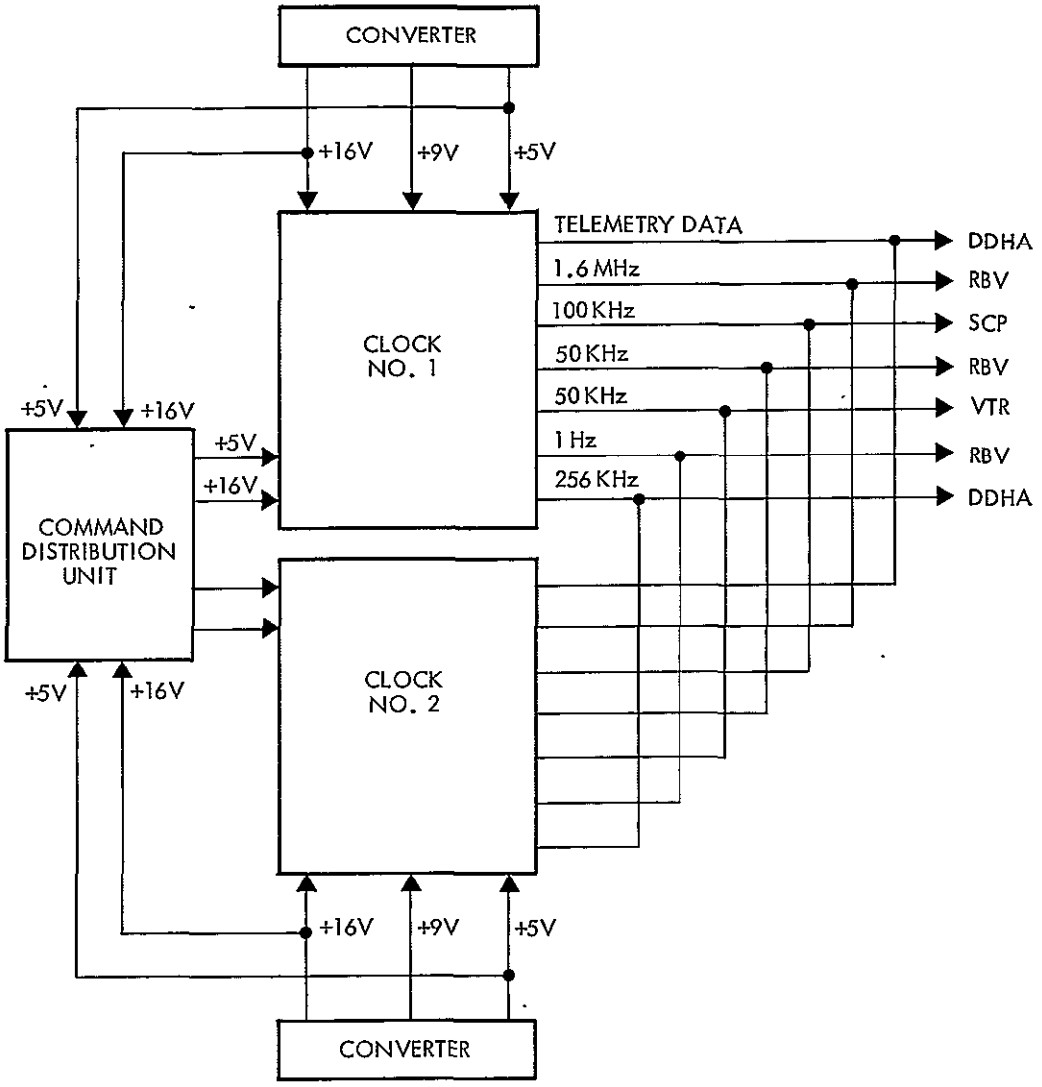

Figure 5-17
INTERFACE BLOCK DIAGRAM showing timing and power connections

the data handling subsystem. Each clock unit will be housed in its respective programmer unit, and the outputs of each will be cross-strapped to provide the redundancy requirements.

As shown in Figure 5-18, the basic clock unit consists of three main blocks:

1) Oscillator. The heart of the clock unit is a Bulova TCXO from which all other frequencies are derived. The output is a 6.4 MHz sine wave with a stability of 1 part in 10^6. It will require a continuous supply of +9 volts at a maximum of 16 ma.

2) Divider Chain. The various frequencies are derived from the 6.4 MHz oscillator by using the appropriate logic divider elements. All output frequencies are submultiples of the oscillator frequency. The scheme for obtaining the required outputs is shown below:

Input	Divide By	Output
6.4 MHz	4	1.6 MHz
6.4 MHz	25	256 kHz
1.6 MHz	16	100 kHz
100 kHz	2	50 kHz
50 kHz	50, 000	1 Hz

The logic elements used are the standard SN54 T^2L series IC's (T.I.). All outputs have a 50 percent duty cycle except the 256-kHz output, which requires a one-shot to provide the 0.2 microsecond pulsewidth.

3) Buffer Amplifiers. All outputs are buffered by using TTL open-collector NAND gates except the 1.6 MHz and the 256 kHz signals. The 1.6-MHz signal is buffered with discrete components because its output requires a level shift from +5 volts to +9 volts. Another buffer amplifier is used for monitoring the oscillator output and for providing a telemetry data signal. This uses a peak input detector, a TTL open-collector NAND gate for inversion, and discrete components for providing the level shift from +5 volts to +9 volts. All outputs are capable of being cross-strapped with the redundant unit since all outputs are derived from discrete components and open-collector gates.

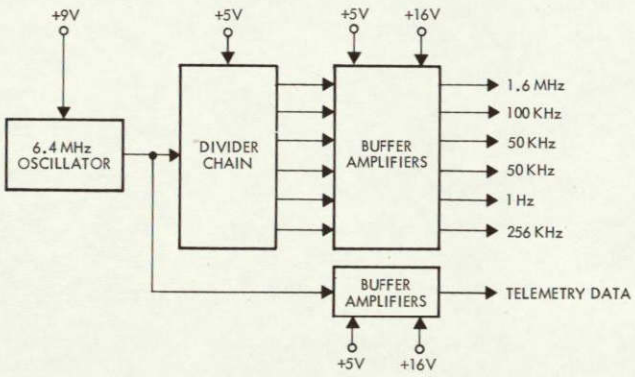

Figure 5-18
CLOCK simplified block diagram

All logic elements in the divider chain and all buffer amplifiers except the telemetry data output amplifier will be power-gated by ground command. The remainder will be continuously supplied with power for monitoring of both oscillators simultaneously.

5.9 COMMAND DECODER

Each command decoder (Figure 5-19) accepts composite audio

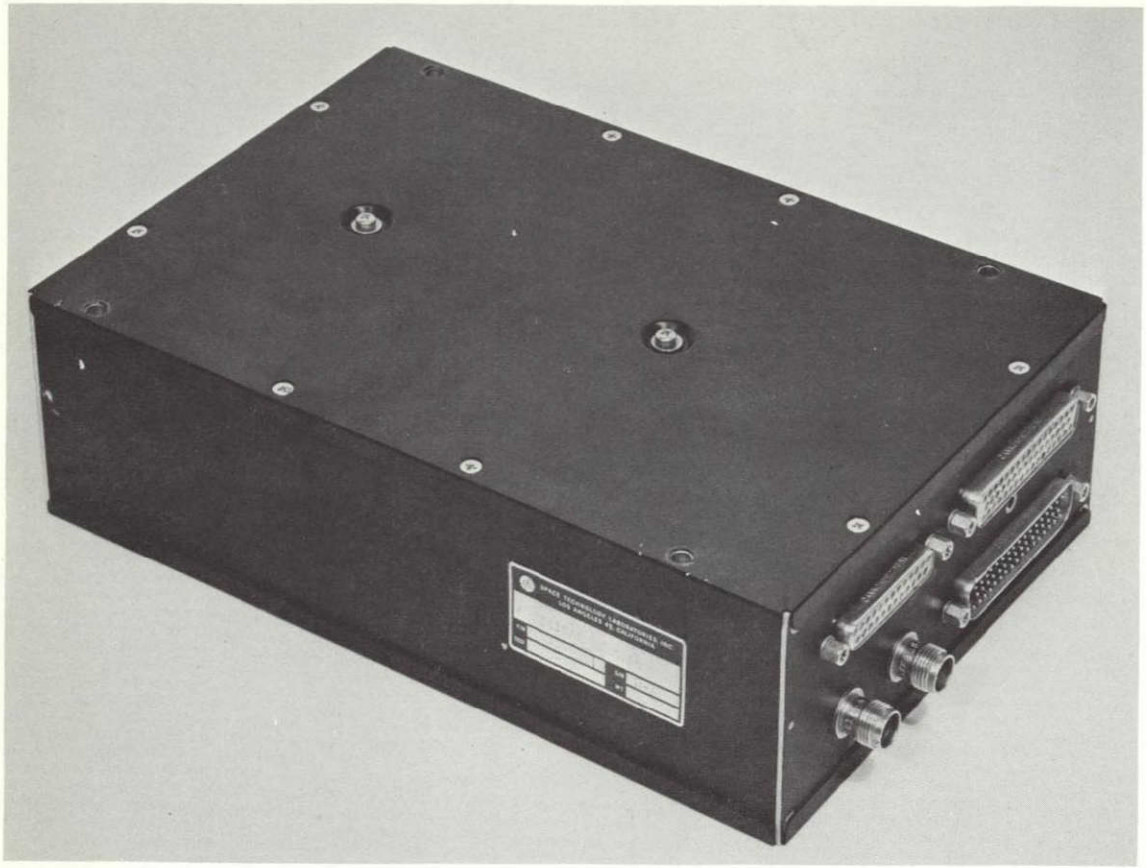

Figure 5-19
THE ERTS COMMAND DECODER is a minor modification of the OGO unit

command from either of the two VHF receivers, detects the 128 bit/sec data and outputs this with the associated clock signal to the stored command programmer. The command decoder accepts serial data, clock, reset, and squelch signals from the programmer and decodes the data signal into matrix commands or stored command data. As shown in Figure 5-20 this command data may be from either the VHF or unified S-band command link and may also have been stored previously in the programmer. The composite audio waveform, input from the VHF receivers, is shown in Figure 5-21.

The digital decoder derives its VHF synchronization from the 120-Hz amplitude modulated. The digital VHF data is derived from a frequency shift keyed subcarrier. The digital command word structure for real time matrix commands and for stored commands is shown in

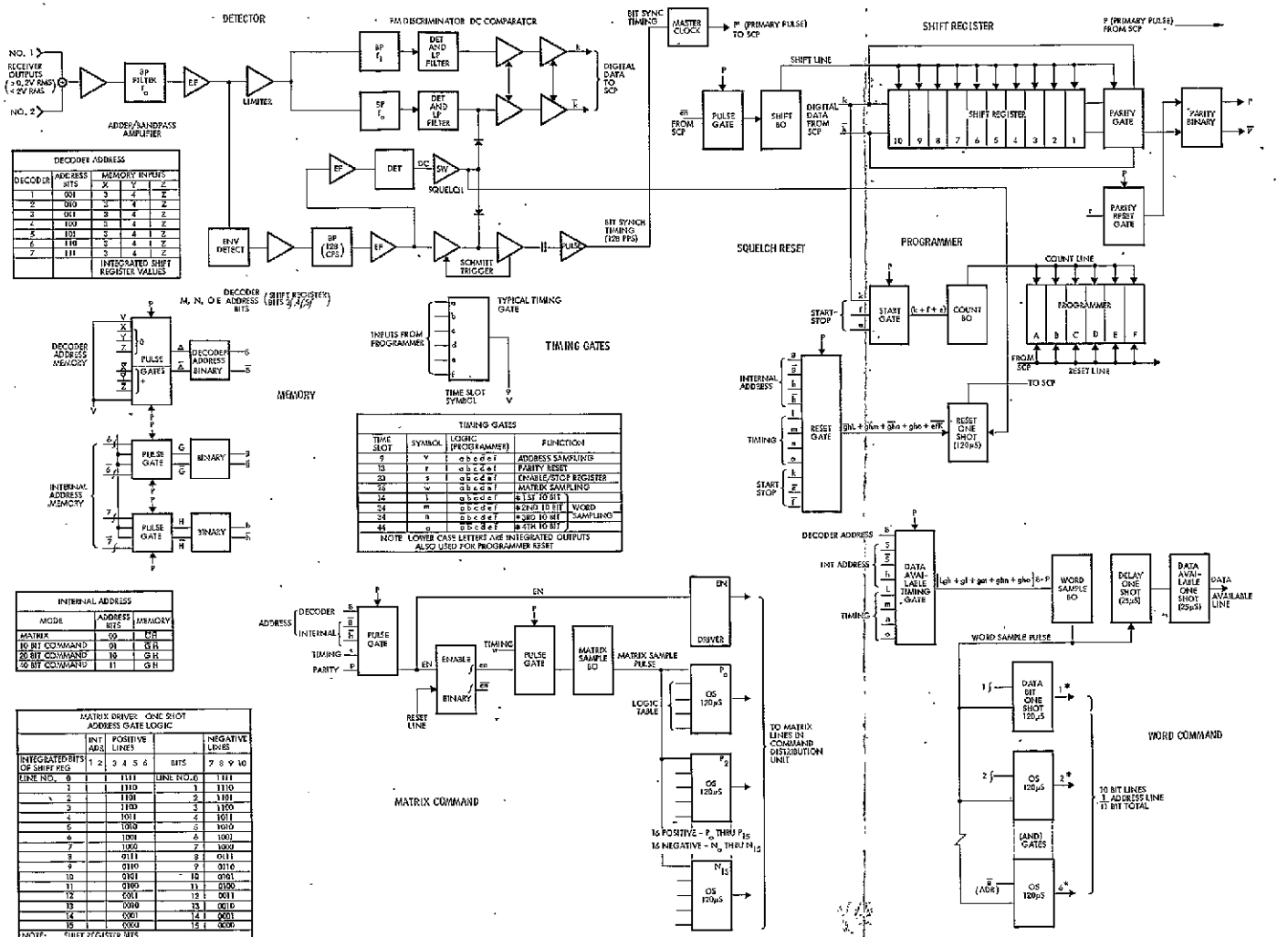

DECODER ADDRESS

DECODER	ADDRESS BITS	MEMORY INPUTS X	Y	Z
1	001	3	4	5
2	010	3	4	5
3	011	3	4	5
4	100	3	4	5
5	101	3	4	5
6	110	3	4	5
7	111	3	4	5
		INTEGRATED SHIFT REGISTER VALUES		

INTERNAL ADDRESS

MODE	ADDRESS BITS	MEMORY
MATRIX	00	GH
10 BIT COMMAND	01	GH
20 BIT COMMAND	10	GH
40 BIT COMMAND	11	GH

TIMING GATES

TIME SLOT	SYMBOL	LOGIC (PROGRAMMER)	FUNCTION
9	v	a b c d e f	ADDRESS SAMPLING
13	r	a b c d e f	PARITY RESET
23	s	a b c d e f	ENABLE/STOP REGISTER
26	w	a b c d e f	MATRIX SAMPLING
34	l	a b c d e f	+1ST 10 BIT
24	m	a b c d e f	+2ND 10 BIT WORD SAMPLING
24	n	a b c d e f	+3RD 10 BIT
44	o	a b c d e f	+4TH 10 BIT

NOTE LOWER CASE LETTERS ARE INTEGRATED OUTPUTS ALSO USED FOR PROGRAMMER RESET

MATRIX DRIVER ONE SHOT ADDRESS GATE LOGIC

	INT ADS. 1	2	POSITIVE LINES 3	4	5	6	BITS	NEGATIVE LINES 7	8	9	10
INTEGRATED BITS OF SHIFT REG											
LINE NO. 0	1	1	1	1	1	1	LINE NO. 0	1	1	1	1
1	1	1	1	1	1	0	1	1	1	1	0
2	1	1	1	1	0	1	2	1	1	0	1
3	1	1	1	1	0	0	3	1	1	0	0
4	1	1	1	0	1	1	4	1	0	1	1
5	1	1	1	0	1	0	5	1	0	1	0
6	1	1	1	0	0	1	6	1	0	0	1
7	1	1	1	0	0	0	7	1	0	0	0
8	1	1	0	1	1	1	8	0	1	1	1
9	1	1	0	1	1	0	9	0	1	1	0
10	1	1	0	1	0	1	10	0	1	0	1
11	1	1	0	1	0	0	11	0	1	0	0
12	1	1	0	0	1	1	12	0	0	1	1
13	1	1	0	0	1	0	13	0	0	1	0
14	1	1	0	0	0	1	14	0	0	0	1
15	1	1	0	0	0	0	15	0	0	0	0

NOTES: SHIFT REGISTER BITS ALSO INTEGRATED 1, 4, 10
0 = PRIMED (-) VALUES
1 = UNPRIMED VALUES
EXAMPLE ONE SHOT DRIVING POSITIVE LINE = 6 IS CONNECTED TO 1, 4, 10, 6

Figure 5-20
COMMAND DECODER block diagram

FOLDOUT FRAME 1

FOLDOUT FRAME 2

PRECEDING PAGE BLANK NOT FILMED.

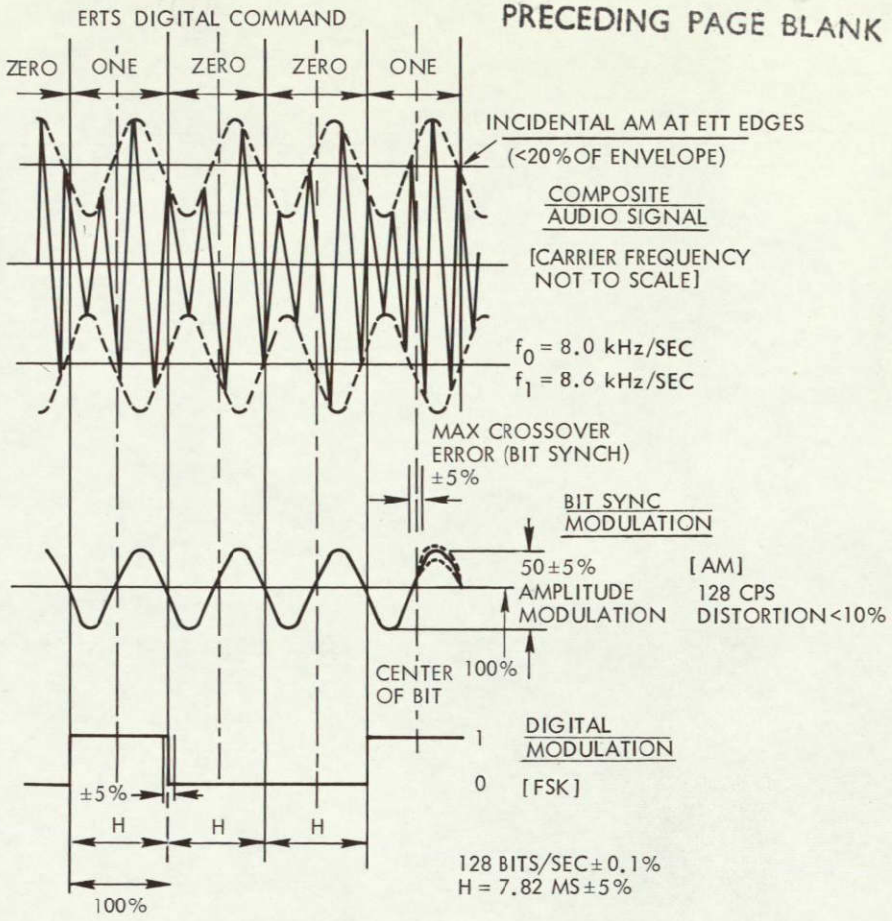

NOTE: SHIFTING TIME < 0.5MSEC

Figure 5-21
VHF COMPOSITE AUDIO WAVEFORM

Figure 5-22. Both types of commands are delivered from the stored command programmer in acceptable format for the command decoder to use without modification. When the command is verified, the decoder energizes a pair of matrix lines which feed relay drivers in the command distribution unit.

5.10 SPECIAL PURPOSE TELEMETRY

The special purpose telemetry unit (Figure 5-23) accepts PCM data from the real time narrowband telemetry equipment or narrowband tape recorder and conditions it for the telemetry transmitters. As

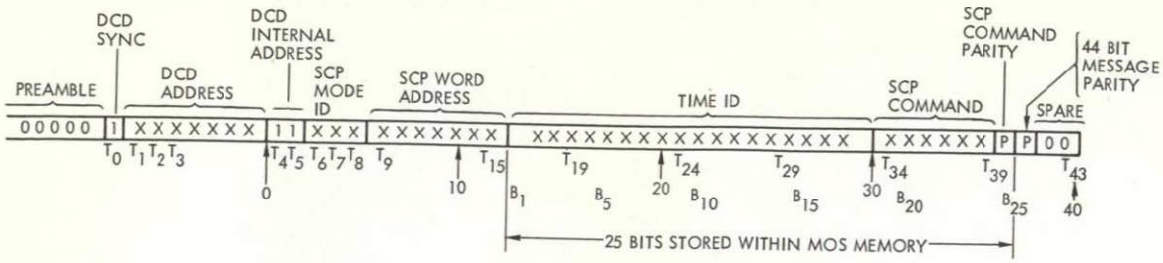

Figure 5-22

STORED COMMAND PROGRAMMER word format

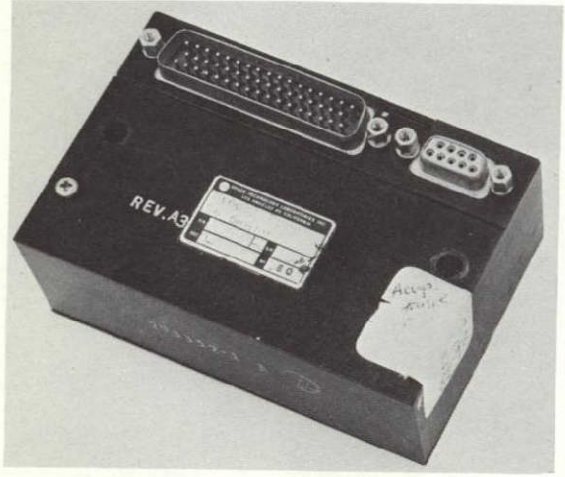

Figure 5-23

SPECIAL PURPOSE TELEMETRY unit for ERTS is a modified OGO unit

shown in Figure 5-24, two redundant conditioning channels are available. Switches allow real-time data and stored data playback to be directed, by command, to the appropriate transmitter or transmitters. In addition, 1 kbit/sec data in the data storage mode is converted to Manchester code and conditioned for transmission to the wideband video tape recorders.

The following are the nominal characteristics of the unit:

Inputs

2 PCM telemetry (real time and/ or data storage)

Bit rate: 1 or 32 kbits/sec real time, 32 kbit/sec data storage

True level: +6 to +10 volts

False level: 0 to +3 volts

Input impedance: 1300 to 1800 ohms

Outputs

3 PCM outputs, 3.4 volts peak-to-peak $\pm$0.2 volts into 10 kohms $\pm$5% to VHF telemetry transmitter and unified S-band baseband assembly

2 PCM outputs to wideband video tape recorders

Weight	0.8 pounds maximum
Size	20 cubic inches maximum
Power input	28 volts DC +5.5 volts - 4.5 volts 20 ma maximum at 28 volts

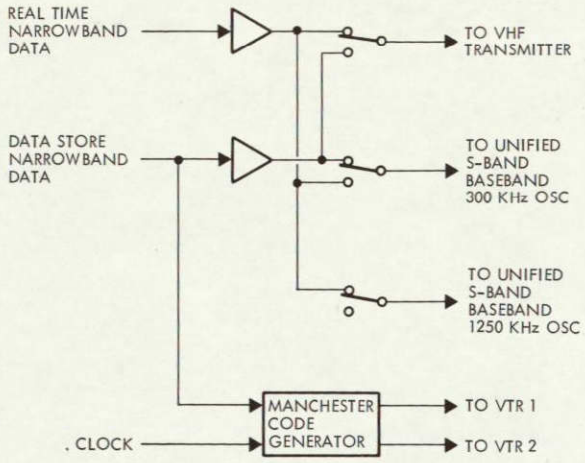

Figure 5-24

SIGNAL CONDITIONER block diagram showing shaping of narrowband data

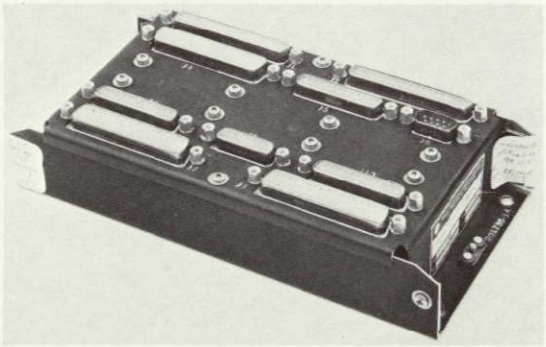

Figure 5-25

THE ERTS SIGNAL CONDITIONER is also an unmodified OGO unit

5.11 SIGNAL CONDITIONER

The signal conditioner (Figure 5-25) converts analog or digital measurement data from the payload and spacecraft subsystems to a form suitable for the narrowband telemetry system. Its nominal characteristics are as follows:

Output impedance: 2500 ohms, maximum

Signal voltage analog: 0 to +5.1 volts full scale, 0 to -6.375 volts full scale

Signal fault voltage: ±33.5 volts maximum

5.12 UNIFIED S-BAND DUAL BASEBAND ASSEMBLY

The dual baseband assembly (Figure 5-26) generates the composite baseband signal which phase modulates the unified S-band transmitter. The composite baseband signal is made up of:

- Four subcarriers frequency modulated by real-time or stored digital data

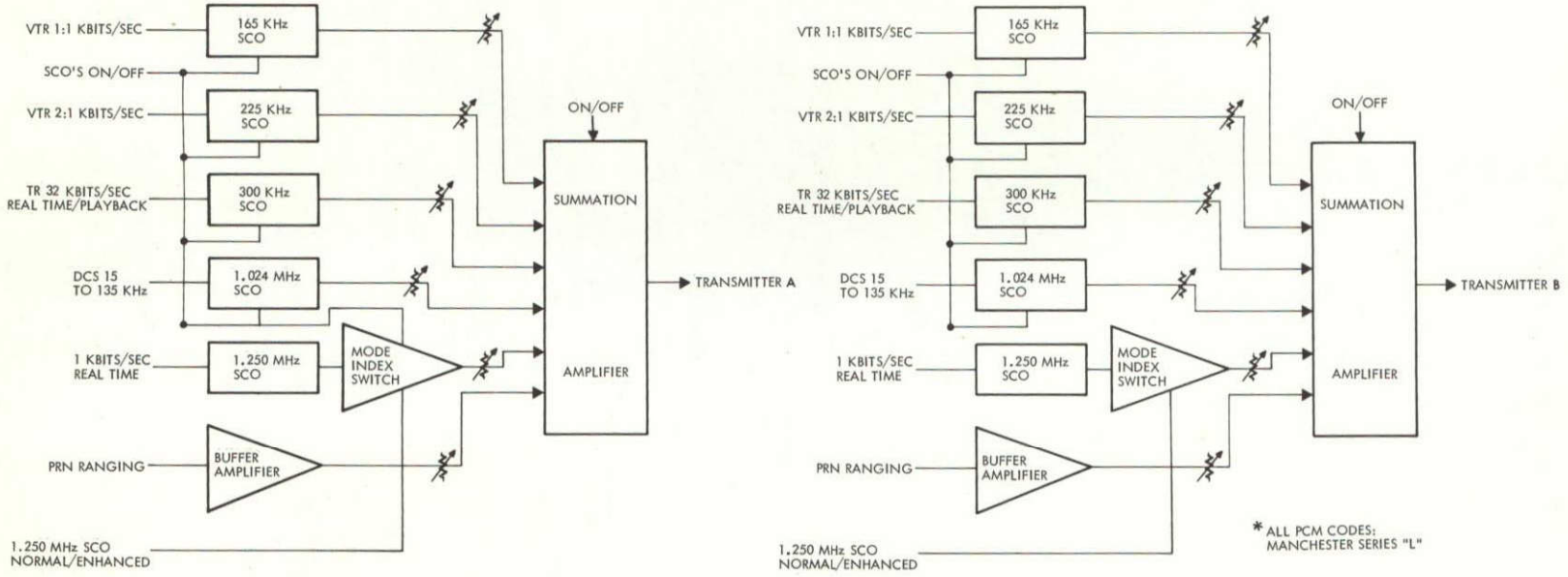

Figure 5-26
DUAL BASEBAND ASSEMBLY block diagram

CONTENTS

- One subcarrier frequency modulated by the output of the DCS receiver
- The turnaround ranging signal from the unified S-band receiver

Each assembly contains two identical units and each unit contains the following circuits:

- Five subcarrier oscillators
- Six gain adjustment circuits to set the output amplitudes of the subcarrier oscillators and ranging signal
- Two buffer amplifiers
- A summation amplifier

The two units have independent power sources. Unit A is powered from unified S-band transponder converter A and unit B is powered from unified S-band transponder converter B.

Parameters of the six data channels are as follows:

Data Channel	Data Form	Center Frequency	Deviation
VTR 1	1 kbit/sec	165.000 kHz	± 1 kHz
VTR 2	1 kbit/sec	225.000 kHz	± 1 kHz
Narrowband tape recorder	32 kbits/sec	300.000 kHz	+ 30 kHz
DCS	(Real time/playback) 15 to 135 kHz	1.024 MHz	150 kHz/volt
Real time	1 kbit/sec	1.250 MHz	± 1 kHz
PRN ranging	1 mbit/sec		

The amplitudes of the outputs from the subcarrier oscillators and the ranging channel buffer amplifier are adjustable in order to set the proper modulation index for each subcarrier. The summation amplifier output is linearly proportional to the sum of the input signals within ± 1 percent over the output signal range of 0.2 volt peak-to-peak to 8.1 volts peak-to-peak. This composite output signal phase modulates the unified S-band downlink.

The operational modes of the baseband assembly are as follows:

Function	Command
165, 225, 300 kHz, 1.024 MHz SCO channel	On
165, 225, 300 kHz, 1.024 MHz SCO channel	Off
PRN ranging channel	On
PRN ranging channel	Off
1.250 MHz SCO channel	On
1.250 MHz SCO channel	Off
1.250 MHz SCO channel modulation index switch	Normal
1.250 MHz SCO channel modulation index switch	Enhanced

The 1.250-MHz subcarrier is unique in that it is followed by a modulation index switch. The modulation index switch has two operational modes. In the normal mode, the other subcarriers are also on. In the enhanced mode, the other subcarriers are turned off and the modulation index of the 1.25-MHz subcarrier is increased by a 5.5 to 1 gain change in the modulation index switch.

6. ANTENNA SUBSYSTEM

The ERTS antenna subsystem consists of antennas, diplexers, hybrids, filters, and power monitors. Four different antenna assemblies are used as required by the several frequency bands being employed:

- STADAN VHF which transmits at 137.86 MHz and receives at 154.2 MHz
- MSFN unified S-band which receives at 2106.4 MHz and transmits at 2287.5 MHz
- Wideband video telemetry channels which transmit at 2229.5 and 2265.5 MHz
- Data Collection System which receives at 401.9 MHz

Only the first three of these antenna systems are discussed in this section. The data collection system antenna is described in Volume 5 Section 3. The installation of these antennas on the spacecraft is shown in Figure 6-1.

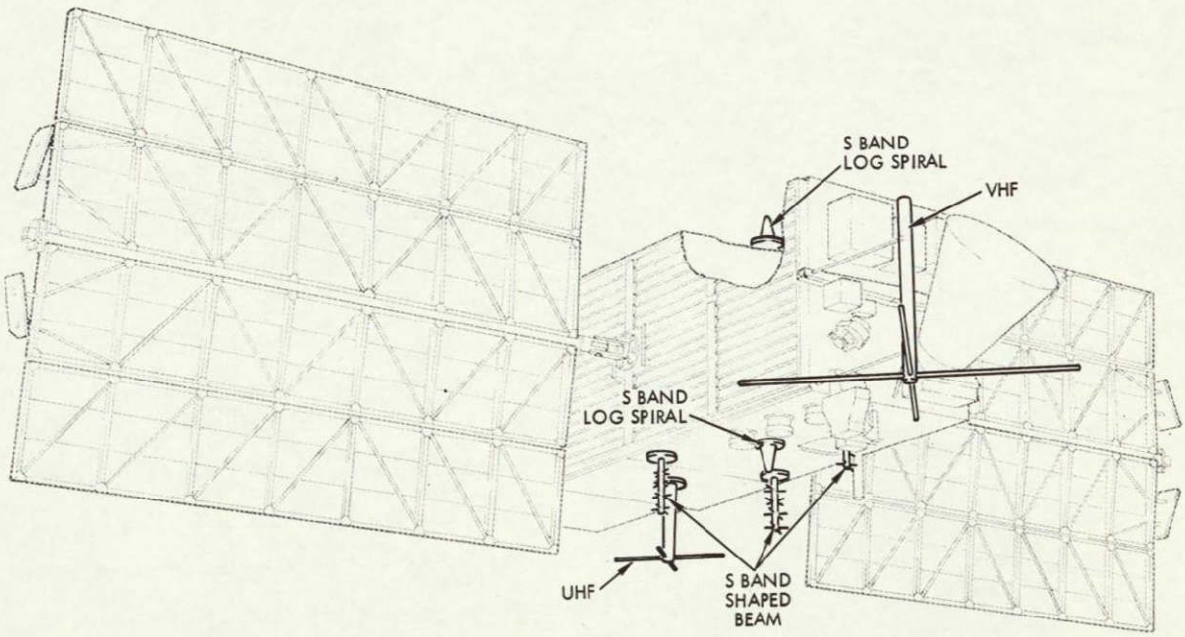

Figure 6-1
RELOCATION OF OGO VHF ANTENNA ON ERTS

6.1 VHF ANTENNA SYSTEM

This system must be able to receive commands from and transmit 1 kbit/sec PCM data to a STADAN ground station under any spacecraft attitude condition. The OGO VHF antenna provides omnidirectional coverage, however in order to simplify the installation and delete the requirement for a deployable boom as used on OGO, a new antenna location was selected for ERTS. The antenna was relocated at Station 307.5 and radiation tests were conducted. The resulting patterns are similar to the patterns provided by the OGO installation.

In addition to the antenna, the VHF system contains a dual diplexer/coupler and a power monitor in each transmitter line. The antenna is coupled to the dual diplexer/coupler which provides right-hand and left-hand circular polarization for the signals from the transmitters, and provides two orthogonal linear polarization outputs for the two receivers. The power monitor at the output of each transmitter indicates both the forward and reverse power conditions of the transmitters. Figure 6-2 shows a block diagram of the VHF antenna system and Figure 6-3 shows the OGO diplexer which will be retuned for ERTS.

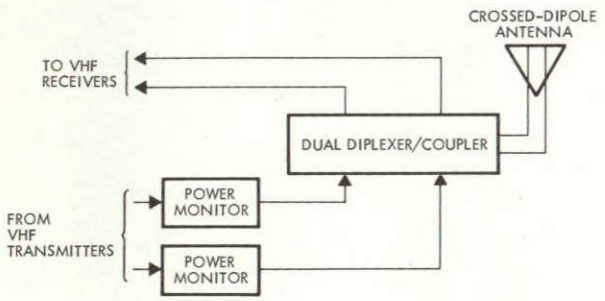

Figure 6-2
VHF ANTENNA ASSEMBLY block diagram

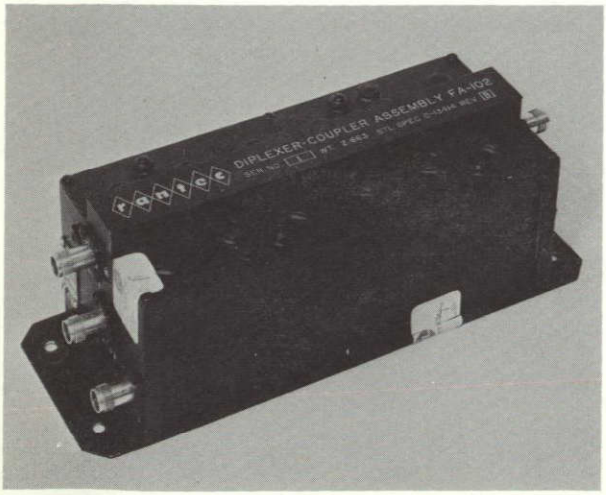

Figure 6-3
DIPLEXER COUPLER

6.2 UNIFIED S-BAND ANTENNA SYSTEM

The unified S-band antenna system, in Figure 6-4, provides two different antenna coverage patterns. Omnidirectional coverage is provided for real-time telemetry transmission and

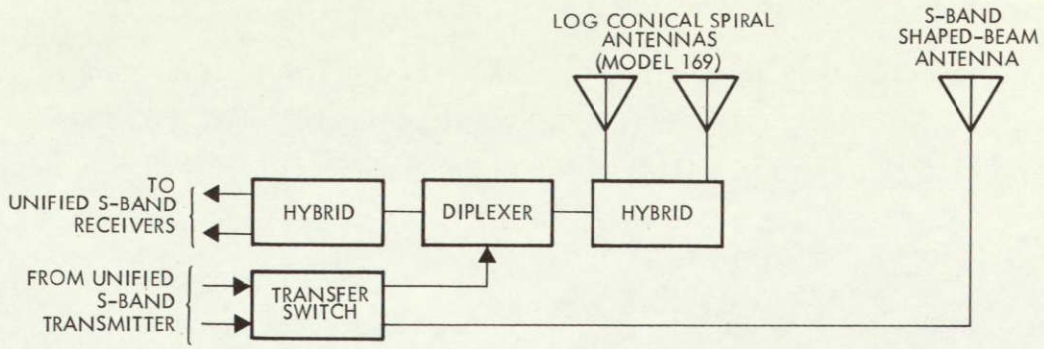

Figure 6-4
UNIFIED S-BAND ANTENNA block diagram

command reception during orbit injection and attitude orientation of the spacecraft. In addition, a variable gain shaped-beam pattern provides constant signal strength over the portion of the earth in view of the spacecraft. This pattern provides the gain required for normal unified S-band transmission of the multisignals being transmitted when the spacecraft is earth oriented.

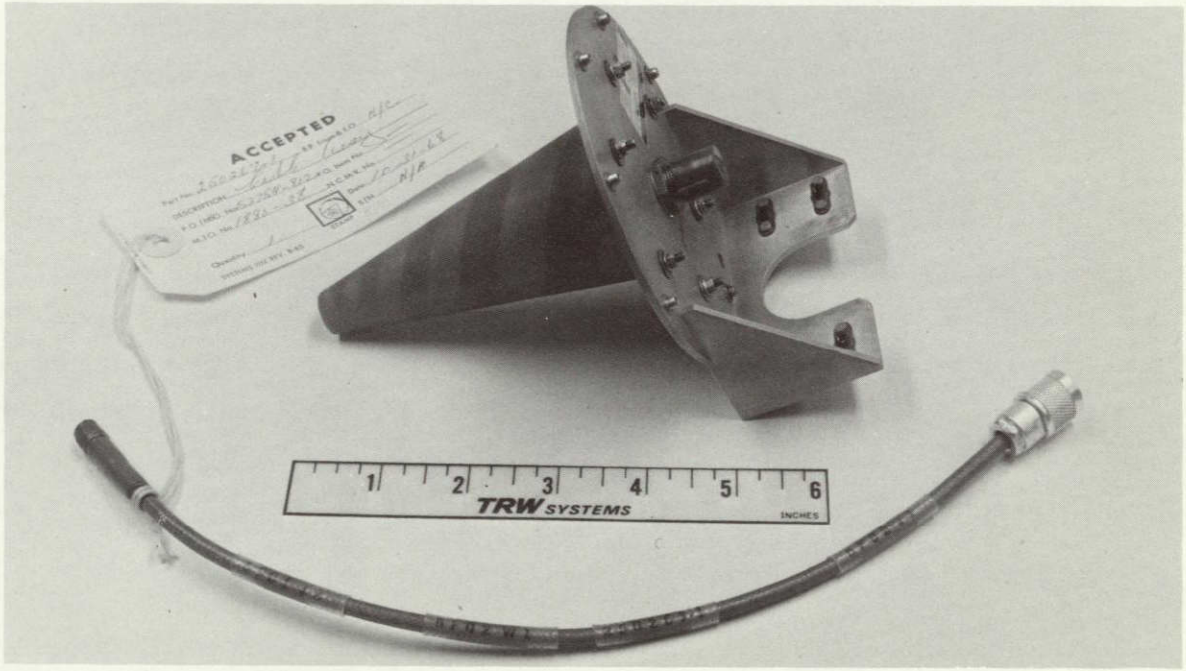

Figure 6-5
OMNIDIRECTIONAL S-BAND ANTENNA

For the omnidirectional requirement, two hemispherical antennas, one mounted on the earth-facing, +Z, side of the spacecraft will provide the necessary pattern. A log spiral antenna used on Program 169 has been selected (Figure 6-5).

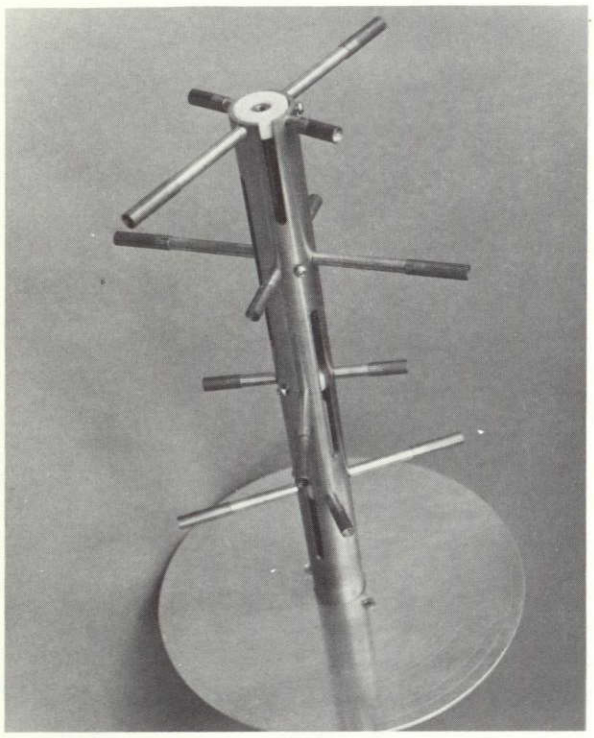

Figure 6-6
S-BAND SHAPED-BEAM ANTENNA

The shaped-beam pattern is satisfied by the use of the turnstile antenna (see Figure 6-6) developed by TRW for the wideband links. Its radiation pattern is shown in Figure 6-7.

Connection of these two different antenna assemblies to the unified S-band transponders is accomplished through the RF distribution assembly.

An RF distribution assembly connects the two omnidirectional units to the two transponder assembly receivers through a hybrid and diplexer, and connects one transmitter of the transponder to the shaped-beam antenna and one to the omni antennas through a transfer switch. In normal spacecraft operation, the transmitter connected to the shaped-beam antenna will be energized. When the spacecraft is not earth oriented, i.e., at launch, orbit injection, etc., the transmitter connected to the omni antenna assembly will be energized. Operation of the coaxial transfer switch will be necessary only in case of a transmitter failure.

6.3 WIDEBAND VIDEO TELEMETRY ANTENNA SYSTEM

The wideband telemetry antenna system consists of two shaped-beam antennas (Figure 6-6) and two band-reject filter units. The antennas equalize the horizon and nadir field strength and to the extent possible all points between. At the horizon the effective gain is 5 db higher than a perfect

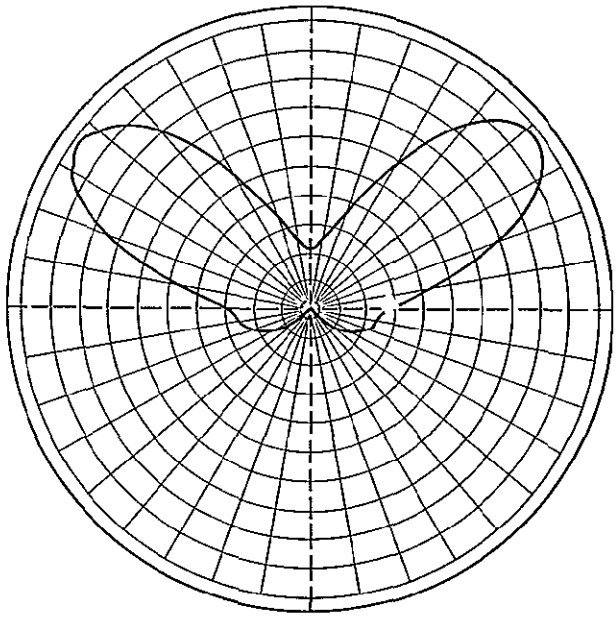

Figure 6-7
SHAPED-BEAM, S-BAND ANTENNA
pattern (measured)

circularly isotropic antenna. The filters remove the wideband TWT amplifier noise in the unified S-band receiving frequency band to prevent degradation of receiver sensitivity. The rejection required at the unified S-band receiver frequency is approximately 70 db. Included in the filter assemblies are power monitors which indicate the forward output power of the traveling wave tube amplifier.

CONTENTS

7. POWER SUBSYSTEM

Primary power for the ERTS is supplied by oriented arrays of silicon solar cells mounted on two large paddles. The arrays are supplemented during heavy load and during eclipses by two packs of rechargeable secondary (nickel-cadmium) batteries. In addition the subsystem includes the charge control devices and the DC-to-DC converters for secondary power. The operation of the ERTS power subsystem is illustrated in Figure 7-1. In concept and design it is almost identical to OGO.

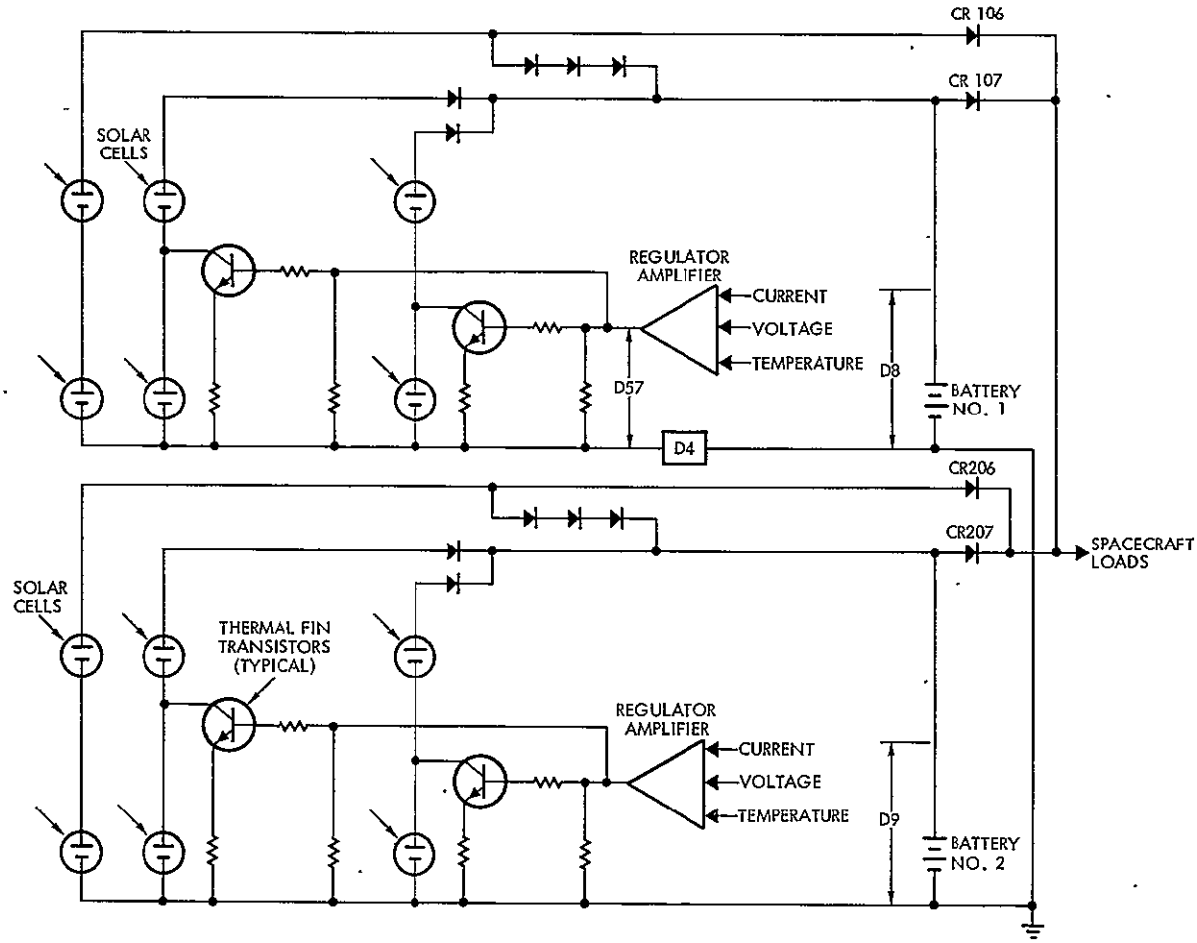

Figure 7-1
POWER SYSTEM block diagram

7.1 SUBSYSTEM CAPABILITY

The total energy capability of the ERTS power subsystem varies between 30,000 and 40,000 watt-minutes per orbit over the one-year

lifetime. This energy is distributed in the following manner to the various power buses.

+28 (24.5 to 31.5) volts DC:	Ordnance bus
	Communication bus
	Attitude control
	Undervoltage bus No. 1
	Payload positive bus (Converted to -24.5 volts DC)
-24.5 (-24.0 to -25.0):	Payload negative bus
-24.5 (-24.0 to -34.0):	Payload shuttering bus (pulse power)
	DCS bus (optional)

The payload positive bus and undervoltage bus No. 1 are connected to the power source through undervoltage relays. Loads on these buses are removed from the power source if the +28 volt supply drops below 23.5 volts. The loads on other buses which are essential to spacecraft operation remain connected to the power source. The payload negative bus is taken from the output of the payload converter. The converter is capable of starting into load resistances as low as 0.9 ohm. Regulation is maintained for load variations from 0 to 300 watts.

The payload pulse power bus utilizes a small battery (1.1 ampere-hour) as its energy source. Its function is to supply the RBV shutter pulse power and DCS power (if required). The DCS requirement comes about if -24.5 volts DC is needed as a power source. This low and continuous power need (1 watt) should not be the sole load on the relatively large payload converter. Charge power for this battery is derived from the synchronizing oscillator in the power control unit.

The electrical power subsystem, with the exception of certain converters, is redundant, i.e., elements of the subsystem (power control unit, batteries, and solar arrays) are dual systems (see Figure 7-1). This duality was achieved without doubling the total power capacity with the attendant weight and volume penalty. Thus, the subsystem is capable of failure mode operation at a somewhat reduced output. As a result, a

charge control or battery failure can be taken out of the subsystem (by ground control) and limited operation continued.

The subsystem operates as follows: solar energy is converted to electrical energy by a solar array made up of two identical paddles that are rotated around the roll axis to maximize solar input. The battery system consists of two identical batteries, and similarly charge control employs two identical units. Under normal conditions, one solar paddle furnishes charge current to one battery and the charge current is controlled by one section of the charge control device. The solar array power is supplemented by the batteries during peak load.

7.2 SOLAR ARRAY

The ERTS two paddle solar array is attached to a shaft through the spacecraft body, and is the primary source of all in-orbit electrical power. Each paddle consists of two outer sections which hinge to a central section along an axis parallel to the array shaft as shown in Figure 2-7. Each expanded paddle measures 7 x 6-1/4 feet and weighs approximately 58 pounds. During boost the outer paddle sections are folded against the center sections and the entire paddle assemblies folded along side the body through hinges in the array shaft, as shown in Figure 7-2. The paddles are retained against the body during launch by pneumatic latches which release after the observatory is separated from the Delta stage.

The size of the solar array has been established to provide all the energy required under the most extreme mission conditions. Anticipated cell degradation has been assumed to be 6 percent per year. Body shading has been analyzed and the array size increased 16 percent to offset this. Finally, a worst case power usage profile has been assumed to arrive at the energy necessary to offset battery charge and discharge inefficiencies. Average array output in sunlight is approximately 450 watts of regulated power. The ERTS array employs 18,816 gridded n-on-p solar cells having 10.5 percent efficiency in space. The cells are assembled into 168 modules before assembly to the panel frames. On each module, groups of four 2 by 2 cm cells are connected in parallel and 28 parallel groups are connected in series forming a 112-cell module. Module size

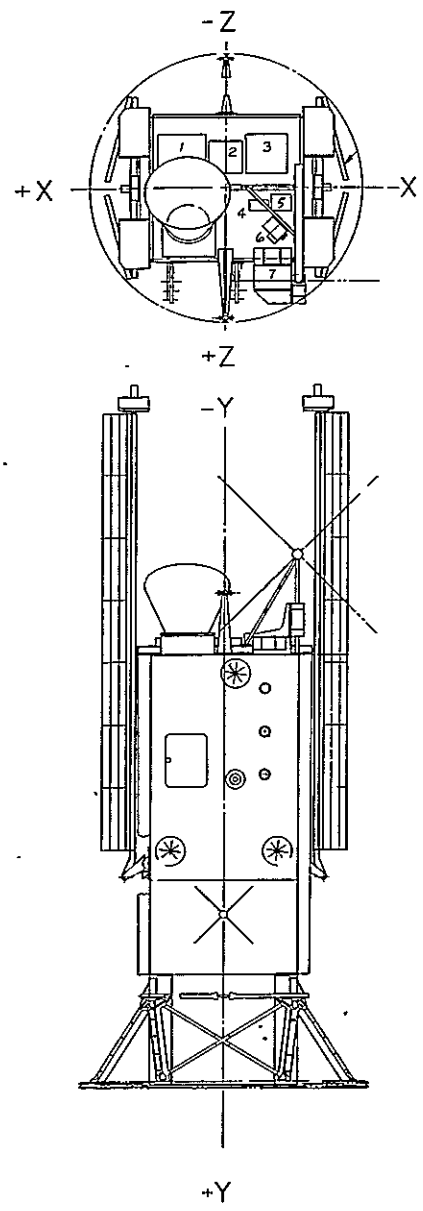

Figure 7-2
FOLDED PADDLE ASSEMBLY

is 5.9 by 13 inches. In assembling the paddle, three modules are connected in series to obtain a minimum degraded voltage of 31.5 volts at the maximum power point during full solar illumination.

Each array is divided into three sections: two sections are regulated by charge control fins; the third section is unregulated. The two regulated sections are made up of three modules in series and eight modules in parallel. Regulation of the two sections is accomplished by shunting part of the section output current through the charge-control-fin transistor which is connected across one half of the section. The location of the modules within each section was determined as a result of a body shadow analysis which utilized a one-tenth scale model of ERTS. The solar array modules are constructed with bypass diodes to minimize the effect of antenna shadows.

The array cabling and interconnections are arranged to minimize the magnetic moment produced by solar array currents. Additional wires for test purposes are incorporated in the array cabling to permit verification of the array's condition during integration and test without breaking any connection.

Radiation which strikes each cell is filtered by 6-mil thick Corning No. 0211 microsheet glass slides over which an electro-optical coating has been applied. This filtering screens out that portion of the solar spectrum which is not convertible to electrical power and would only heat the

cell, causing a reduction in efficiency. In addition, the cover glass protects the adhesive from discoloration by ultraviolet radiation. The temperature of the solar array will vary from -60°C in eclipse to less than 70°C in full sunlight resulting in a 40 percent variation of the voltage at which maximum power transfer occurs. This effect has been included in selecting the number (84) of cells in series. See Volume 4 Section 11 for the detailed discussion of the effect.

7.3 NICKEL CADMIUM BATTERIES

Continuous power to the payload and spacecraft subsystems, despite array output fluctuations and load variations, is provided by a pair of nickel cadmium batteries, each consisting of 22 12-ampere/hour cells. Selection of the 12-ampere/hour cell has been based on mission requirements and on extensive testing undertaken during the OGO program and on OGO flights. The cells are sealed and back-filled with helium for leak detection purposes. A complete battery pack, identical to that used in OGO, is illustrated in Figure 7-3. It includes, in addition to the cells and case, a harness and connector and two thermal packs. Each battery weighs 31 pounds.

Orbital tests have shown nickel-cadmium batteries to be highly reliable. The two thermal packs included in each battery contain a thermal switch that opens when the battery temperature reaches 95°F and closes at approximately 88°F, a thermistor for telemetering battery temperature, and a sensistor for charge-voltage-limit temperature compensation. The thermal switches from each pack of the same battery are connected in series and automatically limit the battery charge current to 0.4 ampere upon opening. The sensistor provides charge-voltage-limit compensation at a rate of approximately -0.30 volts/°F with the voltage limit at 75°F set at 31.9 volts.

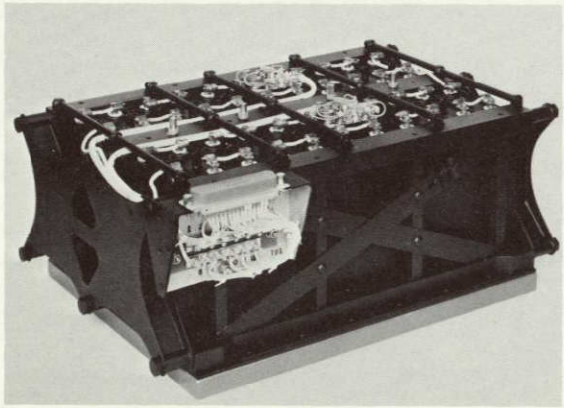

Figure 7-3
NICKEL CADMIUM BATTERY for ERTS is identical to the OGO battery. Total weight of the battery pack is 31 pounds.

The maximum anticipated depth of discharge during the ERTS mission (with 20 minutes of sensor operation) is 27 percent, near the orbital value noted on OGO 4 and somewhat less than that on OGO 6.

Flight history on the OGO spacecraft has shown that the average battery temperatures tend to increase at a rate of 0.6°C per watt of power dissipation. Since the thermal environment on the ERTS will be similar to that of POGO, this value has been used as a guide in the determination of battery thermal behavior.

Battery reconditioning has proven beneficial for OGO satellites, and is being incorporated into ERTS. Because of the necessity to recondition during eclipses (on ERTS), the battery not being reconditioned must carry the entire system load. To limit the number of eclipses for this double depth of discharge and to simplify ground operations, a two-rate reconditioning discharge will be used. The initial rate will be 3 amperes at a battery voltage of 24.2 volts followed by the OGO rate of 0.6 ampere at 18 volts. The switch from one rate to the other occurs automatically; reconditioning is discontinued by command.

7.4 POWER CONTROL UNIT

Battery charge control and bus voltage regulation in the ERTS spacecraft are maintained by the power control unit. In addition, the power control unit (shown in Figure 7-4) acts as a junction box for solar arrays, batteries and load bus, and distributes power synchronizing signals.

The ERTS charge control technique calls for the battery terminal voltage (when compensated for cell temperature and IR drop) to be the measure of state of charge. To reduce circuit complexity the adjustment for current is not incorporated in the power control unit. The control which is incorporated limits the voltage to 32.93 volts minus 0.0294 volts per degree departure from 40°F.

Other limits on charge control are provided in the power control unit in the form of selectable (by ground command) charging modes, charge current limits (0.4, 4.0, 8.4 and 12 amperes), a temperature limit and the facility to completely disconnect the battery and discharge it in orbit.

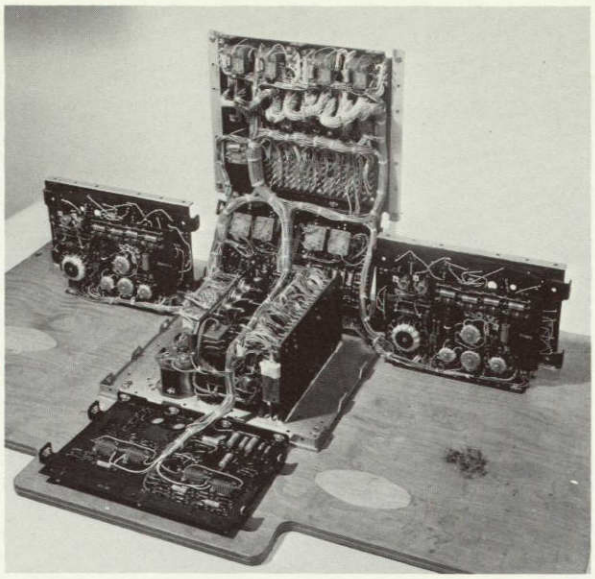

Figure 7-4

ERTS POWER CONTROL UNIT is identical to that used on OGO and maintains spacecraft battery charge control and bus voltage regulation

The charge control modes selectable by ground command include:

- Charge at full selected current to the temperature compensated voltage limit. Current automatically reduced thereafter so as not to exceed the voltage limit as state of charge increases.
- Charge as before to the same voltage limit whereupon current is automatically switched to trickle (0.4 ampere) until a battery discharge occurs.

These two modes are selected in orbit depending on the load requirements. No one method is suitable for all orbital conditions.

7.5 CHARGE CONTROL FINS

The charge control fins provide the power stages of the charge regulators with a suitable thermal environment. One heat sink or fin is provided for each of the four regulating transistors, mounted at the ends of the solar panels (2 fins per panel).

Each thermal fin is composed of a power transistor (2N2124), base emitter resistors, and a power diode. All parts are mounted on a lithium-filled aluminum heat sink and covered with a multilayer reflector material as shown in Figure 7-5 to minimize heat inputs from the sun, earth, and spacecraft. The black honeycomb strip on the end of the thermal fin prevents erroneous reflection into the sun sensor which is also located on the end of the solar paddle.

Parametric studies were undertaken to establish a balance between the size, weight, auxiliary heating requirements, and surface finishes needed to maintain the electronic components within the desired temperature limits, despite power dissipation variation, solar electric input

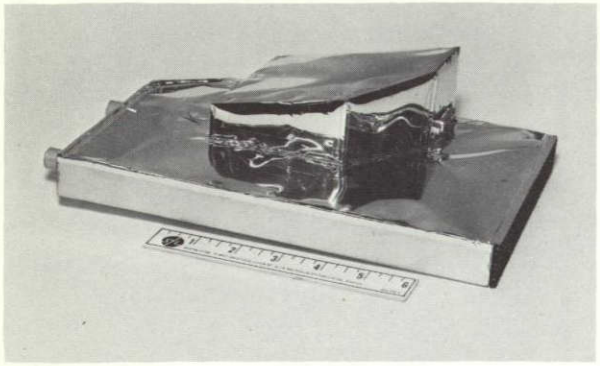

Figure 7-5
POWER REGULATOR HEAT SINK

variation, and eclipses. The selected ERTS design obviates the requirement for auxiliary power to minimize weight and operates with a temperature maximum of 80 to 90°C. Acceptance testing of similar units on OGO has revealed that 80 degrees is generally the upper temperature limit. The weight of each unit is about 2 pounds.

7.6 OPERATION OF MAIN BUS POWER COMPONENTS

The solar array, nickel-cadmium batteries, power control unit and charge control fins operate together to supply main bus voltage between 23.5 and 33.5 volts under all load and solar input conditions. Figure 7-6 is a block diagram which provides a basis for understanding how these elements operate together.

1) The power system consists of two separate parallel sections each made up of a solar paddle, a regulator and a battery. The upper and lower halves of Figure 7-7 portray this division.

2) The solar arrays shown in Figure 7-8 consist of three major strings of cells each. All but two (the "C" sections) of the six strings are regulated by shunting half the string to ground using a power transistor (variable resistor) contained in the thermal fins. The result is that in full sunlight regulation is effective at any load current from full array output down to 5.0 amperes load – the unregulated output of the "C" sections.

3) A current limiter and a voltage limiter are both effective in controlling array current and thus battery current. The center portion of the drawing shows the regulator functions and current limits.

4) A single regulator may be connected by command to control both arrays.

5) Either battery may be disconnected from the bus.

6) Either battery may be discharged through a resistor (reconditioned).

PRECEDING PAGE BLANK NOT FILMED.

7) A flip flop switches to trickle charge upon reaching voltage limit.

8) Battery temperature is sensed and is routed to regulator 1 or 2.

9) An in-flight jumper permits disconnecting the power system for ground test purposes.

10) In-flight telemetry is provided for battery currents, voltages and temperatures; array currents, load bus current and power transistor drive voltages.

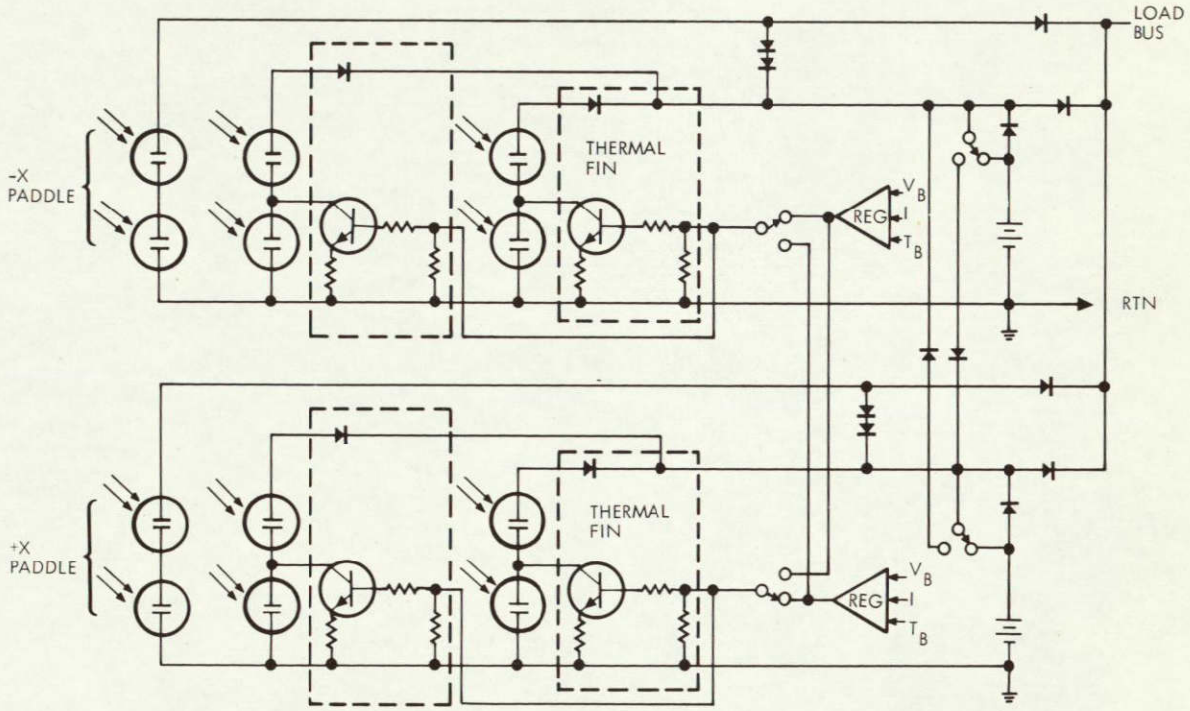

Figure 7-7
CHARGE CONTROL SYSTEM simplified schematic diagram

7.7 SUBSYSTEM CONVERTERS

The communication and data handling subsystem and the attitude stabilization subsystem require voltages at different levels and different regulations than the main spacecraft bus. To supply these needs 7 DC-DC converters are used. Table 7-1 lists key characteristics of these units. Typical units are shown on Figure 7-9. Pulsewidth regulation is used to obtain maximum efficiency in regulating and converting the +23.5 to 32.5 volt bus to the indicated values.

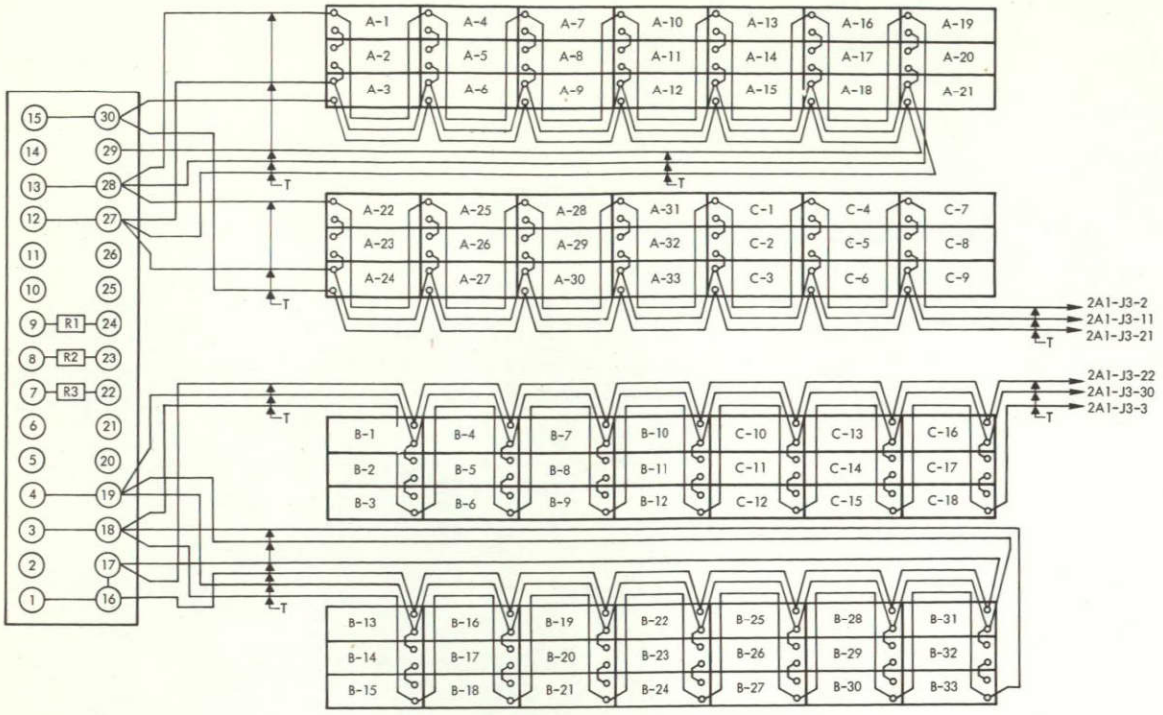

Figure 7-8

PRELIMINARY WIRING DIAGRAM, solar array module interconnection

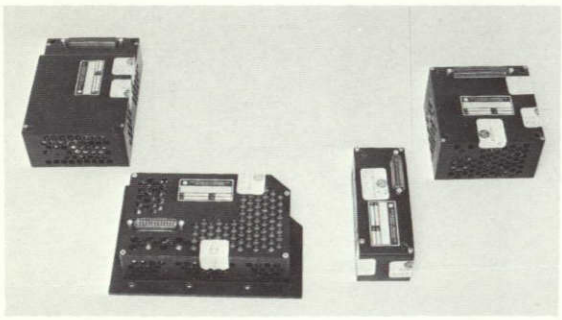

Figure 7-9

TYPICAL OGO DC-DC CONVERTERS
applicable to ERTS

As indicated in the typical converter block diagram, Figure 7-10, DC input power passes through an L/C filter which filters out the high transient current drawn by the series switching element. When first turned on the DC input power activates a unijunction oscillator circuit which pulses the switch element. By pulsing the switch element, output voltage is developed across a second L/C filter, whose output starts the two-core flux oscillation inverter circuit and disables the start circuit. AC voltage from the inverter is fed to a magnetic amplifier, which in turn pulsewidth controls the switching element.

Table 7-1. Converter Characteristics

Converter Module No.	Output Voltage (vdc)	Output Current (ma)	Output Power (watts)	Regulation Envelope (±percent)	Telemetry Output (+ vdc)	Efficiency (percent)	Weight (lb)
2	+16	60	1.0	1.0	3.5		
	+9	560	5.0	1.0	3.5		
	+5	100	0.5	1.0	3.5		
	-6	60	0.36	1.0	2.0		
	-6	20	0.12	1.0	-		
			6.98 total			44	1.8
5,6	+16	300	4.8	1.0	3.5		
	+9	789	7.1	1.0	3.5		
	-6	280	1.7	1.0	2.0		
	-16	10	0.2	1.0	2.0		
			13.8 total			64	1.95
7,8	+16	20	0.32	2.0	3.5		
	+9	107	0.97	2.0	3.5		
	-6	20	0.12	2.0	2.0		
			1.41 total			28	0.71
9	+20	350	7.0	1.5	3.5		
	+10	50	0.5	3.0	3.5		
	-20	350	7.0	1.5	2.0		
	28 vac CT	385	10.8	3.0	2.0		
			25.3 total			74	2.4

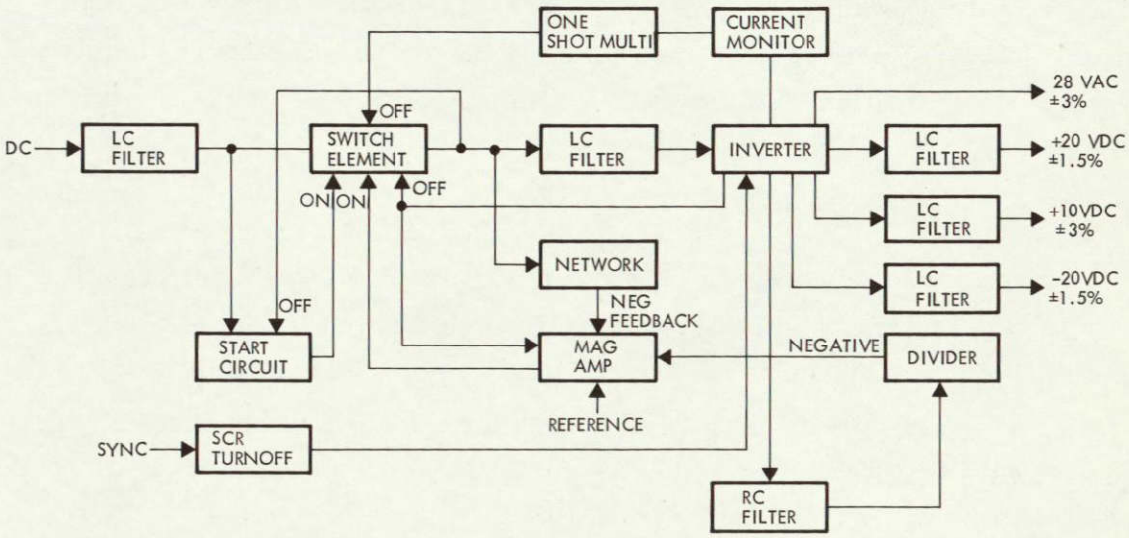

Figure 7-10
OGO CONVERTER NO. 9 block diagram

A current monitor measures the DC current drawn by the inverter. If it is greater than a selected level, it pulses a one-shot multivibrator which overrides the magnetic amplifier and turns off the switching element. Once the converter is turned off, the starting circuit comes into action and turns the converter on. The overload current is again sensed and

the converter is turned off. Under a sustained overload the converter cycles between these two modes of operation and provides overload protection for the converter.

In order to reduce overshoot on the output voltage due to starting or step change in input voltage, a feedback network senses the output of the switching element and controls the magnetic amplifier during the transient, preventing the full effect from reaching the outputs.

The DC-DC converters can be synchronized from an external frequency source. The external frequency source triggers SCR's which short out the base drive of the ON transistor, allowing the OFF transistor to turn on.

AC power from the inverter is rectified and filtered to produce +20, +10 and -20 volt DC outputs. In addition, part of the power from the inverter is taken directly from the inverter to produce a 28 volt p-p AC square wave output, whose frequency is 2461 Hz. Another A-C output is rectified, filtered and divided down by a resistor divider network and compared against a precision reference voltage. The net error controls the magnetic amplifier and the pulsewidth or duty cycle of the switch element to maintain the outputs constant.

7.8 PAYLOAD CONVERTER

Two payload converters (Figure 7-11) provide -24.5 volt regulated power to the payload bus. A breadboard model of one converter, tested in April 1969, will be improved to regulate over a range of 0 to 300 watts. Fail-safe operation at overload and no load is incorporated. The requirements placed on the converter by the payload are:

Output Characteristics:

Voltage	-24.0 to -25.0 volts DC
Current	0 to 12.5 amperes
Output impedance	0.3Ω max.
Ripple	400 ma

Input Characteristics:

Input voltage	23.5 to 32.5

Efficiency: 85%, full load

Redundancy:

Three Converters with switching
to select any two upon command.

The converter utilizes the pulsewidth modulation technique to obtain the required voltage regulation. High efficiency is obtained through the use of the same transistor(s) for regulation and power switching. High efficiency is obtained at low load with load proportionate drive circuitry. No regulator is required between the integrator and load. However, this circuit can be readily incorporated if regulation and/or EMC problems become so acute as to require this refinement.

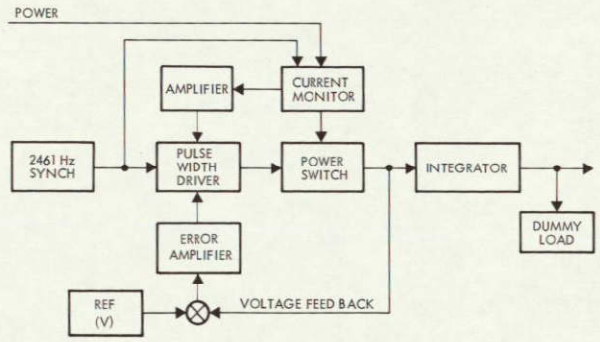

Figure 7-11
PAYLOAD CONVERTER block diagram

As in OGO converters, the payload converter will be synchronized at a power switching frequency that is a multiple of 2461 Hz. In the event of loss of this synchronization signal the converter will continue to operate to specified requirements

Figure 7-12 illustrates the efficiency obtainable with this concept. In order to obtain no load operation a dummy load is incorporated into the converter. This dummy load is turned on when the input current drops to 1.5 amperes. The converter will be turned off when no payload bus load exists, hence the dummy load is provided largely for ground test. The maximum load profile and the power loss within the converter is shown in Figure 7-12. This profile corresponds to that used to size the solar array (Volume 4, Section 7-11).

Redundancy is accomplished by the use of three separate converters, two active and one in reserve (Figure 7-13). Converter No. 3 can upon command replace either converter No. 1 or 2.

Static switching (i. e., biasing the converters off and on) will avoid the use of power relays.

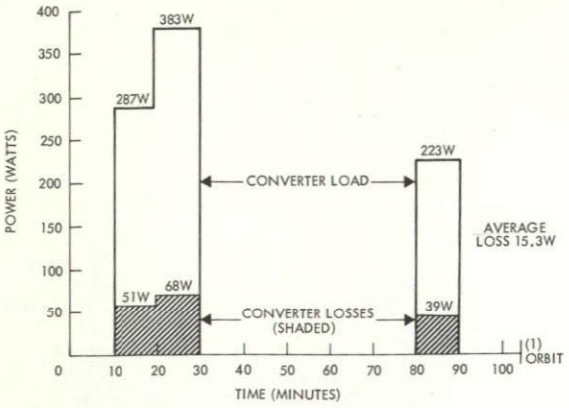

Figure 7-12

PAYLOAD CONVERTER maximum load and loss profile

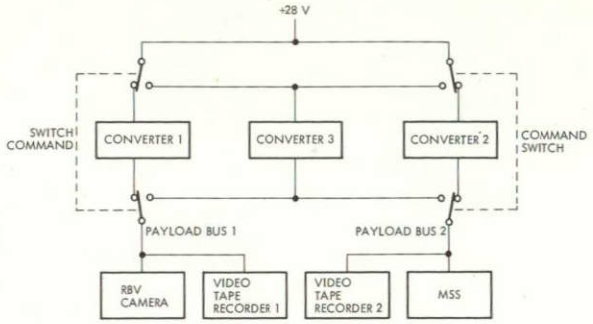

Figure 7-13

CONCEPTUAL SWITCHING of payload converters places one unit in reserve for two functioning units

The converter dimensions are:

Length	12.0 inches
Width	9.0 inches
Height	3.5 inches

The base area (108 square inches) is largely influenced by the thermal flux requirement of 0.2 watt per square inch (average for the orbit) or less. The weight of the unit is 12 pounds.

The input, output, synchronization signal and telemetry will utilize a 37-pin receptacle and a 37-pin plug.

7.9 RBV CAMERA SHUTTERING PULSE

Shuttering of the RBV cameras requires an 18-ampere pulse of current at -24.5 volts enduring for 80 msec. Because this momentarily exceeds the capacity of the payload converter and good regulation is not required, a separate small nickel-cadmium battery is provided to supply this pulse. The battery (Figure 7-14) is made up of 28 1.1-ampere-hour cells, (typically Gulton Industries HVO-1.1). The assembled battery stands 3.87 inches high by 3.62 inches wide by 6.50 inches long and weighs 4.25 pounds. Mounting is provided by two holes at each end of the battery base. A continuous trickle charge maintains the charge condition and is obtained by rectifying part of the synchronizing signal from within

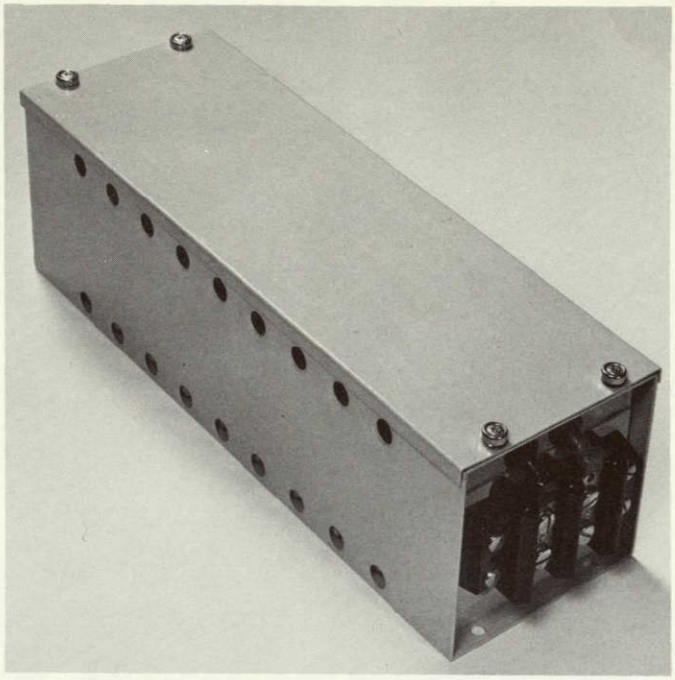

Figure 7-14

GULTON 28-CELL NICKEL-CADMIUM BATTERY for -24 volt RBV current pulse

the power control unit. This design choice reflecting our approach to accomplishing RBV shuttering without imposing RBV changes was selected after considering several alternate approaches. See Section 12, Volume 4. TRW believes, however, that the best overall choice to the satisfaction of RBV shuttering requirements would be to invert the shuttering circuits to permit operation from the spacecraft positive unregulated bus.

CONTENTS

8. ELECTRICAL INTEGRATION

The electrical integration subsystem provides for electrically integrating all equipment into the spacecraft and furnishes a number of attitude control and data elements. The ERTS equipment is essentially identical to that of OGO, with changes made only to satisfy the new payload, velocity correction modifications, and RF subsystem additions for ERTS.

The major elements of the electrical integration subsystem and the percentage of their modification required for ERTS are listed in Table 8-1. The momentum control assembly, digital integration unit, and pyrotechnic junction box are only slightly modified or unchanged from OGO.

Table 8-1. Elements of the Electrical Integration Subsystem

	Percentage Change	Reason for Change
Command distribution unit	50	Added velocity correction, payload timers, negative power bus, and relay telemetry
Payload integration assembly	100	Greatly decreased requirement allows reduction in size and complexity.
Junction box 3A7	100	OPEP removed; volume reduced, and improved access to test points
Junction box 3A5	5	Improved attitude control telemetry, added orbital switching assembly
Junction box 3A13	10	Minor modifications
Momentum control assembly	0	
Harness (subsystem)	10 electrical 80 mechanical	Relocated subsystem boxes, new and modified subsystems boxes
Harness (payload)	100	New payload equipment
Wrap-up	100 electrical 50 mechanical	Single wrap-up required on ERTS

The interconnection cabling for the spacecraft subsystems is electrically identical to that of OGO, although routing is changed because equipment is relocated. These bundles, grouped by functions, consist of conventional wire and cable. The general power routing is shown in Figure 8-1.

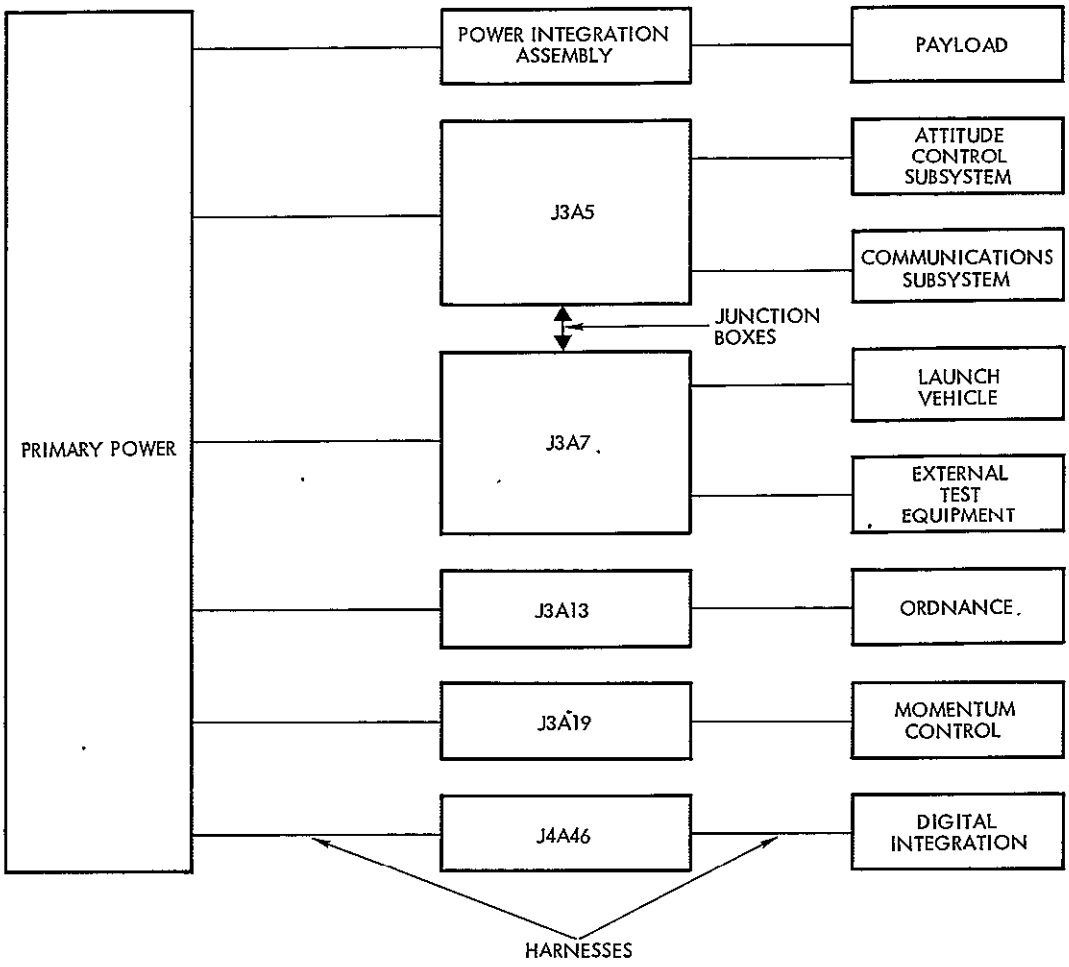

Figure 8-1
TYPICAL POWER ROUTING

8.1 PAYLOAD INTEGRATION ASSEMBLY

The payload integration assembly consists of one or more junction boxes which establish electrical interface locations and equipment for the payload. These interfaces include the connections between each payload assembly and the spacecraft subsystem and between the several assemblies of a given payload. Interassembly connections are generally direct wired. Interfaces between payload and spacecraft subsystems are jumper connected in the integration assembly. This assembly is the gathering place for all subsystem signals routed to payloads, all subsystems input gates receiving signals from payloads, and all other connections to payloads.

The payload integration assembly is mechanically redesigned and reduced in size because the ERTS payload interface requirements are less complex than for OGO. The new design reduces the connector and pin termination requirements from 144 connectors and approximately 4400 pin terminals to 100 connectors and 2300 pin terminals.

The assembly makes it possible to accommodate changes in payload equipment requirements within the assembly without modifying subsystem cables or junction boxes.

The outside dimensions of the assembly are shown in Figure 8-2. The assembly contains terminal boards, connectors, interconnection wiring, fuses, resistors, a bilevel summing network, and passive devices as necessary to satisfy payload requirements. The assembly is an inside-out junction box, which allows ready access to junction points for testing and modification without disassembling the unit or even removing it from the spacecraft.

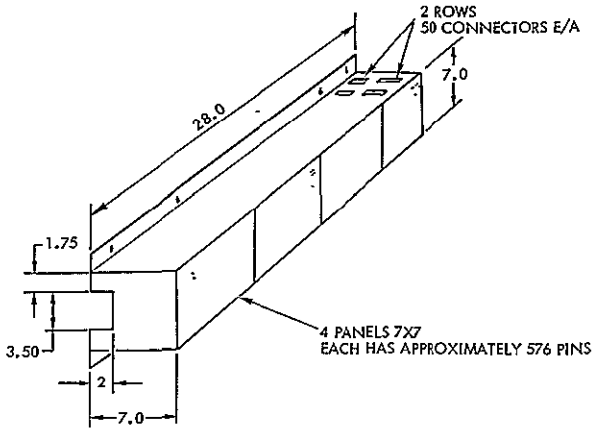

Figure 8-2
EXTERNAL CONFIGURATION of the payload integration assembly

8.2 JUNCTION BOXES

Junction boxes (J boxes) supply protected mounting locations for electrical branch points (terminals) and miscellaneous electrical components (resistors, capacitors, diodes). They also solve the problem of signal and power distribution throughout the spacecraft. In many cases it is necessary for a single function to be delivered to several destinations; 28 volts DC primary power, for example, must be available at a multiple connection branch point for further distribution. They also aid in establishing the concept of separable harnesses.

The central J-box, J3A5, provides a separation point for subsystem interconnections, and a branching point for control signals, power and

analog data. Several large harnesses interface with each other here, harness No. 1 (attitude control system) and harness No. 2 (power and communication), for example. See Figure 8-3. The J-box allows primary DC power to be supplied to harness No. 1 from harness No. 2, allows only harness No. 1 to be associated with the entire attitude control subsystem, and allows both of these major harnesses to be kept to a reasonable size.

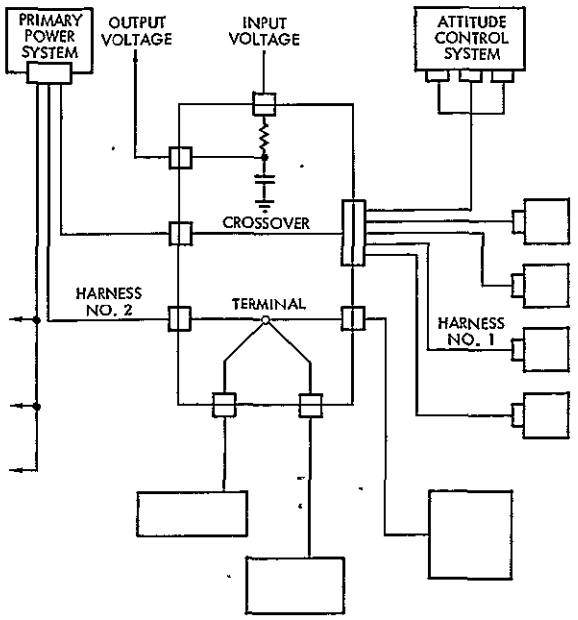

Figure 8-3
THE J3A5 CENTRAL JUNCTION BOX
concept block diagram

The power distribution J-box, J3A7, provides subsystems a power distribution point and an interface with the launch vehicle and external test equipment. The box is redesigned and reduced in size to 14 X 6 X 3 inches and is mounted in the extended compartment on the +Y panel. This mounting configuration allows ease of access to all test points as well as quick access to the in-flight jumper.

The ordnance J-box, J3A13, the momentum control assembly, J3A19, and the digital integration unit, J4A46, are all unchanged from their OGO 6 configurations.

8.3 WRAP-UP ASSEMBLY

ERTS will use the wrap-up designed, developed and flown on all of the OGO series. Since the dual section wrap-up flown on OGO 6 provides an excessive number of conductors for the ERTS application, a savings in cost, weight and volume is realized by reducing the wrap-up assembly to a single section and fewer conductors per cable element. See Figure 8-4. A single section wrap-up assembly with eight wire elements, composed of three elements of 15 hook-up conductors

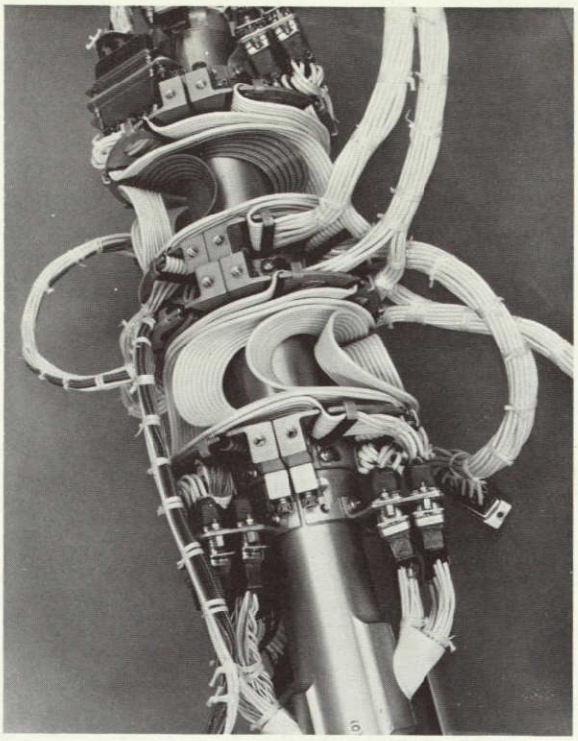

Figure 8-4
DUAL WRAP-UP ASSEMBLY used on OGO will be reduced to a single section for ERTS array application.

each (total of 45 hook-up conductors) and five elements of 10 shielded conductors each (total of 50 shielded conductors), provides a total of 95 conductors.

All connectors are 22 AWG. Twenty-two of them are parallel to handle 12 high current circuits. Thus, the ERTS requirements of 28 connections between the +X solar array and the main body and 29 connections between the -X solar array and main body are easily met. The 50 shielded conductors provide a high percentage of redundancy for the 33 signal and telemetry lines.

The single section wrap-up mounts in the -X position. The array harnesses pass through the drive shaft entry holes on the side only, but branch to both +X and -X paddles.

8.4 BILEVEL TELEMETRY CONDITIONING

Bilevel (discrete) digital inputs from the payload are conditioned into analog signals, four bilevels per analog word slot. The nominal bilevel input characteristics are:

Output impedance	2.5 ohms, maximum
Signal voltages analog	0 to +5.1 volts full scale 0 to -6.375 volts full scale
Bilevels	on -10 to -5 volts off -1 to 0 volts
Signal fault voltage	±33.5 volts maximum

These signals are conditioned by driving digital gates, with resistor-diode input fault protection. The outputs of the digital gates, now at controlled logic voltage levels, are combined by resistive adders to form analog data words, suitable for inputs to the analog digital handling assembly. Four discrete bilevel signals may be combined in this way with no loss of data. Twenty analog words assigned to carry bilevel data thus provide capacity for 80 bilevels to be monitored; 11 more than the present payload requirement of 69.

A bilevel conditioner module is shown in Figure 8-5. Twenty such circuits are included in a single inclosed package. This package mounts within and goes through qualification and acceptance tests as a portion of the payload integration assembly.

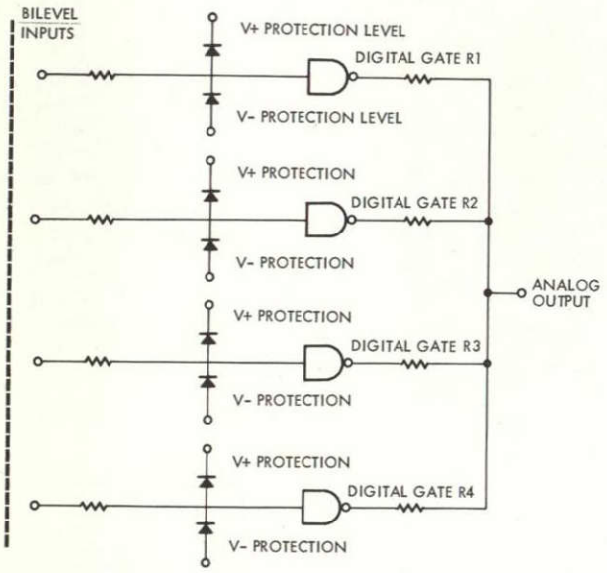

Figure 8-5
BILEVEL COMBINER MODULE

8.5 COMMAND DISTRIBUTION UNIT

The command distribution unit (Figure 8-6) contains a number of latching relays, called power control relays, to control 28 volts DC power for the desired spacecraft loads and -24.5 volts DC power for the payload. A group of nonlatching relays, known as impulse relays, supply a ground connection and a -24.5 volts DC level for a 62 millisecond duration to the payload. These impulse commands are implemented with inverse functions such that -24.5 volts and ground appear at the payload interface when the command is not being activated. (See Figure 8-6.)

The unit is designed with plug-in subassemblies for easy removal and replacement and for ease of modification. The ERTS payload power source impedance is reduced to 1 ohm by the use of relays.

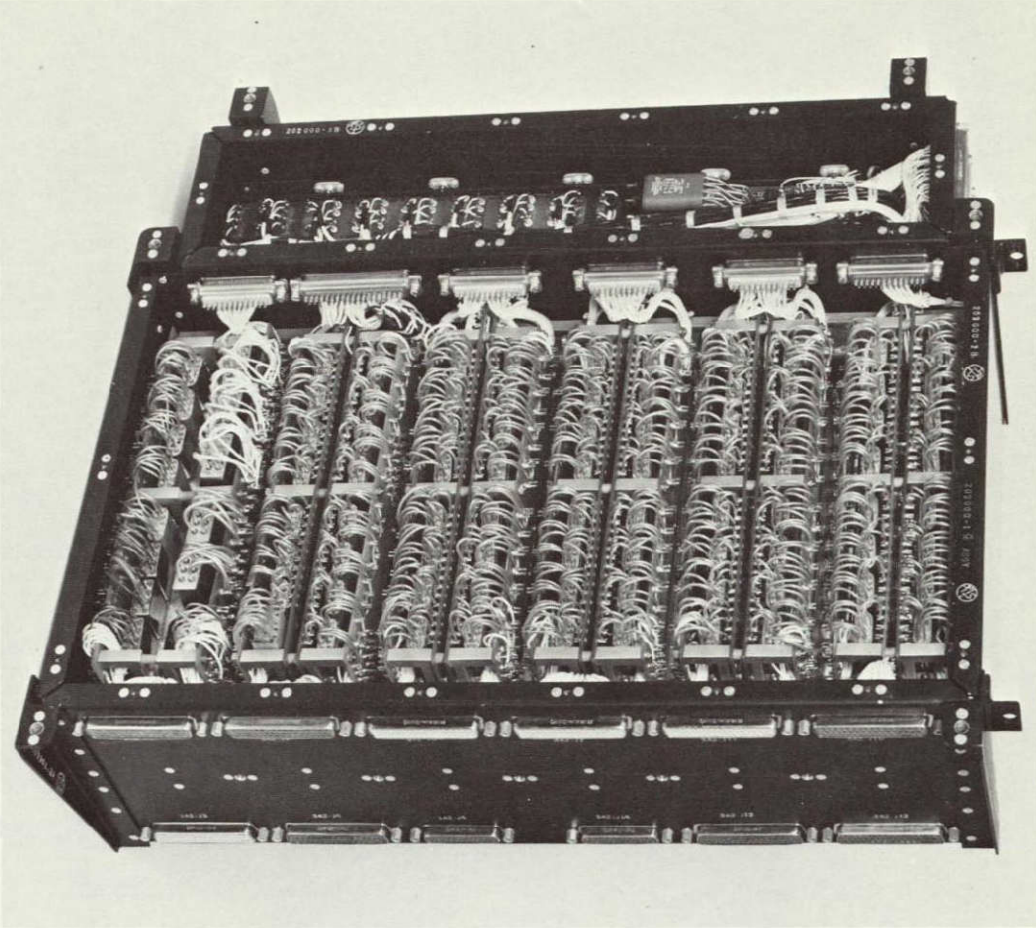

Figure 8-6
COMMAND DISTRIBUTION UNIT

To control the payload, 109 latching and impulse relay commands are utilized. All impulse and latching relays supply grounding and -24.5 volts DC to the payload with 51 commands available for growth. The command matrix is arranged so that the stored mode commands and the Z-axis matrix commands do not interact. (See Volume 4, Section 12.)

For safety, critical functions such as ordnance initiations and gas eject commands are processed by a two-step "arm" and "execute" sequence. All signals are transmitted by the command distribution unit to the payload electrical integration assembly by a standard harness. Each signal is then distributed, as required, by the tailored wiring in the integration assembly and the tailored harnesses to the payload. Other

command functions are distributed to the various spacecraft subsystems by standard harnesses.

Also included within the command distribution unit are sources of three logic signals for use by the spacecraft; switch, mode, and bit rate. The switch signal indicates whether real time data is being transmitted. The mode signal indicates which equipment group is processing real time or storage data. The bit rate signal indicates the bit rate for the real time telemetry system and always consists of one of two possible DC voltages. The unit provides a total of six equipment timers for the video tape recorders, wideband amplifiers, MSS, and the RBV.

The timers are a new design, using a signal from the low frequency timing assembly as its basic timing pulse. The pulse is multiplied through seven flip flop circuits to give a clock time of 24 minutes (Volume 4 Section 12). The timers are reset each time a turn-on command is sent so that a 24-minute interval is provided after each turn-on command. A commandable override bypasses the timers in the event that a timer fails in the off position. The override capability also provides a means of commanding a given payload for a period longer than 24 minutes.

Command status telemetry is provided on five 9-bit digital words. Five shift registers are loaded in parallel for serial readout to the data handling equipment. Status update is automatic for each bit change. Latching relays hold status information and allow the registers to be inhibited during read out.

CONTENTS

9. THERMAL CONTROL SUBSYSTEM

Thermal control for ERTS is provided by a combination of active and passive techniques. Within the main body the mean radiant environment, apart from the immediate vicinity of high power dissipation components, is 20 $\pm 10^{\circ}$C. Materials used in thermal control are sufficiently stable and components so reliable that the probability of maintaining this environment for one year exceeds 0.98. Flexibility in mounting the payload is not limited in any way by thermal considerations. An equally acceptable (though different) environment exists for extra-body components including the solar array, sun and horizon sensors, change control fins, and the antennas.

The thermal control system of the ERTS main box consists of radiating panels under active louver control and insulation. The +Z, -Z, +Y and -Y panels are fully insulated, and both X panels under an active louver control.

To reduce the solar input reflected from the solar arrays and from the earth, the radiating panels are constructed of anodized aluminum covered by aluminized teflon. The solar absorptance of aluminized teflon remains below $\alpha = 0.25$ even after a three-year exposure to the sun, assuring that the solar input remains a minor heat source throughout the ERTS mission. The surface emittance of aluminized teflon is $\epsilon = 0.8$, the same as on OGO. The louvers reduce the effective emittance to approximately $\epsilon = 0.68$ when open and $\epsilon = 0.10$ when closed, maintaining the panel temperature within 20 $\pm 15^{\circ}$C during the most severe conditions. The main benefit of an active thermal control is that it permits changes, relocations, or additions of high-power dissipating experiments for various missions without any change in the system, plus the capability of controlling the temperature when the duty cycle is changed.

The same thermal control is retained on ERTS except that the louvers on the +Y panels are deleted and the surface of the radiating panels on the X panels are covered with aluminized teflon.

To minimize heat losses through the sides not under the louver control, the remaining four surfaces are insulated with multilayer aluminized

Mylar insulation. The effective conductance through this insulation has been demonstrated by several tests to be such that losses amount to approximately 1 watt/ft^2 when the side is in the shade and a negligible amount when the side is exposed to the sun.

The tape recorder compartment on the +Y end of ERTS is treated as an extension of the basic OGO structure. With the exception of the concave corners the entire extension is insulated with multilayer insulation. The corners are utilized as the heat radiating areas. The desired amount of heat rejection is achieved by controlling the thermophysical properties of the corners with a combination of vacuum-deposited aluminum finish and aluminized teflon. Vacuum-deposited aluminum has solar absorptance of $\alpha = 0.12$ and surface emittance of $\epsilon = 0.04$. Heaters are provided for use in event the recorders remain off for extended periods.

The heat losses through the antennas and other external elements are reduced by requiring all the items to be either thermally isolated with fiberglass standoffs, plated with vacuum-deposited aluminum or coated with a colorless conversion coating. The heat losses through such brackets are only 0.25 to 1 watt per bracket.

The only places where the surface emittance is purposely high are the four corner castings at the +Y end. The castings are bulky and well coupled to the panels at places where the highest heat generating components (inverter and power control unit) are located; they thereby add radiating areas in the locations where most needed. They are covered with Mylar tape with an approximate surface emittance $\epsilon = 0.6$. Heat loss through these castings is approximately 20 watts.

The design of the system is based on two most severe conditions; the hot condition, when the external heat input and the internal power are greatest, and the cold condition, when the inputs are the smallest. The two conditions for ERTS are approximately the same, solar input causing most of the variations. Calculations based on the orbital analysis presented in Volume 3, Section 10, indicates that three phenomena contribute to variations in the solar input: changes in distance from the sun, eclipse duration and the cone angle characterizing the orbital motion of the sun relative to the spacecraft body. Each effect has a yearly cycle

with peaks in winter and summer. Fortuitously these effects tend to cancel and leave a nearly uniform total solar input throughout the year.

Predicted temperatures in the ERTS configuration are shown on Figure 9-1. This data, obtained from the thermal analysis computer program, shows that payload temperature specification of 20 ±10°C can be met with payload off entirely or on 20 minutes per revolution. Figure 9-2 shows the detailed temperature distribution.

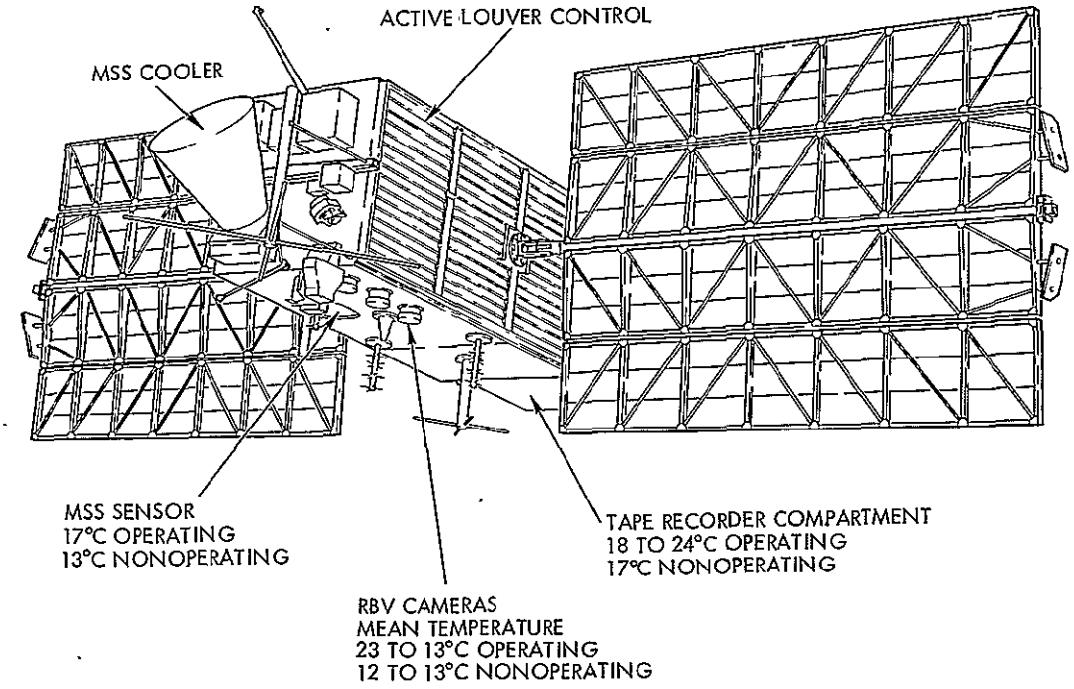

Figure 9-1

THERMAL ENVIRONMENT FOR THE PAYLOAD. The temperature of the payload remains within the required limits because power variation is compensated by an active thermal control system.

The temperatures of the main box are monitored by several thermistors. A complete temperature distribution, covering the areas not sensed by the thermistors, is obtained by the thermal analysis, the accuracy of which is approximately 1 to 3°C. On the OGO flights the agreement between predicted and actual temperatures in orbit has been quite close.

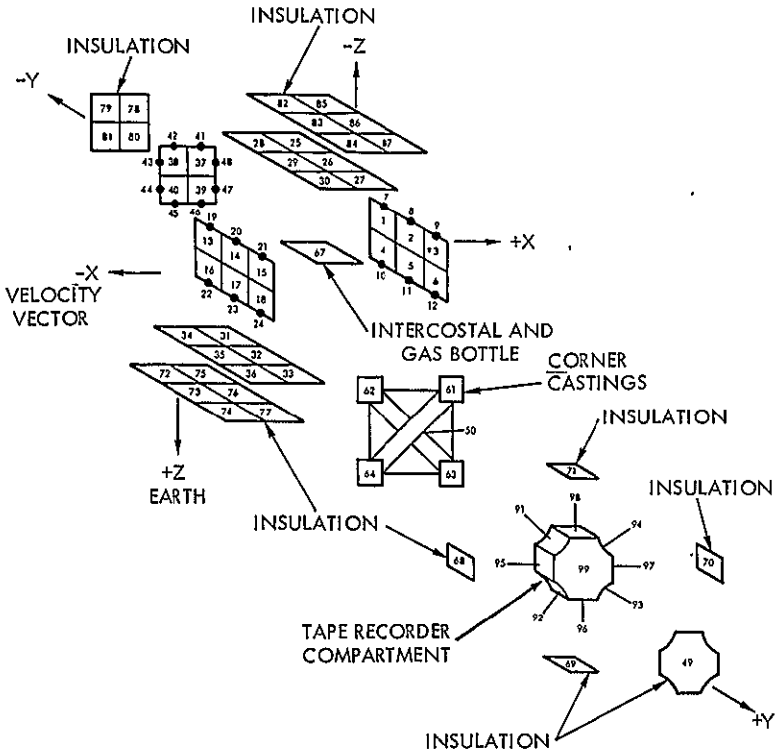

LOCATION	NODE NO	TEMPERATURE °C 69° CONE	50° CONE	69° CONE WITH PAYLOAD TURNED OFF
+X TOP	1	15	15	13
	4	15	15	12
+X MID	2	15	15	13
	5	17	17	15
+X AFT	3	18	18	16
	6	19	18	16
-X TOP	13	15	15	12
	16	12	13	9
-X MID	14	16	16	14
	17	18	18	15
-X AFT	15	20	20	18
	18	20	20	18
+Z TOP	31	17	17	13
	34	16	17	13
+Z MID	32	24	24	17
	35	24	24	17
+Z AFT	33	23	23	20
	36	22	22	20
-Z TOP	25	20	20	17
	28	20	20	17
-Z MID	26	20	20	17
	29	20	20	17
-Z AFT	27	18	18	16
	30	20	20	17
-Y	37-40	16	17	13
+Y	99	19	20	16
GAS BOTTLE	67	18	18	15
AFT STRUCTURE	50	16	16	13
TAPE RECORDER COMPARTMENT	91	18	20	13
	92	18	19	14
	93	18	19	14
	94	18	20	13
	95	23	24	17
	96	21	21	17
	97	23	23	17
	98	21	22	17

Figure 9-2

TEMPERATURE DISTRIBUTION IN ERTS is computed by the TRW Thermal Analysis Computer Program, which takes into account all heat sources, radiant and conducted heat paths, and means of heat rejection. For OGO, similar predictions compared with flight measurements showed an accuracy within 1 to 3°C. Predicted temperatures for ERTS fall between 14 and 25°C, well within the required range of 20 ±10 C during normal operating mode.

9.1 LOUVER SYSTEM

The main body louver system consists of 98 individually actuated louvers (see Figure 9-3). Each X side assembly contains 49 louvers covering 12 square feet. Two louvers near the velocity correction nozzles and two areas covering 2.5 square feet on the +Y end of OGO are deleted on ERTS. The complete louver system, including all hardware, weighs 0.66 pound per square foot for a total of 15.8 pounds. Each louver unit consists of the louver blade, support bearings at each end, plastic end fittings, a bimetallic spring, and stops to limit the fully closed and open positions. See Figure 9-4. The louver blades are lightweight, center-rotating members constructed of two 0.005-inch aluminum sheets spotwelded together along the two edges. The bimetallic actuators serve the double purpose of sensing the local mounting panel temperature and providing the driving torque to rotate the louver blades. The actuators are placed alternately at opposite ends of the louvers, thereby providing a more even distribution of the sensing elements over the equipment mounting panel.

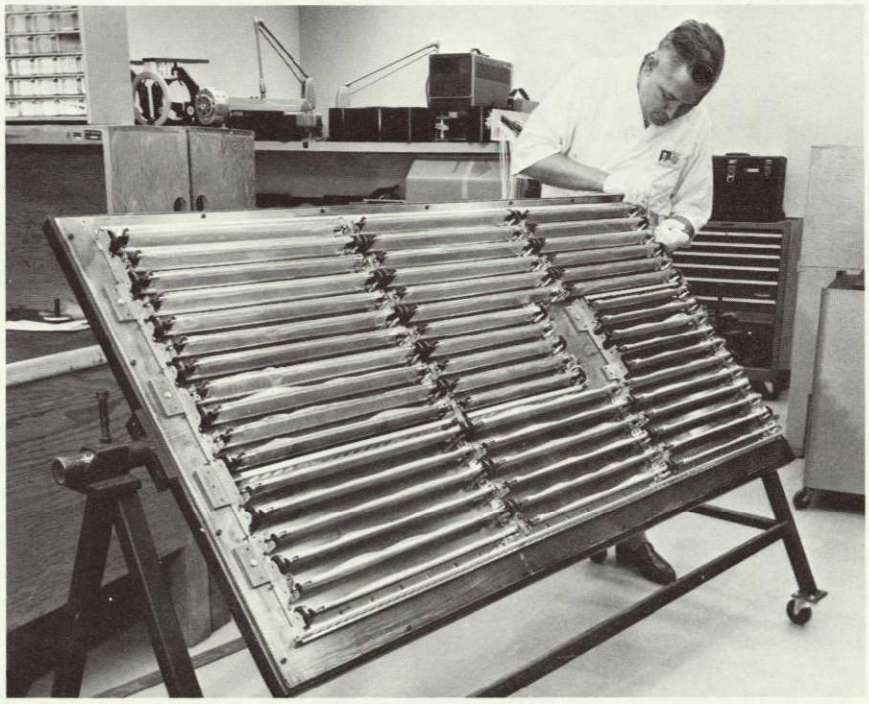

Figure 9-3
SIDE LOUVER ASSEMBLY

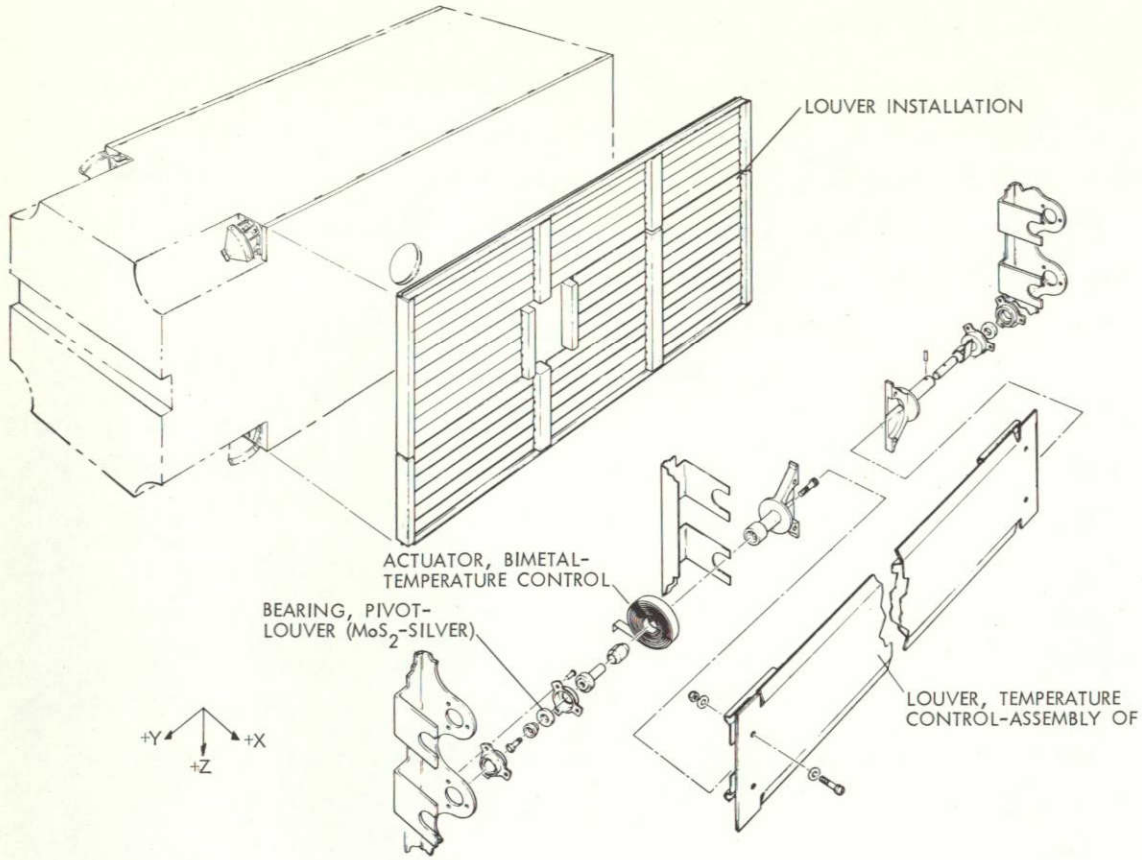

Figure 9-4
DETAILS OF LOUVER ASSEMBLY

The coil has a free length of 38 inches and a torque constant of 0.0029 in.-lb/°C. A 14°C increase in temperature from 70°C rotates the louvers 90 degrees from fully closed to fully open. The bimetal springs are thermally coupled to the mounting panel by anchoring the fixed end to the panel, oxidizing the bimetal to obtain a high infrared emittance, and insulating the free end from the louver by plastic end fitting. In addition, further isolation from the varying external thermal environment is achieved by means of an insulated housing with 10 layers of crinkled aluminized Mylar within an outer jacket of 3-mil aluminized Mylar.

Louver blades rotate in 1/8-inch inside-diameter sleeve bearings housed in a bearing support bracket at each end of the louver assembly. On the basis of extensive tests for OGO a bearing composed of 80 percent silver and 20 percent molybdenum disulfide sintered material was

selected, along with a shaft coating of molybdenum disulfide in a sodium silicate binder. For this combination of materials the highest starting torques experienced were 0.033 in.-oz. This corresponds to a temperature increase of the bimetallic actuator of about 1°C to overcome worst-case static friction torques.

The effective surface emissivity of a radiating panel with a surface emissivity $\epsilon = 0.8$ is shown in Figure 9-5. A substantial portion of the loss in efficiency is attributed to the thickness of the louver blades, since they occupy 11 percent of the panel are in the open position. Because of the space between the louver blades and the actuator housing, and a narrow gap between the louvers themselves, an uncertainty range exists in a region where the louvers are fully closed. In evaluating the louver performance this uncertainty has always been included in the analysis by assuming two values, each value conservative for a given situation. Thus, the larger value was taken in the cold condition and smaller in the hot.

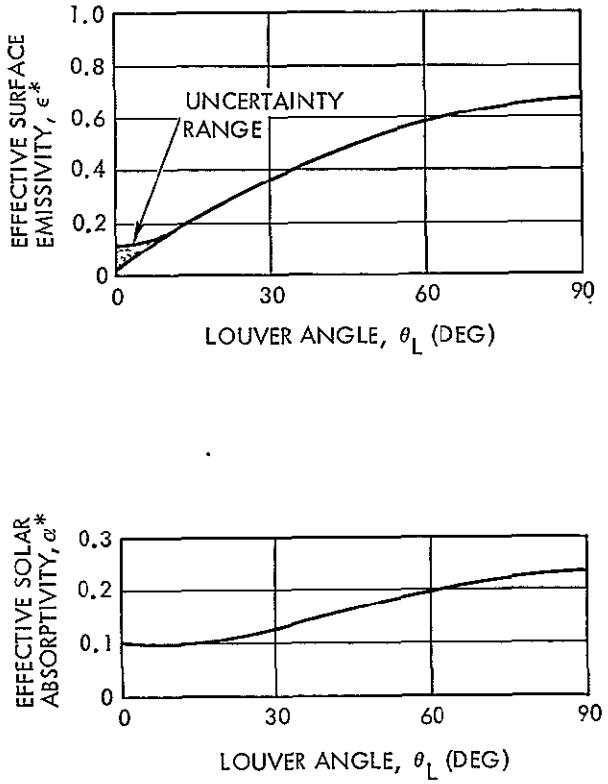

Figure 9-5
EFFECTIVE SURFACE EMISSIVITY and solar absorptivity of the louvered panels

The solar input to the louvered surfaces has not been a problem in controlling the temperature of the mounting panels. The louvered surfaces on OGO 1, 2, and 3 were exposed to sunlight and the flight data indicates that the systems did not thermally degrade. However, as a precaution against excessive louver temperature in the sun and consequent warping, a strip of thermal control paint is added to each blade on ERTS.

9.2 INSULATION

The use of insulation to cover all areas of the spacecraft other than the louvered areas is a key factor in the successful performance of the thermal control system. In order to maintain a conservative and flexible thermal design, a multiple-layered shield has been devised. The insulation selected consists of ten layers of 1/4 mil crinkled aluminized Mylar with an outer layer of 3-mil aluminized Mylar (Mylar side out). Ultrasonic sealing techniques are employed to hold the layers together with spots and seams around the edges and openings. An insulation blanket is thus formed which can be handled but which retains its essential insulating qualities. Air trapped between the layers is vented by means of incomplete sealing on selected edges, thereby directing the gases in preferred directions away from sensitive experiments.

In the transverse direction, the low apparent thermal conductivity is the result of multiple thermal radiation shields minimizing the heat transfer by radiation. Conduction heat transfer is made small by crinkling the Mylar and reducing the contact area between the layers. Low lateral conductivity results from the low thermal conductivity of the Mylar and a small cross-sectional area of each individual sheet.

9.3 PAYLOAD

The payload environment is controlled by the active louver system of the main box. The RBV cameras are mounted on a honeycomb plate to avoid camera misalignment from thermal gradients on the mounting surfaces. The heat dissipated by the cameras is rejected by radiation to the interior of the observatory from the cameras themselves and to the -X panel through the honeycomb plate. Thermal gradient across the thickness of the plate is maintained to less than $1^{\circ}F$ by inserting solid metal fillers where the cameras are attached to the plate and by providing low surface emittance finish ($\epsilon = 0.04$ to 0.10) on the side of the plate facing the interior of the observatory and painting black ($\epsilon = 0.85$) the side facing the -X panel. A combination of these two finishes and solid metal fillers allows the heat to be conducted from the cameras to the plate and to be rejected by radiation from the plate to the -X panel. At the same time

the plate is prevented from absorbing the heat radiated from other components in the interior of the observatory. In a normal operating mode the mean temperature of the plate and the cameras is calculated to be between 22 and 24°C.

No special mounting precautions are required on the MSS scanner. The heat is rejected by conduction to the +X panel and by radiation to the interior of the observatory. The temperature of the scanner is calculated to be 17°C.

The tape recorders for the payload are mounted in a special compartment on the +Y end of the observatory. The temperature of the compartment is controlled by radiation from four concave corners and by the heat exchange between the compartment and the interior of the observatory. Approximately 17 watts (net) are dissipated by the corners and 15 watts are radiated to the interior of the observatory. The amount of heat rejected by the corners is easily adjusted, if required, by changing their thermophysical properties. In a normal operating mode, the temperature of the tape recorders is calculated to be 24°C and the temperature of the electronics 21°C.

9.4 SEPARATION BAND

The separation band fastens all four corner castings of ERTS to the interstage. To avoid excessive thermal stresses in the band during the coast before separation, the band is shielded with insulation consisting of ten layers of crinkled 1/4-mil aluminized Mylar and a single 3-mil shield. There is no hot problem associated with the band.

9.5 HORIZON SCANNER

The entire horizon scanner, with the exception of sensor windows, is wrapped with the multilayer insulation. Since there are no heat sources in the scanner, the temperature control of the scanner head relies almost exclusively on conductive heat flow from the -Y panel. Under all normal orbital conditions, including eclipses, the temperature of the scanner head is about 4°C below the temperature of -Y panel and is calculated to range from 5 to 30°C; well within the -8 to +40°C acceptance range for the units.

9.6 SOLAR ARRAYS

The solar arrays consist essentially of two parts, the solar cell modules and the structure which supports the modules. Each module contains 112 silicon cells with 6-mil microsheet cover glass and a beryllium substrate. A sketch of a solar cell and associated thermal conductivity is given in Figure 9-6. The back side of the arrays are painted with MT6-7 white pigmented silicone rubber paint to minimize unwanted albedo input from the earth. The thermophysical properties of MT6-7 are approximately the same as the MT6-2 used on OGO but, the application and handling of MT6-7 is easier to control than MT6-2. The low solar absorptivity and high surface emittance of this paint virtually eliminates the albedo input. The thermal radiation properties of microsheet cover glass, MT6-7 paint and the beryllium substrate are given below:

	Cover Glass Microsheet	Beryllium Substrate	MT6-7 Paint
Emissivity	0.80	0.06	0.85
Solar Absorptivity	0.82	0.62	0.20 to 0.36*

Figure 9-7 shows the array temperature predicted for the ERTS orbit. OGO flight data has generally indicated that such predictions are quite accurate.

The charge regulator thermal fins are located at the outer edge of each solar array, two fins per array (see Section 9.4). These units must reject surplus array power without exceeding 93°C and maintain the temperature of an internal power transistor above -50°C during eclipses when no surplus power is available.

The hottest case occurs when the heat input from the earth and the surplus electrical power sum to approximately 43 watts per fin. The coldest condition is during eclipses when the temperature of the transistor depends strictly on the thermal capacity of the fin. A high fin thermal

*Three year degradation.

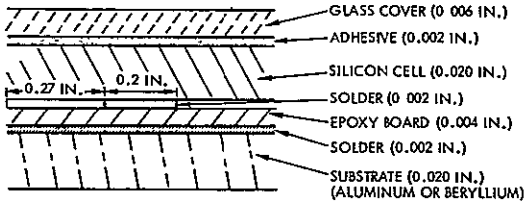

THERMAL CONDUCTIVITY

PART	CONDUCTIVITY BTU/HR FT^2 °F/FT
COVER GLASS	0 4
ADHESIVE	0 1
SILICON	45.0
SOLDER	100.0
EPOXY BOARD	0.1
SUBSTRATE	
ALUMINUM	60.0
BERYLLIUM	80 0

Figure 9-6
CROSS-SECTION OF OGO SOLAR CELL showing thermal conductivity

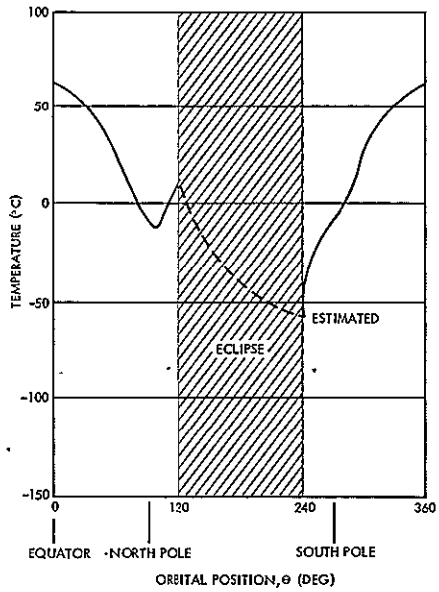

Figure 9-7
APPROXIMATE TEMPERATURE HISTORY of solar arrays on ERTS

capacity, without excessive weight, is achieved by filling a thin aluminum case with lithium. The density of lithium is $\rho = 33.1$ lb/ft and the specific heat $C_p = 0.8$ Btu/lb-°F, as compared to $\rho = 168.5$ lb/ft and $C_p = 0.2$ Btu/lb-°F for aluminum. The required heat balance in the sun is achieved by adding five layers of crinkled Mylar insulation on the side of the fin facing the spacecraft to prevent heat exchange between the solar array and the fin, and by controlling properties of the radiating surfaces. Exposed surfaces are soft anodized to provide solar absorptivity $\alpha = 0.27$ and surface emissivity $\epsilon = 0.85$.

9.7 SUN SENSORS

Temperature control of the two sun sensor packages is achieved by conductively isolating the housing from the solar arrays and the sensors from the housing. The housing is isolated from the solar arrays with a fiberglass mounting bracket, and the sensors thermally isolated from the solar arrays with a fiberglass mounting spool and with multilayer Mylar insulation. The heat loss through the electrical leads is decreased by using wire of the smallest permissible gage and increasing the conduction path by wrapping the wire around the spool. The required temperature level is

achieved by balancing the very small heat loss through the sensors with the severely restricted heat gain from the housing through the fiberglass spool.

The heat gain from the housing is kept steady by coating it with a combination consisting of hard anodized and vacuum-deposited aluminum. The solar absorptivity of the anodized aluminum is approximately $\alpha = 0.87$ and that of vacuum deposited aluminum $\alpha = 0.1$. The surface emittance is approximately $\epsilon = 0.8$ for the anodized and $\epsilon = 0.03$ for the vacuum-deposited aluminum. The stabilization temperatures are individually tailored for each unit by addition of Mylar tape and by proportioning the two coating areas (see Figure 9-8).

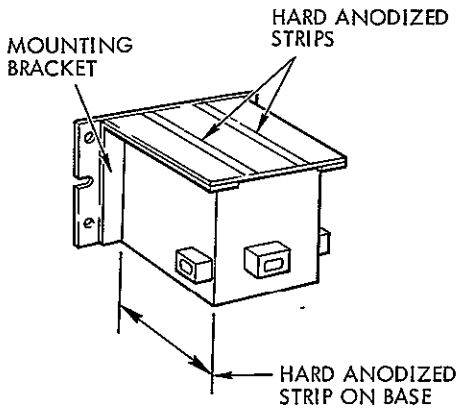

Figure 9-8
OGO SUN SENSORS

During eclipses, the temperature of the sensors is maintained above 20°C by a beryllium heat sink. The sensors, RTT, and the trimming resistors are mounted on a sink having a heat capacity sufficient to counter the heat loss through the fiberglass spool to the rapidly cooling housing.

9.8 YAW GYRO

The temperature of the yaw gyro is maintained between the required values of 57 to 62°C by a proportional heater capable of dissipating approximately 11 watts at 28 volts. The power to the heater is thermostatically controlled between 1 and 8 watts, is never reduced to zero. This assures that the gyro temperature will not drop below 57°C.

The gyro is conductively isolated from the structure with non-conductive washers and the heat rejection is achieved by radiation only. No thermal problems have been experienced with this thermal control on OGO. Flight data indicated that the temperatures were within the required temperature range at all times and the same performance is anticipated for ERTS.

CONTENTS

10. VELOCITY CORRECTION

Establishing and maintaining the precise orbit required for the ERTS mission is the function of the velocity correction subsystem. An analysis of Thor-Delta N injection inaccuracies indicates that 31 ft/sec of velocity correction must be available to remove in-plane errors and 17 ft/sec must be available to remove out-of-plane errors (see Section 3.4 of Volume 2). While operation could continue for one year without additional correction a more precise ground-trace overlap or operation for longer than one year would require additional capability to the extent of approximately 8 ft/sec per year.

Performance of the required velocity corrections is accomplished using heated krypton gas. The tankage is the same as for the attitude control pneumatics. At 4000 psia, 57 pounds of krypton are stored providing 7.7 pounds for attitude control and 49.3 pounds for velocity correction. This allocation of krypton to velocity correction provides 3220 lb-sec of impulse or 74 ft/sec velocity correction capability for the 1425-pound observatory. By increasing the gas pressure to the design limit of 5175 psia an additional 8 pounds could be carried. Because of the common tank any other division of gas between velocity correction and attitude control could be effected.

Achieving the stated total impulse with the weight of gas allocated is accomplished by raising its I_{sp} 92 percent to 71 seconds by heating it in electrothermal thrusters to 1600°F.

Three thrusters are employed, one for each direction of in-plane correction and one for out-of-plane corrections. Either positive or negative inclination errors can be corrected with a single thruster by thrusting only at the proper node. A second and oppositely oriented out-of-plane thruster has not been included because of interference and potential contamination problems with the MSS radiative cooler on ERTS-B.

10.1 DESIGN APPROACH

The addition of electrothermal thrusters to the OGO pneumatic system offers significant reliability, operational, and cost advantages over other approaches to velocity correction. As shown in Figure 10-1,

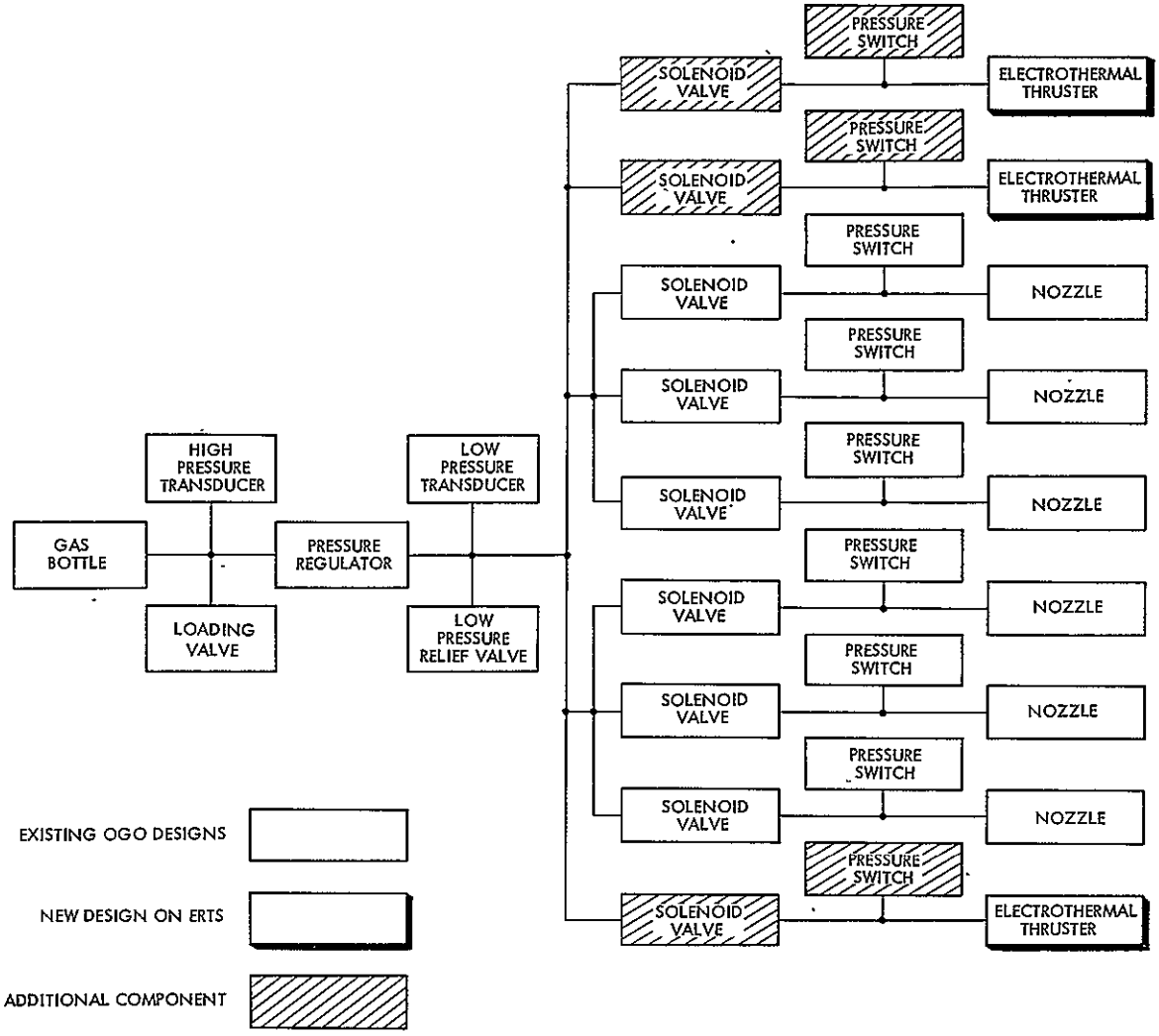

Figure 10-1

OGO PNEUMATICS SYSTEM provides orbit correction capability for ERTS with the addition of three valves, pressure switches, and electrothermal thrusters.

the thrusters use the same gas supply, the same valves, and the same pressure switches as the cold gas attitude control nozzles (see Section 3). In the resulting system the only components that have not already been flight qualified are the electrothermal thrusters, which are currently under development at TRW. In addition to savings in hardware and qualification costs, the use of electrothermal thrusters retains the simplicity and reliability of the cold gas propulsion system and offers the potential for long spacecraft life; since it is unlikely that orbit adjustment

will consume all of the allotted propellant, unused gas will be available for continued attitude control.

The concept of adding electrothermal thrusters to a cold gas propulsion system has been applied successfully to two other TRW satellites. Vela 3 used a single electrothermal thruster to add a translational maneuver capability to the cold nitrogen propulsion system. The advanced Vela used two multi-nozzle electrothermal thrusters for both translational maneuvers and spin rate control. Both configurations used cold gas for attitude control. Specific performance parameters for the ERTS configuration are listed in Table 10-1.

Table 10-1. Capabilities of the ERTS Orbit Adjust System

Thrust level, lb	0.05
Exit temperature, $^{\circ}F$	1600
Heater power, watts	75
Thrust alignment to nozzle symmetry, deg	±0.15
Thrust alignment to spacecraft axes, deg	±5
Propulsive efficiency, percent	92
Gas weight available, lb	49.3*
Thrust sector (orbit), deg	±15
Thrust time (nominal), sec	500
Velocity gained/500 sec, ft/sec	0.56
Orbits to insert 3σ ΔV,	80
Velocity gained per pound of krypton, ft/sec	1.5
Total ΔV capability, ft/sec	74
Specific impulse at $1600^{\circ}F$, sec	71

*After allowance of 7.7 pounds for attitude control, leakage, and residuals.

10.2 OPERATING PARAMETERS

The limit of orbital accuracy obtainable with the low thrust system depends only on the ability of the tracking system to measure errors. The combination of the low thrust level and the small timing uncertainty (0.5 second) in the stored command programmer allows extremely fine

adjustments in velocity. The minimum impulse that can be programmed is less than 50 millipound-seconds, which corresponds to a velocity change of less than 10^{-3} ft/sec.

A further advantage of an electrothermal system with a low thrust level is safety for the spacecraft. Orbit corrections must generally be conducted out of sight of ground stations. A small timing error or even an erroneous command can be counteracted readily if the thrust level is low, but is unacceptable if thrust is high. Only 0.7 percent of the propellant supply is exhausted during an inadvertent 500-second firing, whereas 42 percent of the hydrazine supply would be consumed during the same period by a 3.5-pound thrust hydrazine engine, imparting an intolerable error in velocity.

Orbital corrections will be precisely predictable. After the initial orbit parameters are determined, an orbit-adjust thrust schedule will be compiled. This data will be transmitted to the ERTS and retained in the stored command programmer. Before a thruster is fired, an enable command is transmitted to the spacecraft, allowing the programmer to operate that thruster. At programmed times during the orbit, the programmer commands the propellant valve to open and supply voltage to the thruster heater. As illustrated in Figure 10-2, each of the two in-plane thrusters will operate about 500 seconds per orbit, which corresponds to an orbital angle of about 30 degrees. The single out-of-plane thruster will also fire for 500 seconds, or 30 degrees, per orbit. Choice of the 500-second periods of thrust is based on balancing computed loss of efficiency for various thrust durations against total elapsed time for velocity correction maneuvers. About 1 percent loss of efficiency is experienced with 500 seconds of in-plane thrusting, 0.5 percent with out-of-plane thrusting.

At a thrust level of 0.50 pound, operation of the sensors need not be interrupted during orbit adjustment although body pointing and rates will be increased. No compensation for atmospheric drag is required for the ERTS orbit.

10.3 SYSTEM IMPLEMENTATION

One of the major reasons for selecting the heated gas system is the relative ease with which it can be integrated into the spacecraft.

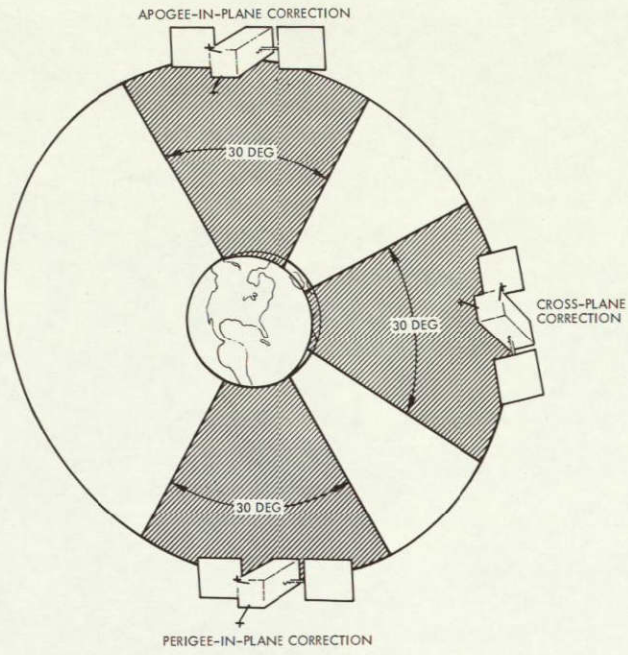

Figure 10-2

ORBITAL OPERATION requires no more than one thruster firing at one time.

Figure 10-3 shows the installation of the pneumatics. Provision is made for adjusting the position of a thruster parallel to the Y-Y axis to allow accurate alignment of the thrust vector to the center of gravity. The thrusters will not protrude from the spacecraft body sufficiently to interfere with the folded solar panels.

The thermal control system is unaffected by the addition of the thrusters. Since the thruster valves are within the spacecraft envelope additional thermal control is unnecessary. Because of the high thermal efficiency of the vortex thrusters, conducting heat to the spacecraft structure will total less than 5 watts. Heating of the solar panels from plume impingement will be negligible.

The commands and telemetry channels required for operation of the thrusters are minimized by using the existing pressure switch to verify thruster operation and by electrically connecting the thruster valve and thruster heater in parallel.

Flow field analysis indicates that exhaust plume impingement on the solar panels of the type shown in Figure 10-4 is readily compensated (see Volume 4, Section 7). The consequent propellant expenditure is equivalent to a thruster inefficiency of no greater than 2 percent. Because of plume impingement, in-plane velocity adjustments have a small out-of-plane component; an in-plane adjustment of 15 ft/sec will have an out-of-plane component of less than 0.25 ft/sec, which is easily compensated. The spacecraft pointing accuracy is not degraded during velocity connections and the payload will remain fully operational.

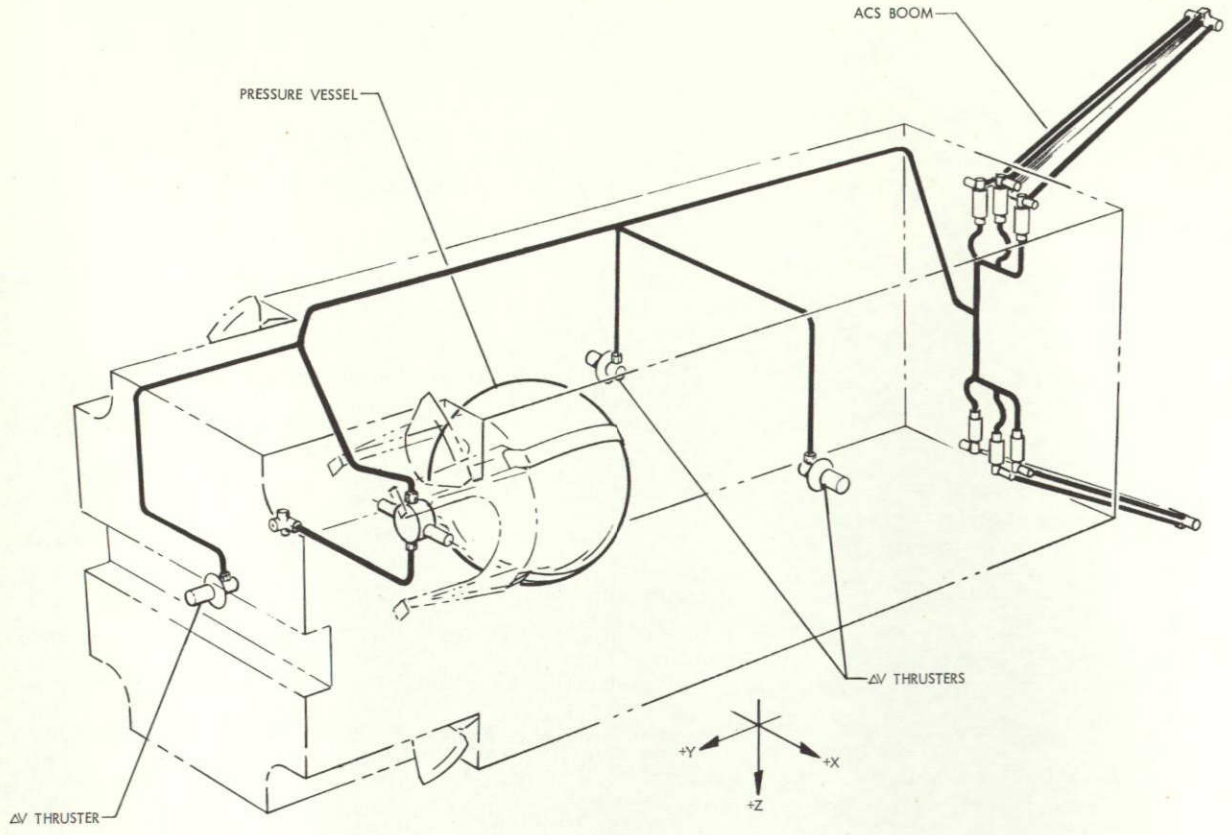

Figure 10-3

INSTALLATION OF THE ELECTROTHERMAL THRUSTERS is readily accommodated by the existing attitude control system

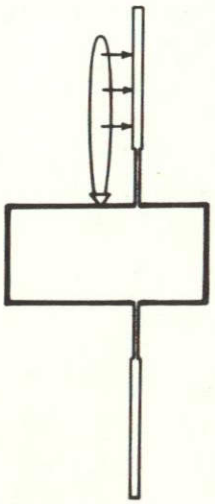

Figure 10-4

HEATED GAS IMPINGEMENT on solar panels will result in a net torque about the Z-Z axis, which can easily be cancelled by the cold-gas thrusters.

The thrusters are positioned to thrust through the ERTS center of gravity. In the case of the X panel thrusters the center of gravity shifts as krypton is depleted; hence these thrusters are positioned at the average center of gravity. Attitude control thrusters must compensate for consequent torques, but since the roll and yaw lever arms of the control jets are each 48 inches only a 1 percent loss of gas is caused by an assumed 0.6-inch error in thrust to c.g.

alignment. There is no less of efficiency due to c.g. misalignments which produce torques along the pitch axis. In the presence of a torque along the pitch axis, the attitude control system will respond with a counter torque, but since it is in the form of a pure couple, no loss in translational thrust will occur. The total movement of c.g. along the Y axis caused by depletion of the 50 pounds of krypton is 0.7 inch. If the thruster is positioned midway in this range, the net loss of efficiency from c.g. movement is 1.5 percent. It is planned to position the X panel thrusters forward of the c.g. (-Y direction) to balance the torque from the average plume impingement.

The power and voltage requirements of the electrothermal thruster are within the capabilities of the power system. Conditioned power is not required for thruster operation. Each electrothermal thruster requires about 75 watts for steady-state operation.

10.4 ELECTROTHERMAL THRUSTER

The thruster consists of a cylindrical cavity with a coaxial spirally-wound wire heater element 75 percent tungsten, 25 percent rhenium) as shown in Figure 10-5. The propellant gas is injected tangentially at high velocity. The gas spirals radially inward with high tangential, but low radial, velocity. In passing around and through the heater element many times, the gas is heated. It is then expelled through a conventional convergent-divergent nozzle.

The thrusters weigh less than 0.1 pound each. The low-mass, helical configuration of the heater element provides fast thermal response and minimizes the effects of the thermal transients on delivered specific impulse. Moreover, a heater element failure will not impair the ability of the thruster to perform in an unheated mode. In the event of a heater failure, the delivered specific impulse will be degraded 50 percent but thrust remains constant.

For a given operating temperature, the thermal and specific impulse efficiencies of the vortex thruster with krypton propellant closely approach the theoretical maxima. The theoretical specific impulse of heated krypton was calculated from standard thermochemical data. Based on data from previous nozzle efficiency studies and OGO experience, these theoretical

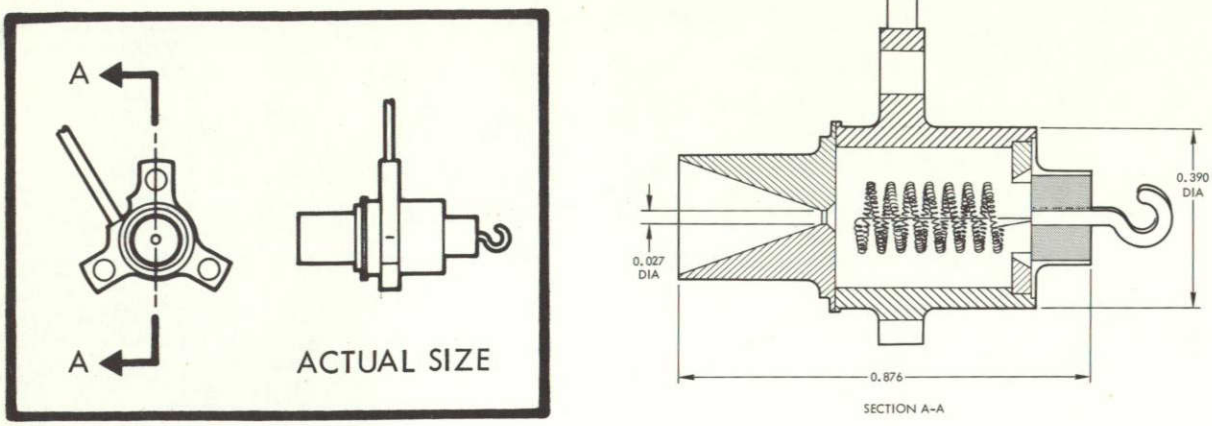

Figure 10-5

VORTEX THRUSTER has been developed for other TRW programs, and has been demonstrated at thrust levels between 0.005 and 0.050 pound.

data were used to predict the delivered specific impulse as a function of temperature (Figure 10-6). The power required to heat the propellant is a function of the delivered specific impulse and the propellant specific heat capacity. Experimental data shown in Figure 10-7 illustrates the relationship between specific impulse and power for nitrogen propellant.

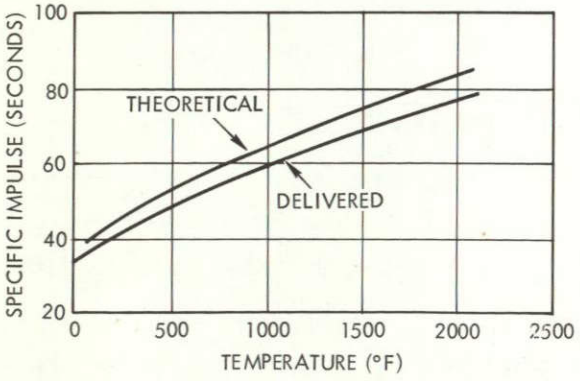

Figure 10-6

DELIVERED SPECIFIC IMPULSE of a vortex thruster with krypton varies from about 94 percent of theoretical at normal spacecraft temperatures to 92 percent at 1600°F, as demonstrated in development tests.

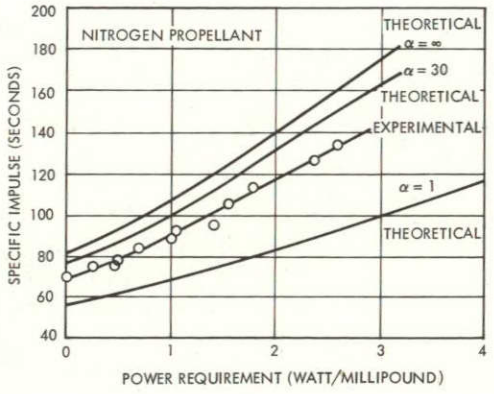

Figure 10-7

PROPULSIVE PERFORMANCE of prototype thruster over the propellant temperature range tested (up to 1600°F) showed a delivered I_{sp} 90 percent of theoretical for an area ratio of 30, including both thermal and viscous flow losses

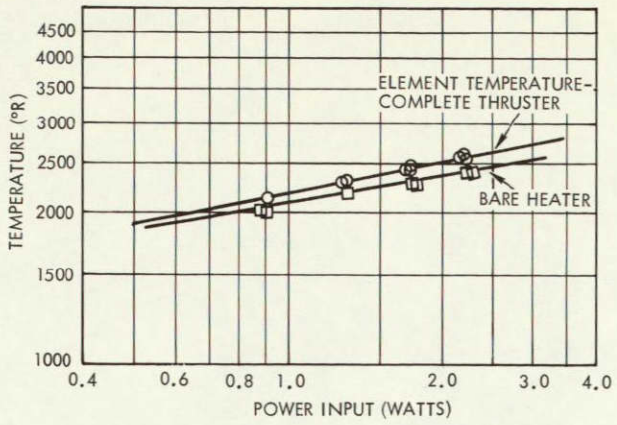

Figure 10-8

HEAT LOSS on the prototype vortex thruster amounted to about 0.7 watt at 1600°F (2059°R).

Because the heater element is the only portion of the thruster that operates at high temperature, the thermal efficiency is quite high. Figure 10-8 shows the no-flow heat losses for a 10-millipound vortex thruster. Under these conditions, the temperature of the outer wall of the thruster does not exceed 300°F. With propellant flow, the outer case is cooled by the incoming gas and thermal losses are reduced.

Extrapolating to the ERTS thrust level of 0.05 pound, the total heat losses do not exceed 5 watts. A photograph of a developmental 10-millipound thruster is given on Figure 10-9.

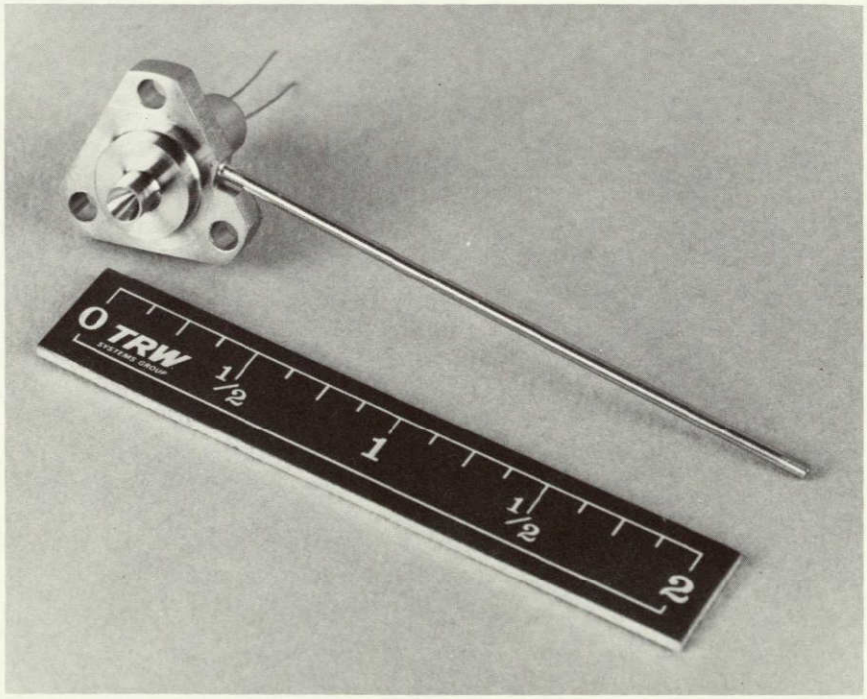

Figure 10-9

VORTEX HEATED THRUSTER, 0.01-pound thrust

CONTENTS

11. GROUND SUPPORT EQUIPMENT

The mechanical and electrical ground support equipment necessary for integration, test, and launch of ERTS-A and -B is described in this section. The only new items of mechanical GSE are installation fixtures for the MSS and the RBV's. For the electrical GSE, however, the new equipment design is more extensive because of the inclusion of the unified S-band and wideband video subsystems.

11.1 MECHANICAL GROUND SUPPORT EQUIPMENT

The mechanical ground support equipment required for ERTS is listed in Table 11-1. As shown, of 30 items needed, only five are new or adapted. The others are applicable unchanged from the OGO program.

11.1.1 Universal Handling Fixture

The universal handling fixture includes a vertical dolly, a horizontal dolly, and a shared center section used for erection of the observatory. This center section becomes a connecting link between the horizontal and

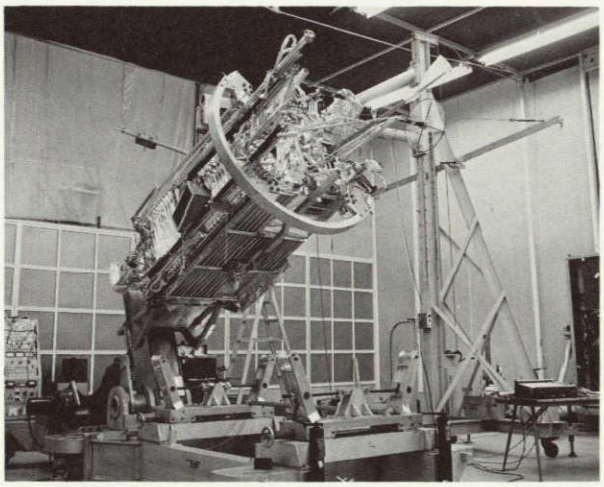

Figure 11-1

THE UNIVERSAL HANDLING FIXTURE provides in-plant support and mobility of the observatory.

vertical dollies during erection and separates at either interface to become part of either dolly. In addition to the motor-driven erection drive, the center section contains a motor-driven drive for rotating the observatory about its Y axis in any orientation from vertical to slightly below

Table 11-1. Mechanical Ground Support Equipment for ERTS

	No. Required	Available from OGO	To Be Built
Universal hand fixture	1	1	
Vertical sling	2	3	
Vertical transporter	1	1	
Solar array handling fixture	2	3	
Horizontal hoist sling	2	2	
Body support beams	2	3	
Center of gravity fixture	1	1	
Thermal vacuum fixture (major change from OGO)	1	0	1
Vibration fixture	1	1	
Solar array spring tool	1	1	
Interstage align tool	2	2	
Strain gage suitcase	1	1	
Ordnance suitcase	2	2	
Separation spring cup tool	1	1	
Horizon scanner hoops (minor change from OGO)	2	2	
Coarse sun sensor GSE	2	2	
Work stands	2	2	
Torque-angle machine	1	1	
Solar array fixture	1	1	
Solar paddle sling	1	2	
High pressure cart	2	2	
Krypton charging system	1	1	
Thermal louver support frame	3	4	
Horizontal MSS installation fixture (new)	1	0	1
Vertical MSS installation fixture (new)	1	0	1
RBV installation fixture (new)	1	0	1
Alignment adapter (new)	1	0	1
Horizon scanner field of view fixture	2	2	

horizontal. The horizontal dolly includes supports for roll rings which attach to the observatory at the -Y end and at the separation plane. The supports allow adjustment of the height and lateral position of the observatory.

The roll rings are designed so that one to three quarters can be removed for access purposes while the observatory is supported by the remaining sections. When a roll ring section is removed a spring loaded piston protrudes from the adjacent section to prevent inadvertent rotation of the observatory.

11.1.2 Vertical Hoist Sling

The vertical hoist sling consists of four cables terminated at one end in fittings which attach to the castings at the observatory separation plane. The cables are suspended from a common point at the hook, through a spreader frame, to take out horizontal loads, and pass through stabilizer arms attached to the observatory at the -Y end.

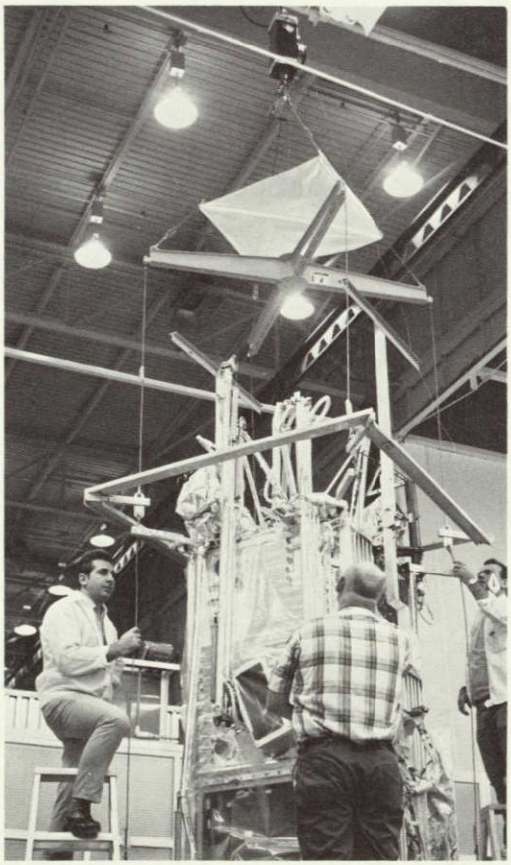

Figure 11-2

THE VERTICAL HOIST SLING provides for attachment of a fully assembled observatory to an overhead hoist.

11.1.3 Horizontal Hoist Sling

The horizontal hoist sling consists of a beam extending the length between roll rings, cables with clevises to attach to the roll rings, and a hoist attach point which is adjustable to be positioned near the longitudinal center of gravity.

11.1.4 Solar Array Handling Fixture

The solar array handling fixture supports the array on a box-beam framework which surrounds the paddle in an unfolded configuration. This frame is supported at each end through pivot points by a rolling dolly. The pivots provide for rotation of the paddle about its long axis into horizontal and vertical orientations. Removable covers protect both the solar cell side and the opposite side, while providing access to both sides.

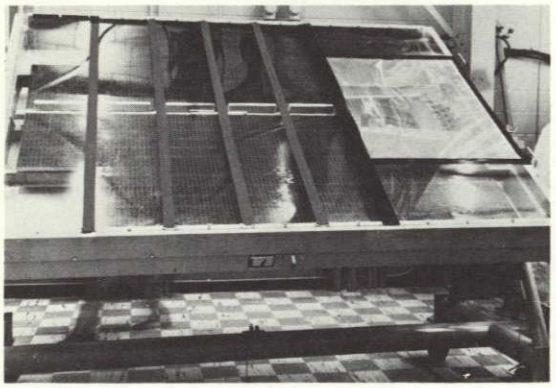

Figure 11-3

THE SOLAR ARRAY HANDLING FIXTURE supports the ERTS solar array during in-plant movement and storage.

11.1.5 Body Support Beams

The body support beams are simple box beams with attach points to pick up the observatory structure at several points along the four X-Z interfaces. These beams also have provisions for mounting plexiglas sheets to protect the thermal louvers installed on the X faces.

11.1.6 Center of Gravity Fixture

The center of gravity fixture is a rectangular frame made of channel members, with sufficient rigidity to permit no significant change of the relative positions of the scale support points and the observatory support points as the load changes.

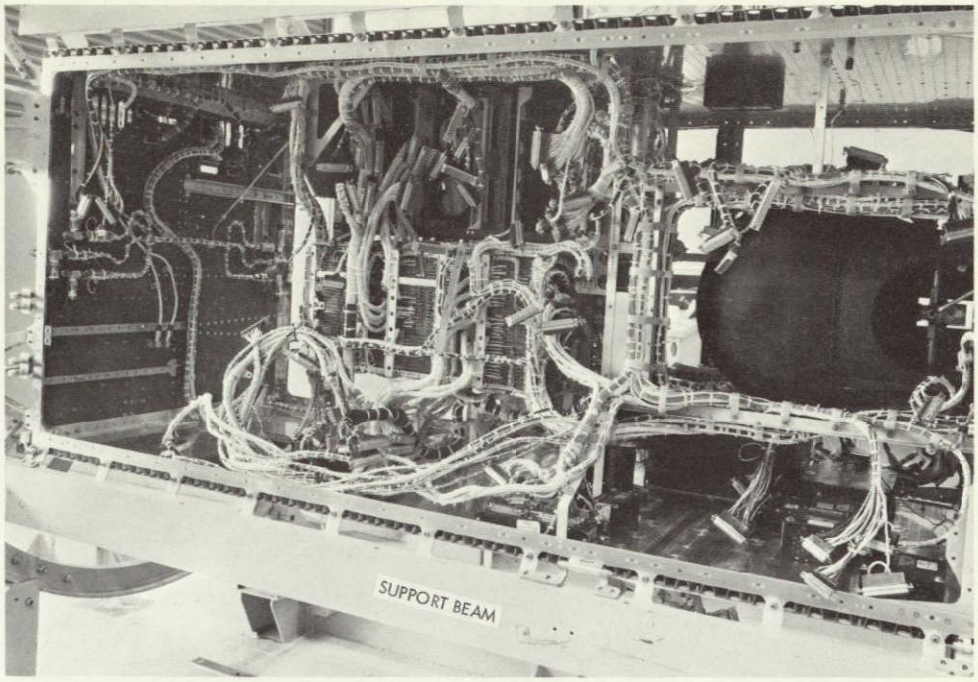

Figure 11-4

BODY SUPPORT BEAMS replace the structural support of the Z doors of the ERTS when the doors are open.

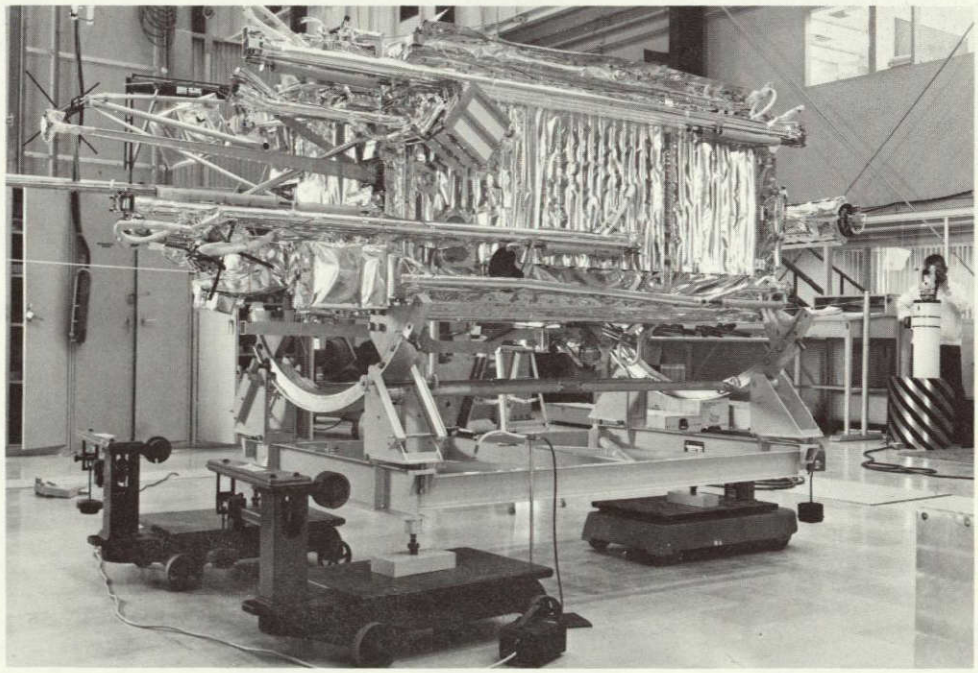

Figure 11-5

THE CENTER OF GRAVITY FIXTURE uses three beam-balance scales to weigh the observatory.

11.1.7 Thermal Vacuum Fixture

The thermal vacuum fixture will support the observatory in the TRW 22 × 46-foot chamber, with the Y axis orientation adjustable to 50 to 69 degrees off the sun vector, and provide rotation of the observatory about the Y axis. Support will also be provided for solar paddle simulators which will simulate solar paddle heat input and shadowing effects. The Y-axis orientation mechanism will be manually driven through a mechanical feed, and the observatory will be rotated about its Y axis by a motor drive housed in a sealed unit inside the chamber but connected to outside ambient.

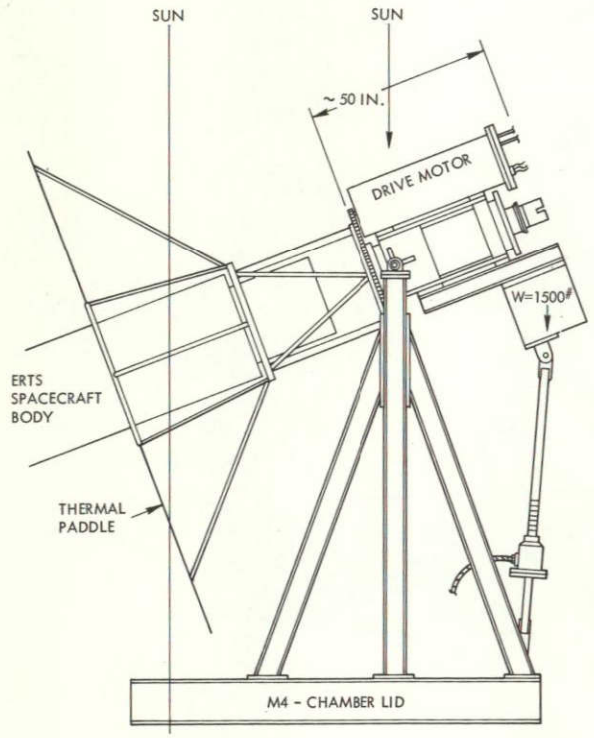

Figure 11-6
THE THERMAL VACUUM FIXTURE rotates about the observatory Y axis through one revolution and return.

11.1.8 Vibration Fixture

The vertical vibration fixture is a hemispherical casting designed to have no resonances in a frequency range that interferes with proper dynamic simulation.

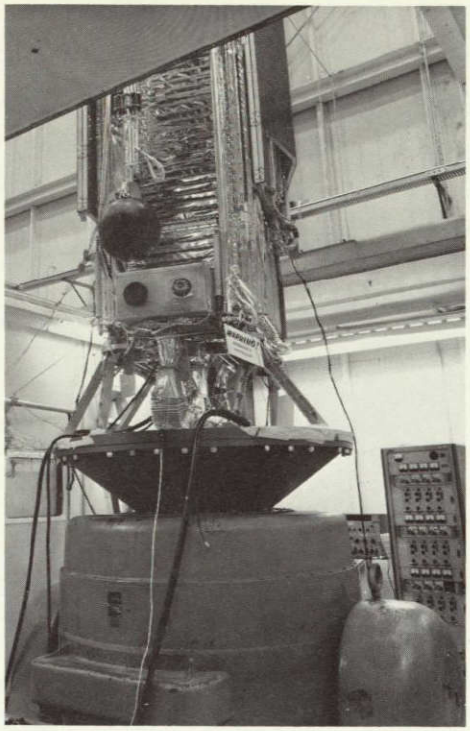

Figure 11-7

THE VERTICAL VIBRATION FIXTURE adapts the launch interstage attachments to the test shaker.

11.1.9 Horizon Scanner Hoops

The horizon scanner earth simulators are black anodized bows which curve around the scanner head and present a black field of view to the scanner. At calibration angles along the bow, heaters are exposed to the scanner through adjustable windows.

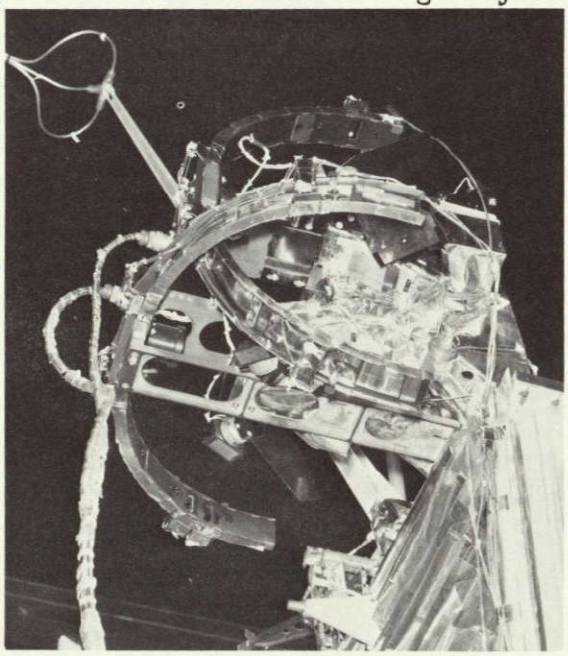

Figure 11-8

HORIZON SCANNER HOOPS simulate the horizon during attitude control tests.

11.1.10 High Pressure Cart

The high pressure cart has provisions for in-plant manual mobility and for hoisting. It holds four 6000-psi bottles and valves and gages for charging and discharging the bottles. It has the following characteristics:

Weight: 1750 lb

Dimensions: 34 × 34 × 68 in. high

High-side working pressure: 6000 psi

High pressure relief setting: 6600 psi

Low pressure working pressure: <3000 psi

Low pressure relief setting: 3600 psi

Component pressure ratings:

	Working	Proof	Burst
Certified ICC3AA pressure bottles	6,000	10,000	18,000
Manifold burst	6,000	9,000	30,000
Relief valve	6,000	6,600	24,000
Blowout disc	6,000	6,600 (disc set)	20,000 (housing)
Gages	6,000	10,000	20,000
Regulator	6,000	10,000	20,000
Tubing	6,000	9,000	45,000
All low pressure components	3,000	4,500	10,000 or more
All low pressure tubing	3,000	4,500	20,000

11.1.11 Krypton Charging System

To fill the attitude control system bottle for flight a two-stage pumping system is used having the following characteristics:

Weight: ~750 lb

Component pressure ratings:

	Working	Proof	Burst
Certified ICC3AA bottles	6,000	18,000	24,000
First stage pump AG4C	600	900	2,400
Second and third stage pump ATS-75-C	16,000	40,000	80,000
Gages	5,000	10,000	20,000
Relief valve, high pressure	6,600	13,200	26,400
Relief valve, low pressure	3,600	7,200	14,400
Tubing	7,000	12,000	20,000
Components	6,000	12,000	24,000

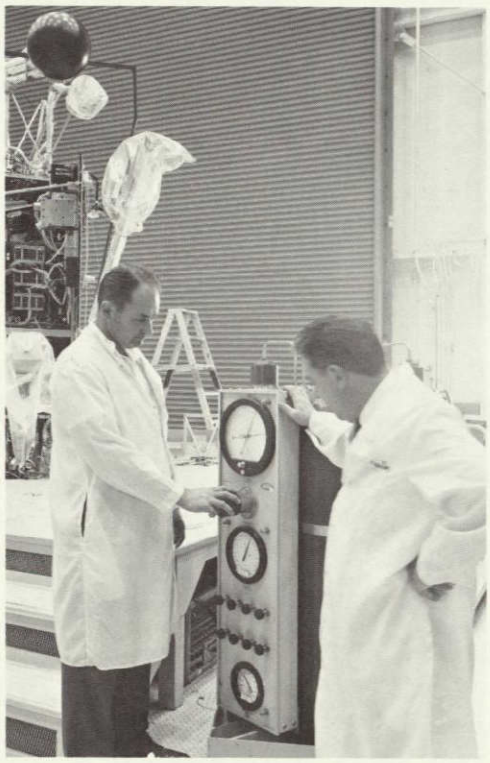

Figure 11-9

THE HIGH PRESSURE CART is used to charge the attitude control system during tests.

11.1.12 Torque-Angle Machine

The torque-angle machine has been refined during its use on OGO to provide friction-free surfaces so that very small defects in deployment systems can be identified and evaluated.

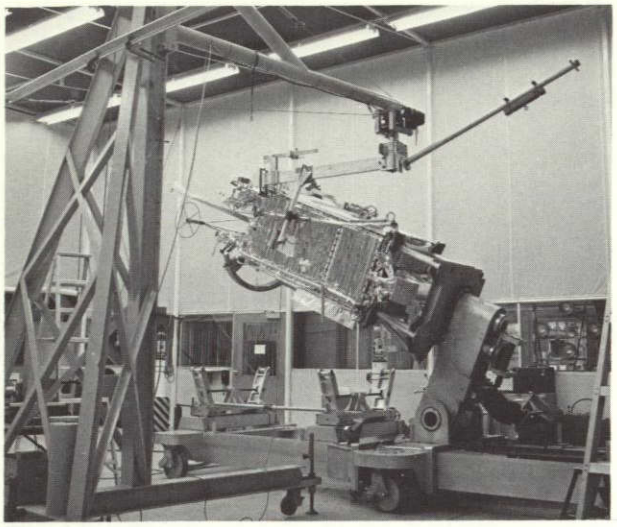

Figure 11-10

THE TORQUE-ANGLE MACHINE drives the solar array deployment mechanism through its travel while measuring the output torque by means of a load cell.

11.1.13 Vertical Transporter

The vertical transporter is a roadable trailer providing thermal and dynamic protection for the observatory at highway speeds up to 60 mph and temperature extremes of 0 to 110°F. Dynamic isolation is provided by four coil springs at the level of the sprung center of mass, with associated dampers. Thermal protection is provided by an insulated container and an automatic refrigeration and heating unit. Control for the air conditioning system includes alarms for out-of-temperature conditions as well as automatic control heating and cooling. The transporter is 14.5 feet high. This height has not been a problem on any of the OGO trips, but if impediment lower than that height should be encountered the transporter can rotate the observatory container to a horizontal position for short periods at low speeds.

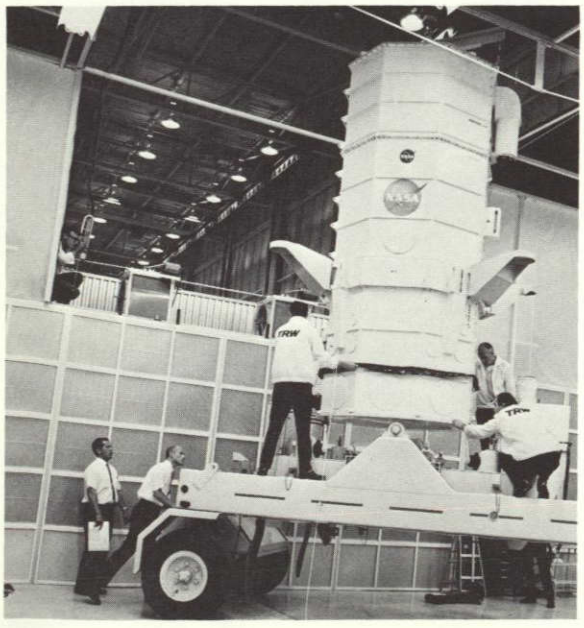

Figure 11-11

THE VERTICAL TRANSPORTER has provided protection for OGO during movement of the observatory from TRW to Vandenberg AF Base and from GSFC to Kennedy Space Flight Center.

11.1.14 Thermal Louver Support Frame

The thermal louver support frame is a flat sheet of honeycomb construction with attach points on one side for the louver assembly and handles on the other for manual handling of louvers.

11.1.15 RBV Installation Fixture

The RBV installation fixture is a counterbalanced sling allowing overhead support of the weight while mounting bolts are installed with the observatory horizontal or vertical.

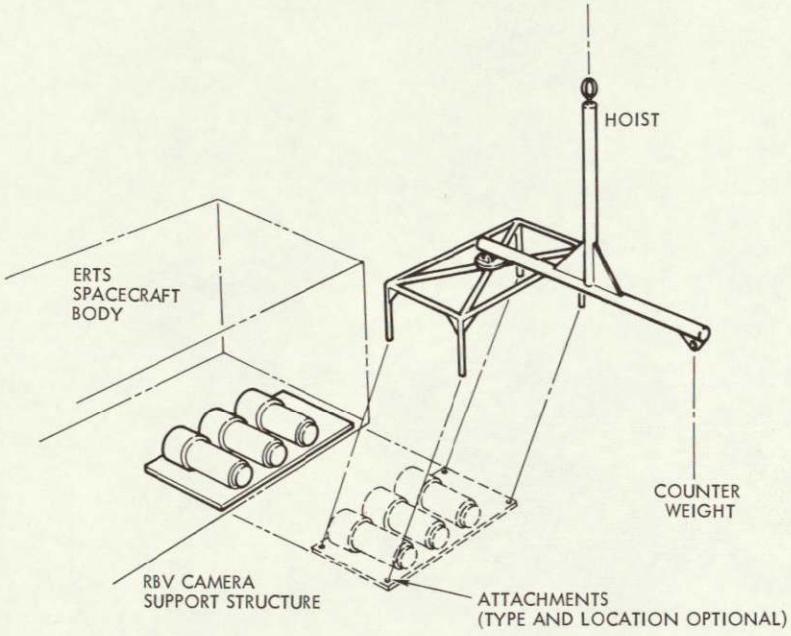

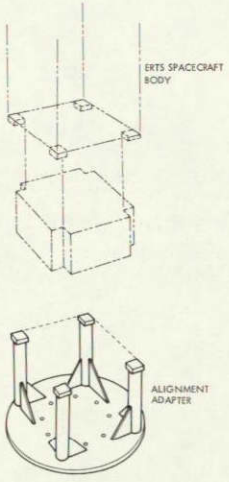

11.1.16 Alignment Adapter

A four-post pedestal is provided to attach the observatory to the indexed rotary table during alignments. The adapter mates with the tapered holes in the corner castings at the separation plane.

11.1.17 Horizontal MSS Installation Fixture

The horizontal MSS installation fixture is a counterbalanced sling which interfaces with two of the six mounting feet on the MSS and allows access to all mounting feet for installation of flight mounting bolts.

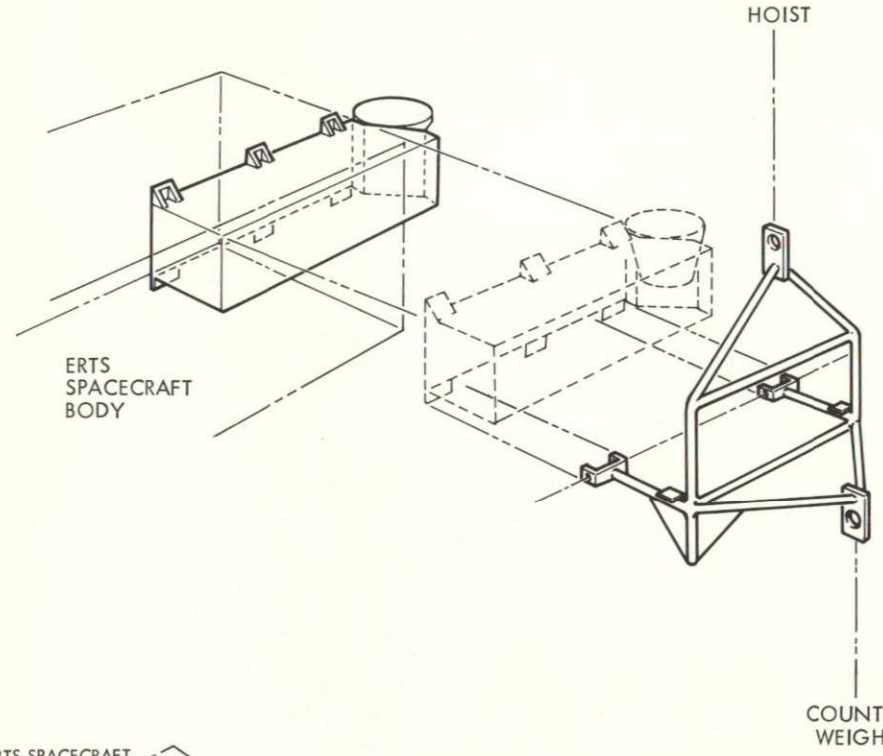

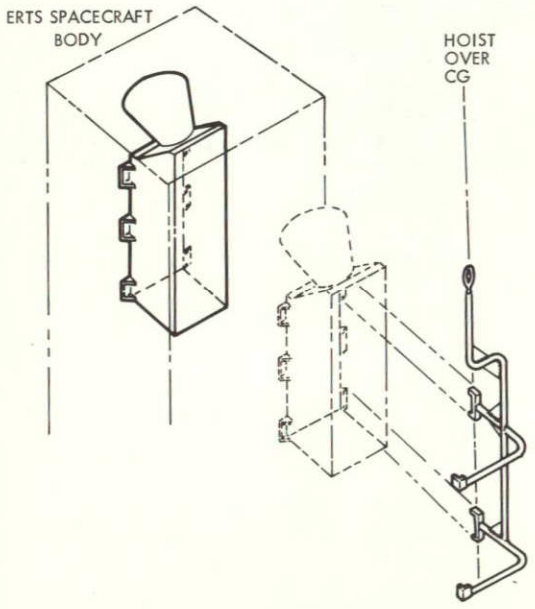

11.1.18 Vertical MSS Installation Fixture

The vertical installation fixture attaches to the MSS mounting feet in the same manner as the horizontal fixture but does not require counterbalancing.

11.1.19 Horizon Scanner Field-of-View Fixture

The field-of-view fixture is a horizon scanner head with the

sensor replaced by a light source which projects a beam with the same angle of divergence as the scanner sensor. When swept through the scanning arc, the light beam illuminates all objects within the field of view of the horizon scanners.

11.1.20 Sun Sensor Stimulator

The sun sensor stimulator is positioned in front of the three elements of the sun sensor. When a light is turned on, the sensor output drives the solar array shaft if the arrays are not installed or actuates the appropriate gas jet. When the solar arrays are not mounted on the observatory, the stimulators are mounted on the solar arrav hinges for convenience in connecting the sensor to the observatory.

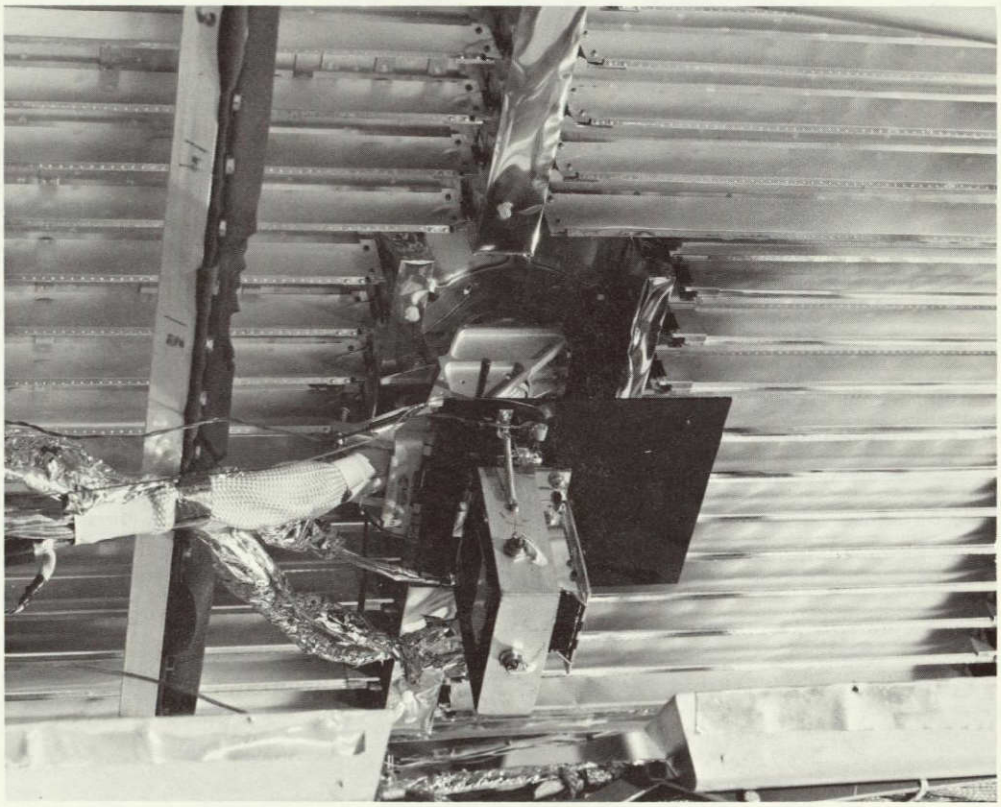

Figure 11-12

SUN SENSOR STIMULATOR consists of three light sources in appropriate housing.

11.2 ELECTRICAL GROUND SUPPORT EQUIPMENT

The ERTS electrical GSE calls essentially for repackaging GFE from the OGO Program, combined with new equipment for the unified S-band equipment in ERTS. The requirements for EGSE are illustrated in the system test layout in Figure 11-13 as are number and status of the major assemblies as shown in Table 11-1.

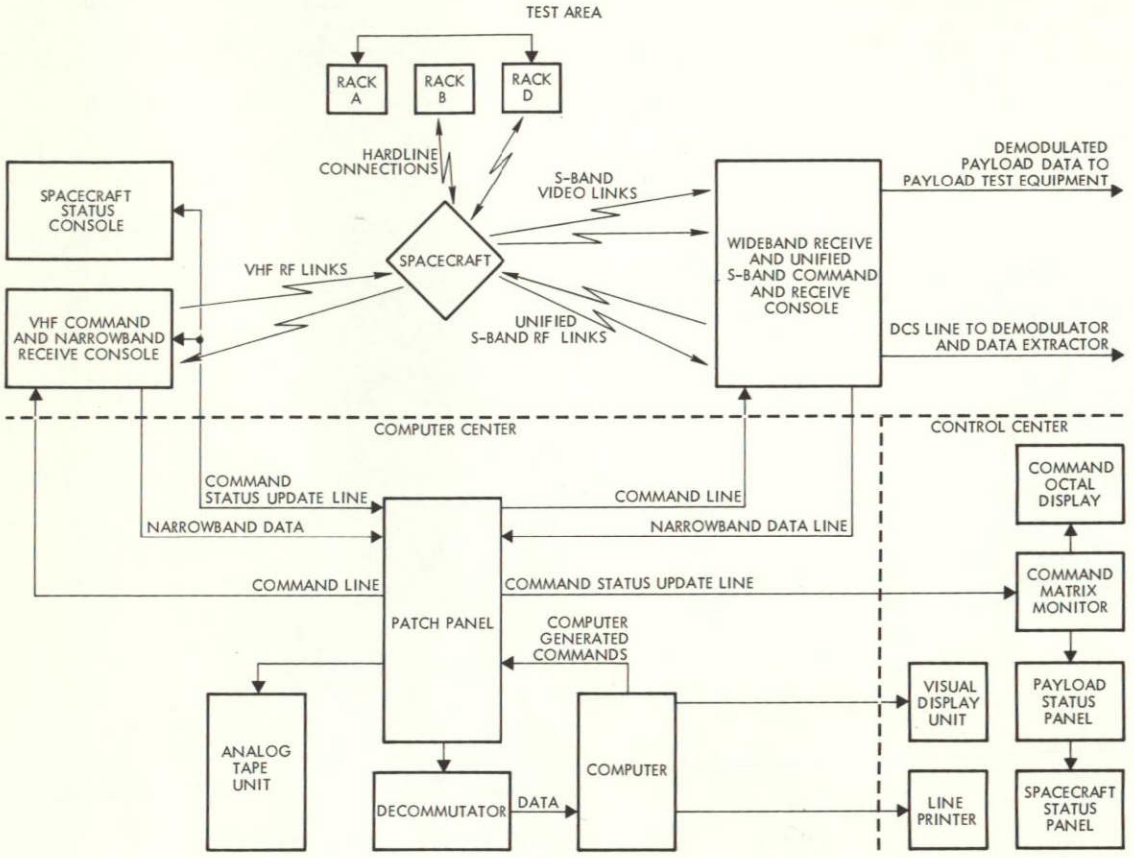

Figure 11-13
OVERALL EGSE SYSTEM TEST block diagram

11.2.1 Computer Station and Control Center

11.2.1.1 Computer Station

The computer station compiles and processes data during system tests and presents to the test conductor a meaningful summary of real-time data from a given test while retaining the capability to present for analysis all the data pertaining to any selected area. Data is accepted

Table 11-1. Major Items of EGSE

	New Design Required	No Changes from OGO	Minor Changes from OGO	Units Required for ERTS	Units Available	Remarks
Control center console		Repackage		1	2	
Peripheral equipment						
Rack A (power)		X		2	3	
Rack D (power)		X		2	3	
Rack B (attitude control)			X	2	2	Deletes extra functions
Narrowband receive console		Repackage		1	3	Buy two telemetry receivers
Command — command/receive console		Repackage		1	3	Add command encoder and decoder
Spacecraft status console		Repackage		1	2	
Wideband receive console	X			1	0	
USB command and receive console	X			1	0	
Launch command console		Repackage		1	1	Buy TWTA for USB commands

through a patch panel by the analog tape unit and the telemetry decommutator. Decommutated data is fed to the computer, from which in turn commands are fed back to the patch panel. The real-time ERTS monitoring program is used to monitor all of the spacecraft real-time telementry in the computer and to present only significant, exceptional data in annotated form for rapid analysis by the test personnel. Control of the program is via computer breakpoints, by console type-ins, and by card input.

The telemetry decommutator formats and assembles all telemetry data into computer words and transfers data in parallel into the computer through a buffered data channel. Input to the decommutator can originate from the spacecraft or tape recordings of spacecraft telemetry.

The decommutators use existing Lear Siegler 610-B-13 systems. The updated systems provide increased operating flexibility and reliability over that of the OGO equipment. A new Model 6203A bit synchronizer and Model 6204A data synchronizer are incorporated. Design

improvements are also incorporated in the Model 6102 data switch and Model 6210 digital-to-analog converters.

11.2.1.2 Control Center Console

The control center console (Figure 11-14) serves as a central point for the direction of system testing and data analysis by the test conductor.

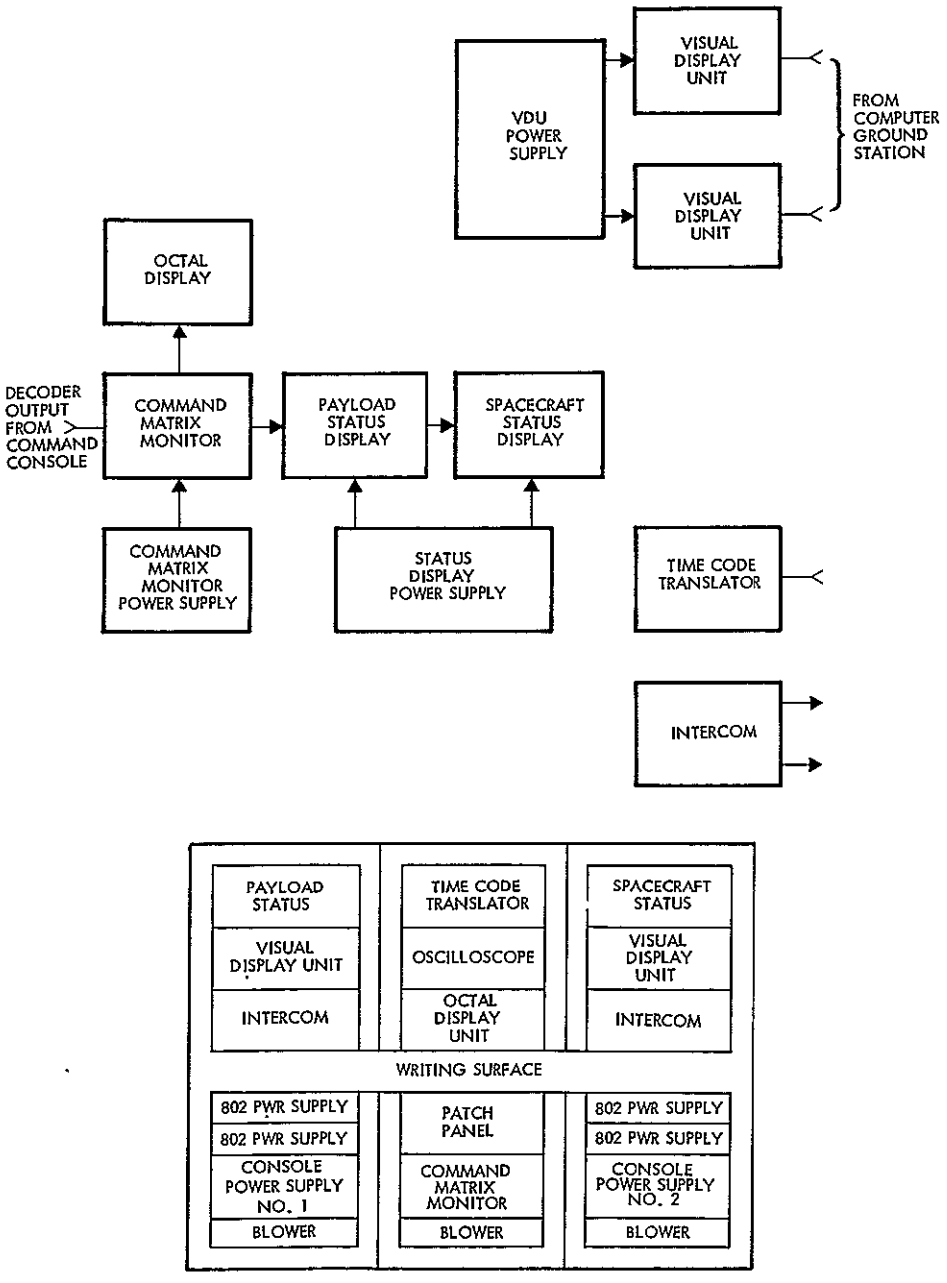

Figure 11-14
CONTROL CENTER CONSOLE and overall block diagram

The console is capable of monitoring spacecraft and payload status, displaying real-time narrowband telemetry, and selecting any word within the telemetry format for display.

The command matrix monitor receives signals from a command decoder in the VHF console via coaxial line. The 16 by 16 matrix signals are converted to octal readout, and the lines energized and octal number of the matrix position commanded are displayed. Command signals are routed from the matrix monitor on 32 lines to the payload status display and then to the spacecraft status display.

Indicators on the payload status display are divided horizontally. The upper half of each indicator lights when the matrix line monitored carries a command pulse that sets a latching-type relay. Receipt of an off command pulse resets the indicator. The lower half is energized and lighted from relay flip-flops on receipt of an impulse command. The first impulse through any pair of matrix lines lights the indicator, and the next impulse through the same pair of lines turns the indicator off.

Indicators on the spacecraft status display represent subsystem status. Latching-type relays are set by command signals on the matrix line monitored, which in turn energize the indicators to show status of spacecraft commands generated. Reset is by off commands.

A time code translator provides the test conductor with accurate Greenwich Mean Time.

The control console is made up of repackaged assemblies from the OGO five-bay console into a new three-bay console. All assemblies will be tested, refurbished, and/or repaired and calibrated if required. Unused indicators are blanked out. A new console is incorporated along with interconsole cabling.

11. 2. 2 Peripheral Equipment

The peripheral equipment (Figure 11-15) consists of three racks classified A, B, and D, to supply, control, and monitor spacecraft power and subsystem functions.

Rack A is a single-bay console containing a power control and monitor panel, digital voltmeters, and a digital recorder. This rack can

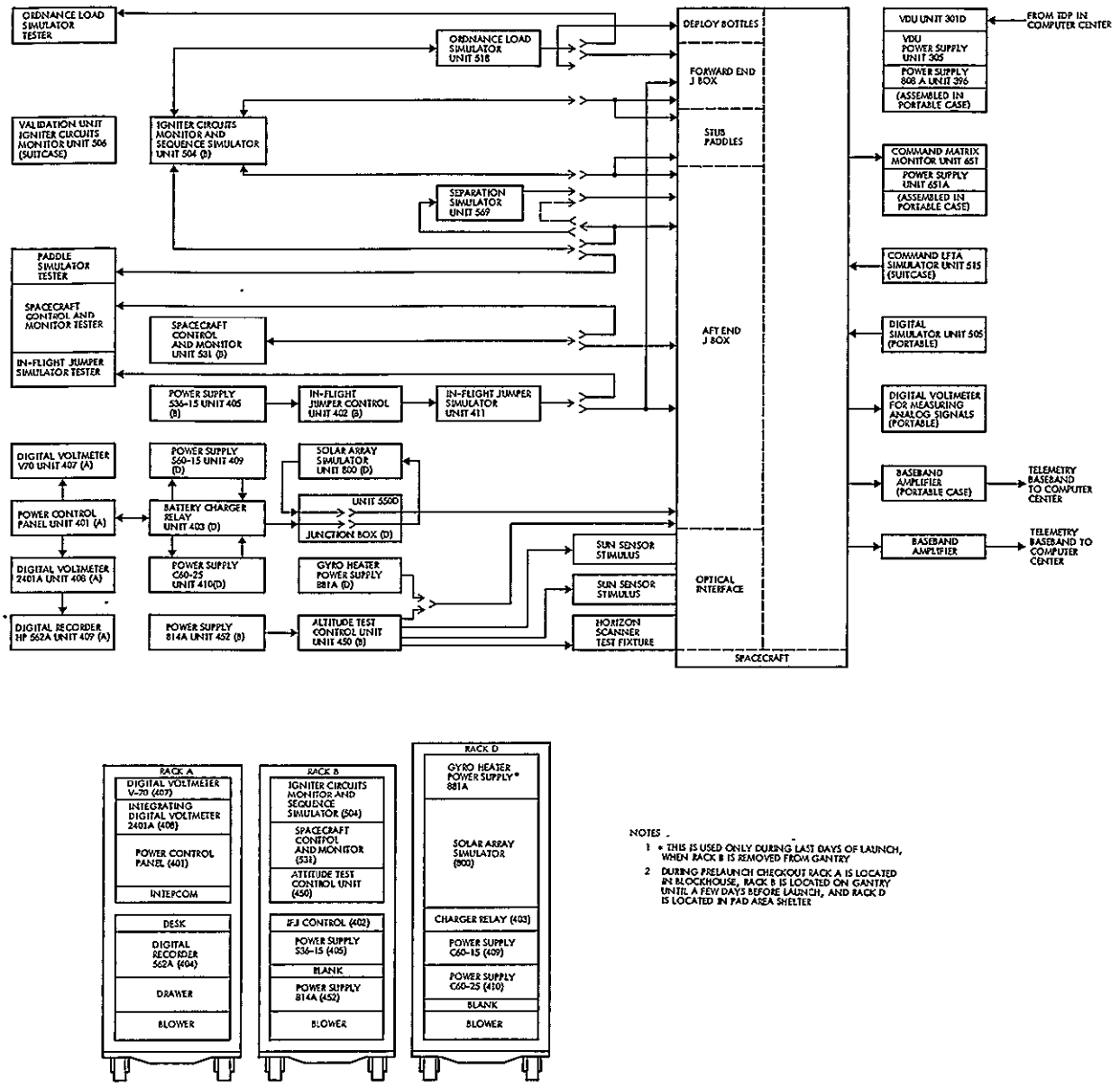

Figure 11-15
PERIPHERAL EQUIPMENT and functional block diagram

control all modes of spacecraft power (supplied by Rack D) for primary bus excitation, battery charging, and solar array simulation. Monitor meters and test points are available for measuring voltages, currents, and battery temperature. The digital voltmeters are used for accuracies greater than panel meter capabilities, and the printer provides permanent records of selected parameters.

Rack B is also a single-bay console containing major assemblies peculiar to controlling and monitoring all spacecraft subsystem functions. The attitude control equipment provides control and monitor capability for that system in each of its modes of operation. Stimuli for the sun sensor, horizon scanner, and gyros are provided. The ordnance monitor sequences the ordnance signals and confirms availability of sufficient igniter current. Any signals within the ordnance no-fire region are also detected. The spacecraft control and monitor assembly provides the capability to control and monitor the various subsystems, including receiver video, ordnance control circuits, and converter and inverter synchronizing signals.

Rack D is a single-bay console containing power supplies, solar array simulator, controllers, and junction box. This rack supplies power for all modes of spacecraft bus excitation and battery processing. Power control is through the interface with Rack A. The console is controlled remotely and located in the terminal room during launch operations.

Racks A and D will be tested, refurbished, calibrated, and used as is with no design changes. Three drawers of Rack B are modified from OGO configuration:

1) Igniter circuits monitor: Eliminate six indicators, eight indicating switches, and 24 toggle switches from front panel. Relocate six indicators and indicating switches on new front panel.

2) Spacecraft control and monitor: Eliminate 13 indicating switches, five RF connectors, three banana jacks, and one potentiometer from front panel.

3) Attitude test control unit: Rewire two unused indicating switches to obtain proper control switching of pitch and yaw gyros torquer current. Change torquer current supply circuits to obtain adequate torque current capability for pitch and yaw gyros.

11.2.3 Spacecraft Status Console

The spacecraft status console (Figure 11-16) is a single-bay console containing equipment to display spacecraft and payload command status.

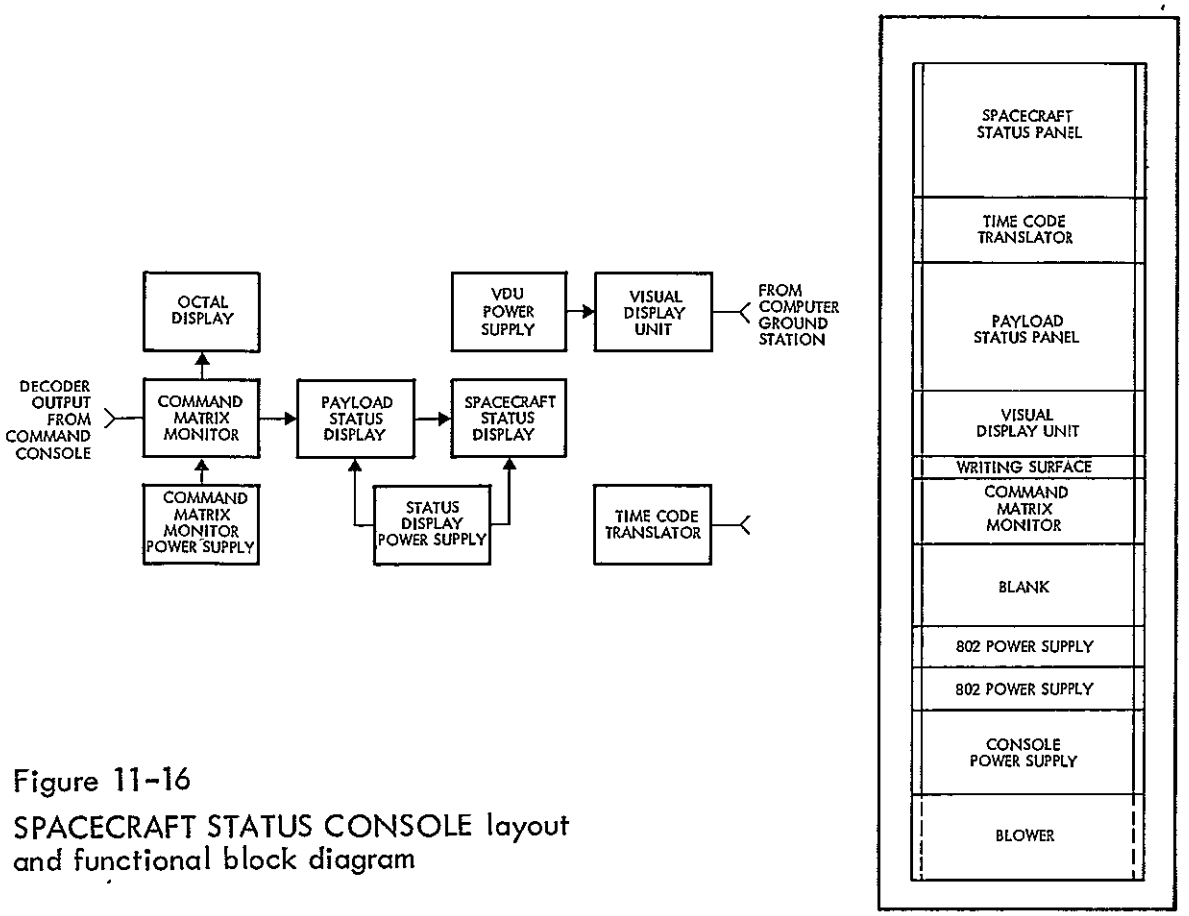

Figure 11-16
SPACECRAFT STATUS CONSOLE layout and functional block diagram

As with the status panels in the control center console, decoded command signals are routed via coaxial line from the VHF console to a command matrix monitor. Outputs from the matrix monitor in turn update the appropriate indicators on either a spacecraft or payload status panel whether the S-band or VHF command RF uplink is used, or both. A visual display unit is provided for monitoring any selected word within the narrowband telemetry format. A time code translator displays accurate Greenwich Mean Time. All major assemblies are identical to like units in the control center console.

The spacecraft status console involves minor modifications of the payload and spacecraft status panels and repackaging and recabling of GFE (existing OGO) into a new single-bay rack. Eight OGO drawers will be refurbished and used as is.

11.2.4 VHF Command and Receive Console

In the VHF command and receive console (Figure 11-17), VHF telemetry is received simultaneously by two narrowband receivers and demodulated data is made available via patch panel for distribution to a data decommutator. Two phase-lock receivers at 137.6 MHz are utilized. Suitable predetection filters and phase demodulators are selectable for

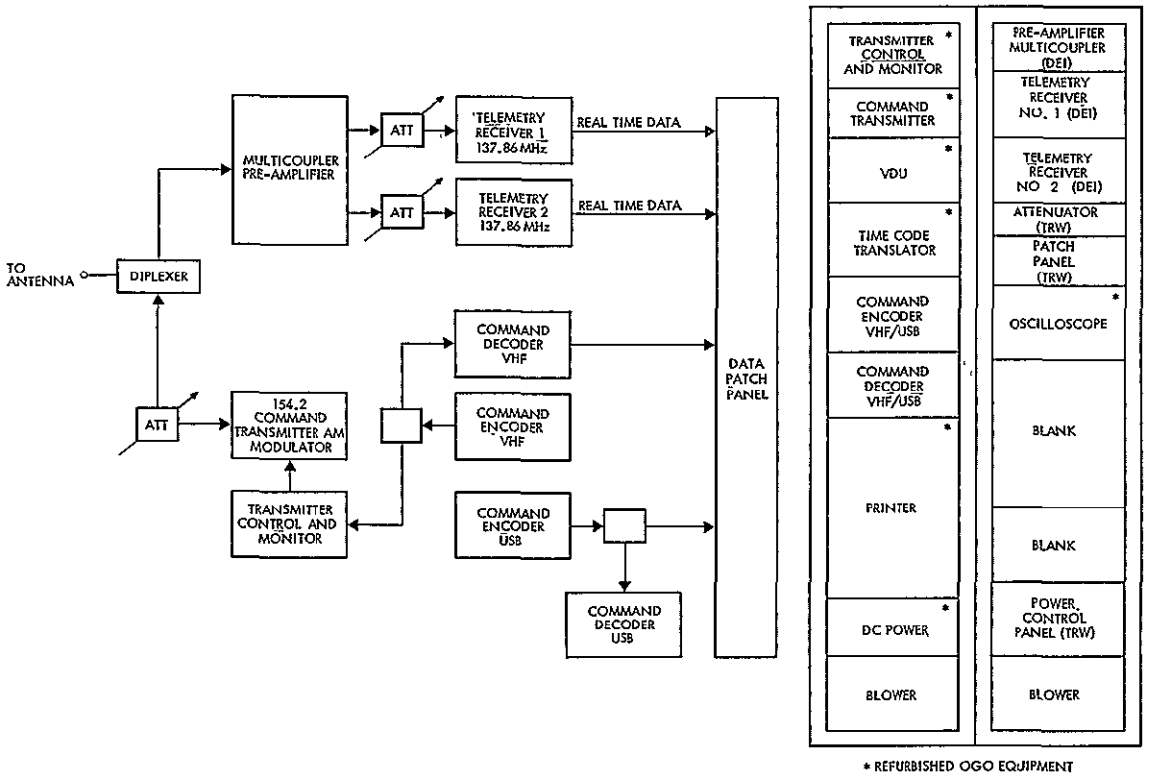

Figure 11-17
VHF RECEIVE AND COMMAND CONSOLE and functional block diagram

bit rates of 1 and 32 kbits/sec. Both receivers with associated multicoupler preamplifier, attenuators, and patch panel are housed in half of the two-bay VHF console.

The narrowband VHF receive rack involves packaging new commerical RF equipment with three new drawers, attenuator, patch panel, and power control, in a new rack.

From the VHF command and receive console, VHF commands are transmitted via hardline or radiated by a low-level (200 mv) transmitter. Decoded command outputs are routed externally to update remote status panels via command matrix monitors. The transmitter with its control and monitor drawer was used on OGO; for ERTS it is retuned to 154.2 MHz. Appropriate command baseband is amplitude-modulated on the transmit carrier.

A dual command encoder (Figure 11-18) is used to construct the command baseband modulating signals for the uplink VHF and unified S-band transmitters. Commands may be formatted by either manual selector (matrix commands only) or by computer request. Both matrix and stored commands can be transmitted using the computer. Both the VHF and unified S-band shift registers are loaded with parallel data from the computer. The data is then shifted in serial at the proper bit rate (128 bits/sec for VHF and 1000 bits/sec for unified S-band) to their respective modulators. Command baseband output can be VHF only, unified S-band only, or both.

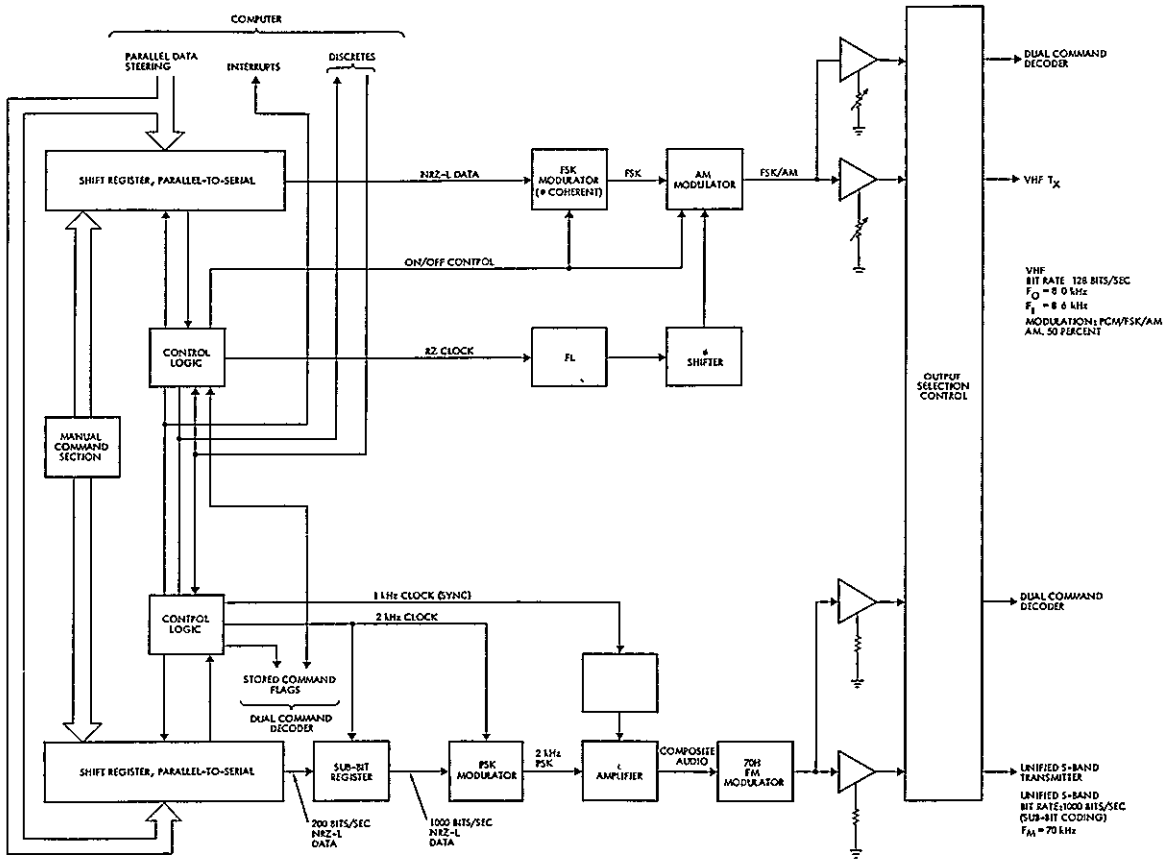

Figure 11-18
DUAL COMMAND ENCODER block diagram

A dual command decoder (Figure 11-19) is used to demodulate and decode the VHF and unified S-band command baseband signals. Decoded outputs are routed to a digital printer for recording of commands generated and to the spacecraft status and control center console for updating

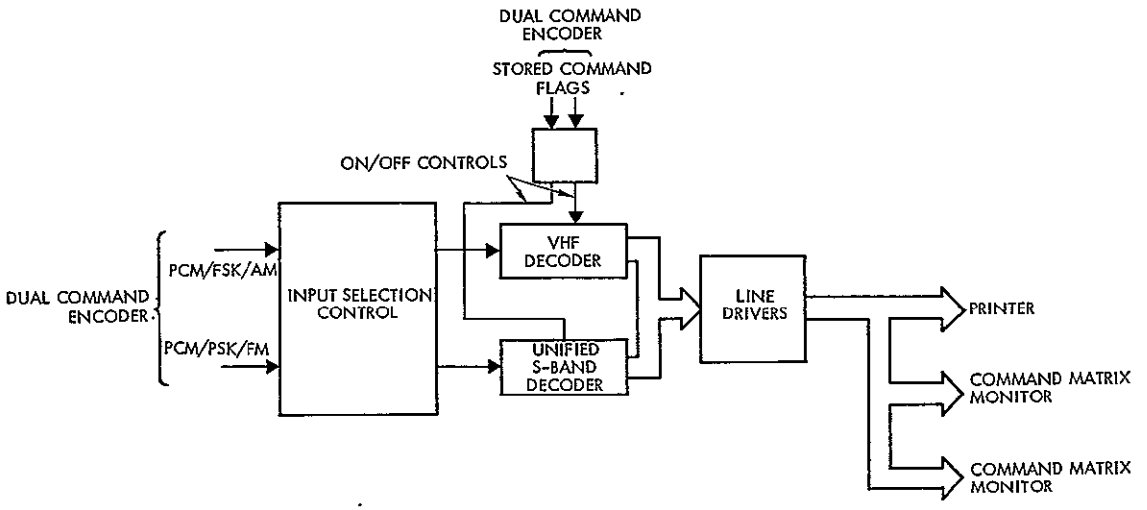

Figure 11-19
DUAL COMMAND DECODER block diagram

status indicators. Both the VHF and unified S-bands are identical to spacecraft units.

The VHF command rack (which is packaged with the narrowband VHF receive rack) involves new design of an encoder-decoder compatible with the unified S-band uplink data rate (1000 baud). These new drawers are packaged and recabled with refurbished OGO drawers.

11.2.5 S-Band Receive and Command Console

11.2.5.1 Wideband Receive

Wideband telemetry data is recovered by two receivers, one for multispectral scanner and one for RBV data. The demodulated payload data is distributed via patch panel to payload test equipment (see Figure 11-20).

An S-band receiver receives the MSS downlink signal at 2230 MHz. To provide sufficient predetection bandwidth for high-rate (15 Mbits/sec) MSS data, the IF passband is approximately 20 MHz. The receiver IF output is applied to a PCM/FM data demodulator for further processing.

Another S-band receiver receives the RBV downlink signal at 2265 MHz. An FM demodulator with baseband capabilities to 6 MHz is

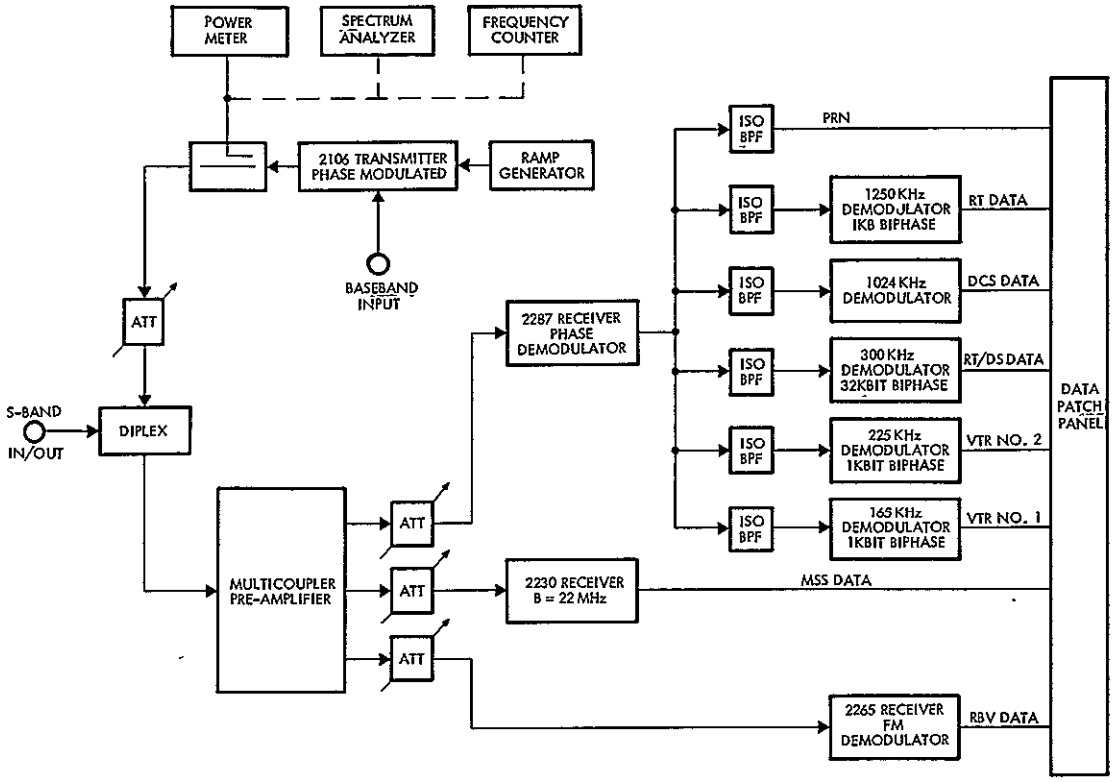

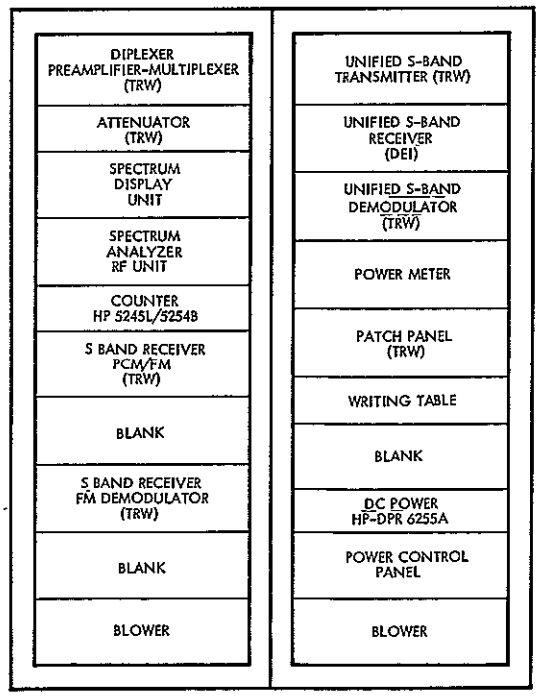

Figure 11-20

S-BAND RECEIVE AND TRANSMIT CONSOLE layout and functional block diagram

incorporated. The receiver-demodulator output is available via patch panel for distribution to payload test equipment.

The two wideband receivers with associated multicoupler preamplifier and attenuators are housed in half of the two-bay S-band console.

The wideband receive console is almost entirely new, requring four new RF drawers. All the equipment is packaged in a new rack. This S-band equipment is packaged side by side with the unified S-band command and telemetry equipment.

11.2.5.2 Unified S-Band Command and Telemetry

Unified S-band-compatible commands are transmitted either hardline or radiated by a low-level transmitter. Telemetry is received, filtered, demodulated, and made available via patch panel for distribution to a data decommutator. The S-band transmitter generates a carrier at a frequency of 2106.4 MHz at a power level of +23 dbm. As shown in Figure 11-20, appropriate command baseband is generated by the command encoder in the VHF console and routed to the transmitter phase modulator. Unified S-band telemetry is received by a phase-lock receiver (2287 MHz) and phase demodulated. Demodulator output contains all unified S-band-compatible subcarriers and PRN code. This output is routed to a data demodulator drawer for further processing. The data demodulator drawer contains suitable filtering and five demodulators, one for each subcarrier. Serial two-phase data from the demodulators is available via patch panel for distribution.

The unified S-band equipment is all new. A mix of TRW new design and new commercial equipment constitute the unified S-band command/command receive rack.

11.2.6 Launch Command Console

The launch command console (Figure 11-21) provides radiated signal levels to the spacecraft during tests at the launch site. Selectable redundant VHF power amplifiers with associated power supplies are available to boost power to levels sufficient for on-stand testing. Excitation is obtained from the low-level transmitter in the VHF console. A traveling wave tube assembly with associated power supply boosts the

S-band power, and excitation is from the low-level transmitter in the S-band console.

The launch command console requires four new TRW-designed drawers to be integrated with refurbished OGO VHF equipment, in a new one-bay rack.

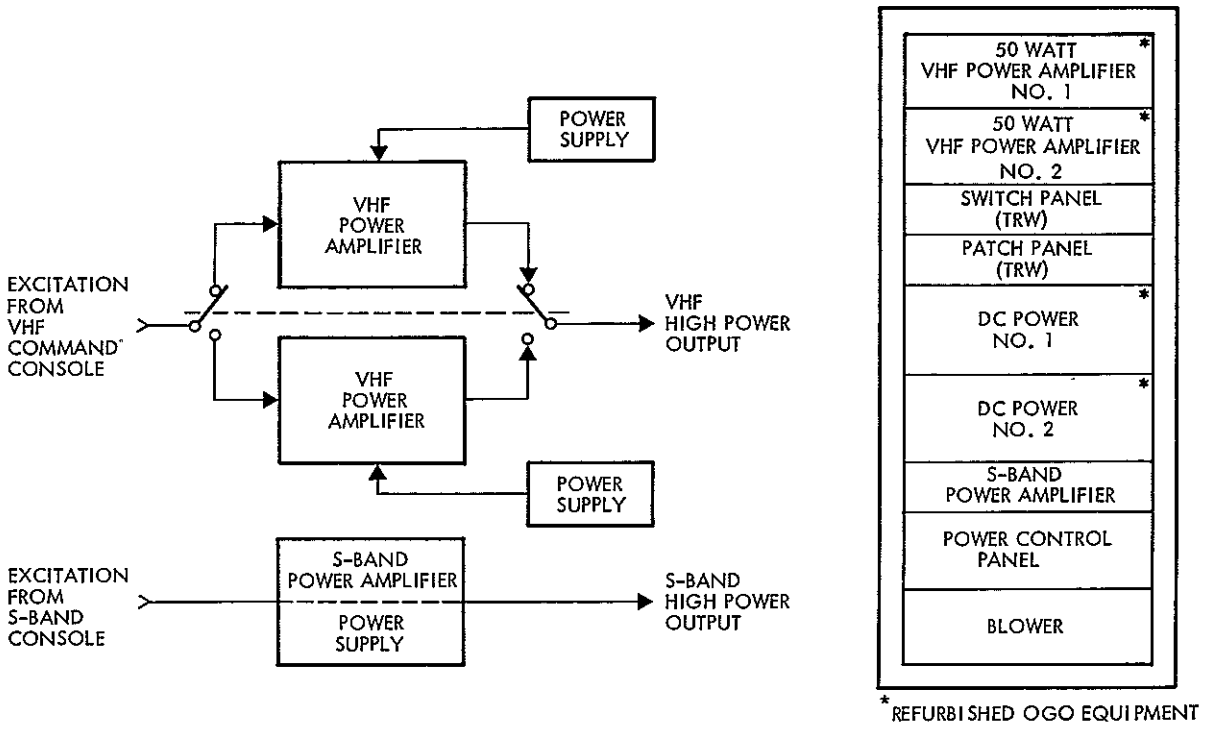

Figure 11-21

HIGH-POWER COMMAND TRANSMITTERS, VAFB launch operations console layout and functional block diagram